

Biochemical and Microbiological
Investigations of Inhibitors for
 β -Lactamases from Human Pathogenic
Bacteria

by

Carol Anne Tanner

A thesis

presented to the University of Waterloo

in fulfillment of the

thesis requirement for the degree of

Doctor of Philosophy

in

Chemistry

Waterloo, Ontario, Canada, 2019

©Carol Anne Tanner 2019

Author's Declaration

I hereby declare that I am the sole author of this thesis. This is a true copy of the thesis, including any required final revisions, as accepted by my examiners.

I understand that my thesis may be made electronically available to the public.

Abstract

The majority of antibiotics prescribed for treatment of bacterial infections are β -lactam antibiotics. Resistance to these has evolved in a few different ways, notably by regulating permeability and by the expression of β -lactamases which hydrolyze the antibiotic before it reaches its target. Three of the classes of β -lactamases (classes A, C and D) are serine- β -lactamases (SBLs) and the fourth class (Class B) consists of metallo- β -lactamases (MBLs) that rely on one or two zinc ions for their catalytic activity. Bacteria producing β -lactamases that are capable of hydrolyzing the β -lactam bond in all of the classes of β -lactam antibiotics including penicillins, monobactams, cephalosporins and carbapenems are of great clinical concern. As a consequence of the increasing prevalence of resistance, there is much interest in the discovery of inhibitors for such clinically important β -lactamases as well as in the discovery of β -lactam antibiotics that are less susceptible to inactivation by β -lactamases.

Described in this thesis are the kinetic properties of new chromogenic cephalosporin-type substrates that are susceptible to hydrolysis by clinically important SBLs and MBLs but that exhibit a much more pronounced colour change upon hydrolysis than does the commercially available and widely used chromogenic cephalosporin called nitrocefin. Some of these substrates also offer more favourable kinetic properties for assaying MBLs *in vivo*.

Also in this thesis, biochemical as well as microbiological investigations of several classes of SBL and MBL inhibitors are described as well as one class of cephalosporins that exhibit inhibition of MBLs and surprising antibacterial potency against certain clinically significant MBL-producing Gram negative bacteria.

More specifically, 6-phosphonomethylpyridine-2-carboxylates (PMPCs) and a number of derivatives thereof, synthesized previously in this research group have been shown in this thesis research to be potent inhibitors (low to submicromolar K_i) of the major Class B1 MBLs, IMP-1, VIM-2, NDM-1 and SPM-1 as well as the Class B3 MBL L1, all of which are dizinc enzymes, and somewhat less potent inhibitors of the monozinc Class B2 MBL, SFH-1, which is of lesser clinical significance. These compounds that are expected to exhibit metal-binding characteristics were found to exhibit a time-dependent inhibition mechanism which fits a kinetic mechanism that is consistent with slow binding to the active site and even slower release of the inhibitor without expulsion of the metal ions from the MBL active site. Microbiological investigations were also carried out involving

combinations of PMPCs with the carbapenem antibiotic meropenem and demonstrated an ability of the PMPCs to lower the MICs of meropenem against of MBL-producing clinical strains of *Escherichia coli*, *Klebsiella pneumoniae*, *Pseudomonas aeruginosa*, *Acinetobacter baumannii* and *Stenotrophomonas maltophilia* thus encouraging further research on even more potent PMPCs for potential clinical use in combination with carbapenems.

Another class of MBL inhibitors that was studied consist of cephalosporin derivatives that incorporate an aromatic thioester linked to C3' of the cephalosporin core. It was found that inhibition of the Class B3 MBL L1 was likely the consequence largely of the binding of an arylthioacid conjugate base to the active site zinc ions after its expulsion from the hydrolysis product of the cephalosporin. This led to a study of the MBL-inhibitory properties of a series of synthetic arylthioacids, a class of compounds that have not been well studied as metallo enzyme inhibitors. These compounds were found to be poor inhibitors of Class B1 MBLs (IMP-1, VIM-2, NDM-2 and SPM-1) but good inhibitors of the B3 MBL L1. These observations are consistent with inhibition of Class B1 MBLs arising not from the arylthiocarboxylate released but from binding the cephalosporin-derived metal-binding species formed upon expulsion of the arylthiocarboxylate from the active site.

A further enzyme kinetic study revealed that synthetic samples of pyridine-2,6-bis(carbothioic) acid and 6-thiocarboxy-picolinic acid, previously known as Fe³⁺-binding siderophores produced by some species of *Pseudomonas*, were good inhibitors of Class B1 and B3 MBLs and also exhibited an ability to lower the MIC of meropenem against MBL-producing clinically important Gram negative bacteria.

One cephalosporin called UW-123 with at C3'-arylacetylthio group and a siderophore mimic attached to the amide group at C7 was studied in some detail microbiologically and found to exhibit good standalone antibiotic activity against certain MBL-producing Gram-negative bacteria especially those producing the widespread MBL VIM-2. UW-123 was also shown to be bacteriostatic and to bind preferentially to induce filamentation of *E. coli* cells. It was found to bind most strongly to PBP 3 and 1a but also significantly to PBP1b and 4 in *P. aeruginosa*. In *E. coli*, UW-123 bound most tightly to PBP3 but also significantly to PBP1a/b and PBP2.

Finally, the ability of a cyclobutanone mimic of penem antibiotics JJ05-1058, previously prepared in this laboratory, to inhibit both SBLs and MBLs was demonstrated and the ability of this compound to bind to the low molecular weight penicillin binding proteins was observed suggesting that such

compound may have some promise as broad spectrum MBL/SBL inhibitors and possible also as antibiotics that inhibit penicillin binding proteins.

Acknowledgements

First and foremost I would like to thank Dr. Gary Dmitrienko for sharing his knowledge and expertise in the field of β -lactam resistance these many years. His patience and assistance with the thesis writing process has made the production of this document tolerable.

I would also like to thank our collaborators Dr. James Spencer and Dr. Philip Hinchliffe without whom many of the insightful conclusions about binding modes could not have been achieved. My advisory committee Dr. Guy Guillemette, Dr. Thorsten Dieckmann, Dr. Richard Manderville, and Dr. Stefan Siemann have been excellent sources of advice and thought provoking questions, challenging me to push the boundaries of my knowledge and expertise. My external examiner, Dr. Steven Seah, and my internal-external examiner, Dr. Trevor Charles should be thanked for the time and effort they put forth in reviewing my thesis and offering suggestions.

I am also grateful to Cathy Van Esch, a fount of knowledge for the inner workings of graduate studies in the Department of Chemistry.

The ladies of the Dmitrienko biochemistry lab, Dr. Geneviève Labbé, Valerie Goodfellow, and Dr. Laura Marrone taught me everything I know about running experiments and living life to the fullest – no amount of thanks could be enough. The excellent undergraduate thesis students that have passed through this lab over the years, Melinda Lam, Karan Malik, Alicia Tjahjadi, and Jessica Duong must be thanked and credited for giving us a reason to purify more proteins, actually performing the purification, and breaking the silence that took over the lab in 2015.

To Dr. Anthony Krismanich, Dr. Ahmad Ghavami, Dr. Ahmed Desoky, Dr. Nan Chen, Dr. Glenn Abbott, Dr. Jarrod Johnson, Karan Teckwani and Peizhi Qui, this work would not have been possible without your synthetic talents and the religious observation of the 10 am coffee break. Upon the dispersal of the Dmitrienko organic lab, I thank my friends throughout the department for keeping me company as I continued to observe – though less religiously – the daily coffee break.

The biological nature of this work necessitated use of equipment or facilities in the Biology Department, and I would like to thank Dr. Trevor Charles, Dr. Josh Neufeld, Katja Engel, Sura Ali, Dr. Brenden McConkey, and Dr. Roland Hall for training me and allowing me to use your facilities to complete my work.

Finally, I would like to thank my husband, Taylar Cameron for his unending love and support throughout my graduate studies and his understanding when I say that I have done enough dishes for one day. Our beloved cats, Lily and Pickles, must also be thanked for being my primary source of purr-crastination.

Table of Contents

Author's Decarlation.....	ii
Abstract	iii
Acknowledgements	vi
Table of Contents	viii
List of Figures	xii
List of Schemes	xv
List of Tables	xvi
List of Abbreviations.....	xix
Chapter 1	1
1.1 Antibiotic Classes and Targets.....	1
1.1.1 Overview of Antibiotics.....	1
1.1.2 β -Lactam Antibiotics.....	4
1.1.3 Bacterial Resistance	7
1.2 Penicillin Binding Proteins	9
1.2.1 Bacterial Cell Wall Structure	9
1.2.2 PBP Functional and Structural Classification	10
1.2.3 PBP Expression in Bacterial Strains	15
1.2.4 Role of PBPs in Bacterial Resistance to β -Lactams.....	17
1.3 β -Lactamases.....	18
1.3.1 Role of β -Lactamases in Bacterial Resistance to β -Lactams	19
1.3.2 Classification of β -Lactamases.....	20
1.3.3 Class A β -Lactamases	23
1.3.4 Class C β -Lactamases	28

1.3.5 Class D β -Lactamases.....	31
1.3.6 Class B β -Lactamases.....	33
1.3.7 Established Methods for Assaying β -lactamases.....	37
1.4 β -Lactamase Inhibitors	38
1.4.1 β -Lactams as β -Lactamase Inhibitors	38
1.4.2 Serine- β -Lacamase Inhibitors.....	40
1.4.3 Metallo- β -Lactamase Inhibitors.....	47
1.4.4 Dual Serine- and Metallo- β -Lactamase Inhibitors	57
1.5 Clinical Significance of β -Lactamase Inhibition	58
Chapter 2 Phylogenetic Analysis, Purification, and Biochemical Characterization of β -Lactamases	60
2.1 Introduction	60
2.2 Methods	62
2.2.1 Protein Sequence Alignment	62
2.2.2 Enzyme Purification	63
2.2.3 Characterization of Chromogenic Substrates	74
2.2.4 Biochemical Characterization.....	76
2.3 Results	78
2.3.1 Metallo- β -Lactamase Protein Sequence Alignment	78
2.3.2 Protein Purification.....	84
2.3.3 Characterization of Chromogenic Substrates	88
2.3.4 Biochemical Characterization.....	93
2.4 Discussion.....	99
2.5 Future Work.....	105

Chapter 3 Inhibition of Metallo- β -Lactamases by Phosphonomethyl Pyridine Carboxylates	106
3.1 Introduction	106
3.2 Methods	109
3.2.1 Enzyme Kinetics	109
3.2.2 Microbial Experiments	113
3.3 Results	114
3.3.1 Enzyme Kinetics	114
3.3.2 Potentiation of meropenem against MBL producing Gram negatives	123
3.4 Discussion	124
3.5 Future Work	132
Chapter 4 Thioacids and 3'-Acylthio-Cephalosporins as B3 Inhibitors	134
4.1 Introduction	134
4.2 Methods	137
4.2.1 Synthetic Thioacids and 3'-acylthiocephalosporins	137
4.2.2 β -Lactamase Enzyme Kinetics	140
4.2.3 Antimicrobial Susceptibility	141
4.2.4 Mode of Action	142
4.3 Results	146
4.3.1 Released Phenyl Thioacids as β -Lactamase Inhibitors	146
4.3.2 MICs of UW-123	155
4.3.3 Bacterial Synergy of UW-123 with Meropenem	163
4.3.4 Mode of Action Studies of UW-123	164
4.3.5 Pyridine thioacids – a more potent alternative to phenyl thioacids	173
4.4 Discussion	179

4.4.1 Phenyl Thioacid Inhibitors of B3 MBLs	179
4.4.2 3'-Acylthiocephalosporins as delivery systems for phenyl thioacid inhibitors of L1	182
4.4.3 UW-123	183
4.5 Future Work.....	185
Chapter 5 Other β -Lactamase Inhibitors.....	187
5.1 Introduction	187
5.2 Methods.	191
5.2.1 β -Lactamase Enzyme Kinetics	191
5.2.2 Penicillin Binding Protein Binding Assay	193
5.3 Results	194
5.3.1 Inhibition of β -Lactamases	194
5.3.2 Competitive binding to Penicillin binding proteins	198
5.4 Discussion.....	200
5.5 Future Work.....	202
Appendix A Structures of β -Lactamase Inhibitors	203
Appendix B Statistical Methods for IC_{50} Averages	206
Appendix C Clinical Isolates and Control Strains	207
Appendix D K_i Graphs of DPA, PMPC-3, and PMPC-4	209
Appendix E Protein Sequence Alignments.....	212
Bibliography	242

List of Figures

Figure 1.1 Critically important antimicrobials for human medicine.....	2
Figure 1.2 Representative antibiotics from each major class of β -lactams.....	4
Figure 1.3 Chemical structures of imipenem and cilastatin.....	6
Figure 1.4 Core structures of β -lactam antibiotic families.....	7
Figure 1.5 Gram positive and Gram negative cellular envelope composition.....	9
Figure 1.6 Structure of Lipid II, the peptidoglycan precursor.....	11
Figure 1.7 3-Dimensional structure of Class A SBLs, exemplified by KPC-2.....	24
Figure 1.8 Locations of phenotype changing mutations in TEM-1.....	26
Figure 1.9 Overall MBL $\alpha\beta\alpha$ fold.....	34
Figure 1.10 Penicillins that are inhibitory towards some SBLs.....	39
Figure 1.11 Mechanism-based serine- β -lactamase inhibitors.....	41
Figure 1.12 Other mechanism-based inhibitors: penicillanic acid sulfones, 6-halo penicillins, and alkylidene penams.....	42
Figure 1.13 A selection of the diazabicyclooctanes that are clinically available or in development...	43
Figure 1.14 Transition state analog inhibitors of SBLs: boronates and phosph(on)ates.....	45
Figure 1.15 Cyclobutanones: β -lactam mimics that are inhibitory towards β -lactamases.....	46
Figure 1.16 Demetallating inhibitors of MBLs.....	48
Figure 1.17 Dicarboxylate inhibitors of MBLs.....	49
Figure 1.18 Thiol inhibitors of MBLs.....	51
Figure 1.19 D-Captopril bound to various MBLs from all subclasses.....	53
Figure 1.20 Thioester and other non-thiol MBL inhibitors that contain sulphur.....	55
Figure 1.21 Structurally unique MBL inhibitors.....	57
Figure 1.22 Structural evidence for cyclic boronate inhibition of SBLs and MBIs.....	58
Figure 2.1 Chromogenic and fluorogenic substrates for β -lactamases excluding the UW series substrates.....	60
Figure 2.2 Chromogenic β -lactamase substrates synthesized by the Dmitrienko group.....	61
Figure 2.3 Chromogenic β -lactamase substrates synthesized by the Dmitrienko group.....	75
Figure 2.4 Phylogenetic tree of NDM Variants.....	79
Figure 2.5 Phylogenetic Tree of VIM variants.....	81
Figure 2.6 Phylogenetic tree of IMP family variants.....	83

Figure 2.7 SDS-PAGE of pure β -lactamases.	87
Figure 2.8 Visual appearance of 200 μ L of increasing concentrations of unhydrolyzed and hydrolyzed chromogenic substrates synthesized by the Dmitrienko lab.....	89
Figure 2.9 Spectral scans of chromogenic substrates before and after hydrolysis	90
Figure 2.10 Stability spectra of 100 μ M chromogenic substrates before and after hydrolysis.	92
Figure 2.11 DMSO sensitivity of β -lactamases.....	93
Figure 2.12 Michaelis-Menten plots of CTX-M-15 kinetic parameter determination.	94
Figure 2.13 Michaelis-Menten plots of VIM-1, SFH-1, OXA-23, and OXA-48 kinetic parameter determination.....	96
Figure 2.14 NDM-1 crystal structure with residues that are changed among the variants highlighted	99
Figure 2.15 Overlay of VIM-1 and VIM-2 crystal structures with variable residues within 10 Å of the Zn atoms highlighted.....	100
Figure 3.1 MBL inhibitors based off the DPA core structure.	107
Figure 3.2 PC1 from <i>S. aureus</i> covalently inactivated by a phosphonate monoester	108
Figure 3.3 Phosph(on)ate based inhibitors of β -lactamases.	109
Figure 3.4 Structures of picolinic acid derivatives used in this chapter.	110
Figure 3.5 Dose response curves of MBLs with PMPCs and related compounds.	118
Figure 3.6 Time-dependent K_i graphs for PMPC-1 against representative MBLs.....	121
Figure 3.7 Binding of 3-(4-hydroxypiperidin-1-yl)-aminophthalic acid and PMPC-1 to the active site IMP-1.	127
Figure 3.8 Crystal structures of PMPCs bound to L1.....	127
Figure 3.9 Binding of the S-enantiomer of PMPC-3 to the active site of L1.....	128
Figure 3.10 Fits of initial and steady state rates on representative progress curves of MBLs inhibited by PMPC-1.....	130
Figure 3.11 Binding of PMPC-1 to the active site of IMP-1, highlighting opportunities for development of future PMPCs.	133
Figure 4.1 Protection of meropenem hydrolysis by synthetic and commercial cephalosporins.....	136
Figure 4.2 Generation of a MBL inhibitor from 8-thioxo-cephalosporins.....	137
Figure 4.3 Potent inhibitors of CcrA and L1 determined from natural product screen.....	137
Figure 4.4 Structure of pyridine based thioacids and related compounds presented in this chapter. .	138

Figure 4.5 Serine- β -lactamase inhibitors used in microbiological experiments in the Dmitrienko lab.	141
Figure 4.6 MH agar spot plates of thioacid potentiation of meropenem against L1 and L2 producing <i>S. maltophilia</i>	151
Figure 4.7 UW-123 time kill curves against wild type <i>E. coli</i>	165
Figure 4.8 SDS-PAGE of UW-123 bound to <i>P. aeruginosa</i> PBPs competing with Bocillin.	168
Figure 4.9 Dose response curves of the relative competitive binding of UW-123 to PBPs from <i>P. aeruginosa</i> with Bocillin.	169
Figure 4.10 SDS-PAGE of UW-123 bound to <i>E. coli</i> PBPs competing with Bocillin.....	171
Figure 4.11 Dose response curves of the relative competitive binding of UW-123 to PBPs from <i>E. coli</i> with Bocillin.	172
Figure 4.12 Dose response curves of MBLs and GC-1 inhibited by PMTC and PDTC	176
Figure 4.13 Spot plates of UWB 33 on MH agar to determine the MBCs of thioacid potentiated..	181
Figure 4.14 Binding of thiols to the L1 active site.....	182
Figure 4.15 Bis-PDTC-cephalosporin.....	186
Figure 5.1 Examples of cyclobutanone mimics of β -lactam antibiotics.	188
Figure 5.2 Conformations of C3-substituted cyclobutanones and the steric interactions of the hydrates.....	189
Figure 5.3 X-Ray crystal structures of cyclobutanones bound to β -lactamases.	191
Figure 5.4 Inhibition of SBLs by JJ05-1058.....	195
Figure 5.5 Inhibition of MBLs by JJ05-1058.	196
Figure 5.6 SDS-PAGE of JJ05-1058 bound to <i>P. aeruginosa</i> PBPs competing with Bocillin.....	198
Figure 5.7 JJ05-1058 competition for PBP binding with Bocillin.....	199
Figure 5.8 Time Dependent KI graphs for DPA against representative MBLs	209
Figure 5.9 Time Dependent K_I graphs for PMPC-3 against representative MBLs.....	210
Figure 5.10 Time Dependent K_I graphs for PMPC-4 against representative MBLs.....	211

List of Schemes

Scheme 1.1 Generalized hydrolysis of β -lactam by a β -lactamase.	8
Scheme 1.2 Reactions catalyzed by PBPs: glycosyl transfer, transpeptidation, carboxypeptidation, and endopeptidation.	12
Scheme 1.3 Inactivation of PBPs by a β -lactam.....	13
Scheme 1.4 Mechanism of penicillin hydrolysis by Class A β -lactamases.....	25
Scheme 1.5 Mechanism of cephalosporin hydrolysis by Class C β -lactamases.	30
Scheme 1.6 Mechanism of penicillin hydrolysis catalyzed by Class D SBLs.	32
Scheme 1.7 Hydrolysis of carbapenems by B1 and B3 MBLs.....	37
Scheme 1.8 Hydrolysis of carbapenems by B2 MBLs.	37
Scheme 1.9 Inhibition of SBLs by cephalosporins and carbapenems.	40
Scheme 1.10 Inhibition of Class A SBLs by mechanism-based inhibitors eg. clavulanate.	42
Scheme 1.11 Avibactam mediated inhibition of SBLs and other reactions with Avibactam catalyzed by β -lactamases.	44
Scheme 1.12 Covalent adducts formed by boronates, phosphonates, and cyclobutanones that mimic the transition-state of β -lactam acyl-enzyme formation with serine- β -lactamases.	47
Scheme 1.13 Activation of rhodanine to a mercaptocarboxylate MBL inhibitor.....	54
Scheme 2.1 Panbio homogeneous immunoassay technology.	61
Scheme 2.2 Hydrolysis of nitrocefin by β -lactamases.	89
Scheme 3.1 Enzyme inhibition mechanisms that can exhibit time-dependent inhibition.	120
Scheme 4.1 Formazan dye strategy for a chromogenic cephalosporin.	135
Scheme 4.2 Abridged method for thioacid synthesis.	138
Scheme 5.1 Comparison of hemiketal formation with TS and intermediate in acyl enzyme mechanism.....	187
Scheme 5.2 Parallels between the binding of penems and cyclobutanones to SBLs and MBLs.	190

List of Tables

Table 1.1 Mode of action of established antibiotics.	3
Table 1.2 Penicillin binding proteins present in <i>E. coli</i> and <i>P. aeruginosa</i>	16
Table 1.3 Richmond and Sykes functional classification scheme for β -lactamases.	21
Table 1.4 Functional and molecular classification of β -lactamases.....	22
Table 1.5 Amino acid residues that coordinate zinc ions in the three subclasses of metallo- β - lactamases.	34
Table 2.1 Enzyme and substrate concentrations used for DMSO stability studies.....	76
Table 2.2 Amino acid differences between NDM-1 and other NDM variants.	80
Table 2.3 CTX-M-15 purification table.....	84
Table 2.4 KPC-2 purification table.	85
Table 2.5 VIM-1 purification table.....	85
Table 2.6 GC-1 purification table.	86
Table 2.7 OXA-48 purification table.	87
Table 2.8 Masses of pure β -lactamases as predicted using ExPASy ProtParam and determined by mass spectroscopy	88
Table 2.9 Molar extinction coefficients for UW substrates	91
Table 2.10 Kinetic parameters of CTX-M-15 with and without its His-tag against NC and UW substrates.....	95
Table 2.11 Kinetic parameters of serine- β -lactamases (except CTX-M-15) against NC and UW substrates.....	97
Table 2.12 Kinetic parameters of metallo- β -lactamases with NC and UW substrates	98
Table 2.13 Literature values for serine- β -lactamase kinetic parameters with nitrocefin.	103
Table 2.14 Literature values for metallo- β -lactamase kinetic parameters with nitrocefin.....	104
Table 3.1 Kinetic parameters and conditions for PMPC inhibitor screening.....	111
Table 3.2 Conditions of time-dependent K_I determination.....	112
Table 3.3 Screening of PMPCs and related commercial compounds against MBLs.....	115
Table 3.4 Screening of PMPCs and related commercial compounds against SBLs.	116
Table 3.5 IC_{50} 's of PMPCs against MBLs	119
Table 3.6 K_I of DPA, PMPC-1, -3, and -4 against select MBLs.....	122

Table 3.7 On and off rates of metallo- β -lactamase inhibition by PMPCs.....	122
Table 3.8 Sensitization of MBL producing Gram negatives to meropenem by DPA and PMPCs. ...	124
Table 4.1 Structures of phenyl thioacids presented in this chapter	138
Table 4.2 Structures of cephalosporins presented in this chapter.....	139
Table 4.3 Relationships indicated by FIC	142
Table 4.4 pH of DMSO stocks of TA-1 when prepared with and without NaOH.	147
Table 4.5 Phenyl thioacid screening against L1 when prepared in the presence and absence of NaOH (presented as % inhibition).....	148
Table 4.6 Phenyl thioacid inhibitor screening against SBLs.....	149
Table 4.7 Phenyl thioacid inhibitor screening against MBLs.....	150
Table 4.8 Potentiation of meropenem against <i>S. maltophilia</i> strains by TA-1, TA-5, and TA-6 as determined using agar spot plate technique.....	152
Table 4.9 MICs of 3'-acylthiocephalosporins and control β -lactams against β -lactamase producing strains of <i>S. maltophilia</i>	154
Table 4.10 Potentiation of meropenem by 3'-acylthiocephalosporins (Ceph) against β -lactamase producing strains of <i>S. maltophilia</i>	155
Table 4.11 MICs of UW-123 in the presence and absence of 4 mg/L BLI-489 against select bacteria from the UW collection.....	156
Table 4.12 MICs of UW-123 against select strains from UW collection and its potentiation by avibactam.	157
Table 4.13 MICs of UW-123 in the presence and absence of an undisclosed avibactam-like inhibitor against a Merck panel of IMP producers.....	159
Table 4.14 MICs of UW-123 in the presence and absence of an undisclosed avibactam-like inhibitor against a Merck panel of NDM-1 producers.	161
Table 4.15 MICs of UW-123 in the presence and absence of an undisclosed avibactam-like inhibitor against a Merck panel of VIM producers.	162
Table 4.16 Synergy of UW-123 and meropenem against select strains from the UW collection.	163
Table 4.17 Sucrose stabilized, β -lactam treated <i>E. coli</i> under 1000x magnification by phase contrast microscopy.	166
Table 4.18 IC ₅₀ s of the competitive binding of UW-123 to PBPs from <i>P. aeruginosa</i> with Bocillin.	170

Table 4.19 IC ₅₀ s of the competitive binding of UW-123 to PBPs from <i>E. coli</i> with Bocillin.	173
Table 4.20 Pyridine thioacid inhibitor screening against SBLs.	174
Table 4.21 Pyridine thiocarboxylate inhibitor screening against MBLs.	175
Table 4.22 IC ₅₀ s of pyridine thiocarboxylates against class B and C β-lactamases.	177
Table 4.23 Sensitization of MBL producing Gram negatives to meropenem by pyridine thiocarboxylates.	178
Table 5.1 Kinetic parameters and conditions for inhibitor screening.	192
Table 5.2 IC ₅₀ of β-Lactamases with JJ05-1058 with variable pre-incubation times and detergent concentrations.	197
Table 5.3 IC ₅₀ s of JJ05-1058 competing with Bocillin for binding to <i>P. aeruginosa</i> PBPs.	200
Table 5.4 Comparison of literature values for JJ05-1058 IC ₅₀ s to those presented in this study.	201

List of Abbreviations

6-MPA	6-Methyl picolinic acid
aa	Amino acid
ACE	Angiotensin-converting enzyme
AMA	Aspergillomarasmine A
BLI	β -Lactamase inhibitor
BSA	Bovine Serum Albumin
CAZ	Ceftazidime
CDC	Centers for Disease Control
clav	Clavulanate
CNMR	¹³ C Nuclear Magnetic Resonance Spectroscopy
CTX	Cefotaxim
DBO	Diazabicyclooctanes
DHP-1	Renal dehydropeptidase I
DMF	Dimethylformamide
DMSO	Dimethylsulfoxide
DNA	Deoxyribonucleic acid
dNTP	Deoxynucleotide triphosphate
DPA	Dipicolinic acid, specifically 2,6-dipicolinic acid
DPMP	Diphosphonomethyl pyridine
EDTA	Ethylenediaminetetraacetic acid
ESBL	Extended spectrum β -lactamase
ESI-MS	Electrospray ionization mass spectrometry
ESKAPE	<i>Enterococcus faecium</i> , <i>Staphylococcus aureus</i> , <i>Klebsiella pneumoniae</i> , <i>Acinetobacter baumannii</i> , <i>Pseudomonas aeruginosa</i> , and the <i>Enterobacter</i> species
FDA	Food and Drug Administration
FIC	Fractional Inhibitory Concentration
HEPES	(4-(2-hydroxyethyl)-1-piperazineethanesulfonic acid)
HMM	High molecular mass (regarding PBPs)
HNMR	Proton Nuclear Magnetic Resonance Spectroscopy
HRV 3C	Human rhinovirus 3C protease

IC ₅₀	50% Inhibitory concentration
IgM	Immunoglobulin M
Imi	Imipenem
IPTG	Isopropyl β-D-1-thiogalactopyranoside
IR	Inhibition resistant
k _{cat}	Catalytic constant
kDa	Kilodalton
K _I	Inhibition constant
K _M	Michaelis constant
LB	Luria Bertani
LMM	Low molecular mass (regarding PBPs)
LMW	Low molecular weight (regarding SDS PAGE standards)
MBC	Minimum Bactericidal Concentration
MBL	Metallo-β-lactamase
MBP	Maltose binding protein
<i>m</i> -DAP	<i>meso</i> -Diaminopimelic acid
Mero	Meropenem
MES	2-(N-morpholino)ethanesulfonic acid
MH(A/B)	Mueller Hinton (Agar/Broth)
MIC	Minimum inhibitory concentration
MRSA	Methicilin resistant <i>Staphylococcus aureus</i>
NAG	N-acetylglucosamine
NAM	N-acetylmuramic acid
NaPi	Sodium phosphate (buffer)
NC	Nitrocefin
NCBI	National Center for Biotechnology Information
Ni NTA	Nickel coordinated Nitrilotriacetic acid
nPB	Non-penicillin binding (domain)
OD	Optical density
PA	Picolinic acid
PAR	4-(2-pyridylazo)resorcinol

PB	Penicillin binding (domain)
PBP	Penicillin binding protein
PCMB	<i>para</i> -chloromercuribenzoate
PCR	Polymerase chain reaction
PDCA	Pyridine dicarboxylic acid
PDTC	Pyridine dithiocarboxylate
penG	Penicillin G or Benzylpenicillin
PMPC	Phosphonomethyl pyridine carboxylate
PMS	Phenazine methosulfate
PMTC	Pyridine monothiocarboxylate
Q-TOF	Quadripole time of flight (with respect to mass spectrometry)
RNA	Ribonucleic acid
RT	Room temperature
SAR	Structure activity relationship
SBL	Serine- β -lactamase
SDS PAGE	Sodium dodecyl sulphate polyacrylamide gel electrophoresis
SIT	Spiro-indolino-thiadiazoles
spp	Species (plural)
sul	Sulbactam
tazo	Tazobactam
TB	Terrific broth
TPEN	<i>N,N,N',N'</i> -tetrakis(2-pyridylmethyl)ethylenediamine
TS	Transition State
UPLC	Ultra Performance Liquid Chromatography
UV	Ultraviolet
UWB	University of Waterloo bacterial collection
WHO	World Health Organization

Throughout this thesis, the three and one letter codes for amino acids are used in accordance with IUPAC convention.

Chapter 1

1.1 Antibiotic Classes and Targets

1.1.1 Overview of Antibiotics

Prior to the advent of antibiotics, approximately one third of deaths were the result of bacterial infection.¹ The discovery of penicillin by Sir Alexander Fleming in 1929 and its subsequent identification and use as a clinical therapeutic in 1940 and 1941 respectively by Chain and Florey, heralded the age of antibiotics.²⁻⁴ The sulfa drugs were discovered in the 1930's in Germany, and represent the first synthetic antibiotics.⁵ Over the next few decades the discovery and development of a wide variety of antibiotics burgeoned, reducing the relative number of deaths from bacterial infection substantially.^{1,6} Among the bacterial pathogens that remain problematic, are the nosocomial “ESKAPE” pathogens: *Enterococcus faecium*, *Staphylococcus aureus*, *Klebsiella pneumoniae*, *Acinetobacter baumannii*, *Pseudomonas aeruginosa*, and the *Enterobacter* species (spp.). These pathogens are considered important for the study of antibiotic susceptibility due to the incidence of infections from these as well as their pathogenesis, transmission, and resistance.⁷ These ESKAPE pathogens also represent 5 of the 9 pathogens designated by the World Health Organization (WHO) as critical or high priority targets for the development of new antibiotics.⁸ Other high priority pathogens on the WHO list are *Helicobacter pylori*, *Campylobacter* spp., *Salmonellae*, and *Neisseria gonorrhoeae*.

In addition to designating which target pathogens are most in need of new antibiotics, the WHO has designated which current antibiotics are most important. Critically important antibiotics have been defined as those that are the only therapy (or one of limited available therapies) for serious bacterial infections and can either treat bacterial infections that can be transmitted from non-human sources or acquire resistance from non-human sources.⁹ As of 2017, the critically important antibiotic classes are aminoglycosides, ansamycins, β -lactams (carbapenems, 3rd, 4th, and 5th generation cephalosporins, monobactams, and penicillins), glycopeptides, glycylicyclines, isoniazid, lipopeptides, macrolides, oxazolidinones, fosfomycin, polymixins, and quinolones.⁹ Representative drugs from each of these classes are shown in Figure 1.1

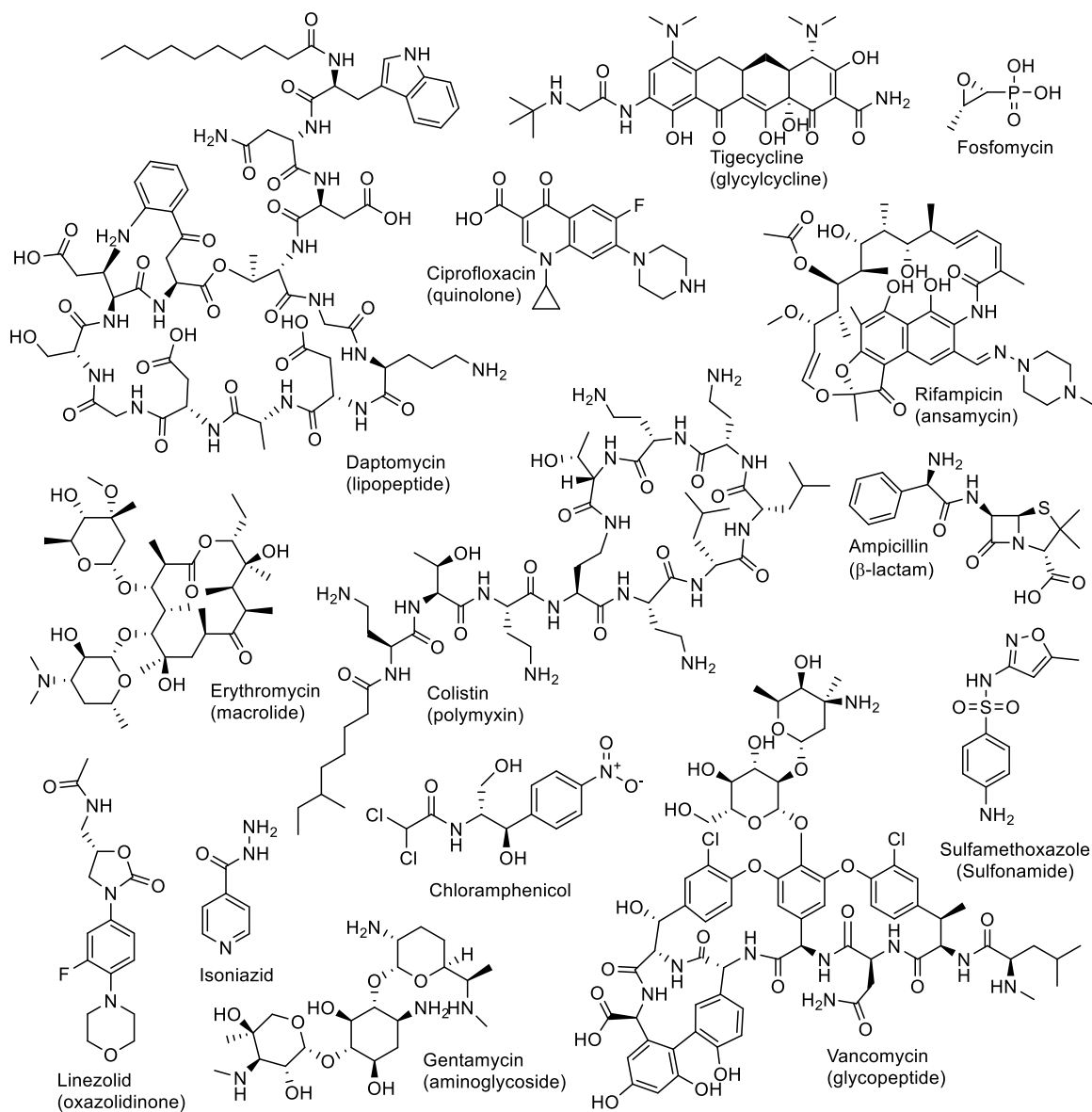


Figure 1.1 Critically important antimicrobials for human medicine.

The structural diversity of antibiotics seen in Figure 1.1 correlates with target diversity.¹⁰ The most common target systems are protein synthesis and cellular envelope stability with several molecular targets existing within each system. Protein synthesis can be inhibited through binding of antibiotics to either the 30S or 50S subunit of the ribosome.¹¹ Destabilization of the cellular envelope can occur through several mechanisms targeting either the cell wall or the bacterial membranes. The cell wall integrity can be compromised by either capping the polymerizing cell wall subunit or inhibiting the

enzymes responsible for subunit synthesis or polymerization.¹² The membrane integrity can be compromised by pore formation causing membrane depolarization or dissolution by detergent-like antibiotics.^{13,14}

Table 1.1 Mode of action of established antibiotics.¹⁵

Drug / class	Target System	Molecular Target
β -lactams	Cellular envelope	Penicillin binding proteins
Fosfomycin	Cellular envelope	MurA (NAM synthesis)
Vancomycin	Cellular envelope	Peptidoglycan
Daptomycin	Cellular envelope (Gram positive)	Cytoplasmic membrane
Colistin	Cellular envelope (Gram negative)	Outer membrane
Isoniazid	Cellular envelope (Mycobacteria)	InhA (Mycolic acid synthesis)
Quinolones	DNA replication	Gyrase and Topoisomerase IV
Ansamycins	Transcription	RNA polymerase
Aminoglycosides	Protein synthesis	30S ribosomal subunit
Tetracyclines	Protein synthesis	30S ribosomal subunit
Chloramphenicol	Protein synthesis	50S ribosomal subunit
Macrolides	Protein synthesis	50S ribosomal subunit
Oxazolidinones	Protein synthesis	50S ribosomal subunit
Sulfonamide	Folic acid synthesis	Dihydropteroate synthetase

Despite the wide array of established antibiotics, the β -lactams are the most prescribed class of antibiotic consisting of 50 % of antibiotic usage in Canada in 2017.^{16,17} There are 4 main structural classes of β -lactam antibiotics: penicillins, cephalosporins, carbapenems, and monobactams (Figure 1.2) which can be distinguished by the size and heteroatom composition of the ring fused to the β -lactam or by the lack of a fused ring.

β -Lactam antibiotics exert their antibacterial activity through inhibition of critical cell wall synthesis proteins known as penicillin binding proteins (PBPs). PBPs are enzymes that can be membrane anchored or associated with peptidoglycan, which catalyze the elongation and crosslinking of peptidoglycan to form the rigid component of the cell wall. Each bacterial strain has a different complement of PBPs and generally, each class of β -lactams preferentially inhibits one or more PBPs.¹⁸

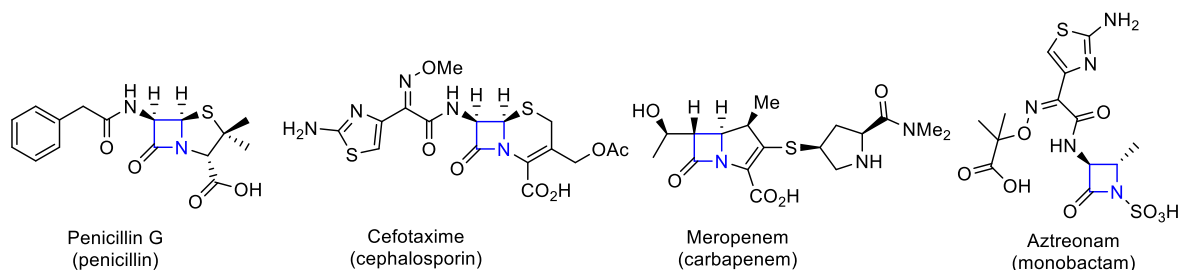


Figure 1.2 Representative antibiotics from each major class of β -lactams with the β -lactam functionality highlighted in blue.

Bacteria have developed resistance to antibiotics through three main mechanisms: target modification, antibiotic inactivation, and reduction of drug accumulation.^{19–21} Resistance to β -lactams occurs through all of the aforementioned mechanisms although primarily by antibiotic inactivation through the expression of enzymes, known as β -lactamases, that hydrolyze the β -lactam ring.²² There are two mechanistic classes of β -lactamases, serine- β -lactamases (SBLs) and metallo- β -lactamases (MBLs) both of which are present and problematic in bacterial pathogens.^{23–26} With the increasing prevalence of β -lactamases in pathogenic bacteria, inhibition of β -lactamases through combination therapy is vital for reinstating the efficacy of β -lactam antibiotics.^{27,28}

This introductory chapter provides a brief overview of β -lactam antibiotics and penicillin-binding proteins with emphasis on those present in *E. coli* and *P. aeruginosa*, followed by a more in depth look at β -lactamases and β -lactamase inhibitors.

1.1.2 β -Lactam Antibiotics

1.1.2.1 Discovery of Penicillin

As indicated above, Sir Alexander Fleming is widely credited with the discovery of penicillin which arose from a *Penicillium notatum* contaminant on one of his *Staphylococcus* culture plates. He observed that the bacteria in the vicinity of the mould had lysed and become transparent. Subsequent experiments with subcultures of the mould determined that the *Penicillium* mould was excreting an antibiotic into the medium which was responsible for the death of the staphylococci in the original plate.² Although Fleming was the first to understand the significance of these results, he was not the first to observe them: John Burdon Sanderson observed a similar phenomenon in liquid media in 1870 but incorrectly interpreted the results to mean that fungi were airborne but bacteria were not.²⁹

Inspired by Sanderson's observations, Joseph Lister, John Tyndall, and Thomas Henry Huxley also explored the antibacterial properties of *Penicillium* spp. through the 1870's.³⁰ Lister disproved Sanderson's hypothesis that bacteria could not be airborne and suggested that *Penicillium* spp. make liquid media less favourable for bacterial growth.³¹ Tyndall then suggested that they made liquid media unfavourable by covering the surface of the media, thereby depriving the bacteria of oxygen.³² Huxley disproved Tyndall's hypothesis, showing that oxygen deprivation was not the cause of the antibacterial effect but rather the mould in solution was making the media unfavourable for growth.³³ Throughout the late-1800's and early-1900's, several scientists noted the antibacterial properties of moulds and the abilities of extracts of moulds to be used as treatments for bacterial infections, but none of them had identified the causative agent for these effects.³⁴ It was Fleming's work in 1928 that finally established that the antibacterial effect of this mould was being caused by a compound excreted from *Penicillium notatum* which was not excreted from other moulds.²

In the summary of Fleming's 1929 paper, he suggests that penicillin could be an effective antibiotic with clinical applications, although he did not do any studies on infected patients (human or animal).² The clinical usefulness of penicillin was established by Chain and Florey in their 1940 paper where they showed the efficacy of penicillin in treating mice infected with *Streptococcus pyrogenes*, *Staphylococcus aureus*, or *Clostridium septicum* (modern name: *Clostridium septicum*^a).⁴ Human trials of penicillin began in January 1941 when a penicillin infusion was injected into a terminally ill breast cancer patient to determine toxicity in humans – she showed no adverse effects initially and within a few hours developed a high temperature and died. It was determined that the cause of the increased temperature was an impurity, not penicillin itself. The first patient treated with penicillin was a policeman with combined staphylococcal and streptococcal septicemia who was “desperately and pathetically ill”. He showed improvement within the first day and was almost healthy after five days. Unfortunately, they had exhausted Florey's supply of penicillin and could not treat the man any further – he died a month later from the infection. After shifting the trials towards children (less

^a The strain referred to in Chain et al. 1940⁴ is denoted “*Cl. septicum* Nat. coll. type-cultures No. 458”. The NCTC entry for No. 458 is *Bordetella bronchiseptica* which does not cause the gas gangrene described by Chain et al.⁵⁵³ It is probable that this is a typographical error in which the NCTC entry should be No. 547 (548 does not exist) which is *Clostridium septicum* (formerly *Vibrio septicum*), the strain used by Henderson and Gorer in the paper referenced by Chain et al. in the methods section.⁵⁵⁴ The change in nomenclature from *V. septicum* to *C. septicum* appears to have occurred in 1935 and references to *C. septicum* occur throughout the 1940's (referring to NCTC No. 547).⁵⁵⁵⁻⁵⁵⁸

penicillin was required for smaller patients), there was a string of successes in which the patient was saved or only died because the treatment was too late.³ Fleming, Chain, and Florey were awarded a Nobel Prize in Physiology or Medicine in 1945 for their contributions to the discovery and development of penicillin.

1.1.2.2 Modern β -Lactams

In the decades that followed Fleming's discovery of penicillin, a host of other antibiotics were discovered and developed.³⁵ The next leap forward in β -lactam antibiotics was discovery of cephalosprin C in 1948 from a strain of *Cephalosporium* (modern name: *Acermonium*) fungus by Guisepe Brotzu.³⁶ The natural cephalosporins had modest antibacterial activity but had a stable ring system that made them ideal for chemical modification which lead to the four generations of semi-synthetic cephalosporins which were much more potent than their natural counterparts.^{34,37} In 1976, a new family of β -lactams were discovered in extracts from *Streptomyces olivaceus*, the olivanic acid family carbapenems.³⁸ Another family of carbapenems, the thienamycin carbapenems, was discovered around the same time from *Streptomyces cattleya*; although, neither of these families of natural carbapenems were stable enough for clinical use.^{39,40} A semi-synthetic effort in the late-1970's by scientists at Merck yielded imipenem (Figure 1.3), a carbapenem that had a broader spectrum of activity than any of the cephalosporins, and was resistant to hydrolysis by many of the enzymes that hydrolyze penicillins and cephalosporins.⁴⁰⁻⁴² Imipenem, like thienamycin, is susceptible to inactivation by renal dehydropeptidase I (DHP-I) and has to be administered in combination with cilastatin, a DHP-I inhibitor, to prevent degradation and the formation of nephrotoxic metabolites.⁴⁰

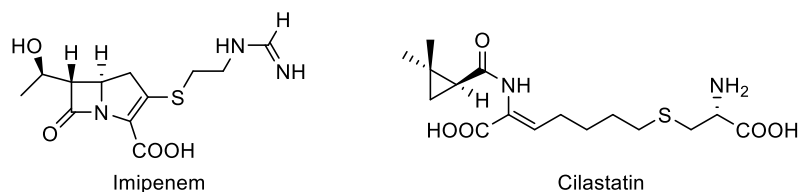


Figure 1.3 Chemical structures of imipenem and cilastatin.

To date, there are four major structural classes of β -lactam antibiotics: penicillins (penams), cephalosporins (cephems), carbapenems, and monobactams. Other β -lactam classes include penems,

cephams, penamycins, oxapenems, cephamycins, oxacephems, oxacephamycins, and carbacephems (Figure 1.4).^{34,43}

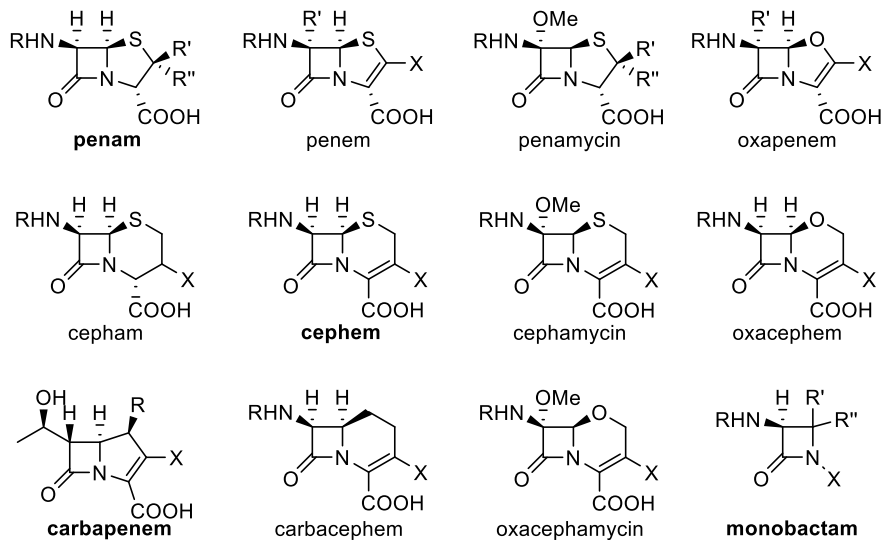


Figure 1.4 Core structures of β -lactam antibiotic families.

While antibiotics from all four major classes of β -lactams are still used clinically, many pathogens have developed resistance to some or all of them.

1.1.3 Bacterial Resistance

In human medicine, antimicrobials are one of the most prescribed drugs, although the Centers for Disease Control (CDC) has estimated that as many as 50 % of these prescriptions are unnecessary.⁴⁴ As a result of this systemic misuse through over-prescribing, not abiding by treatment regimens, and addition to feed stocks for food animals; bacteria have developed resistance to all of the antibiotic classes mentioned in Table 1.1.³⁵ The first report of the incidence of bacterial resistance to antibiotics was in 1940 when enzyme (β -lactamase)-mediated resistance to penicillin was observed in *E. coli*.⁴⁵ It has been suggested that the existence of β -lactamases pre-dates the antibiotic era by millions of years since penicillin is a naturally occurring antibiotic used in signaling and potentially germ warfare among microbes.^{46,47} In response to spreading resistance, the use of some antibiotics, such as third-generation cephalosporins and carbapenems, has been restricted to hospitals.⁴⁸

Bacteria can acquire resistance through random chromosomal mutation or horizontal gene transfer. These adaptations lead to resistance through one of three general mechanisms: target modification,

1.2 Penicillin Binding Proteins

1.2.1 Bacterial Cell Wall Structure

The cellular envelopes of bacteria are responsible for creating a stable barrier between the cell and its environment that is rigid enough to maintain cell shape and resist lysis in dilute solutions while being permeable enough to transport nutrients in and waste out. There are three types of cellular envelope: Gram-positive, Gram-negative, and atypical which are broadly classified by Gram staining. The cellular envelope of Gram-positive bacteria consists of an inner cell membrane coated in a thick layer of peptidoglycan – the rigid component of bacterial cell walls. Gram-negative bacteria have a similar inner membrane coated in a much thinner layer of peptidoglycan which is covered by another membrane layer referred to as the outer membrane. Both Gram positive and Gram negative cellular envelopes have a space between the inner membrane and peptidoglycan known as the periplasm that contains numerous proteins in a reducing environment.⁵⁷ Atypical bacteria lack peptidoglycan either as part of their native state (eg. *Mycoplasma spp.*) or due to degradation of their peptidoglycan (L-forms).⁵⁸ Atypical bacteria will not be discussed further as they do not respond to β -lactam antibiotics due to their lack of peptidoglycan; however, more information on this topic can be found in reviews.^{59–61}

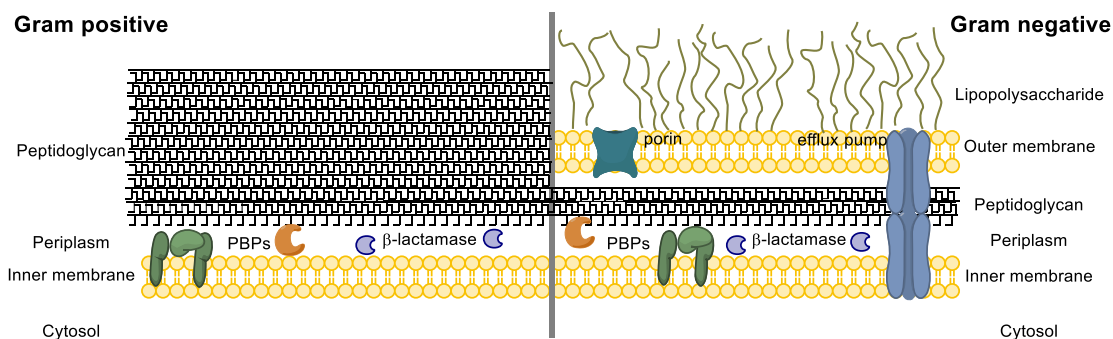


Figure 1.5 Gram positive and Gram negative cellular envelope composition.^{62,63} Membrane graphics were generated using ChemDraw Pro v. 17.0.

The bacterial cell wall is constructed using several enzymes, key among them, the penicillin binding proteins (PBPs). These proteins are responsible for the synthesis and recycling of peptidoglycan as well as some regulation of its size and the extent of crosslinking. As should be expected, these proteins are primarily located on the periplasmic face of the inner (cytosolic)

membrane in complexes with other PBPs and proteins involved in cell shape maintenance and septation.⁶⁴ Some of the smaller PBPs such as *E. coli* PBP 4 are associated with peptidoglycan instead of being membrane bound.⁶⁵ The localization and function of PBPs as well as other proteins involved in cell shape and septation in rod shaped bacteria has been reviewed by den Blaauwen.⁶⁴

1.2.2 PBP Functional and Structural Classification

Historically, penicillin-binding proteins were defined as membrane associated proteins that would bind penicillin G. Much of the early work in this field was performed using gel based assays with ¹⁴C isotopically labelled penicillin G, and as such, the nomenclature for PBPs has been broadly defined by molecular weight where the heaviest PBP was denoted PBP 1 and lighter ones followed in sequence.⁶⁶ An appreciable difference in the necessity and functionality of PBPs was observed and they were split into two groups: high molecular mass (HMM) and low molecular mass (LMM). The naming of PBPs by molecular mass has proven inconvenient as different organisms express different quantities of PBPs and functionality is not strictly correlated with mass; thus PBP 2 from one organism may have a different function than PBP 2 from another organism.

1.2.2.1 Reactions Catalyzed by PBPs

Peptidoglycan (or murein) is a highly crosslinked polymer made from the precursor, lipid II, which is synthesized in the cytoplasm before being flipped into the periplasm using a flippase. Lipid II is composed of three major groups: the membrane anchor, the glycan backbone, and the pentapeptide, as shown in Figure 1.6. The membrane anchor is embedded in the inner membrane, keeping this substrate in close proximity to the HMM PBPs which are responsible for its polymerization as they are also membrane bound. The polymerization of lipid II into peptidoglycan is achieved by sequential additions of the N-acetylmuramic acid-N-acetylglucosamine (NAM-NAG) disaccharide portion of the molecule to form a glycan backbone. Finally, the pentapeptide is the portion of peptidoglycan that is crosslinked to increase the structural integrity of the cell wall. In the majority of Gram negative bacteria, the sequence of the pentapeptide is L-Ala- γ -D-Glu-*m*-DAP-D-Ala-D-Ala (*m*-DAP: meso-diaminopimelic acid).⁶⁷

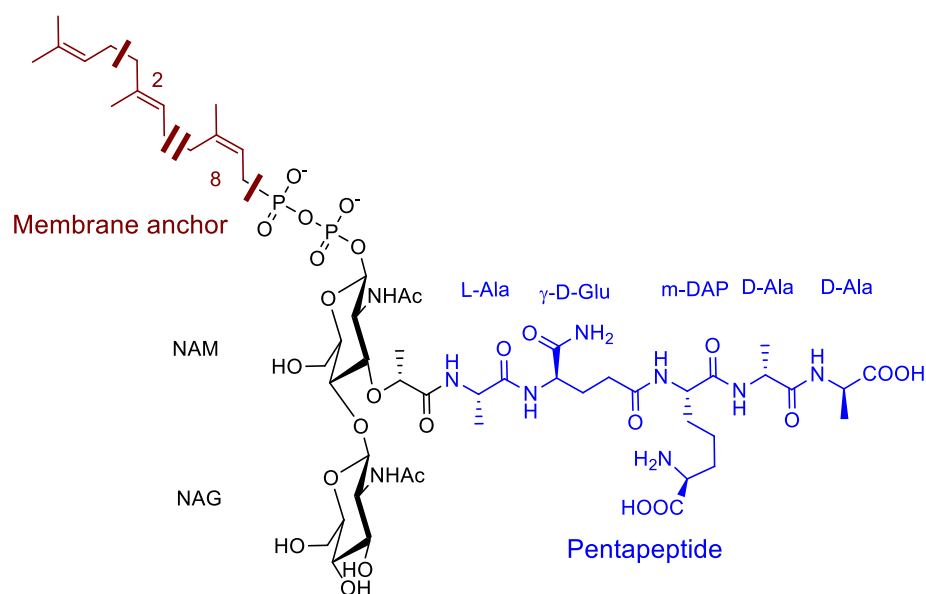
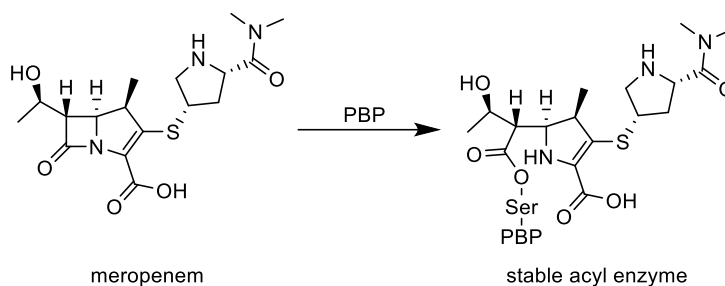


Figure 1.6 Structure of Lipid II, the peptidoglycan precursor with the membrane anchor highlighted in red, the glycan backbone in black, and the pentapeptide in blue.

There are four reactions that are catalyzed by the various PBPs in the periplasm: glycosyltransfer, transpeptidation, DD-carboxypeptidation, and DD-endopeptidation. The glycosyltransferase capabilities of certain HMM PBPs polymerize the carbohydrate moieties of the lipid II substrate to make a linear layer of the cell wall. The different layers are crosslinked at the pentapeptide between the fourth member of the donor peptide, D-Ala, and the amine on the sidechain of the *m*-DAP of the acceptor peptide using the transpeptidase functionality of HMM PBPs which offers structural stability to the cell wall.⁶⁸ The degree of crosslinking is controlled by LMM PBPs that act as DD-carboxypeptidases which remove the terminal D-alanine, preventing crosslinking.^{69,70} A few of the LMM PBPs also have DD-endopeptidase activity which hydrolyzes the peptide crosslink as part of septation and murein turnover.^{71,72} The penicillin binding domain of each PBPs use a catalytic serine residue and a water molecule in their active site to first form an acyl-enzyme with the substrate which is then subsequently attacked by an acceptor (transpeptidase) or hydrolyzed (DD-carboxypeptidase and DD-endopeptidase).⁶⁸ The reactions carried out by PBPs are summarized in Scheme 1.2. For a more comprehensive depiction of the reactions involved in bacterial cell wall biosynthesis and recycling, see Fisher and Mobashery's 2014 review.⁷⁰

The critical role of PBPs in the synthesis of bacterial cell walls makes them an ideal target for antibiotics, namely β -lactams. The inhibition of a PBP by a β -lactam occurs when the active site serine of the PBP binds and attacks the amide of the β -lactam, forming an acyl enzyme as shown in Scheme 1.3. Unlike with its natural substrate, the acyl enzyme formed between a PBP and a β -lactam is very slow to hydrolyze with a half-life of around 10 hr, leading to covalent inactivation of the PBP.⁷³



Scheme 1.3 Inactivation of PBPs by a β -lactam.

1.2.2.2 Classification of PBPs

A classification system for the PBPs was developed by Goffin and Ghuyssen based on the nomenclature of *E. coli* PBPs which focused on the functionality and amino acid sequence of HMM PBPs.⁶⁸ This system has been further refined by Sauvage et al. to include classification of LMM PBPs and PBPs from Actinomycetes and Cyanobacteria using structure and function as classification determinants.¹⁸ For simplicity, this section will only cover PBPs in Gram positive and Gram negative bacterial pathogens with most attention being paid to *E. coli*, *P. aeruginosa*, *B. subtilis*, *S. aureus*, and *S. pneumoniae*. Several excellent reviews are recommended for more detailed information on the structural and functional classification of PBPs.^{18,68,73,76}

The high molecular mass PBPs are multimodular, membrane bound proteins that can be classified as one of two classes: Class A consists of any PBP with a transglycosylase functionality at the N-terminal and Class B consists of PBPs with a C-terminal transpeptidase module and an N-terminal module that is involved in the cell cycle. The nomenclature of these two classes are based upon the numbering of *E. coli* PBPs for Gram negative organisms, while *B. subtilis*, *E. faecium*, and *S. pneumoniae* were used in combination to describe the PBPs for Gram positive organisms.⁶⁸ *B. subtilis*

will be used where possible as the example for describing PBPs classification in Gram positive organisms as it contains the widest variety for a Gram positive organism.

Class A PBPs are further divided into 7 subclasses based on sequence analysis of the penicillin binding (PB) cores and are denoted A1-A7. Subclasses A1 and A2 contain the major bifunctional transpeptidases/transglycosylases in Gram negative organisms of which *E. coli* PBP 1a and 1b are the prototypes respectively.⁷⁷⁻⁸⁰ The bifunctional transpeptidases/transglycosylases in Gram positive organisms comprise subclasses A3, A4, and A5 as exemplified by *B. subtilis* PBPs 1, 2c, and 4 respectively. Subclass A6 contains the “outliers” such as *E. coli* PBP 1c which contains both modules characteristic of Class A PBPs; however, the PB domain is very substrate specific and does not seem to act as a transpeptidase.^{81,82} Finally, subclass A7, which was added by Sauvage, contains monofunctional glycosyltransferases such as MgtA from *E. coli*.^{83,84} It is worth noting that subclass A7 enzymes do not appear in traditional gel based assays as they lack a PB core and that subclass A6 enzymes may not appear under certain conditions due to their evolutionarily divergent PB core.

The class B PBPs are multimodular like the class A PBPs with a C-terminal penicillin-binding transpeptidase module; however, the non-penicillin binding (nPB) module in class B PBPs is implicated in cellular morphology and division rather than transglycosylation.^{18,64} Five subclasses of class B PBPs are present in Gram positive and Gram negative organisms: B1-B5, defined by Goffin and Ghuysen using sequence alignment.⁶⁸ The subclass B1 PBPs are most commonly found in Gram positive organisms and are characterized by their low affinity for β -lactams, most famously, PBP 2a from methicillin resistant *S. aureus*. B1 PBPs have been thoroughly reviewed by Zapun et al..⁸⁵ Subclass B2 PBPs are predominantly found in Gram negatives, such as *E. coli* PBP 2, and are associated with rod shaped bacteria as the nPB module is specific to the elongase complex.⁶⁴ Consequently, selective inhibition of subclass B2 PBPs causes the formation of spherical cells.^{66,86} The B3 subclass PBPs, such as *E. coli* PBP 3 are part of the divisome, and their selective inhibition causes filamentation.^{64,86} The Gram positive counterpart to B3 PBPs are B4 PBPs, such as *B. subtilis* PBP 2b, in that they contribute to cell division.^{87,88} The B5 PBPs are Gram positive PBPs such as *B. subtilis* PBP 2a, most of which have no known function for the nPB module.^{68,89,90} *B. subtilis* PBP 2a is known to be involved in maintaining rod shape along with PBP H, another B5 PBP.⁹¹ This function in elongation cannot be a sole characteristic of B5 PBPs as many cocci express these.¹⁸

The final class of PBPs are the Class C PBP, commonly referred to as the low molecular mass (LMM) or non-essential PBPs. Class C PBPs are monofunctional PBPs that play a role in peptidoglycan regulation and recycling through carboxypeptidase and/or endopeptidase mechanisms.^{18,76} As with Class A and Class B PBPs, the nomenclature of Class C PBPs is based on the separation pattern of *E. coli* PBPs; however, there is no differentiation between Gram positive and Gram negative organisms in this class. The Class C PBPs are divided into three types: type 4, type 5, and type 7.¹⁸ Type 4 PBPs, whose archetype is PBP 4 in *E. coli*, function as both a DD-carboxypeptidase and a DD-endopeptidase and have been implicated in maintaining normal cell morphology and in recycling the cell wall.^{65,76,92,93} These PBPs do not contain a transmembrane helix and are thought to be loosely associated with the cytoplasmic membrane (Gram positive), the inner leaflet of the outer membrane (Gram negative) or directly with peptidoglycan since they overproduce in the soluble form for *E. coli* and can be washed off *B. subtilis* with 1 M KCl.^{18,65,94-96} In *Neisseria gonorrhoeae*, the type 4 PBP, PBP 3, has been found to be associated with both the outer membrane and peptidoglycan.^{97,98} Type 5 PBPs are often the most abundant PBPs in cells and are the strict DD-carboxypeptidases.⁹⁹⁻¹⁰¹ Functionally, type 5 PBPs have been implicated in normal septum formation and in the maintenance of normal cell diameter.^{92,102,103} In *E. coli*, this type is represented by PBP 5 and PBP 6 of which PBP 5 performs the normal regulatory functions of this type, and PBP 6 is involved in the onset of stationary phase.^{69,104,105} The final type of Class C PBPs is type 7 which are structurally similar to the penicillin binding domain of type 5 PBPs and as such exhibit the same carboxypeptidase/endopeptidase activity but are largely absent in Gram positive organisms.¹⁸ Much like type 4 PBPs, these are loosely membrane associated and, as of yet, their function in cell cycle or morphological regulation is unknown.^{101,106} In *E. coli*, this class is represented by PBP 7 and its proteolytic product, PBP 8.¹⁰⁷

1.2.3 PBP Expression in Bacterial Strains

In this study, assays of both *E. coli* and *P. aeruginosa* penicillin binding proteins were employed, so it is important to discuss which PBPs are present in these organisms, how they compare, and to examine any controversy in the literature. Much of the comparison of *E. coli* and *P. aeruginosa* PBPs was performed by Noguchi et al. in 1979; however, this study was limited to the PBPs that react with radiolabeled benzylpenicillin and remain on an SDS PAGE gel.¹⁰⁸ Using binding kinetics, thermal sensitivity, correlations in β -lactam specificity, and morphological impacts as criteria, they determined that *E. coli* PBPs 1a, 1b, 2, 3, 4, and 5 correspond with *P. aeruginosa* PBPs 1b, 1a, 2, 3, 4,

and 5 respectively. It was also noted that expression of PBPs may vary between *P. aeruginosa* strains with PBP 2 being nearly invisible on the gels of certain strains, and PBP 3x appearing on others.¹⁰⁸

Recently, *P. aeruginosa* PBPs have been studied individually, bringing the understanding of the function, and in some cases structure, of these proteins to the level of *E. coli* PBPs. Comparative genetic sequence alignment of *P. aeruginosa* PBP 1a with PBP 1a and 1b from *E. coli* determined that *P. aeruginosa* PBP 1a most closely correlates with *E. coli* PBP 1a, not 1b as was previously suggested.^{108,109} Several studies have confirmed that PBP 2, 3, 4, and 5 from *P. aeruginosa* have the same function and similar structures as their *E. coli* counterparts.^{99,110–113} Gene names can be used as a clearer way to compare PBPs across species as they more closely correlate structure and function than electrophoretic mobility, although some inconsistencies in naming still occur. Table 1.2 is a compilation of the PBPs present in *E. coli* and *P. aeruginosa* with their respective gene names. It is worth noting that there is no relationship between the proteins encoded by *pbpC* in *E. coli* and *P. aeruginosa*, it is seemingly just an unfortunate naming coincidence.^{81,114}

Table 1.2 Penicillin binding proteins present in *E. coli* and *P. aeruginosa*^{76,111}

<i>E. coli</i> Protein	Genes	<i>P. aeruginosa</i> Protein
PBP 1a	<i>ponA</i>	PBP 1a
PBP 1b	<i>mrcB</i>	PBP 1b
PBP 1c	<i>pbpC</i> †	
PBP 2	<i>pbpA</i>	PBP 2
PBP 3	<i>ftsI</i>	PBP 3
	<i>pbpC</i> †	PBP 3x
PBP 4	<i>dacB</i>	PBP 4
PBP 5	<i>dacA</i>	
PBP 6	<i>dacC</i>	PBP 5/6
PBP 6b	<i>dacD</i>	
PBP 7/8	<i>pbpG</i>	PBP 7

†The genes denoted as *pbpC* are not homologs

Aside from the naming coincidence with the *pbpC* genes in *E. coli* and *P. aeruginosa*, there is controversy in the literature with respect to the names of the high molecular weight PBPs in *P. aeruginosa*. The first report of *P. aeruginosa* PBPs labelled them as 1a, 1b, 2, 3, 3', 4, 4', 5, and 7/8, some of which are only conditionally present, notably 3' which also goes by the names 3x and 3a.^{68,76,108,114,115} While there is some differences between the original labelling of the Class B and C PBPs and the current labelling, the nomenclature of these PBPs has become consistent across the literature. The point of contention seems to be whether the two Class A PBPs are 1a and 1b or 1b and 1c. The origin of the 1b/c nomenclature seems to be a publication by Moyá et al. in 2010, in which four classic papers about *P. aeruginosa* PBPs are referenced in the introduction with respect to the PBPs present in *P. aeruginosa*; none of these papers mention PBP 1c and all use the 1a/b nomenclature.^{18,108,116–118} Since the paper by Moyá, several other papers have used the 1b/c nomenclature, mostly in reference to the proteins inhibited by ceftolozane (which is the subject of Moyá et al. 2010)^{119–121} Additionally, PBPs 1b and 1c are named in the mode of action description of ceftolozane on Drugbank; although, PBP 1c is not listed in the targets section.¹²² Papers describing new experiments on *P. aeruginosa* PBPs since the release of Moyá et al. 2010 tend to use the 1a/b nomenclature, including another paper by Moyá, which may suggest that the 2010 paper had a typographical error that has been carried through later literature on the subject.^{113,116,123,124} Putting this to rest, Dhar et al. released a review in 2018 that included a survey of the *P. aeruginosa* genome database, and found no genes corresponding to PBP 1c.⁷⁶ For this work, the major PBPs in *P. aeruginosa* will be labelled as PBPs 1a, 1b, 2, 3, 4, 5/6 according to the most common nomenclature, excluding those that are not visible.

1.2.4 Role of PBPs in Bacterial Resistance to β -Lactams

Penicillin-binding proteins contribute to bacterial resistance to β -lactams through either being inherently resistant to inhibition by β -lactams or through inducing the production of β -lactamases upon inhibition. The most well-known of the β -lactam resistant PBPs is PBP 2a from *Staphylococcus aureus*, a Class B PBP that confers methicillin resistance.^{125,126} PBP 2a is encoded by the *mecA* gene which is found in a mobile genetic element that integrates into the chromosome of *Staphylococci* and whose origin appears to be *Staphylococcus fleurettii*.^{127,128} β -Lactam resistance by PBP 2a acquisition is primarily due to its poor affinity for β -lactams allowing it to compensate for other inhibited transpeptidases.^{129–133} Additionally, PBP 2a accounts for 43% of expressed PBPs in methicillin resistant *S. aureus* cells while the number of other PBPs expressed per cell remains

constant.¹³⁴ Similar β -lactam resistant PBPs exist in other bacteria and are covered in several excellent reviews.^{73,85,135}

In bacteria that do not produce inherently resistant PBPs, the inhibition or mutation of certain native PBPs has been shown to up-regulate the production of Class C chromosomal β -lactamases such as AmpC. Chromosomal *ampC* genes has been found in many Gram negative pathogens including *E. coli*, *P. aeruginosa*, *K. pneumoniae*, *E. cloacae*, and *Serratia marcescens* and can be constitutively expressed (as in *E. coli*) or induced by β -lactams.^{136–139} β -Lactam induced production of the β -lactamase AmpC occurs primarily through one of two pathways: AmpR regulation or two component CreBC(D) regulation both of which are thoroughly reviewed by Zeng and Lin.¹⁴⁰ The AmpR regulation pathway involves the inhibition of a LMM PBP (usually PBP 4 or 5) which shifts the equilibrium of peptidoglycan recycling, releasing NAG-anhydro-NAM-pentapeptides which are transported into the cytoplasm through the AmpG transporter.^{113,141–144} Once in the cytoplasm, the NAG is removed from the NAG-anhydro-NAM-pentapeptides by NagZ and the peptide portion is shortened by AmpD, creating a molecule that interacts with the AmpR regulator, derepressing AmpC production.^{139,143–146} The CreBC(D) system has been shown to regulate the expression of OXA-12 and other chromosomal β -lactamases in *Aeromonas jandaei* and to interact with AmpR regulation in PBP 4 mutants of *P. aeruginosa* to confer higher β -lactam resistance than the AmpR pathway alone.^{144,147,148} The CreBC(D) two component regulation system responds to PBP 4 inhibition or mutation in *P. aeruginosa* through an unknown signal causing the CreC inner membrane histidine kinase to phosphorylate CreB, the response regulator, which induces CreD overexpression in *P. aeruginosa* or induces β -lactamase production in *A. jandaei*.^{144,147–149} It is not well understood how CreD overexpression influences β -lactam resistance, but it is known to contribute to cell envelope stability and biofilm formation.^{148,150}

Despite the importance of PBPs in conferring and inducing β -lactam resistance, these tend to be narrow spectrum resistance mechanisms, making the expression of extended spectrum β -lactamases a more important resistance mechanism.

1.3 β -Lactamases

β -Lactamases are periplasmic enzymes that efficiently hydrolyze β -lactam antibiotics, conferring resistance to the bacterium. There are two general mechanisms by which these enzymes hydrolyze β -

lactams: using a catalytic active site serine or zinc ions. The serine β -lactamases (SBLs) react with β -lactams in a mechanism similar to that of PBPs, except they are capable of rapidly hydrolyzing the acyl enzyme. A common misconception is that β -lactamases evolved from PBPs as a response to the use of β -lactams as antibiotics in humans. It is thought that β -lactamases and PBPs evolved from a common DD-peptidase ancestor hundreds of millions of years ago and clinical use of β -lactam antibiotics has just selected for resistance, making it more prevalent.^{151,152} Additionally, the use of β -lactams in a clinical setting had been shown to accelerate the evolution of β -lactamases with about 170 β -lactamases having been identified by 1997 and around 2000 having been identified today.^{53-55,152}

1.3.1 Role of β -Lactamases in Bacterial Resistance to β -Lactams

The first observation of a β -lactamase capable of conferring resistance to a bacterium was reported in 1940 by Abraham and Chain, although they state in their letter that Fleming had also observed the resistance due to these enzymes in his 1929 paper detailing the discovery of penicillin.^{2,45} Early β -lactamases were referred to as penicillinases or cephalosporinases depending upon their ability to hydrolyze penicillins or cephalosporins respectively. When semisynthetic penicillins were introduced in the 1970's as less β -lactamase susceptible alternatives to natural product penicillins, they were lauded for their efficacy against highly resistant pathogens such as *Pseudomonas* spp., although resistance was observed in clinical trials.^{34,153} Likewise, the third-generation of semi-synthetic cephalosporins, such as ceftazidime in 1979, were thought to be highly resistant to hydrolysis by β -lactamases but some Gram-negative pathogens developed resistance in clinical trials.^{154,155} Many of first identified β -lactamases had relatively narrow-spectrum activity against either penicillins or cephalosporins and the few that were capable of hydrolyzing the more stable β -lactams were chromosomally encoded.^{156,157}

In the early 1980's, enzymes were discovered on transferrable plasmids in *Klebsiella* spp. isolates that were capable of hydrolyzing many of the available β -lactams which represented the first of the extended spectrum β -lactamases.¹⁵⁶ In the 1980's, extended-spectrum β -lactamases (ESBLs) were considered those capable of efficiently hydrolyzing common semi-synthetic penicillins and first-generation cephalosporins but exhibiting poor activity against third-generation cephalosporins and monobactams.¹⁵⁶ The definition of the term ESBL has evolved with the advent of new β -lactams and

the identification of β -lactamases with even broader spectrum activity such that it now includes only enzymes that are, at least, capable of conferring resistance to penicillins, first-, second- and third-generation cephalosporins, and monobactams.¹⁵⁸ The β -lactam therapy of choice for ESBL-producers has been carbapenems for the last few decades, although ESBLs that also hydrolyze carbapenems (carbapenemases, e.g. KPC-2) and metallo- β -lactamases have rendered this option less effective.¹⁵⁹

Recently, mobile genetic elements coding for multiple β -lactamases as well as resistance enzymes for other classes of antibiotic have been discovered in Gram negative pathogens.^{160,161} One such *K. pneumoniae* isolate harbouring 4 resistance plasmids was found to be carrying genes for 6 β -lactamases, conveying resistance to all β -lactams, as well as genes coding for resistance to gentamicin (and related compounds), streptomycin, sulfonamides, aminoglycosides, trimethoprim, quinolones/fluoroquinolones, macrolides, and fosfomycin in addition to 9 efflux pumps with a wide range of specificity.¹⁶² Multidrug resistant bacteria are becoming more and more prevalent and have moved from being associated only with nosocomial infections to community-acquired infections as well.¹⁶³ The Infectious Disease Society of America has declared that antimicrobial resistance is “one of the greatest threats to human health worldwide”, and with over 50% of prescribed antibiotics being β -lactams, combatting β -lactam resistance is of the utmost importance.^{16,17,164}

1.3.2 Classification of β -Lactamases

The earliest nomenclature for the enzymes that were capable of hydrolyzing penicillins was “penicillinase” in accordance with the naming conventions of the time.⁴⁵ The discovery of cephalosporins in the mid-1950’s and the enzymes capable of hydrolyzing them brought about a new term – cephalosporinase.^{165,166} These functional names failed to accurately categorize the enzymes that they were describing as they only indicated whether or not that enzyme could hydrolyze that type of substrate, omitting enzymes that hydrolyze both cephalosporins and penicillins. Additionally, there was no distinction between broad spectrum enzymes that could hydrolyze every member of a class of β -lactams and a narrow spectrum one that could only hydrolyze a few members of a class (e.g. Only first-generation cephalosporins, but not second-generation).

After some early efforts to establish a classification system,¹⁶⁷⁻¹⁶⁹ Richmond and Sykes came up with the first widely accepted classification scheme in 1973.¹⁵⁷ This scheme split the known β -lactamases into five classes denoted by the Roman numerals I-V according to their substrate

specificity as well as their sensitivity to inhibition by both cloxacillin and *p*-chloromercuribenzoate as illustrated in Table 1.3.¹⁵⁷ Unlike the previous nomenclature, this scheme allows for classification of β -lactamases that can hydrolyze both cephalosporins and penicillins and uses additional information such as the susceptibility to inhibitors to further subdivide. The classes proposed by Richmond and Sykes were subdivided into lettered subgroups according to their relative activities with six substrates.¹⁵⁷

Table 1.3 Richmond and Sykes functional classification scheme for β -lactamases.¹⁵⁷

Class	Preferred Substrate	Sensitivity to Inhibition	
		Cloxacillin	<i>p</i> -chloromercuribenzoate
I	cephalosporin	S	R
II	penicillin	S	R
III	cephalosporin/penicillin	S	R
IV	cephalosporin/penicillin	R	S
V	cephalosporin/penicillin	R	R

S = sensitive to inhibition, R = resistant to inhibition

While the Richmond and Sykes classification system was adequate for the time, it introduced confusion since Roman numerals were also used in the names of β -lactamases to distinguish between two β -lactamases produced by the same organism (e.g. BcI and BcII from *Bacillus cereus*). Ambler proposed a simplification of the classification of β -lactamases in 1980 based on their structure and changed designations from Roman numerals to letters. The β -lactamases analysed by Ambler fell into two groups: Class A and Class B which used an active site serine residue and divalent zinc ions respectively to perform the hydrolysis.¹⁷⁰ The serine- β -lactamases (SBLs) studied by Amber: PC1, BcI, TEM-1, and *B. licheniformis* 749/C, had a high sequence homology and thus did not require further division although Ambler addressed the likelihood of other classes existing.¹⁷⁰ Another molecular class, Class C, was proposed by Jaurin and Grundström in 1981 to encompass chromosomally encoded SBLs from *Enterobacteriaceae* such as AmpC which had low sequence homology with the class A β -lactamases.¹⁷¹ The final molecular class, Class D, was proposed in 1987 by Ouelette et al. on the basis of the lack of sequence homology between the OXA-type SBLs and the Class A and C SBLs.¹⁷²

Table 1.4 Functional and molecular classification of β -lactamases. ^{173,174}

Bush-Jacoby	Ambler	Distinctive substrate(s)	Inhibited by		Characteristics	Representative enzymes
			Clav/Tazo	EDTA		
1	C	Cephalosporins	-	-	Greater hydrolysis of cephalosporins than PenG; hydrolyze cephamycins	<i>E. coli</i> AmpC, P99, ACT-1, CMY-2, MIR-1, DHA-1
1e	C	Cephalosporins	-	-	Increased hydrolysis of ceftazidime and often other oxyimino- β -lactams	GC-1, CMY-10
2a	A	Penicillins	+	-	Greater hydrolysis of PenG than cephalosporins	PC1, BcI
2b	A	Penicillins, early cephalosporins	+	-	Similar hydrolysis of PenG and cephalosporins	TEM-1, SHV-1
2be	A	Extended-spectrum cephalosporins	+	-	Increased hydrolysis of oxyimino- β -lactams (cefotaxime, ceftazidime, cefepime)	CTX-M-15, SHV-2A, SHV-12, TEM-3
2br	A	Penicillins	-	-	Resistance to clav/sul/tazo	TEM-30, SHV-10
2ber	A	Extended-spectrum cephalosporins, monobactams	-	-	Increased hydrolysis of oxyimino- β -lactams combined with resistance to clav/sul/tazo	TEM-50
2c	A	Carbenicillin	+	-	Increased hydrolysis of carbenicillin	PSE-1, CARB-3
2ce	A	Carbenicillin, cefepime	+	-	Increased hydrolysis of carbenicillin, cefepime, and cefpirome	RTG-4
2d	D	Cloxacillin	\pm	-	Increased hydrolysis of cloxacillin and oxacillin	OXA-1, OXA-10
2de	D	Extended-spectrum cephalosporins	\pm	-	Hydrolyzes cloxacillin or oxacillin and oxyimino- β -lactams	OXA-11, OXA-45
2df	D	Carbapenems	\pm	-	Hydrolyzes cloxacillin or oxacillin and carbapenems	OXA-23, OXA-48
2e	A	Extended-spectrum cephalosporins	+	-	Hydrolyzes cephalosporins. Inhibited by clav but not aztreonam	CepA, L2
2f	A	Carbapenems	\pm	-	Increased hydrolysis of carbapenems, oxyimino- β -lactams, cephamycins	KPC-2, KPC-3, SME-1, IMI-1
3a	B1	Carbapenems	-	+	Broad-spectrum hydrolysis including carbapenems but not monobactams	BcII, IMP, NDM, VIM, SPM-1
	B2	Carbapenems	-	+	Broad-spectrum hydrolysis including carbapenems but not monobactams	L1, GOB-1, FEZ-1
3b	B3	Carbapenems	-	+	Preferential hydrolysis of carbapenems	CphA, Sfh-1
4	?	Penicillins	-	-		SAR-2

Adapted from ^{173,174} with representative enzymes focused towards ones used in this work. ¹⁷⁵⁻¹⁷⁷ clav = clavulanic acid, tazo = tazobactam, sul = sulbactam, PenG = penicillin G = benzylpenicillin.

Some small updates have been made to the Ambler molecular class classification system since the 1980's including subdividing the Class B's into three subclasses (B1, B2, and B3) based on the amino acids used to bind the zincs as well as rearranging the phylogenetic tree of the Class B's to emphasize the relationship between B1 and B2.^{178,179}

The Ambler molecular classification scheme, along with its many updates, is the most widely used classification system to this day because of its simplicity and the limited amount of information (primary sequence) needed for classification of new β -lactamases. Throughout the late-1980's and early-1990's, Bush and Jacoby championed another functional classification system, culminating in their 2010 update that divides the β -lactamases into 4 groups (one of which is for "others") and 17 subgroups based upon their preferred substrate(s) and their inhibition by clavulanic acid/tazobactam and EDTA.^{173,174,180-182} While this scheme excels at categorizing β -lactamases according to the finer details of their function, it is exceedingly complicated and related enzymes can be scattered across subgroups (e.g. TEM-type β -lactamases are spread across 4 functional subgroups: 2b, 2be, 2br, and 2ber), leading to its lack of widespread use.¹⁷³ For the purposes of this work, the Ambler class will be referred to as the molecular class and the Bush-Jacoby class will be referred to as the functional class.

The names of β -lactamases are abbreviations that indicate the source organism (Bc = *Bacillus cereus*), the target substrate (IMP = imipenem), the location where a family of β -lactamases was first discovered (NDM = New Delhi Metallo- β -lactamase), the name of the patient (TEM = Temoneira), or a combination of thereof (CTX-M = cefotaxime, isolated from Munich). The number that follows the abbreviation is often assigned sequentially to variants within a family as they are discovered. An in depth listing of the nomenclature conventions of β -lactamases was compiled by Jacoby in 2006.¹⁸³

1.3.3 Class A β -Lactamases

When the molecular classes of β -lactamases were first defined, only four Class A SBLs were identified: the chromosomally encoded PC-1 from *S. aureus*, BcI from *B. cereus*, and 749/C from *B. linchiformis* as well as the plasmid encoded TEM-1 (R-TEM) from *E. coli*.¹⁷⁰ This class tends to prefer penicillins as their substrate rather than cephalosporins. Much of the work on this class has been on the TEM-type Class A SBLs due to their clinical significance as a result of being plasmid encoded. The mobility of plasmids between bacterial strains and species facilitated the rapid

dissemination of TEM-1 from one *E. coli* isolate in Greece in the early 1960s into other *Enterobacteriaceae*, *P. aeruginosa*, *Haemophilus influenzae*, and *Neisseria gonorrhoeae* worldwide in only a few years.¹⁸⁴ To this day, TEM-type β -lactamases are responsible for almost 90% of ampicillin resistance in Gram negative pathogens.¹⁸⁵

Class A SBLs are composed of two globular domains: one composed entirely of α -helices (pink) and another composed of 5 β -strands (green) surrounded by α -helices (blue) as depicted in Figure 1.7. The active site sits between the two domains with the β_3 strand defining one wall and an Ω -loop (Arg164-Asp179) as the other wall shown in green and purple respectively in Figure 1.7.¹⁸⁶ An oxyanion hole composed of the backbone NH groups of Ser70 and Ala237 orients the substrates correctly by binding the carbonyl oxygen of the β -lactam amide.¹⁸⁷ The catalytic serine residue, Ser70, as well as other critical active site residues such as Lys73, Glu166, and Lys234 are invariant among all Class A SBLs.

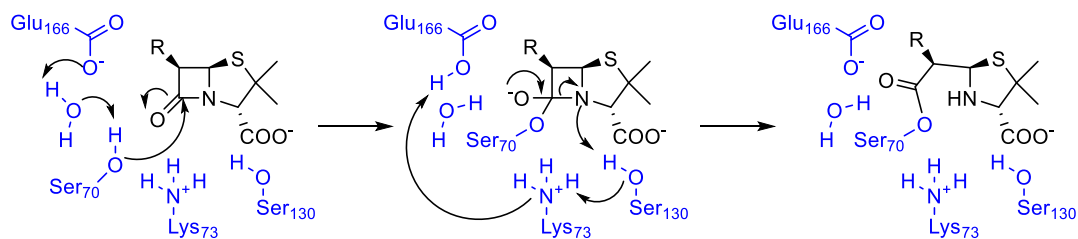


Figure 1.7 3-Dimensional structure of Class A SBLs, exemplified by KPC-2.¹⁸⁸ This figure was generated using UCSF Chimera v. 1.12 from protein databank file 2OV5.

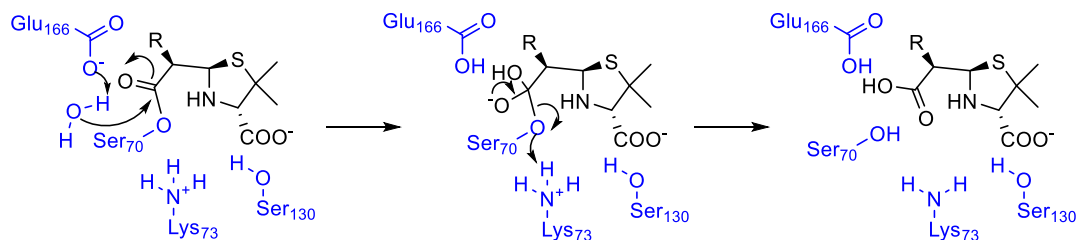
Early studies on the mechanism of SBLs determined that an acyl enzyme was formed and that it was likely that a serine residue, then referred to as Ser44, was the nucleophile.¹⁸⁹⁻¹⁹³ In the early 1990's, X-ray crystallography and site directed mutagenesis were used to further elucidate the mechanism and the discussion shifted to whether Glu166 or Lys73 was the general base used to

activate Ser70 (formerly Ser44).^{194,195} The consensus is that the formation of the tetrahedral intermediate occurs through a “proton shuttle” mechanism in which the proton from Ser70 is shuttled to Glu166 through a water molecule, activating the serine to perform a nucleophilic attack on the carbonyl carbon of the β -lactam amide. Likewise, the collapse of the tetrahedral intermediate to the acyl enzyme proceeds through a proton shuttle in which the proton from Lys73 is shuttled to the substrate nitrogen through Ser130. This shuttle is assisted by Lys234 which increases the acidity of Ser130.¹⁹⁶ Deacylation occurs through activation of a water molecule by Glu166 which performs the hydrolysis.¹⁹⁴ A summary of this mechanism is presented in Scheme 1.4.

Acylation



Deacylation



Scheme 1.4 Mechanism of penicillin hydrolysis by Class A β -lactamases.

The largest family of Class A β -lactamases are the TEM family which is comprised of 237 variants as of December 2018, spanning 4 functional classes.⁵⁵ Mutations to TEM-1 over the decades have broadened the substrate profile of certain TEM-type β -lactamases to include oxyimino- β -lactams such as cefotaxime and ceftazidime as is the case for the EBSL TEM-3 from functional class 2be. The mutations responsible for this extended substrate profile occur only at a limited number of positions on the TEM framework (pink and blue residues in Figure 1.8) with any given variant having only a few of these mutations. Some variants, such as TEM-30, do not have an extended substrate profile but are resistant to inhibition by mechanism-based inhibitors such as clavulanate and tazobactam and

represent another functional class, 2br. Like TEM-type ESBLs, the inhibitor resistant (IR) TEMs contain a couple mutation(s) from a small set (yellow and blue residues in Figure 1.8), some of which are common in ESBLs as well (blue/bold).¹⁸⁴ The frequency and function of the common TEM mutations has recently been reviewed by Grigorenko et al..¹⁹⁷ Complex mutant TEMs such as TEM-50 have mutations that confer both the extended substrate profile and inhibition resistance, and represent another functional class, 2ber.¹⁷³

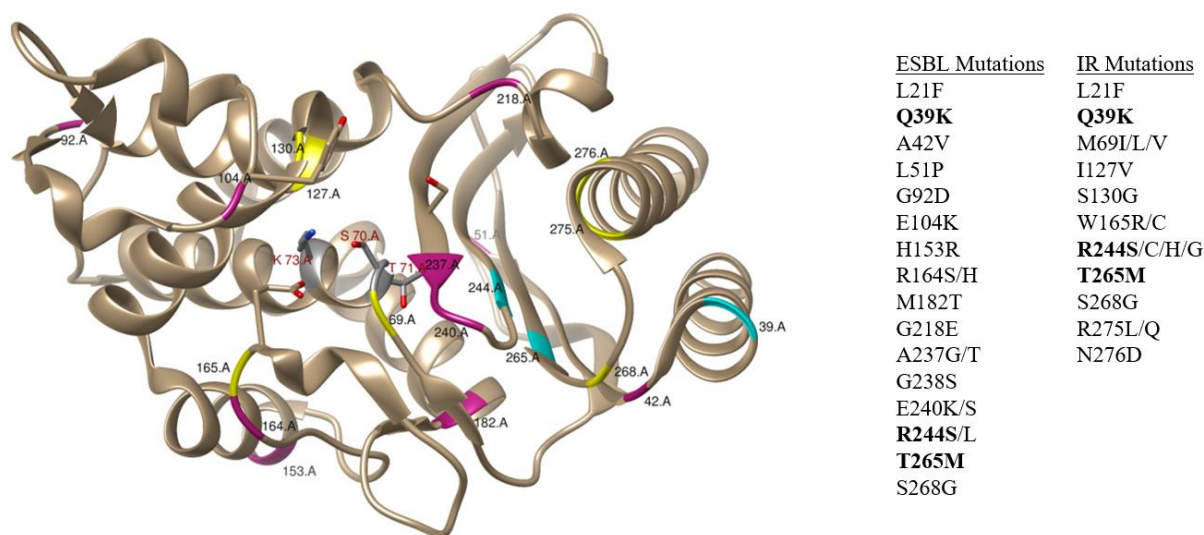


Figure 1.8 Locations of phenotype changing mutations in TEM-1 that contribute to ESBL (pink), IR (yellow), or a combination of ESBL and IR phenotypes (blue). The catalytic triad (STXK) in the active site is highlighted in grey.¹⁸⁴ This figure was generated using UCSF Chimera v. 1.12 from protein databank file 5VHI.

The mutations that confer ESBL character to the TEM variants widen the active site so they can better accommodate the larger oxymino side chains of the third generation cephalosporins or improve their alignment in the active site. Inhibitor resistance is a consequence of mutations that disrupt the active site through misalignment of Ser70 and Ser130 or disrupting the H-bonding network around Ser130. This causes decreased turnover and apparent decreased affinity, particularly with inhibitors such as clavulanic acid, altering the balance between acylation and rearrangement.¹⁹⁸

The second largest family of Class A SBLs is the SHV-family with 228 variants from primarily the 2b and 2be functional classes with a few 2br variants.⁵⁵ Unique to this family, the A146V mutation^b in SHV-38 confers limited carbapenemase activity, but is still categorized in the 2be functional class.¹⁹⁹ Unlike the TEM-family β -lactamases which are found in many different Gram negative pathogens, members of the SHV-family are found primarily in *K. pneumoniae* and other *Enterobacteriaceae*.¹⁷⁶

Although the TEM- and SHV-type Class A SBLs are clinically important, they are becoming overshadowed by another family: the CTX-M's. Named for their ability to hydrolyze cefotaxime (and their first identification in Munich, Germany), this family is entirely composed of ESBLs.^{183,200} The vast majority of the CTX-M-type SBLs belong to the 2be functional class, although recently, a CTX-M-variant, CTX-M-190, was discovered in a clinical isolate in China and demonstrates significant resistance to tazobactam and sulbactam but not clavulanate.^{201,202} This family of ESBLs has disseminated worldwide, primarily in *Enterobacteriaceae*, in large part due to its presence on transferable plasmids.²⁰³ Of the 224 identified CTX-M-variants, CTX-M-15 is the most prevalent in most parts of the world although CTX-M-14 is most prevalent in Southeast Asia, China, South Korea, Japan, and Spain. It has been predicted that in the coming years, CTX-M-27 will out-compete the other CTX-M-variants as it confers increased resistance for ceftazidime compared to CTX-M-14 and has been shown to be more transmissible in nosocomial *E. coli* clones compared to CTX-M-15.²⁰³

Other Class A ESBLs include: ACI-1, BEL-type, BES-1, CARB-10, CfxA-type, CGA-1, CIA-type, CphA-type, CSP-1, DES-1, ERP-type, FAR-1, GES-type, KLUC-type, LRG-1, LUT-type, OHIO-1, OXY-type, PER-type, RAHN-type, SFO-1, SGM-1, SPU-1, TLA-type, and VEB-type.⁵⁵ As is the case for the TEM- and SHV-type SBLs, not all members of a family are ESBLs, but the families listed above include at least one ESBL. Despite the wide diversity of ESBLs, CTX-M-, TEM-, and SHV-type ESBLs are the most common in clinical pathogens and are consequently the most important targets for inhibition.¹⁸⁵

The hydrolysis of cephalosporins is problematic since cephalosporins represent the single most prescribed class of antibiotic in Canada but the ESBLs listed above are not capable of hydrolyzing carbapenems and as such, those infections can be treated with β -lactams.¹⁷ In 1996, a patient in North

^b The A146V mutation is also present in SHV-168; however, the mature protein is the same as SHV-38.⁵⁵⁹

Carolina presented with a carbapenem resistant *K. pneumoniae* infection which marked the first instance of a Class A carbapenemase: KPC-1.²⁰⁴ In 2008, a 73-year-old man in a Toronto-area hospital presented with the first Canadian case of a KPC-producing infection despite having no known risk factors (e.g. recent travel to the USA) – he succumbed to the infection before an appropriate therapy could be determined.²⁰⁵ KPC-producing *Enterobacteriaceae* are now found worldwide, particularly in the USA, China, South/Central America, the Middle East and Mediterranean Europe, with KPC-2 and KPC-3 being the most prevalent variants.^{206,207}

Class A carbapenemases comprise the 2f functional group with the KPC's being the most prevalent. The members of this group (as of 2007), including NMC-A, GES-, SME-, and IMI-type carbapenemases, have been thoroughly reviewed by Walther-Rasmussen and Høiby.²⁰⁸ Of these, the GES-type enzymes are generally the least efficient carbapenemases (the authors suggest that they are more appropriately 2e than 2f) while NMC-A is the most efficient carbapenemase. Additionally, many of these enzymes have higher affinity for meropenem than imipenem (as much as 33-fold greater affinity for SME-2).²⁰⁸ Other Class A carbapenemases have been recently discovered including FRI-1 and BKC-1 from clinical isolates of *E. cloacae* and *K. pneumoniae* respectively, as well as FPH-1 from an opportunistic pathogen that rarely causes infection found in a Utah river (*Francisella philomiragia*), VCC-1 from *Vibrio cholerae* found in shrimp imported to Canada from India, and BIC-1 from an environmental *Pseudomonas fluorescens* sample in France.^{209–213}

Class A carbapenemases harbour mutations that make the active site wider and shallower. These changes are stabilized by a disulfide bond between C69 and C238 which is characteristic of Class A carbapenemases. Additionally, the active site residues 237T, 274H, and 220R interact with the carboxyl.²¹⁴

1.3.4 Class C β -Lactamases

In Ambler's original classification system, β -lactamases were divided based on whether they used a serine or bound zinc ion(s) to hydrolyze β -lactams.¹⁷⁰ All of the SBLs with known sequences at that time were coincidentally Class A's, so when a SBL was sequenced shortly afterwards that had very low sequence homology with the Class A's, another class was established.¹⁷¹ Class C SBLs differ functionally from Class A SBLs in that their preferred substrate is cephalosporins rather than penicillins (in most cases). This establishes them as their own functional group: group 1.¹⁷³

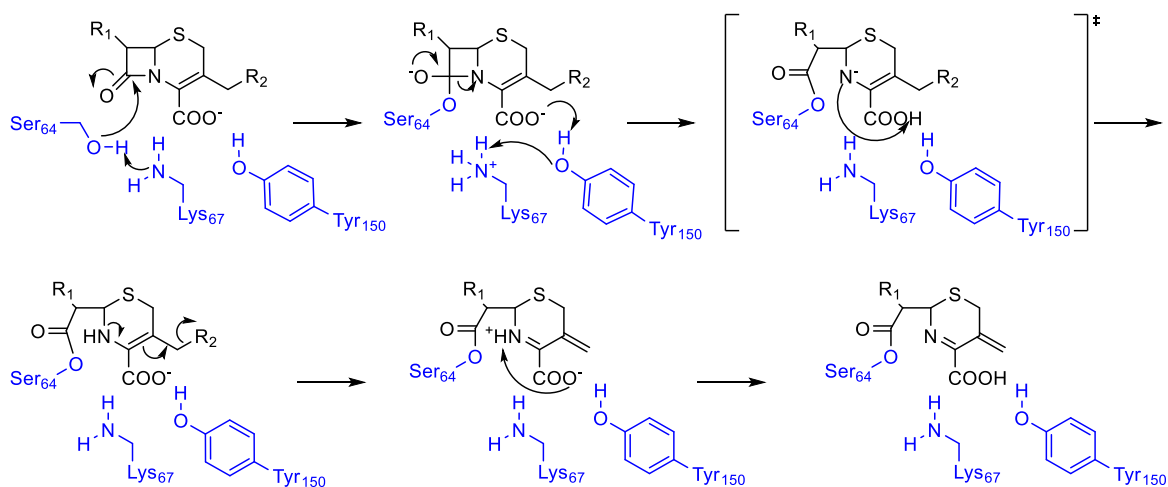
Many of the Class C SBLs are chromosomally encoded by the *ampC* gene in Gram negative bacteria but tend to be expressed in low levels once expression is induced by a β -lactam. Strains that produce high levels of a Class C SBL often harbour mutations in genes involved in the induction pathway, particularly *ampD* or *ampR*, that cause them to become hyperinducible or constitutive hyperproducers.²¹⁵ The chromosomal AmpC-type β -lactamases tend to be named for the organism from which it arises (e.g. *E. coli* AmpC or *P. aeruginosa* AmpC) although some have adopted a short form where they are referred to by the strain identifier (e.g. P99 from *E. cloacae* P99).^{173,216} Plasmid mediated AmpC enzymes have also been discovered such as the ACC, BIL, CMY, DHA, FOX, LAT, and MIR family β -lactamases.²¹⁷ The most prevalent plasmid mediated Class C SBLs are related to CMY-2, although plasmid mediated Class C SBLs are far less prevalent than those that are coded chromosomally in resistant clinical isolates.²¹⁸

Hydrolysis of cephalosporins is considered one of the characteristics of Class C SBLs, although there are a few that are markedly better at hydrolyzing third-generation cephalosporins such as ceftazidime which define the functional group 1e.¹⁷³ These “extended-spectrum cephalosporinases” often have mutations in the Ω -loop, R2 loop, or H-9 helix that open parts of the active site to better bind substrates with bulky sidechains.²¹⁵ The first cephalosporinase discovered to have an extended-spectrum was GC-1 from *E. cloacae* GC1 which has a three amino acid (Ala208 Val209 Arg210) insertion in the Ω -loop relative to P99 from *E. cloacae*, increasing its flexibility.²¹⁹ Other ESBL Class C’s include members from the ADC, CMY, EC, OCH, and PDC families and SRT-1.⁵⁵

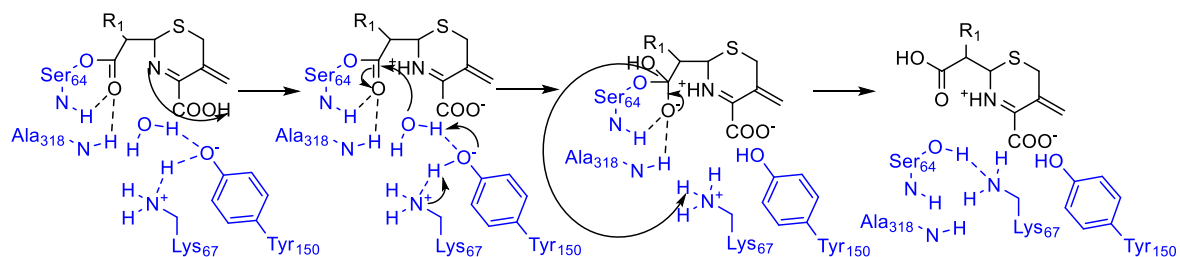
Class C SBLs are structurally similar to Class A SBLs in many ways – they have a similar overall fold and many of the active site residues are the same. The canonical numbering system for Class Cs differs slightly from Class A, the critical active site residues in Class C are Ser64, Lys67, Lys315, and Tyr150 instead of Ser70, Lys73, Lys234, and Ser130 from Class A.²²⁰ From a mechanistic standpoint, Class A and Class C SBLs are very similar in broad strokes: both use a catalytic serine residue to form a tetrahedral acyl-enzyme followed by deacylation using a water molecule found in the active site. Looking in greater detail, differences start to arise – the rate limiting step in Class A β -lactamases is acylation whereas it is deacylation in Class C, the water molecule involved in deacylation approaches from opposite faces of the β -lactam, and Class C β -lactamases do not contain a residue analogous to Glu166 from Class A.^{220–223}

Throughout the years, several groups have attempted to address how Class C β -lactamases function without Glu166. It was originally thought that Tyr150 in its anionic form could act as the general base for acylation; however, this was disproved by NMR experiments that show that the pKa of Tyr150 is greater than 11 and site-directed mutagenesis experiments that showed that Tyr150 is not critical for β -lactam turnover.^{220,224,225} Using hybrid quantum mechanics / molecular mechanics (QM/MM), Tripathi and Nair determined that Lys67 acts as the general base for acylation and Tyr150 acts as a proton shuttle for the collapse of the tetrahedral intermediate to form the initial acyl enzyme as depicted in Scheme 1.5.²²⁶ Following formation of the initial acyl enzyme, many cephalosporins undergo rearrangement to eliminate the R₂ group.

Acylation



Deacylation



Scheme 1.5 Mechanism of cephalosporin hydrolysis by Class C β -lactamases. ^{226,227}

The mechanism of deacylation has also been debated through the years. As with acylation, Tyr150 was originally thought to be the general base for activating the water molecule which was disproven by NMR experiments^{220,224} Substrate-assisted catalysis, in which the ring nitrogen activates the water

was also considered, although Patera et. al. note that the oxygen of Tyr150 is ideally placed to act as the general base if it were in its anionic form.^{228,229} Tripathi and Nair point out that the NMR studies commonly used to eliminate the theories involving Tyr150 were performed on the apo enzyme and do not reflect the nature of the enzyme active site when the β -lactam is bound.²²⁷ In computational studies, the estimated pKa of Tyr150 in the acyl enzyme has supported the idea that it likely exists as the phenolate or partially protonated. This, with QM/MM studies supports the deacylation mechanism in which the water molecule is activated by Lys67 using Tyr150 as a proton shuttle.^{227,230}

1.3.5 Class D β -Lactamases

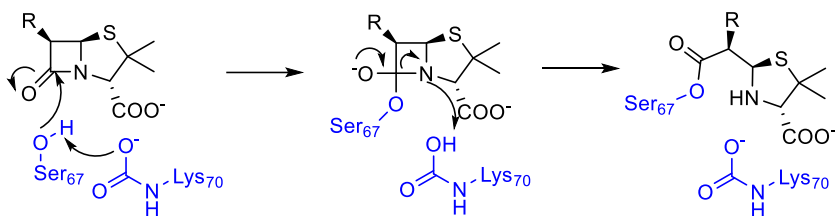
Among the penicillinases, a small group were set apart by their ability to hydrolyze oxacillin, cloxacillin, and other isoxazoyl β -lactams. Once members of this family had been sequenced, they were found to have little sequence homology with Class A and C SBLs and were defined as their own molecular class: Class D.¹⁷² As of 2000, only 20 OXA-variants had been identified,²³¹ however, this group has grown exponentially in recent years: 50 variants had been identified by 2005,²²¹ 250 by 2013,²³² and there are currently over 700 identified OXA-variants.⁵⁵ Several excellent reviews have been written about the Class D β -lactamases over the years.²³²⁻²³⁴

The Class D β -lactamases can be chromosomally encoded or plasmid borne, and are found in many Gram negative pathogens, notably *A. baumannii* and *K. pneumoniae*.²³⁴ The early Class D β -lactamases are narrow spectrum enzymes, defining functional class 2d, and are often related to OXA-1, OXA-2, or OXA-10. There are many extended spectrum variants that are closely related to the narrow spectrum variants, particularly OXA-10 which define the functional class 2de. Some ESBL Class Ds, such as OXA-18, OXA-45, and OXA-53 are not structurally related to the narrow spectrum variants.²³⁵ As with Class A, there are Class D variants with carbapenemase activity (functional class 2f). The carbapenemases are further grouped by structural similarity, such as OXA-23-like, OXA-48-like, OXA-58-like, and OXA-143-like.²³⁴ There is no unified numbering system for the amino acid sequences of Class D SBLs, so all amino acid numbering in this section will refer to OXA-10 since it was the first Class D crystal structure and is one of the best studied in this class.

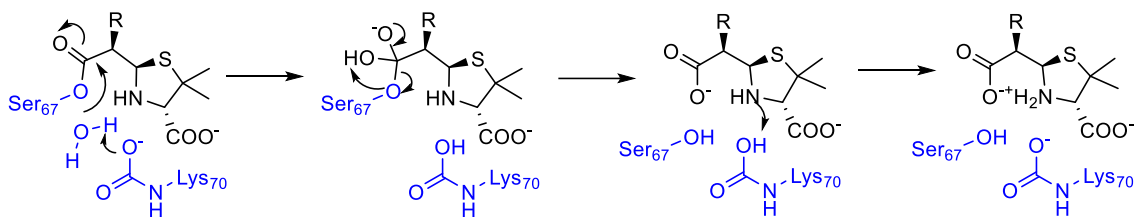
Class D β -lactamases share many mechanistic similarities with Class A β -lactamases: a general base activates the catalytic serine to form the acyl enzyme, the same general base activates a water molecule for deacylation from the α face of the substrate. The general base in Class A β -lactamases,

Glu166, is not present in Class D β -lactamases and early crystallographic studies suggested that a lysine residue in the active site, Lys70 in OXA-10, acted as the general base.^{231,236} This suggestion was found to be incomplete later that year when it was discovered that the lysine is carboxylated in the active form of the enzyme.²³⁷ It is widely accepted that the carboxylated lysine acts as the general base for both the acylation and deacylation half reactions as depicted in Scheme 1.6.

Acylation



Deacylation



Scheme 1.6 Mechanism of penicillin hydrolysis catalyzed by Class D SBLs.²³⁸

Unlike Class A β -lactamases, Class D β -lactamases have a highly hydrophobic active site which is thought to promote the carboxylation of the lysine by lowering its pKa and provide favourable interactions for substrates with bulky hydrophobic groups such as oxacillin.²³² The post-translational modification of the active site lysine is known to be reversible, pH dependent, and necessary for enzyme activity.²³⁹ To prevent spontaneous decarboxylation, the carboxylated lysine is stabilized by hydrogen bonds and salt bridges with nearby residues – notably Trp154 and Ser67.²³²

Prior to the crystallographic and mechanistic studies, Class D β -lactamases were notoriously difficult to work with for kinetic studies due to their biphasic kinetics (burst phase followed by a slower steady state) and irreproducibility. The revelation that a critical active site residue needed to be carboxylated, and that assay buffers should be supplemented with bicarbonate to mimic physiological conditions made kinetic assays reproducible and gave typical progress curves.²⁴⁰ The carboxylated lysine was not the only factor that complicates kinetics with Class D β -lactamases, many of the

OXA's are thought to exist as dimers in solution. Paetzel et. al. demonstrated that optimal enzyme activity was achieved when OXA-10 was in its dimeric form, and suggested that the biphasic kinetics could be, in part, the result of shifting of the dimerization equilibrium.²³⁶ For OXA-10, dimerization is heavily dependent on the presence of divalent cationic metals; however, this is not true for all dimeric OXA's – OXA-48's dimerization is metal ion independent.²⁴¹ Although many OXA's are dimeric (e.g. OXA-2,²⁴² OXA-10,^{236,237} OXA-13,²⁴³ OXA-29,²⁴⁴ OXA-46,²⁴⁵ and OXA-48²⁴¹) there are also several monomeric OXA's (e.g. OXA-1,²⁴⁶ OXA-24,²⁴⁷ OXA-85,²⁴⁸, and OXA-205²⁴⁹

1.3.6 Class B β -Lactamases

The Class B, or metallo-, β -lactamases are characterized by the active site metal ions used to perform catalysis and their ability to efficiently hydrolyze carbapenems. Within this class, there are three subclasses: B1, B2, and B3 which are primarily differentiated by the amino acid residues used to coordinate the zinc ions and the number of those zinc ions in the active form of the enzyme. The subclass B1 MBLs, which represent the majority of Class B MBLs, have 3 His residues that coordinate Zn1 and an Asp, Cys, and His that coordinate Zn2. A hydroxide molecule is also coordinated between the two zinc ions as well, a second water is coordinated to Zn2 such that the coordination about Zn1 is tetrahedral and the coordination about Zn2 is trigonal bipyramidal.^{250–253} The B1 MBLs also have a unique structural feature: a loop (residues 61-66) that closes over the active site and contributes to reaction rate.²⁵⁴ In the B2 MBLs, one of the His residues that coordinates Zn1 is replaced with an Asn residue, decreasing the binding affinity of that site such that CphA is often a monozinc enzyme. The difference between the B1 and B3 MBLs reside primarily in the Zn2 binding site where Cys221 is replaced with His121.^{255,256} A few B3s, such as GOB-1, also have His116 substituted with a Gln.^{178,257} Unlike the B1 (and B3) MBLs, the molecule that coordinates Zn1 is a water molecule, a water molecule also occupies the Zn2 binding site.^{258,259} In the functional classification scheme, B1 and B3 MBLs occupy group 3a which hydrolyze penicillins, cephalosporins, and carbapenems efficiently while group 3b which contains the B2 MBLs only efficiently hydrolyze carbapenems.¹⁷³

Table 1.5 Amino acid residues that coordinate zinc ions in the three subclasses of metallo- β -lactamases.

MBL Subclass	Zn1 ligands			Zn2 ligands		
B1	His116	His118	His196	Asp120	Cys221	His263
B2	Asn116	His118	His196	Asp120	Cys221	His263
B3	His/Gln116	His118	His196	Asp120	His121	His263

Residues numbered using the standard MBL numbering scheme^{178,260}

Unlike the previously described classes of β -lactamase, the Class B β -lactamases use an activated water molecule coordinated by zinc ion(s) to perform β -lactam hydrolysis rather than a serine residue. The MBLs also have a different overall protein fold: they are an $\alpha\beta\alpha$ sandwich with the active site nestled in the crevice between the two β -sheets as depicted in Figure 1.9.²⁶ The structural and mechanistic differences between the metallo- β -lactamases and serine- β -lactamases have suggested that they evolved independently of one another.

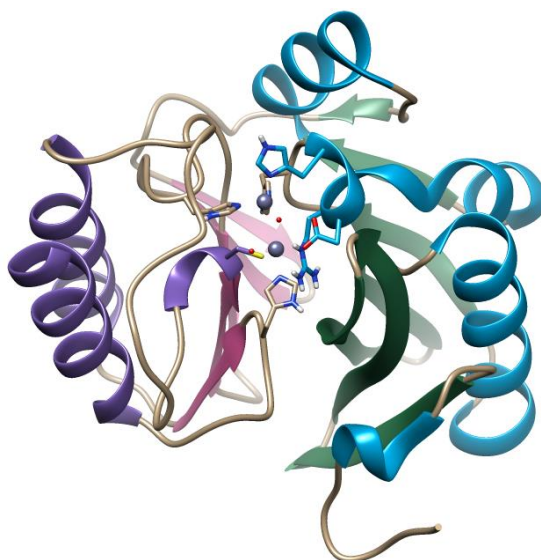


Figure 1.9 Overall MBL $\alpha\beta\alpha$ fold with the N-terminal $\alpha\beta$ motif in blue and green and the C-terminal $\alpha\beta$ motif in purple and pink. This figure was generated using UCSF Chimera v. 1.12 from protein databank file 5N5G, an unpublished structure of VIM-1.

The serine- β -lactamases are thought to have evolved from a DD-peptidase similar to the PBPs, whereas the MBLs are thought to have evolved from a superclass of zinc hydrolases with a possible divergence that differentiated the B3 group from the B1 and B2 groups.^{151,179,261,262} Other proteins from the zinc hydrolase superfamily (sometimes referred to as MBL fold proteins) include flavoproteins, glyoxylase II, SNM1 which repairs DNA interstrand crosslinks, and many more.²⁶¹

The first metallo- β -lactamase was identified by Abraham and Newton in the mid-1950's when it was realized that the penicillinase they were pursuing from *Bacillus cereus* 569H was a mixture of two enzymes termed BcI and BcII.^{263,264} The first of these, BcI, is a Class A penicillinase discussed briefly in 1.3.3. The second, BcII, was found to be a metal-dependent cephalosporinase that lost activity upon treatment with EDTA.²⁶⁵ For decades, BcII was the only known MBL until L1 was discovered in *Pseudomonas maltophilia* (also known as *Xanthomonas maltophilia*, now *Stenotrophomonas maltophilia*) in 1982.²⁶⁶ Shortly after, two more MBLs were identified: CcrA from *Bacteroides fragilis* and CphA from *Aeromonas hydrophilia*.^{267,268} All of the early MBLs: BcII (B1), L1 (B3), CcrA (B1), and CphA (B2) were chromosomally encoded so despite their ability to efficiently hydrolyze cephalosporins and carbapenems, they were not considered clinically important. Recently, L1 has become considered much more clinically relevant since *S. maltophilia* has become increasingly prevalent (third most common non-fermentative Gram negative pathogen after *P. aeruginosa* and *A. baumannii*) and highly resistant to most antibiotics.²⁶⁹

In 1991, the first mobile MBL, IMP-1 (B1), was identified in a *P. aeruginosa* isolate from Japan encoded in a class 1 integron.²⁷⁰ Since then, 70 IMP variants have been identified in several Gram negative pathogens including other *Pseudomonas* spp., *Klebsiella* spp., *Citrobacter* spp., *Acinetobacter* spp., and *E. cloacae*. Pathogens expressing IMP are found worldwide, but are most prevalent in southeast Asia and Australia.²⁷¹⁻²⁷⁶ Another major family of transferrable MBLs was identified in 1997 in a *P. aeruginosa* isolate from Verona, Italy – VIM-1 (B1).²⁷⁷ The VIM-family of MBLs has quickly become the most prevalent MBL in Europe in a variety of Gram negative pathogen with over 50 VIM-variants having been identified to date.^{55,278}

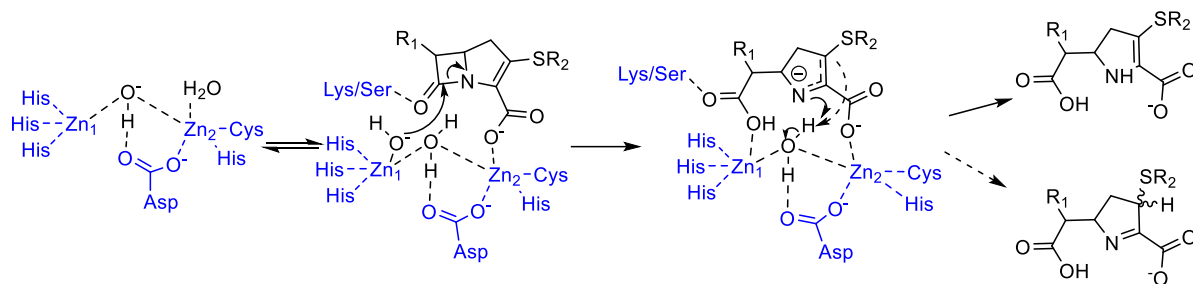
A relatively new family of MBLs, the NDMs, has risen to fame in recent years over their ability to confer resistance to almost every clinically used β -lactam, presence on highly multidrug resistant plasmids, and rapid dissemination into nosocomial and community acquired pathogens. The first report of a pathogen harbouring NDM-1 came in 2009 from a *K. pneumoniae* strain in New Delhi that

expressed NDM-1 (B1 MBL), CMY-4 (Class A SBL), and an erythromycin esterase. In that same report, they also noted that an *E. coli* strain isolated from the patient's feces was also carrying and NDM-1 gene, leading to speculation about *in vivo* conjugation.²⁷⁹ Two years after the first report, NDM-1 was found in clinical isolates worldwide, primarily *E. coli*, *K. pneumoniae*, *A. baumannii*, and *P. aeruginosa*, and in environmental isolates in India (many of which are potential human pathogens).^{56,280,281} NDM-1-producing isolates often produce other resistance proteins – one was shown to have genes for 3 SBLs, as well as aminoglycoside, fluoroquinolone, sulfonamide, trimethoprim, fosfomicin, macrolide, chloramphenicol, and rifampin resistance.^{56,282,283}

Through the 2000's and early 2010's, several novel MBLs were discovered in the chromosomes of pathogens such as FEZ-1 (B3)²⁸⁴ and SFH-1 (B2)²⁸⁵ or on mobile genetic elements such as integrons or transferable plasmids such as SPM-1 (B1/B2 hybrid),^{286,287} GIM-1 (B1),²⁸⁸ SIM-1 (B1),²⁸⁹ KHM-1 (B1),²⁹⁰ DIM-1 (B1),²⁹¹ AIM-1 (B3),²⁹² and FIM-1 (B1).²⁹³ Of these, only SPM-, GIM-, and FIM-producing pathogens are reported with any regularity in epidemiological surveys of metallo- β -lactamase-producers with VIM-, IMP-, and NDM-producers being far more prevalent.^{207,294–297}

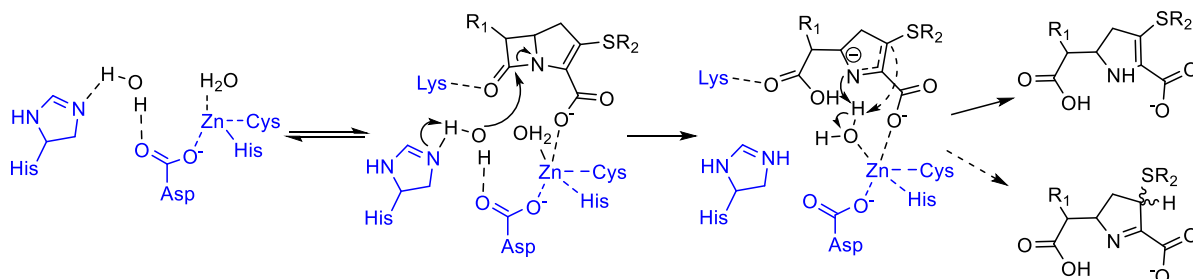
The hydrolytic mechanisms of MBLs are divided into dizinc (B1/B3) and monozinc (B2). For both groups, the predominant questions address the identity and nature of the nucleophile and the identity of the proton source for protonating the ring nitrogen. The history and key studies in this area have been thoroughly reviewed by Meini et. al..²⁹⁸

The primary candidates for the nucleophile in dizinc MBLs are Asp120 (which coordinates Zn2) or the water/hydroxide bound between the zinc ions.^{250,299,300} The consensus is that Zn1 lowers the pKa of the water molecule enough that it exists as a hydroxide ion which acts as the nucleophile for the ring opening.²⁹⁸ Asp120 was seriously considered as the proton source for the second step of the mechanism; however, this would require transient dissociation from Zn2. Also, studies with BcII and L1 mutants have demonstrated that Asp120 is not the proton source.^{301–303} It has been suggested that the proton source is most likely the non-hydrolytic water molecule that coordinates Zn2 and that the two tautomeric products of carbapenems occur through protonation of different resonance structures.²⁹⁸ A summary of the mechanism of B1 and B3 hydrolysis of carbapenems can be found in Scheme 1.7.



Scheme 1.7 Hydrolysis of carbapenems by B1 and B3 MBLs. ²⁹⁸

There has been much less controversy regarding the B2 mechanism – the water molecule bound in the Zn1 binding site is activated by His118, forming a hydroxide that attacks the amide.^{258,259} As with the dizinc MBLs, the water that coordinates Zn2 acts as the proton source which can protonate either resonance structure to form the two carbapenem tautomers.²⁹⁸ A summary of the mechanism of carbapenem hydrolysis by B2 MBLs can be found in Scheme 1.8.



Scheme 1.8 Hydrolysis of carbapenems by B2 MBLs. ²⁹⁸

1.3.7 Established Methods for Assaying β -lactamases

Early methods for assaying β -lactamase activity used traditional analytical chemistry techniques adapted to this unique system such as pH indicators, iodometric titration, or manometric quantitation of the CO_2 evolved. Upon hydrolysis by a β -lactamase, penicillin becomes penicillanic acid which can be quantified using pH indicators such as phenyl red using spectrophotometry.³⁰⁴ Later methods were developed that used a pH meter to monitor penicillanic acid formation.³⁰⁵ The iodometric titration exploited the ability of penicilloic acid to reduce iodine, turning the blue starch/iodine complex clear. The earliest version of the iodometric assay involved adding a known excess of the starch/iodine indicator after hydrolysis had preceded for a set amount of time, and determining the

amount of unreduced indicator by titration with thiosulfate.³⁰⁶ Later versions of this assay added the β -lactamase to a solution containing both the indicator and the substrate and monitoring the colour change from blue to clear spectrophotometrically in either a continuous or discontinuous manner.^{307,308} The manometric method quantifies the hydrolysis of penicillin in sodium bicarbonate by the CO₂ evolved from the bicarbonate in response to the pH change caused by penicillanic acid.³⁰⁹

The hydrolysis of all β -lactam antibiotics causes a shift in the absorption peak in the UV-range. In the early 1970's, a novel cephalosporin, termed nitrocefin, was developed that showed a visible colour change from yellow to red upon hydrolysis.³¹⁰ This allowed for the direct quantitation of the hydrolysis of a cephalosporin using spectrophotometry. By the mid-1970's UV-spectrophotometers had become affordable enough for direct quantitation of β -lactam hydrolysis by spectrophotometry.³¹¹ Since then, several chromogenic substrates have been developed, including PADAC, CENTA, and Chromacef for visual or spectrophotometric determination of β -lactamases, although nitrocefin remains the standard for chromogenic substrates.³¹²⁻³¹⁵

In the early 2000's a fluorogenic cephalosporin was developed that releases an umbelliferone fluorophore upon hydrolysis for use in cell imaging and localization studies.³¹⁶ Recently, another fluorogenic cephalosporin, FC4, was developed that releases a 7-hydroxycoumarin fluorophore. FC4 was found to be an excellent substrate for fluorescence based kinetic assays of MBLs and has also found limited use with SBLs.^{317,318}

1.4 β -Lactamase Inhibitors

1.4.1 β -Lactams as β -Lactamase Inhibitors

The first inhibitor of β -lactamases was actually a β -lactam itself: cephalosporin C which was found to be resistant to inactivation by a penicillinase in 1955.¹⁶⁵ Cephalosporin C was later shown to protect benzylpenicillin (Penicillin G) from hydrolysis by a penicillinase by competitive inhibition of the enzyme.²⁶³ The inhibition of β -lactamases by β -lactams relies entirely upon the substrate specificity of the different classes of β -lactamase. Many of the early β -lactamases were narrow-spectrum Class A SBLs, and consequently were able to efficiently hydrolyze penicillins but not cephalosporins. As such, β -lactams that are inhibitory towards β -lactamases due to unfavourable substrate specificity are often referred to as "poor" or "slow" substrates.

Methicillin was the first semi-synthetic penicillin developed that was resistant to hydrolysis by some penicillinases and acted as a competitive inhibitor of others.³¹⁹ Other penicillins, such as nafcillin, cloxacillin, and quinacillin were also determined to inhibit β -lactamases (Figure 1.10).^{320–322} A structural study by Fink et al. in 1987 suggested that inhibition of β -lactamases by methicillin and related compounds was due to steric interactions of the bulky aromatic sidechains causing the acyl enzyme to adopt a conformation that cannot be deacylated.³²²

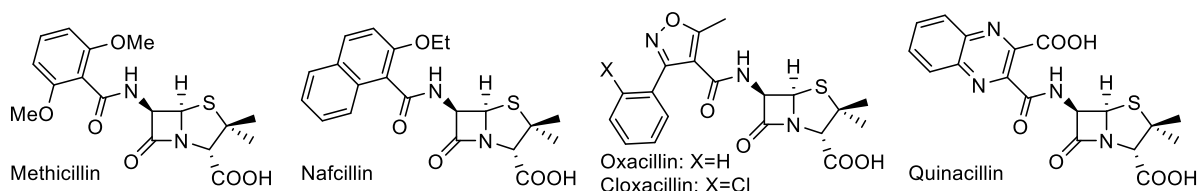
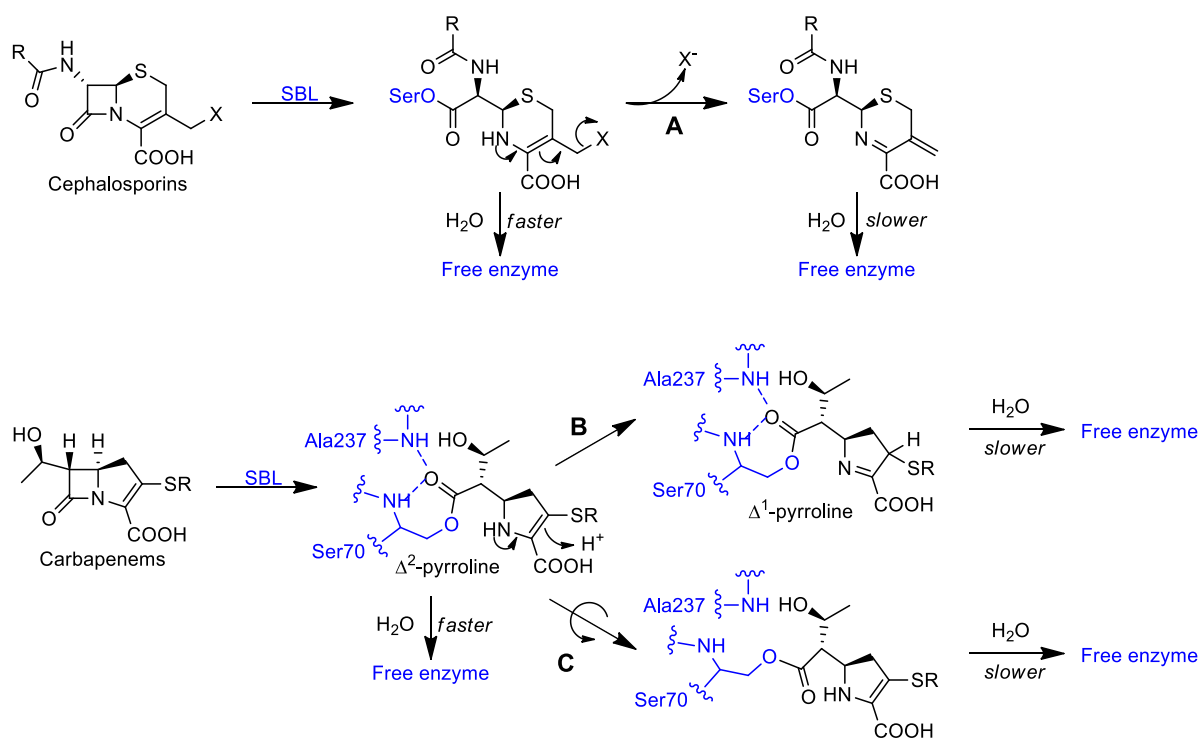


Figure 1.10 Penicillins that are inhibitory towards some SBLs.

Some cephalosporins and carbapenems are capable of inhibiting Class A and Class C β -lactamases through rearrangements that stabilize the acyl enzyme. With cephalosporins, this rearrangement occurs if X is a sufficiently good leaving group and favours elimination over deacylation (Scheme 1.9A) which has been kinetically observed with the Class A SBLs PC1 and RTEM-2 as well as the Class C SBLs *E. cloacae* 908 R and P99.^{323–326} The elimination product of ceftazidime has been captured in crystal structures of AmpC (C) where steric clashes prevented the correct conformation for deacylation and in deacylation impaired mutants of CTX-M-14 (A) and OXA-160 (D).^{327–329} Carbapenems are known to demonstrate biphasic kinetics with Class A SBLs, a phenomenon that was attributed to tautomerization of the acyl enzyme from a Δ^2 -pyrroline to a Δ^1 -pyrroline (Scheme 1.13B) as observed using NMR methods.^{330–332} In crystal structures of carbapenems bound to TEM-1 (A), SHV-1 (A), and AmpC (C) the Δ^1 -pyrroline tautomer is not observed but rather the rotation of a carbonyl formed upon acyl enzyme formation out of the oxanion hole (Scheme 1.13C).^{333–335} This rotation disrupts the ideal geometry for acyl enzyme hydrolysis, leading to a long-lived acyl-enzyme intermediate and consequently, inactivation of the β -lactamase.



Scheme 1.9 Inhibition of SBLs by cephalosporins and carbapenems.

Although metallo- β -lactamases are typically efficient carbapenemases, a series of carbapenems, the 1 β -methylcarbapenems, have been discovered that are poor substrates for MBLs and potent inhibitors. The most potent in this series, J-110,441, was inhibitory towards TEM-1 (A), IMP-1 (B1), BcII (B1), CcrA (B2), L1 (B3), and a Class C cephalosporinase from *E. cloacae* with K_{IS} ranging from 0.0037 μ M to 2.54 μ M. This compound was found to be a modest antibiotic against several MBL-producing strains but was potently synergistic with imipenem, reducing the MIC as much as 64-fold.³³⁶ Unfortunately, this mechanism of MBL inhibition by J-110,441 has not been elucidated and the compound has not led to a clinically useful MBL inhibitor.

1.4.2 Serine- β -Lactamase Inhibitors

Most of the β -lactamases discovered early in the history of β -lactam antibiotic use, particularly those that were prevalent in clinical isolates, were serine- β -lactamases. As a result of this, much of the early work to find a clinically useful β -lactamase inhibitor focused on SBL inhibition. The first success came with the mechanism-based inhibitors, clavulanate, sulbactam, and tazobactam (Figure 1.11) which are inhibitory towards many of the Class A SBLs and some Class D SBLs. Much of the

work over the next few decades focused on transition state analogs such as the boronates and phosphonates, although none of these made it into clinical use. More recently, the diazobicyclooctanes were discovered in the mid-2000's which inhibit Class A, C and some Class D SBLs – these have been approved for clinical use since 2015.^{337,338} Finally, a cyclic boronate, Varborbactam, was approved for clinical use in combination with meropenem in August of 2017 as a inhibitor of Class A and C SBLs.

1.4.2.1 Mechanism Based Inhibitors

Clavulanic acid was the first of the mechanism-based inhibitors to be discovered in the late-1960's but was not disclosed until the late-1970's as part of a program by Beecham pharmaceuticals to identify natural product β -lactamase inhibitors.^{38,339} This compound was a potent inhibitor of penicillinases (Class A SBLs) but was ineffective against the chromosomal cephalosporinases (Class C SBLs).³⁴⁰ Shortly after the disclosure of clavulanic acid, a sulfone derivative of penicillin, sulbactam, was discovered by Pfizer which had a similar spectrum of inhibitory activity as clavulanic acid but slightly inferior potency.^{341,342} Nearly a decade later, tazobactam, a triazole-substituted derivative of sulbactam was prepared by a group led by R. Micetich at SynPhar labs in Edmonton, Alberta, and was determined to have increased potency against Class C SBLs while also improving upon sulbactam's inhibition of Class A SBLs.^{342,343}

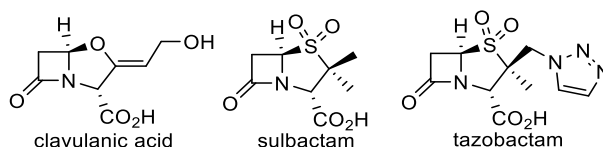
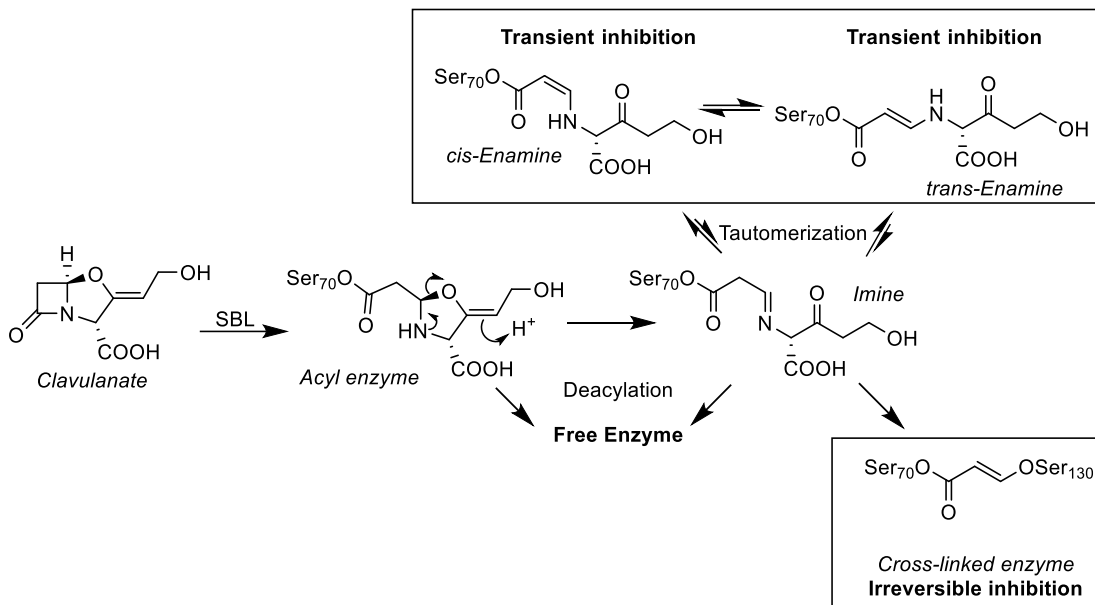


Figure 1.11 Mechanism-based serine- β -lactamase inhibitors.

The mechanism by which these compounds inhibit SBLs has been thoroughly studied and appears in many reviews. The most complete analysis of the mechanism was done by Brown et al. in 1996.^{23,344–349} As summarized in Scheme 1.10, the first step for inhibition by these compounds is similar to the hydrolysis of β -lactams by SBLs: the catalytic serine (Ser70) attacks the β -lactam bond to form the acyl enzyme. From this point, the enzyme can deacylate, releasing the free enzyme, or rearrange to form the imine intermediate. The imine can then tautomerize to form the cis or trans enamine which is transiently inhibitory or alternatively can react with another serine (Ser130), irreversibly crosslinking the active site and inactivating the β -lactamase. Other side reactions

including decarboxylation of the imine or enamines, and hydrolysis of the imine to an aldehyde which is slowly hydrolyzed can also occur.



Scheme 1.10 Inhibition of Class A SBLs by mechanism-based inhibitors eg. clavulanate. ^{344,346,348}

Other mechanism-based inhibitors such as other sulfone derivatives of penicillin,^{350–352} 6-halo penicillins,^{189,353–355} and alkylidene penams^{356–360} have also been studied but have not been brought into clinical use.

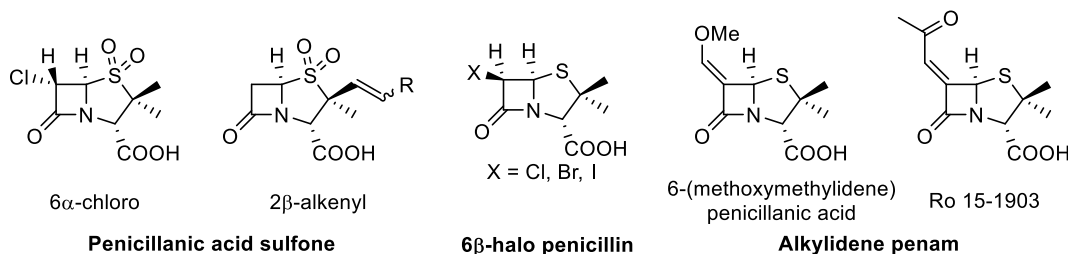


Figure 1.12 Other mechanism-based inhibitors: penicillanic acid sulfones, 6-halo penicillins, and alkylidene penams. ^{189,350,351,354,356,358}

1.4.2.2 Diazabicyclooctanes

The major drawback of the clinically available mechanism-based inhibitors is that they only inhibit some Class A and C SBLs which greatly limits their usefulness for highly resistant pathogens. A new

class of inhibitor, the diazabicyclooctanes (DBOs), was discovered in the mid-2000's that were nanomolar inhibitors of Class A and C SBLs including extended spectrum SBLs not inhibited by clavulanate nor the penicillanic acid sulfones (e.g. KPCs) and some Class D SBLs.^{337,361,362} The first inhibitor from this class to be approved for clinical use is Avibactam (formerly AVE1330A or NXL104) although another, Relebactam, is in phase 3 clinical trials.^{338,363} Earlier this year, a DBO (WCK 4234) was published in the literature that has K_I 's comparable to avibactam for critical Class A and C SBLs but greatly improved activity against Class D SBLs such as OXA-10 and OXA-24 which are uninhibited by Avibactam and Relebactam.³⁶⁴

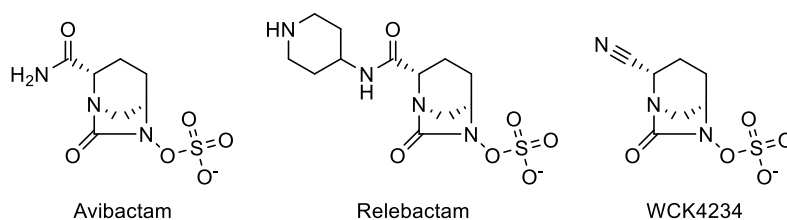
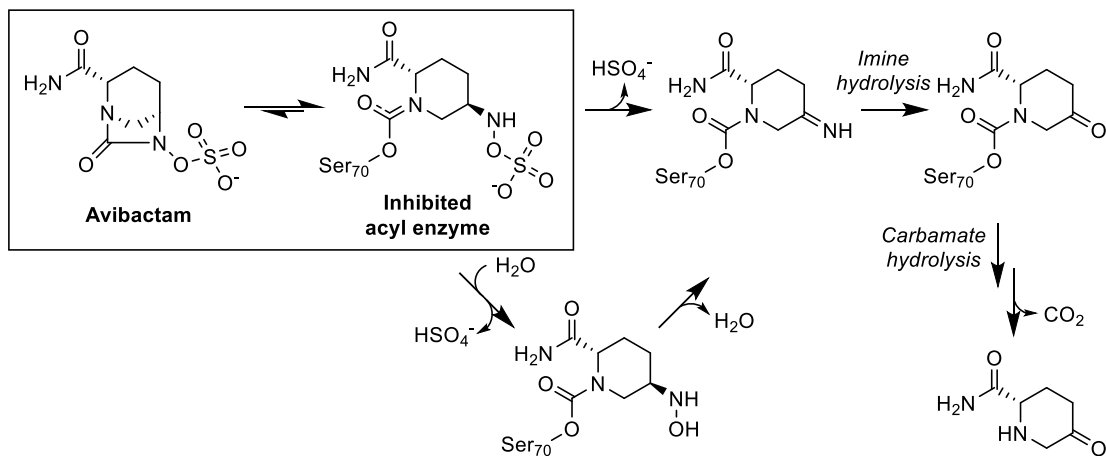


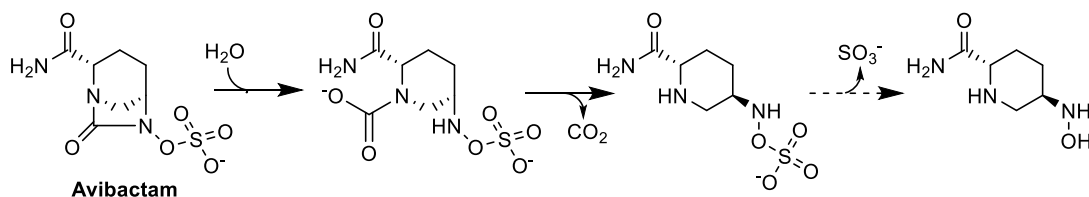
Figure 1.13 A selection of the diazabicyclooctanes that are clinically available or in development.³⁶⁵

The mechanism of SBL inhibition by DBOs (Scheme 1.11) is simple at first glance; the catalytic serine (Ser70) attacks the diaza group carbonyl carbon, breaking the amide bond on the sulfate side to form the inhibited acyl enzyme.³⁶⁶ The details of this mechanism make it very interesting: in the structure of the active inhibitor, the lone pair of electrons on the bridgehead nitrogen are constrained and cannot exist in amide resonance making the carbonyl more reactive than expected from an amide. Once the ring is opened, as in the acyl enzyme shown in Scheme 1.11, the nitrogen lone pair is no longer geometrically constrained and exists in amide resonance. This makes the amide linkage in the acyl enzyme relatively unreactive towards nucleophilic attack by the water in the SBL active site resulting in a relatively long-lived acyl enzyme.³⁶⁶

SBL



MBL



Scheme 1.11 Avibactam mediated inhibition of SBLs and other reactions with Avibactam catalyzed by β -lactamases. ^{361,366,367}

Acylation of the catalytic serine can slowly reverse in many SBLs to regenerate the active inhibitor. Some SBLs, such as KPC-2, are capable of hydrolyzing and inactivating Avibactam by desulfonating (through either a one or two step mechanism), then hydrolyzing the imine, followed by carbamate hydrolysis but these are slow processes shown in Scheme 1.11.³⁶¹ MBLs are not inhibited by DBOs, but have been shown to slowly inactivate the DBOs through the hydrolysis depicted in Scheme 1.11. The subsequent desulfonation in the MBL mechanism was only observed at low levels and it was not conclusively determined whether or not it was the result of enzymatic catalysis.³⁶⁷

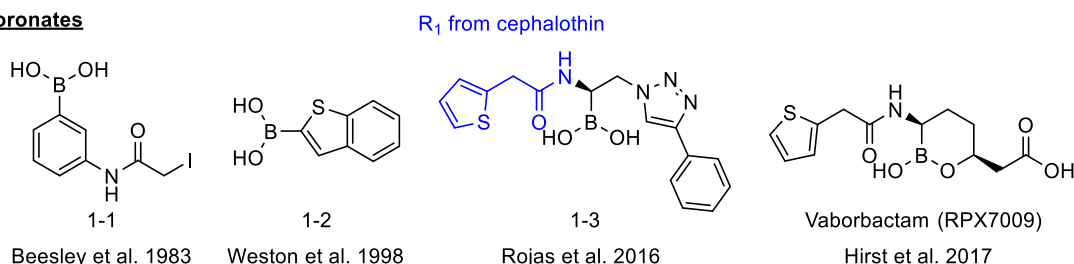
1.4.2.3 Transition State Analogs and β -Lactam Mimics

Mechanism based inhibitors and DBOs both inhibit through the opening of an amide ring (either β -lactam or DBO) forming a stable acyl-enzyme complex. Not all inhibitors of SBLs require a cyclic amide, others function by forming a covalent complex with the active site serine that mimics the

tetrahedral intermediate formed during catalysis or mimics the natural substrate without being able to complete the catalytic cycle.

The earliest β -lactamase inhibitor to be discovered was boric acid in 1978 which inhibited BcI (A) with a K_I of 1 mM.³⁶⁸ Boronate inhibitors were vastly improved in the 1980's with simple aromatic boronic acids such as 1-1 and 1-2 from Figure 1.14 that inhibited Class A and C SBLs with K_I 's as low as 0.5 μ M.³⁶⁹⁻³⁷¹ Increasing the complexity of boronic acids to include two R groups (one of which is derived from a cephalothin R group – highlighted in blue) such as 1-3, improved the potency of these inhibitors to 60 nM (IC_{50}) against Class A SBLs.³⁷² Cyclization of the boronate improved potency even more with Vaborbactam (RPX7009) inhibiting Class A and C SBLs with K_I 's as low as 30 nM.³⁷³ Vaborbactam was first reported and patented in 2010 and was approved for clinical use in combination with meropenem in 2017.^{374,375} Recently, boronic acid inhibitors have also been shown to be inhibitory towards a Class D SBL, OXA-24/40, although the inhibition is much less potent than against Class A and C SBLs.³⁷⁶ The inhibition of Class A, C, and D SBLs by phosphonates (1-4) and both cyclic and linear phosphates (1-5 and 1-6 respectively) have been thoroughly studied by the Pratt group; however the kinetics are reported in terms of rate constants making it difficult to compare their efficacy to that of other inhibitors reported in terms of K_I or IC_{50} .³⁷⁷⁻³⁸⁶

Boronates



Phosph(on)ates

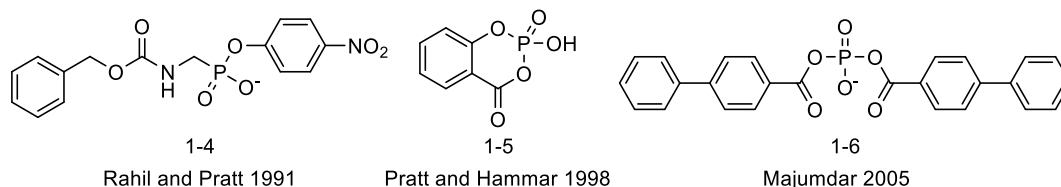


Figure 1.14 Transition state analog inhibitors of SBLs: boronates and phosph(on)ates.

369,371,372,374,377,381,385

Many β -lactam mimics have been studied in the context determining the pharmacophore of β -lactam antibiotics and diversifying pharmacophores, some of which (imidazolidinones and cyclobutanones) were determined to be inhibitory towards β -lactamases. The topic of β -lactam mimics has been well reviewed by Jungheim and Ternansky in 1993 and cyclobutanones in particular have been recently reviewed by Devi and Rutledge.^{387,388} The first cyclobutanones (such as 1-7 from Figure 1.15) were synthesized by Gordon et al. in 1981 and were found to have no inhibitory activity towards R-TEM β -lactamase.³⁸⁹ A few years later, Lowe and Swain prepared a series of cyclobutanones, including 1-8, that inhibited R-TEM and *B. cereus* 568/H β -lactamases in a slow, time-dependent manner but they did not report a value that indicates inhibitory potency.³⁹⁰ Most recently, Johnson et al. from the Dmitrienko laboratory described the synthesis of dichlorocyclobutanones such as JJ05-1058 and JJ05-802, that weakly inhibited all classes of β -lactamases with the best activity being demonstrated against Class C.

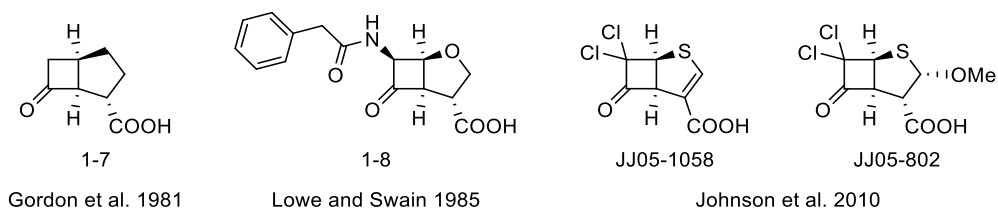
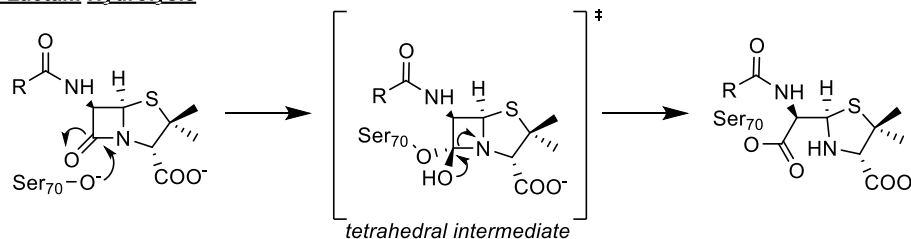


Figure 1.15 Cyclobutanones: β -lactam mimics that are inhibitory towards β -lactamases. ^{389–391}

Both the transition-state analogs and the cyclobutanones inhibit SBLs by forming a reversible covalent acyl enzyme with the catalytic serine (Ser70) of the β -lactamase that mimics the tetrahedral transition-state of β -lactam binding as shown in Scheme 1.12. Crystal structures of Vaborbactam, 1-4, and JJ05-802 bound to the active sites of SBLs have been obtained which confirm the formation of a covalent bond between the catalytic serine and the inhibitor as well as the release of the *p*-nitrophenyl group from the phosphonate.^{373,379,391} A crystal structure of JJ05-1085 bound to the active site of the B1 MBL SPM-1 has also been determined.³⁹²

β -Lactam Hydrolysis

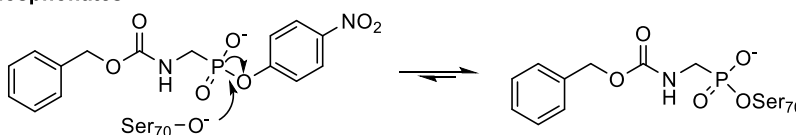


Transition State / Tetrahedral Intermediate Analogs

Boronates

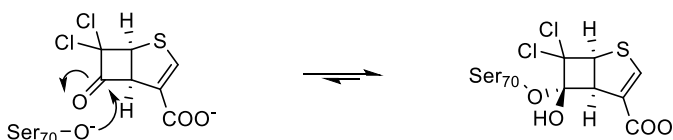


Phosphonates



β -Lactam Mimics

Cyclobutanones



Scheme 1.12 Covalent adducts formed by boronates, phosphonates, and cyclobutanones that mimic the transition-state of β -lactam acyl-enzyme formation with serine- β -lactamases. ^{373,379,391}

1.4.3 Metallo- β -Lactamase Inhibitors

Metallo- β -lactamases have become increasingly prevalent in recent years, and their broad substrate specificity confers resistance to many of the β -lactam antibiotics. Unlike the SBLs which can be inhibited by clavulanate, sulbactam, tazobactam, and the DBOs (Figure 1.11 and Figure 1.13 respectively), MBLs do not yet have a clinically available inhibitor. Many MBL inhibitors have been reported in the literature since the mid-1990's, although none of them have been developed for clinical use. Combination therapy of aztreonam with avibactam is currently being explored by Pfizer in phase 3 clinical trials as a potential treatment for complicated intra-abdominal infections and pneumonia (ventilator associated or hospital acquired) involving bacteria that co-express SBLs and MBLs.³⁹³ This strategy exploits a gap in the MBL substrate profile, their inability to hydrolyze

monobactams, while protecting the antibiotic from the SBLs that can degrade it with avibactam. *In vitro* studies on over 60 000 clinical isolates from 40 countries have shown that the aztreonam and avibactam combination is a potent combination against MBL-producing *Enterobacteriaceae* and *P. aeruginosa*.³⁹⁴ Despite the promise of a treatment for MBL-producing infections in the near future, the pursuit of an MBL inhibitor (for combination therapy with carbapenems) continues to be an important area of research. The following section covering MBL inhibitors is by no means exhaustive but covers many of the main themes in MBL inhibitor development; several excellent reviews exist in the literature.^{27,395–398} Common strategies for MBL inhibition involve completely or partially demetallating the active site with chelators, binding the zinc ions with dicarboxylates or sulphur groups without metal ion removal. Inhibitors have either been designed rationally or been discovered by screening natural product or known chemical libraries for activity using high-throughput methods.

1.4.3.1 Demetallating chelators

When trying to inactivate a protein that uses metal ions to perform its catalytic function, an obvious strategy is to remove the metal from the protein. For decades, this has been used in the classification of β -lactamases as MBLs since only the MBLs would be inactivated by EDTA.³⁹⁹ Although EDTA is adequate as a characterization tool, EDTA inactivation of MBLs often requires hours of incubation which, in combination with its promiscuity, makes it a poor drug candidate. Other common commercial chelators such as o-phenanthroline, PAR, TPEN, and DPA have been investigated as inactivators of IMP-1 although even the most effective of these inactivators, DPA, had only removed one zinc ion from 13% of the IMP-1 molecules after 3 hours of incubation.⁴⁰⁰

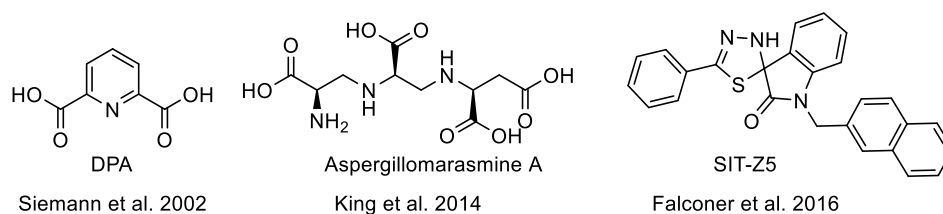


Figure 1.16 Demetallating inhibitors of MBLs. ^{400–402}

More recently, a natural product, Aspergillomarasmine A (AMA), was found to be a potent inactivator of NDM-1 and VIM-2, capable of removing one zinc ion from NDM-1 in as little as one hour. While AMA was shown to potentiate meropenem against NDM and VIM producing bacterial strains, it was much less effective against strains that produce AIM, IMP, or SPM – type MBLs,

making it a relatively narrow-spectrum MBL inactivator.⁴⁰¹ The same group also discovered the potential for spiro-indolino-thiadiazoles (SIT) to inactivate MBLs with IC₅₀s for NDM-1 as low as 6.6 μM. Despite the favourable response from NDM-1, VIM-2 and IMP-7 were unaffected by even the most potent compound from this series, SIT-Z5, likely due to their zinc ions being more tightly bound.^{402–405} Demetallating chelators pose problems for clinical use since compounds that are potent enough to pull the zinc ions out of MBLs will potentially have toxicity problems in humans and those that are weak enough to be non-toxic have very narrow-spectrum activity. As a potentially less toxic alternative to demetallating chelators, inhibitors that can bind the zincs rather than remove them are desirable.

1.4.3.2 Dicarboxylates

The earliest MBL inhibitors in this class were the succinic acid derivatives, the most potent of which is 1-9 (Figure 1.17). This compound was reported to be an extremely potent inhibitor of IMP-1 with an IC₅₀ of 3 nM, although neither the article nor the patent that disclose this compound address its ability to inhibit other MBLs.^{406,407} Further analogs of the succinic acids have been pursued by chemists at Merck who have proven that these compounds can potentiate meropenem against *E. coli* strains transformed with an IMP-1 expressing plasmid, although none of those compounds approach the potency of 1-9.⁴⁰⁸ Olsen et al. explored the inhibitory potency of analogs of 1-9 with BcII and L1 and did not observe inhibition, suggesting that these compounds may not have a sufficiently broad-spectrum to be clinically useful.⁴⁰⁹

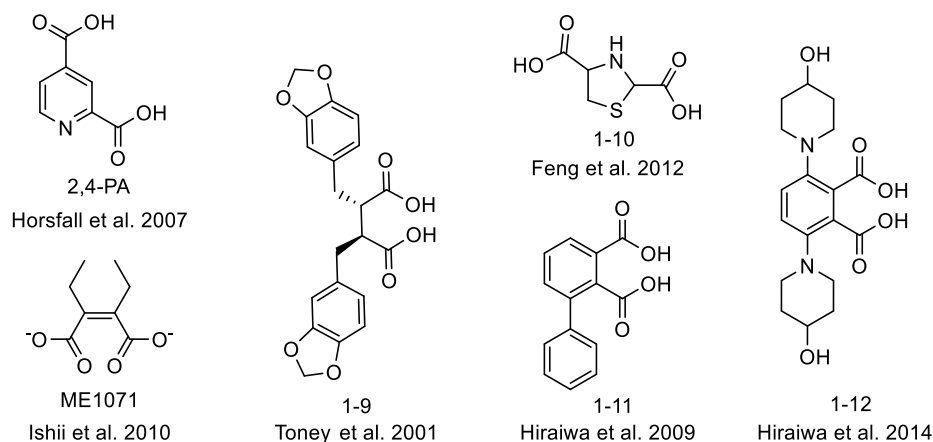


Figure 1.17 Dicarboxylate inhibitors of MBLs.^{406,410–414}

The succinic acid derivatives have flexibility in the bond connecting the carboxylic acid groups, although this is not necessary as several conformationally rigid dicarboxylates have been found to be MBL inhibitors. DPA (2,6-PA), which is capable of abstracting one zinc ion from IMP-1 at long incubation times, also inhibits MBLs in a time dependent competitive manner at short incubation times.^{400,415} Horsfall et al. demonstrated that other substitution patterns of DPA are also inhibitory, notably 2,4-PA which inhibits the B2 MBL CphA with a K_I of 5 μM but has little effect on B1 and B3 MBLs. Their study also demonstrated that the monocarboxylate, 2-picolinic acid, is capable of partially inhibiting all MBL subclasses at 100 μM .⁴¹⁰ Feng et al. explored nitrogen containing heterocycles as MBL inhibitors, and found that those with carboxylate groups on either side of the nitrogen (such as 1-10) were inhibitors of all MBL subclasses with IC_{50} s of compound 1-10 ranging from 0.64 μM to 7.1 μM .⁴¹³

Although the nitrogen in the picolinic acid derivatives is advantageous for zinc binding (see Chapter 3 for more details), it is not a necessary feature for the aromatic dicarboxylate inhibitors. Researchers at Meiji Seika pharmaceuticals have demonstrated that dicarboxylate inhibitors derived from phthalic acid such as 1-11 and 1-12 are capable of inhibiting IMP-1. Although the IC_{50} s for 1-11 and 1-12 (0.97 μM and 0.27 μM respectively) indicate that these are much more potent than the DPA derivatives, they have only been tested against IMP-1, so it is unknown whether or not these represent broad-spectrum MBL inhibitors.^{411,414,416}

Another discovery in this area at Meiji Seika pharmaceuticals is ME1071, a maleic acid derivative that has been demonstrated inhibit IMP-1, VIM-2, and NDM-1. The inhibition constants determined for ME1071 remains consistent between publications for IMP-1 ($K_I = 0.41 \mu\text{M}$ or $0.46 \mu\text{M}$); however, that of VIM-2 varies greatly ($K_I = 120 \mu\text{M}$ or $1 \mu\text{M}$), while that of NDM-1 has only been reported once ($K_I = 24 \mu\text{M}$). When correlated with the bacterial data, it becomes clear that this compound is most active against IMP variants and least active against NDM variants.^{412,417}

1.4.3.3 Sulphur Containing Inhibitors

The affinity of sulphur compounds for zinc ions is one of the fundamental relationships in biology, allowing for zinc binding to proteins through cysteine containing zinc fingers, the Lewis acidity of zinc ions in proteins, some forms of redox activity, and much more.⁴¹⁸ This relationship can also be exploited for inhibition of proteins, such as MBLs, that use zinc in their catalysis.

The most common sulphur moiety used in MBL inhibitors is the thiol (Figure 1.18) which often accompanies a carboxylate. Early mercaptocarboxylates identified as MBL inhibitors included compound 1-13 and R-thiomandelic acid, both of which were inhibitors of multiple subclasses of MBL with submicromolar IC_{50} s and K_i s respectively.^{251,419} In 2003, members of the Dmitrienko lab tested the inhibitory potential of 23 commercial thiols, the most potent of which was mercaptoacetic acid against IMP-1 and also inhibited BcII 5/B/6 and CcrA. This study concluded that thiols with an α -carboxylate (or similar anionic group) were classical competitive inhibitors, while those without an anionic group behave as time-dependent competitive inhibitors under neutral conditions due to the deprotonation necessary to make the most stable EI complex. Additionally, it was observed that esterifying the carboxylates, adding an amine, and using an aromatic molecule as the core structure all reduced inhibitory potency against IMP-1.⁴²⁰ Jin et al. found that using aliphatic chains to distance the thiol from an aromatic group increased potency as compound 1-14 from Figure 1.18 exhibits IC_{50} s of 1.2 μ M and 1.1 μ M with IMP-1 and VIM-2 respectively while the equivalent compound with only one carbon between the phenyl ring and the carboxylate had IC_{50} s of 16.4 μ M and 14.3 μ M respectively.⁴²¹

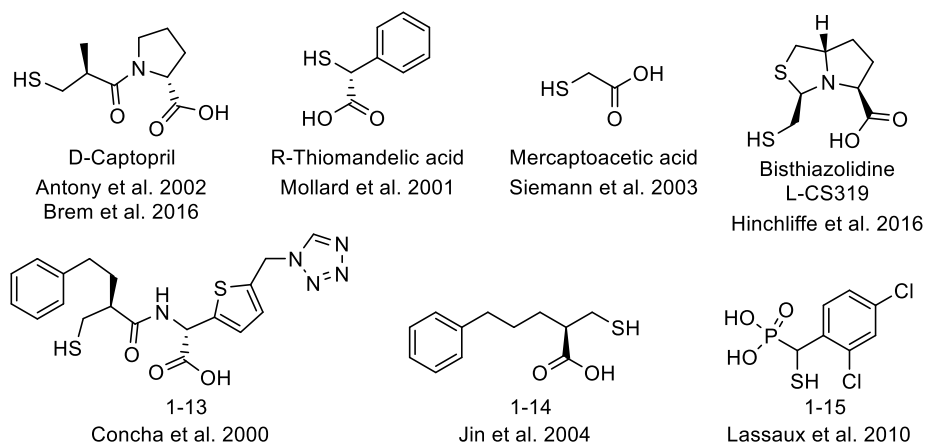


Figure 1.18 Thiol inhibitors of MBLs. ^{251,419–425}

The most thoroughly studied MBL inhibitor is captopril, a known inhibitor of angiotensin-converting enzyme (ACE) in humans that has been used for many years to treat hypertension.⁴²⁶ Two stereoisomers of captopril have been used in most investigations: D-captopril (Figure 1.18) and L-captopril, referring to the stereochemistry of the proline ring. Crystal structures of MBLs have been acquired with both stereoisomers bound; however, the D-isomer is frequently the more potent

inhibitor (2- to 61- fold more potent) and consequently generates higher occupancy crystal structures of the enzyme-inhibitor complexes.^{423,427} Although D-captopril is able to inhibit enzymes in all subclasses of MBL, some MBLs such as SPM-1 (B1) and FEZ-1 (B3) are resistant to inhibition.^{256,423} Additionally, D-captopril does not bind to all MBLs in the same manner: the sulphur atom binds between the zinc atoms in all MBLs except in the monozinc CphA (B2) in which the carboxylate binds the zinc atom as seen in Figure 1.19E. Binding even differs within subclasses, for example the B1 MBLs BcII (Figure 1.19A) and VIM-2 (Figure 1.19B) bind in very similar modes with the proline ring stacked over the His residue that coordinates Zn2 (His240) and the carbonyl H-bonded to Asn210 whereas in IMP-1 (Figure 1.19C) the Asn210 interaction is weaker (4.4 Å as opposed to <3 Å) but the tryptophan on the capping loop, Trp45, makes the proline stacking tighter.⁴²³ The most different of the B1 MBL structures is BlaB (Figure 1.19D) in which the proline ring sits over one of the histidine residues that coordinates Zn1 (His118) rather than the His residue that coordinates Zn2 (His 240).⁴²⁸ The two structures of B3 MBLs differ greatly since L1 (Figure 1.19F) is inhibited by D-captopril with a K_I of 8 μM , corresponding to D-captopril binding the active site tightly, whereas FEZ-1 (Figure 1.19G) is only weakly inhibited with a K_I of 400 μM and in the crystal structure, D-captopril is well removed from the active site.^{255,256}

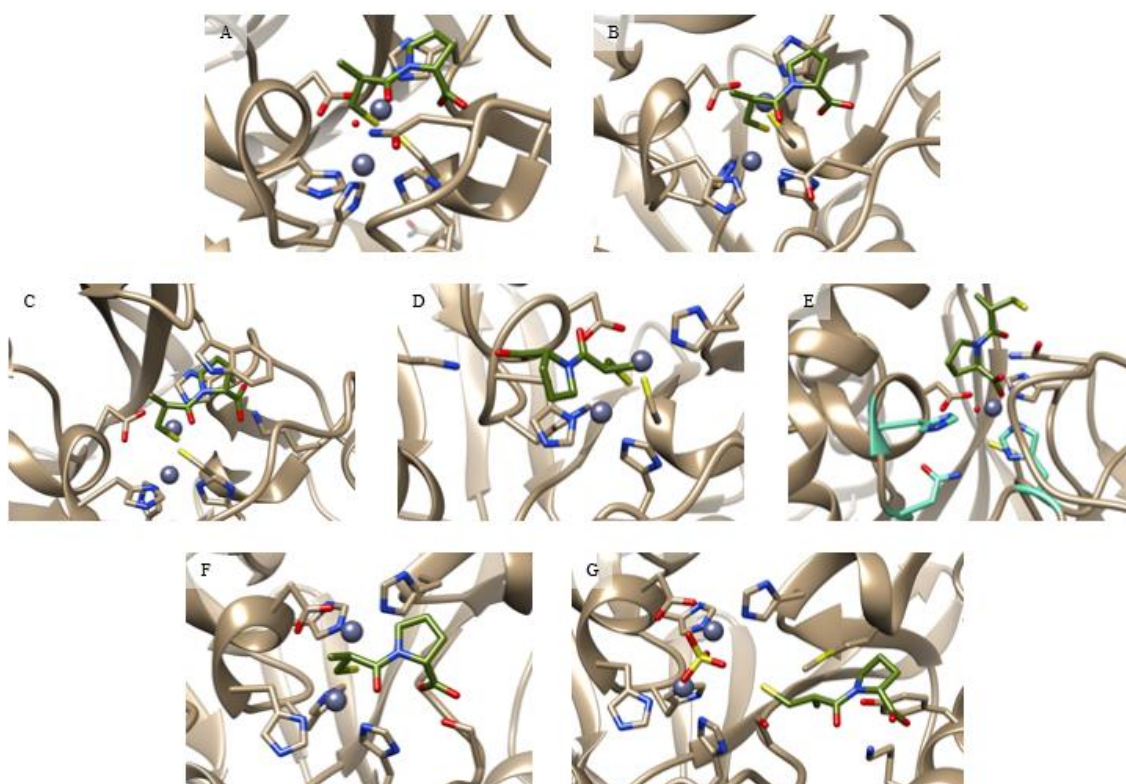
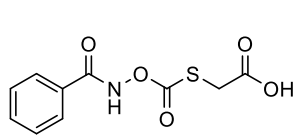


Figure 1.19 D-Captopril bound to various MBLs from all subclasses : B1 MBLs (A) BcII, (B) VIM-2, (C) IMP-1, (D) BlaB, the B2 MBL (E) CphA with the putative Zn1 binding site highlighted in blue, and the B3 MBLs (F) L1, and (G) FEZ-1 (This figure was generated using UCSF Chimera v. 1.12 from protein databank files 4C1C, 4C1E, 4C1G, 1M2X, 2QDS, 2FU8, and 1JT1 respectively).^{255,256,423,428,429} All structures are oriented with Zn1 (or equivalent binding site) towards the bottom of the image.

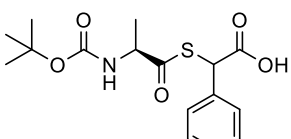
Recent work on thiol inhibitors of MBLs has focused on taking advantage of their ability to inhibit all subclasses of MBL and reducing the *in vivo* toxicity. The mercaptophosphonate 1-15 (Figure 1.18) addressed cross-class inhibition of MBLs by introducing a phosphonate which coordinates the zinc ion of CphA in a tetrahedral geometry while also making contacts with nearby His and Lys residues (PDB: 3IOG) while the thiol is predicted to bind the zincs in the B1 and B3 enzymes as observed for D-captopril.⁴²⁴ The bisthiazolidines, particularly L-CS319 (Figure 1.18), were shown to inhibit all subclasses of MBL with K_{iS} ranging from 0.26 μM to 41 μM with most K_{iS} being in the low micromolar range for the 7 tested MBLs (B1: NDM-1, VIM-2, IMP-1, BcII; B2: Sfh-1; B3: L1, GOB-18). Crystal structures of Sfh-1 (B2) and L1 (B3) were obtained with L-CS319 and showed the

17 inhibited BcII and CfiA with IC_{50} s of 23 μ M and 724 μ M respectively in the presence of 1 μ M zinc and all inhibition was abolished when the Zn^{2+} concentration was increased to 100 μ M. Although it was weakly effective against B1 MBLs, this inhibitor was very potent against L1 with an IC_{50} of less than 1.9 μ M in high and low zinc conditions.⁴³⁶ Compound 1-18 was developed by Merck scientists as a potent IMP-1 inhibitor ($IC_{50} = 0.0004 \mu$ M), although their publications are inconsistent about the stereochemistry of the active inhibitor.^{437,438} The stereochemistry denoted in Figure 1.20 is consistent with the Greenlee paper which actually addresses the differences in the activity of the R and S isomers.⁴³⁷ The extreme potency of 1-18 against IMP-1 (B1) did not translate to the only other MBL tested, CcrA (B1), which has an IC_{50} of only 180 μ M.^{437,438} No crystal structures have been published with a thioester inhibitor bound to an MBL.

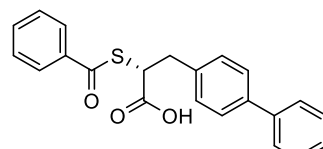
Thioesters



Payne et al. 1997
FEMS Microbiol Lett

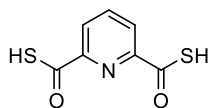


Payne et al. 1997
Antimicrob Agents Chemother

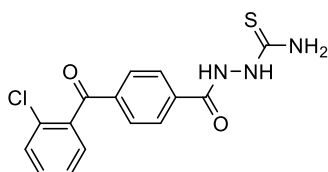


Greenlee et al. 1999

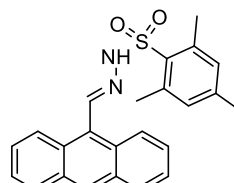
Other



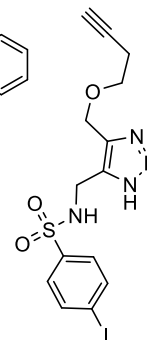
Thiocarboxylate
Roll et al. 2010



N-acylated thiosemicarbazide
Faridoon et al. 2012



N-Arylsulfonyl hydrazone
Siemann et al. 2002



Sulfonyl triazole
Minond et al. 2009

Figure 1.20 Thioester and other non-thiol MBL inhibitors that contain sulphur. ^{435-437,439-442}

Other MBL inhibitors have been discovered with sulphur containing moieties, some of which fit better into the other categories laid out in this section such as the demetallating chelator SIT-Z5 from Figure 1.16 and the dicarboxylate 1-10 from Figure 1.17.^{402,413} Inspired by the inhibition of MBLs with DPA and thiols, Roll et al. investigated the inhibition of CcrA (B1) and L1 (B3) with thioacid and methyl thioester derivatives of DPA and found that PDTC (Figure 1.20) is the most potent inhibitor of these two MBLs with IC_{50} s of 0.14 μ M and 0.6 μ M respectively.⁴³⁹ Faridoon et al. used fragment-based screening to suggest that 3-mercapto-1,2,3-triazoles and N-acylated thiosemicarbazides could be inhibitory towards IMP-1. After investigation of several compounds from each group, they

determined that the triazoles were not inhibitory and the thiosemicarbazoles were moderate inhibitors. The most potent inhibitor from this series, 1-19 in Figure 1.20, inhibited IMP-1 with a K_I of 14 μM which is comparable to the inhibitory potency of L-captopril.⁴⁴⁰

Two groups of inhibitors have been published with sulfones as a key feature of their structure: the N-arylsulfonyl hydrazones (1-20 in Figure 1.20) and sulfonyl triazoles (1-21 in Figure 1.20).^{441,442} The N-arylsulfonyl hydrazones were developed as IMP-1 inhibitors, the most potent of which (1-20) inhibited IMP-1 with an IC_{50} of 1.6 μM . These inhibitors were unfortunately not broad-spectrum as many in this series were unable to inhibit BcII 5/B/6, and even 1-20 only elicited 30 % inhibition at 25 μM .⁴⁴¹ The sulfonyl triazoles were discovered as VIM-2 inhibitors using high-throughput screening of a click-chemistry library, the most potent compound in this series, 1-21, inhibited VIM-2 in a competitive manner with a K_I of 0.41 μM ($\text{IC}_{50} = 3.3 \mu\text{M}$) but was uninhibitory towards IMP-1.⁴⁴² Compound 1-21 was used as a lead to develop a more potent inhibitor which was able to inhibit VIM-2 with a K_I of 0.01 μM but all 47 compounds developed in this series were uninhibitory towards IMP-1.⁴⁴³

1.4.3.4 Other Metallo- β -Lactamase Inhibitors

Identification of structurally unique inhibitors of MBLs occurs primarily through screening large databases of natural products, pharmaceuticals, and chemical collections from pharmaceutical companies. Scientists from GlaxoSmithKline screened their natural products database and identified three tricyclic natural products as MBL inhibitors, the most potent of which is SB236049 which inhibits BcII (B1) and CfiA (B2) with IC_{50} s of 0.3 μM and 2 μM respectively. This compound was not as effective against IMP-1 ($\text{IC}_{50} = 151 \mu\text{M}$) and all three compounds in this series were inactive against L1 (B3).⁴⁴⁴ Chemists at Merck screened their chemical collection to identify biphenyl tetrazoles as inhibitors of MBLs, the most potent derivative of which was L-161,189 which inhibited a CcrA (B1) with an IC_{50} of 0.3 μM .⁴⁴⁵

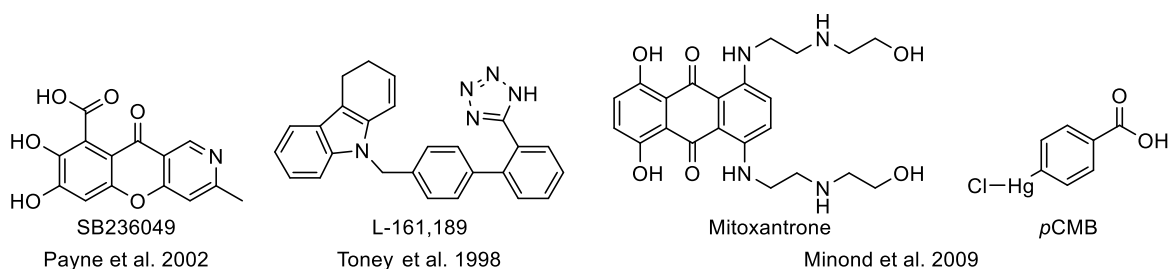


Figure 1.21 Structurally unique MBL inhibitors. ^{442,444,445}

Minond et al. screened a collection of pharmacologically active compounds to identify inhibitors of VIM-2. They found mitroloxantrone (Figure 1.21), a DNA intercalator and topoisomerase II α inhibitor used to treat advanced multiple sclerosis and certain cancers, to be an uncompetitive inhibitor of VIM-2 ($K_I = 1.5 \mu\text{M}$) and uninhibitory towards IMP-1.^{442,446-449} The other pharmacologically active compound identified from the screen as a VIM-2 inhibitor was para-chloromercuribenzoate (*p*CMB) which is known to react with cysteine residues. *p*CMB inhibits both VIM-2 and IMP-1, likely by covalently modifying the cysteine that coordinates Zn²⁺ (Cys172 in VIM-2, Cys158 in IMP-1).^{260,442}

Inhibitors of metallo- β -lactamases vary widely in structure and specificity. Many of the inhibitors presented in this section were only tested against one or two MBLs and do not offer any insight into whether or not they would be useful as broad-spectrum inhibitors. Of those that were tested widely, the thiol (particularly the mercaptocarboxylates) and dicarboxylate functionalities had the broadest spectrum of inhibition. The mercaptophosphonate 1-7 in Figure 1.18 introduces a phosphonate into a thiol inhibitor, a novel solution to the problem of thiols being less inhibitory towards B2 MBL. The dithioacid derivative of DPA (PDTC) in Figure 1.20 is also an interesting approach to that problem, potently inhibiting both a B2 and B3 MBL. The phosphonate and thioacid moieties are understudied in the literature considering their potential to be broadly inhibitory: this thesis addresses furthering the understanding of the prospects for these functionalities in MBL inhibitors (see Chapter 3 and Chapter 4 respectively).

1.4.4 Dual Serine- and Metallo- β -Lactamase Inhibitors

Although it is useful to inhibit either SBLs or MBLs, this poses a challenge for clinical applications against pathogens that produce both types of β -lactamases. It is challenging enough to get combination therapies involving only two compounds approved but is significantly more difficult to get approval for a three-compound combination (antibiotic, SBL inhibitor, MBL inhibitor). Ideally, a dual serine- and metallo- β -lactamase inhibitor would be administered in combination with a broad-spectrum β -lactam (such as meropenem) which would protect it from all β -lactamases. The only dual SBL/MBL inhibitors that have been discovered are the cyclic boronates, notably CB-1 and CB-2 (Figure 1.22).^{450,451}

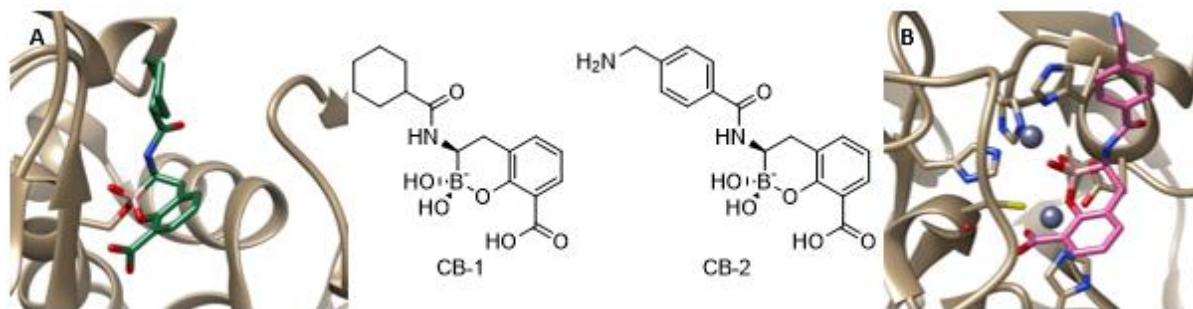


Figure 1.22 Structural evidence for cyclic boronate inhibition of SBLs and MBLs exemplified by CB-1 bound to the SBL CTX-M-15 (A) and CB-2 bound to the B1 MBL VIM-2 (B). This figure was generated using UCSF Chimera v. 1.12 from protein databank files 5T66 and 5FQC.^{450,451}

Kinetic studies on the cyclic boronates CB-1 and CB-2 have determined that while both show activity against SBLs and MBLs, CB-1 is more potent against SBLs and CB-2 is more potent against MBLs.⁴⁵¹ Crystal structures of CTM-M-15 (PDB: 5T66) and OXA-10 (PDB: 5FQ9) have been determined with CB-1 bound, and VIM-2 (PDB: 5FQC) and BcII (PDB: 5FQB) have been determined with CB-2 bound (Figure 1.22).^{450,451} The crystal structures of the SBLs illustrated that the inhibition of SBLs occurs through nucleophilic attack of the boronate by the catalytic serine (Ser73 in CTX-M-15) forming a covalent adduct.⁴⁵⁰ In binding the MBLs, such as VIM-2, CB-2 was found to coordinate Zn1 with both boronate hydroxyl groups and Zn2 with the oxygen in the ring.⁴⁵¹ Although the cyclic boronate pharmacophore is capable of being inhibitory towards both SBLs and MBLs, not all cyclic boronates behave in this manner. The newly FDA approved β -lactamase inhibitor Vaborbactam (Figure 1.14) is a cyclic boronate with activity against only Class A and C β -lactamases as covered in 1.4.2.3.³⁷⁵

1.5 Clinical Significance of β -Lactamase Inhibition

Combination therapy with the mechanism-based inhibitors has proven to be a useful strategy for combating β -lactam resistance in bacteria that express certain SBLs although resistance to these inhibitors is already prevalent. The recent introductions of Avibactam and Vaborbactam into clinical use have addressed resistance from many, but not all, SBLs including some ESBLs. These solutions to an ever-growing problem provide hope that β -lactams can remain a viable option for antimicrobial therapy for decades to come. The biggest threat to β -lactams as a therapeutic option is the increasingly widespread expression of MBLs which are capable of breaking down last-line of defense

β -lactams, such as the carbapenems, and are unaffected by the current SBL inhibitors. Metallo- β -lactamase inhibitors are necessary for the future of antimicrobial therapy, especially in the light of increasingly common multidrug resistant pathogens. Ideally, novel β -lactamase inhibitors should aim to inhibit both SBLs and MBLs since it is not uncommon for resistant pathogens to express multiple β -lactamases from both mechanistic families.

Inhibition of PBPs and β -lactamases – specifically metallo- β -lactamases – is crucial for treating increasingly problematic resistant pathogens. This work explores the potential use of several classes of MBL inhibitors and inhibitor releasing cephalosporins in increasing the efficacy of clinical antibiotics, such as meropenem, against β -lactamase-producing pathogens.

Chapter 2

Phylogenetic Analysis, Purification, and Biochemical Characterization of β -Lactamases

2.1 Introduction

The objective of the research described in this chapter was to overexpress and purify adequate amounts of a variety of β -lactamases for kinetic testing and to characterize their ability to hydrolyze chromogenic cephalosporins as well as their stability to organic co-solvents commonly used in kinetic assays. While the hydrolysis of any β -lactam can be detected using spectrophotometry, it is advantageous to use chromogenic substrates that exhibit larger changes in absorbance in the visible range rather than the UV range upon hydrolysis of the β -lactam bond. This means that these substrates can be assayed in affordable 96-well plates made of polystyrene rather than those made from quartz or expensive UV-transparent plastics. An additional benefit of the assay wavelength being relatively high is that it is uncommon for other compounds in the assay, such as cosolvents or inhibitors, to interfere with the assay as they typically absorb only in the UV range.

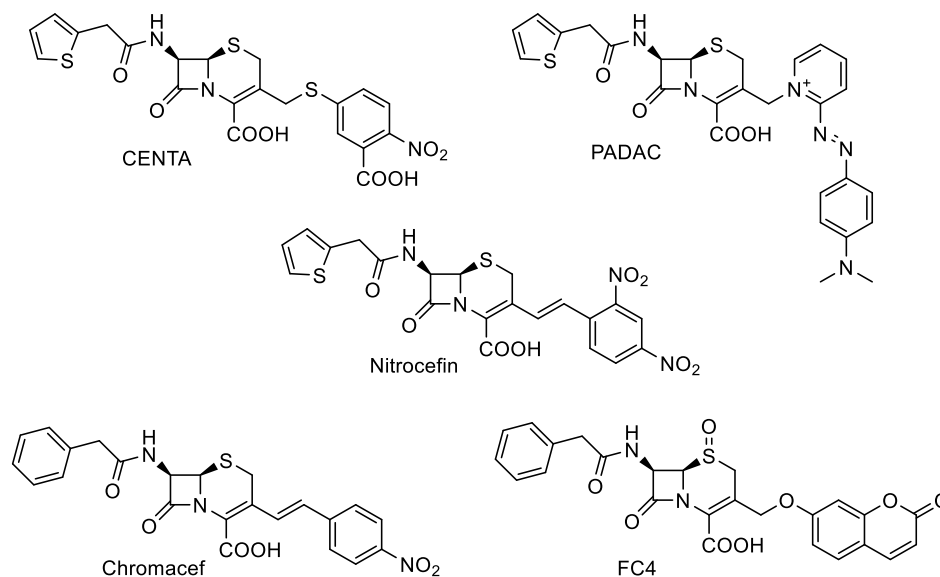
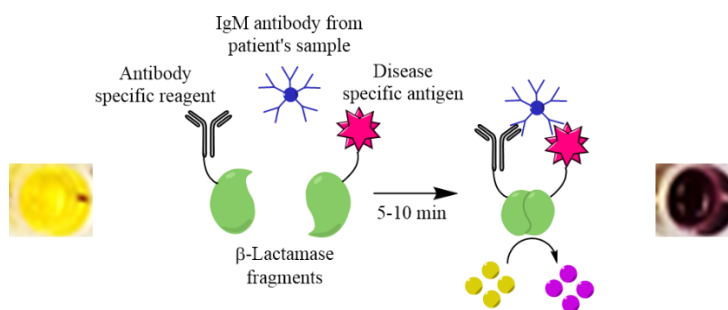


Figure 2.1 Chromogenic and fluorogenic substrates for β -lactamases excluding the UW series substrates.

In the 1970s and early 1980s, several chromogenic β -lactams were developed (eg. nitrocefin, PADAC, and CENTA (Figure 2.1)). PADAC is no longer commercially available and nitrocefin has become the chromogenic substrate of choice.^{310,312–314,452} A drastic increase in the cost of nitrocefin in the early 2000's motivated another surge of chromogenic β -lactam development resulting in Chromacef and the fluorogenic FC4 (Figure 2.1).^{315,317,453}



Scheme 2.1 Panbio homogeneous immunoassay technology.⁴⁵⁴

The Dmitrienko group, in collaboration with Panbio, undertook the development of a series of chromogenic cephalosporins that could be used in a homogeneous immunoassay pictured in Scheme 2.1. In a homogeneous immunoassay, β -lactamase fragments that are independently inactive are tethered to an antibody and a disease specific antigen. Upon binding to IgM from a patient's sample, the β -lactamase fragments are brought together into their active form, catalyzing the hydrolysis of a chromogenic cephalosporin.⁴⁵⁴ The substrates used for this assay need to have a more distinct colour change than provided by nitrocefin hydrolysis and must be more cost effective. The Dmitrienko lab pursued several strategies to make a better chromogenic cephalosporin, finally yielding the UW series of substrates: UW-57, UW-58, and UW-154 (Figure 2.2).

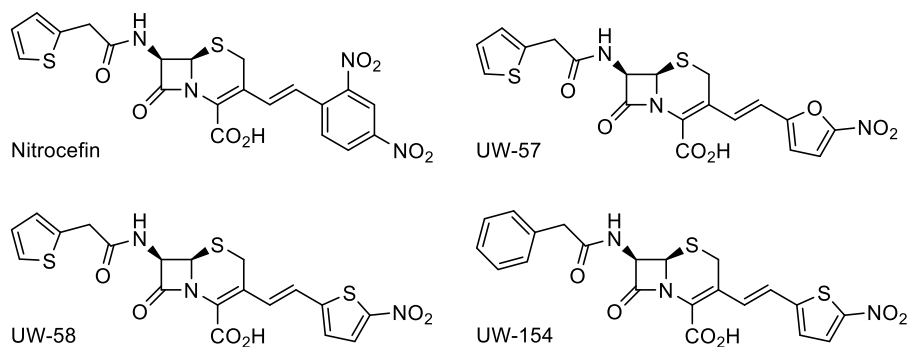


Figure 2.2 Chromogenic β -lactamase substrates synthesized by the Dmitrienko group.

The UW series of substrates have the advantage of a shorter and more cost effective synthetic method while maintaining similar kinetic parameters to nitrocefin with many β -lactamases. In some cases, the kinetic parameters of the UW substrates make them better for kinetic assays than nitrocefin through either raising the K_M sufficiently to make substrate depletion less of a problem in assays performed at K_M concentrations, or higher k_{cat} values which require less enzyme to achieve reasonable rates, allowing savings on precious enzyme stocks.

2.2 Methods

Unless otherwise stated, all spectrophotometric readings were done using a SpectraMax 190 plate reader (Molecular Devices, Sunnyvale, CA) with SoftMax 6.0 (Molecular Devices, Sunnyvale, CA) software. Analysis of kinetic data was performed using GraphPad Prism 5.00 for Windows (GraphPad Software, San Diego, CA). The 96-well plates were always clear, flat bottomed, polystyrene plates and were purchased from either Corning (Corning, NY) or Greiner Bio-One (Monroe, NC) for enzyme kinetics. Plates for bacteria experiments were purchased from either Corning (Corning, NY) or Sarstedt (Nümbrecht, Germany). Initially, cation adjusted Mueller Hinton broth powder was purchased from Sigma (Burlington, MA) when problems with inconsistency were encountered between batches late in 2017, the supplier was changed to BD (Franklin Lakes, NJ). Other bacterial media components were purchased from BioBasics (Markham, ON). Most buffer salts were purchased from BioShop (Burlington, ON), phosphate buffer salts from Alfa Aesar (Haverhill, MA), and other chemicals from companies now owned by MilliporeSigma (Burlington, MA) such as EMD and Sigma. The dialysis membrane used throughout was SpectraPor dialysis membrane with a 6-8 kDa molecular weight cutoff from the Spectrum labs division of Repligen (Waltham, MA).

2.2.1 Protein Sequence Alignment

The protein sequences of IMP-1, NDM-1, and VIM-2 were acquired from the NCBI Database in FASTA form and entered into the BLAST Explorer functionality of phylogeny.fr which searched the NCBI database prior to 9 Nov 2017 for similar, non-redundant protein sequences.^{455,456} The 100 closest matches were displayed and the whole protein sequence for every variant within that family was selected to make a phylogenetic tree using the “One Click” tool. A check was done to ensure all variants with sequences in the NCBI database as of 20 Jan 2018 were in the data set, and any variants that were missing were manually added to the data set prior to tree generation. The “One Click” analysis tool aligned sequences using MUSCLE, curated these results with Gblocks, determined

phylogenetic relationships with PhyML. The phylogenetic tree was rendered with TreeDyn.⁴⁵⁷⁻⁴⁶¹ The sequence alignment was downloaded as a Clustal file then formatted using BioEdit v. 7.0.5.3.⁴⁶² Formatting of the phylogenetic tree was done using both the TreeDyn web applet on phylogeny.fr and the TreeDyn v. 198.3 desktop program.

2.2.2 Enzyme Purification

Characterization of the inhibition of serine- and metallo- β -lactamases by PMPCs (Chapter 3) necessitated the purification and acquisition of a variety of enzymes. Pure protein samples of the MBLs IMP-1, L1, and SFH-1 as well as the SBL OXA-23 were generous gifts from Dr. James Spencer of the School of Cellular and Molecular Medicine at the University of Bristol. Dr. Spencer also provided expression plasmids for VIM-1 and OXA-48. Two batches of pure SPM-1 were obtained; one from Dr. Spencer, and the other from Dr. Christopher Schofield of the Department of Chemistry at the University of Oxford. The experiments presented in this thesis were performed with Dr. Schofield's SPM-1 preparation. NDM-1 with the first 41 amino acids truncated including the signal peptide and the 13 amino acids that follow it, from the Schofield group at the University of Oxford was used throughout these studies.³¹⁷ Dr. Natalie Strynadka of the Department of Biochemistry and Molecular Biology at the University of British Columbia provided the expression plasmid for CTX-M-15 and pure NDM-1 stocks that were used in preliminary experiments not presented in this work. Expression plasmids for VIM-2, GC-1, and KPC-2 were provided by Dr. Patrice Nordmann of L'Université Paris-Sud, Dr. Michiyoshi Nukaga of Josai International University in Togane City, Chiba, Japan, and Dr. Focco van den Akker of Case Western Reserve University respectively. Purification of proteins was carried out with the assistance of Dr. Geneviève Labbé and various undergraduate research students as part of their projects.

2.2.2.1 Preparation for Protein Purification

Media for Bacterial Cultures

Luria-Bertani (LB) and Terrific broth (TB) were made using standard recipes from Molecular Cloning Laboratory Manual 2nd Ed. with tryptone, yeast extract, and NaCl. Salts for buffering TB were prepared separately from the media and added after autoclaving.⁴⁶³

Calcium chloride competent E. coli for Transformation

LB broth (5 mL) was inoculated with 50 μ L *E. coli* cells (BL21, BL21 DE3, or BL21 PLYS as appropriate) and incubated overnight at 37 °C shaking at 225 rpm. The overnight culture was inoculated into fresh LB in a ratio of 1:20 (culture:media) and shaken at 225 rpm at 37 °C until the OD was between 0.25 and 0.3 (approximately 1.5 hr) the chilled on ice for 15 min. Cells were isolated by centrifugation in sterile 50 mL conical vials at 1600 xg for 10 min at 4 °C. The supernatant was decanted and discarded. Cells were resuspended and pooled in 30 mL cold 0.1 M CaCl₂ and allowed to accommodate for 30 min on ice. Centrifugation and resuspension were repeated twice as previously described. The final resuspension was performed with 6 mL cold 0.1 M CaCl₂ in 15 % glycerol which was then aliquoted and flash frozen on dry ice for storage at -80 °C.

2.2.2.2 Analysis of Protein Purification

Nitrocefin Activity Assay

Aliquots of protein collected during purification were diluted as appropriate in the buffer used in the respective purification step and incubated in a flat bottom 96 well plate at 30 °C for 5-10 min before addition to nitrocefin (final concentration 100 μ M for GC-1, and 25 μ M for CTX-M-15). The activity was determined by monitoring this reaction at 482 nm for 5 min at 30 °C and measuring the initial rate. At least two replicates of this assay were generally performed.

Bradford Assay

A standard curve of bovine serum albumin (BSA) from 0.05 mg/mL to 0.5 mg/mL was made fresh each day. Four technical replicates of standards and appropriately diluted samples were simultaneously incubated with Bradford reagent (BioRad, Hercules, CA) in a 96 well plate for 5 min at room temperature. The absorbance was then read at 595 nm using either a Powerwave XS2 (BioTek) plate reader or the SpectraMax 190.

SDS PAGE

Protein samples or diluted protein samples were added to 5x SDS PAGE loading buffer (0.25 M Tris-HCl, 10 % SDS, 5 % 2-mercaptoethanol, 30 % glycerol, 0.02 % bromophenol blue, pH 6.8) then boiled for 5 min. If condensation was observed on the lid of the tubes, they were centrifuged briefly. The prepared sample (10-20 μ L) was loaded onto 12.5 % polyacrylamide:bisacrylamide gel and run at 200 V with a low molecular weight protein standard (GE Healthcare UK, Buckinghamshire, UK or BioBasic, Markham, ON) in at least one of the wells. Gels were stained with Coomassie Blue

(BioRad, Hercules, CA) containing stain (50 % (v/v) methanol, 10 % (v/v) acetic acid, 0.025 % (w/v) Coomassie Blue R-250) then destained with 50 % methanol, 10 % acetic acid. Gels were soaked in water prior to visualization using either the white plate with a Gel Doc EZ Imager (BioRad, Hercules, CA) or a camera. Purification of all β -lactamases in this chapter was monitored using SDS PAGE. Gels from individual purifications will not be presented in this work, only a summary gel.

Mass Spectrometry

The molecular weights of purified proteins were determined by electrospray ionization mass spectrometry (ESI-MS) in positive ion mode at the University of Waterloo Mass Spectroscopy Facility. Pure proteins with their affinity tags cleaved were exchanged into 20 mM ammonium acetate using Amicon Ultra Ultracel 10 K membrane centrifugal filters (Millipore). VIM-2 and KPC-2 were then appropriately diluted in 1:1 MeOH:H₂O, 0.2 % FA and injected into the Micromass Q-TOF Ultima Global mass spectrometer equipped with a Z-spray electrospray ionization source (Micromass) with the aid of a syringe pump. CTX-M-15, GC-1, NDM-1 (received from the Schofield group at Oxford), SPM-1 (received from the Spencer group at Bristol), L1 (also received from Spencer), and OXA-48 were appropriately diluted in 1:1 MeOH:H₂O, 0.1 % FA then injected into the Thermo Scientific Q-Exactive Orbitrap mass spectrometer (Thermo Fisher Scientific Inc.) by electrospray ionization with the aid of a syringe pump. Protein deconvolution was done using Thermo Protein Deconvolution v. 1.0 (Thermo Fisher Scientific Inc.).

2.2.2.3 CTX-M-15

The transformation and purification of CTX-M-15 was done with the assistance of Jessica Duong as part of her undergraduate research.

Transformation

The cloning of CTX-M-15 into a pET28 vector with a thrombin cleavable N-6His tag was performed by Dr. Strynadka's lab before being sent to the Dmitrienko lab. The CTX-M-15 plasmid was transformed into CaCl₂ competent *E. coli* BL21 DE3 cells by incubating them together for 40 min on ice before heat shocking at 42 °C for 1.5 min. The cells were allowed to recover from transformation with the addition of 200 μ L of LB media then incubated for 2 hours at 37 °C. Transformants were plated on LB agar supplemented with 50 μ g/mL kanamycin and incubated overnight at 37 °C then stored at 4 °C until ready to proceed to liquid cultures.

Growth of Liquid Cultures for CTX-M-15 Expression

One colony from the CTX-M-15 transformation was inoculated into 50 mL TB media supplemented with 50 µg/mL kanamycin which was incubated at 37 °C overnight, shaking at 200 rpm. Two 4 L flasks containing 1 L TB media supplemented with 50 µg/mL kanamycin were inoculated with 10 mL each of the overnight culture then incubated at 37 °C, shaking at 220 rpm until the culture had reached an OD₆₀₀ of approximately 0.9 (this should have been 0.6, but was overgrown). Expression of CTX-M-15 was then induced with 1 mM isopropyl β-D-1 thiogalactopyranoside (IPTG) overnight, shaking at 200 rpm at room temperature. Cells were harvested by centrifugation in a JA-10 rotor at 6000 xg for 20 min at 4 °C yielding 25.7 g of pellet. The pellet was then washed twice with 54 mL of 0.85 % NaCl and cells were harvested again by centrifugation in a F34-6-38 rotor at 6000 xg for 5 min at 4 °C then flash frozen on dry ice and stored at -80 °C. Cell pellets were thawed then resuspended in 20 mL of Lysis buffer (50 mM Tris HCl, 300 mM NaCl, 20 mM imidazole, 10 % (v/v) glycerol, 0.2 % NP-40, 1 mg/mL lysozyme, 2 µg/mL DNase I, pH 8.0) and lysed using a large probe on a Heat Systems Ultrasonic processor W-255 sonicator set to 50 % cycle and 50 % power 5 times for 30 sec each with 1 min rest on ice between bursts. Cellular debris was separated from the lysate by centrifugation at 20 000 xg for 60 min at 4 °C using a JA-25.5 rotor. The supernatant was retained and stored at 4 °C overnight.

Affinity Chromatography

An Omnifit column housing filled with HisPur™ Ni-NTA Superflow Agarose (Thermo Scientific) was mounted on a BioCad Sprint Perfusion Chromatography system and equilibrated with 1 column volume of CTX-M-15 Elution buffer (50 mM Tris HCl, 300 mM NaCl, 300 mM imidazole, 10 % (v/v) glycerol, pH 8.0) then 12 column volumes of CTX-M-15 Chelating buffer (50 mM Tris HCl, 300 mM NaCl, 20 mM imidazole, 10 % (v/v) glycerol, pH 8.0) through 2 different lines at 1 mL/min. The lysate was filtered through at 0.2 µm syringe filter to sterilize and remove any particulates before loading onto the column. Over the course of 3 purifications, 9.5 mL of lysate was applied to the column through the pump at 0.5 mL/min then that line was flushed with CTX-M-15 Chelating buffer for 2 column volumes. The column was then washed with 5 column volumes of CTX-M-15 Chelating buffer at 1 mL/min. CTX-M-15 was eluted from the column using a gradient from 100 % CTX-M-15 Chelating buffer to 100 % CTX-M-15 Elution buffer over 5 column volumes with an additional column volume of CTX-M-15 Elution buffer at the end to ensure complete elution. Fractions were

collected every 3 min starting from the loading of the protein onto the column. The 2-3 fractions from each day that contained the highest CTX-M-15 activity by nitrocefin assay were pooled and dialyzed into 50 mM HEPES pH 7.2 until both the imidazole and NaCl concentrations were calculated to be below 10 nM. Dialyzed CTX-M-15 was concentrated using an Amicon Ultra-15 centrifugal filter with a 10 kDa molecular weight cutoff then stored in 50 % (v/v) glycerol at -20 °C.

Thrombin Cleavage of His Tag

Cleavage of the His tag from CTX-M-15 was performed using a Thrombin Cleavage Capture kit (Novagen) which uses biotinylated thrombin and streptavidin agarose. An 80 µL aliquot of concentrated CTX-M-15 was incubated with 20 µL 1:100 diluted thrombin in Thrombin Cleavage Buffer (20 mM Tris HCl, 150 mM NaCl, 2.5 mM CaCl₂, pH 8.4) at room temperature for 4 hr. The reaction was stopped with the addition of 25 µL streptavidin agarose slurry and incubated for 30 min at room temperature to bind all of the thrombin. Cleaved CTX-M-15 was eluted using a spin filter at 1000 xg for 10 min then stored at -20 °C in 50 % (v/v) glycerol.

2.2.2.4 KPC-2

PCR Amplification of KPC-2

The gene for KPC-2 was amplified from a KPC-2 containing pBr322 vector supplied by Dr. Focco van den Akker to introduce restriction sites for insertion into pET28a.²¹⁴ Two sets of primers were used to code for an N-terminal 6-His tag: one that adds the His tag onto the signal peptide of KPC-2 and another one that adds the His tag directly onto KPC-2 without coding for the signal peptide. Polymerase chain reactions (PCR) were prepared using a PWO DNA polymerase kit (Roche) with 1 mM dNTP mixture, 0.25 µM of the NdeI forward primer and EcoRI reverse primer, 1 µL or 5 µL of KPC-2 template, and 2.5 units of PWO polymerase in 10 mM Tris HCl, 25 mM KCl, 5 mM (NH₄)₂SO₄, 2 mM MgSO₄, pH 8.85 then vortexed and centrifuged briefly. PCR was initiated with a 2 min denaturation at 95 °C, followed by 34 cycles consisting of denaturation at 92 °C for 15 sec, annealing at 65 °C for 30 sec, and elongation at 72 °C for 1 min. The final cycle of PCR ended with a 7 min elongation at 72 °C. PCR products were purified on a 1% agarose gel in TAE (40 mM Tris, 20 mM acetic acid, 1 mM EDTA, pH 8.3) where bands were excised, and DNA was isolated using a Qiagen Gel Extraction kit.

Cloning KPC-2 into pET28a

Both PCR products (His-SP-KPC-2 and His-KPC-2) and a pET28a vector were digested with FastDigest EcoR1 and FastDigest Nde1 in FastDigest Green buffer (Fermentas). The digestion of the PCR products was incubated for 1 hr at 37° C while the digestion of the vector was only incubated for 10 min at 37 °C before purification on 1 % agarose gel in TAE where bands were excised, and digested DNA was isolated using a Qiagen Gel Extraction kit. The digested pET28a vector was ligated with each of the two digested PCR products using T4 DNA Ligase for 2 hr at 37 °C.

From this point on, the purification of KPC-2 was taken over by the undergraduate research student Melinda Lam under the supervision of Dr. Laura Marrone.

Transformation

The two KPC-2 containing plasmids, His-SP-KPC-2 and HIS-KPC-2, were transformed into 50 µL of CaCl₂ competent *E. coli* BL21 DE3 cells by incubating cells and plasmid on ice for 30 minutes followed by heat shock at 42 °C for 20 seconds. Transformation reactions were placed back on ice for 2 min then allowed to recover in 950 µL of LB media for 1 hr at 37 °C while shaking. Transformants were plated on LB agar supplemented with 50 µg/mL kanamycin and incubated at 37 °C overnight. Small scale expression tests of these transformants indicated that the construct without a signal peptide was not active and this avenue was not pursued further.

Growth of Liquid Cultures for KPC-2 Expression

Initial cultures were prepared by inoculating 5 mL of LB media supplemented with 50 µg/mL kanamycin with His-SP-KPC-2 transformants then incubating these overnight at 37 °C while shaking. The entirety of this initial culture was used to inoculate 0.5 L LB media supplemented with 50 µg/mL kanamycin which was then grown at 37 °C, shaking at 220 rpm overnight. Small scale tests indicated that expression of KPC-2 was best when not induced with IPTG so this step was forgone. Bacterial cells were harvested by centrifugation at 6000 rpm for 15 min at 4 °C then subjected to periplasmic lysis at room temperature for 10-15 min in 50 mM HEPES, 0.5 M NaCl, pH 7.5 and 0.1 µg of lysozyme. DNase I and RNase I were added to the lysate to degrade any DNA and RNA released by spheroplast lysis then the periplasmic lysate was isolated from spheroplasts and cellular debris by centrifugation at 12 000 xg for 10 min.

Chromatographic Purification of KPC-2

Periplasmic lysate was loaded onto a nickel affinity column but did not bind due to cleavage of the signal peptide and consequently the His tag during cellular processing. The flow through from the affinity column was dialyzed into 20 mM Tris-HCl, 50 mM NaCl, pH 8.7 and loaded onto a Poros 20HQ anion exchange column (Poros) at 2 mL/min using the BioCad Sprint High Perfusion Chromatography system. Again, KPC-2 did not bind to the anion exchange column and the flow through was then loaded onto a Poros 20S cation exchange column but did not bind due to inappropriate pH conditions. The flow through from the Poros 20S column was dialyzed into 10 mM acetate pH 5.0 and loaded again onto the Poros 20S cation exchange column at 2 mL/min using the BioCad Sprint. The column was washed with acetate buffer then KPC-2 was eluted using a gradient of NaCl from 0 to 1 M in buffer over 32 mL. Fractions were tested for activity using nitrocefin as a substrate using the procedure in 2.2.2.2 and some fractions were stored at -20 °C in 50% glycerol while the remainder was frozen on dry ice and stored at -80 °C. Fraction 4, which exhibited the highest activity and was the only fraction with just one band by SDS PAGE, was used for all kinetic studies.

2.2.2.5 VIM-1

The purification of VIM-1 was performed primarily by the undergraduate research student Karan Malik under the co-supervision of Dr. Geneviève Labbé and myself as part of his undergraduate thesis project.

Transformation

Cloning of codon-optimized VIM-1 with a carboxypeptidase A cleavable C-6His tag into pOPIN vector E and the N-terminal signal sequence expressed was performed by Dr. Spencer's lab and given to the Dmitrienko lab as a generous gift. The VIM-1 containing plasmid was transformed into 50 µL of *E. coli* BL21 DE3 cells by incubating them together on ice for 30 min then heat shocking at 42 °C for 45 sec and resting them on ice for 2 min. Transformants were allowed to recover in 900 µL LB media at 37 °C for 2 hr before being plated on LB agar supplemented with 100 µg/mL ampicillin and incubated at 37 °C overnight.

Growth of Liquid Cultures for VIM-1 Expression

A single colony of from the plate of VIM-1 transformants was used to inoculate 50 mL of LB media supplemented with 100 µg/mL ampicillin and incubated at 37 °C, overnight, shaking at 250

rpm. Two flasks with a 4 L capacity containing 1 L of LB media supplemented with 100 µg/mL ampicillin were each inoculated with 20 mL of overnight culture and shaken at 225 rpm and 37 °C. As the OD₆₀₀ of the culture reached 0.4, expression of VIM-1 was induced with 1 mM IPTG for 4 hours shaking at 225 rpm and 37 °C. Cells were harvested by centrifugation at 6000 rpm for 20 min at 4 °C; nitrocefin tests determined that the majority of the VIM-1 activity was in the supernatant.

Affinity Chromatography

VIM-1 containing supernatant was filtered through a 0.45 µm filter to remove particulates, then imidazole was added to the solution to a final concentration of 20 mM. A HisPur™ Ni-NTA Superflow Agarose (Thermo Scientific) in an Omnifit column housing mounted on a BioCad Sprint Perfusion Chromatography system was equilibrated with VIM-1 Chelating buffer (50 mM Tris-HCl, 300 mM NaCl, 20 mM imidazole, 10 % (v/v) glycerol, pH 8.0) before 200 mL VIM-1 supernatant was loaded onto the column at 4 mL/min through the pump. The column was washed with 90% VIM-1 Chelating buffer and 10 % VIM-1 Elution buffer (50 mM Tris-HCl, 300 mM NaCl, 150 mM imidazole, 10 % (v/v) glycerol, pH 8.0) until the OD₂₈₀ was reading less than 0.1. VIM-1 was eluted from the column using VIM-1 Elution buffer then dialyzed 50 mM Tris-HCl, 150 mM NaCl, pH 8.0 at 4 °C. Pure His-tagged VIM-1 was stored in 50 % glycerol at -20 °C. Due to time constraints and low yield, the tag was not cleaved; however, the kinetic parameters of His-VIM-1 did not differ significantly from literature values.⁴⁶⁴ The concentrations of VIM-1 fractions were determined by A₂₈₀ ($\epsilon = 29910 \text{ M}^{-1}\text{cm}^{-1}$) using NanoDrop (Thermo Scientific) instead of Bradford due to low concentrations. The concentration of the final VIM-1 stock was determined by Bradford as described in 2.2.2.2.

2.2.2.6 VIM-2

Dr. Geneviève Labbé cloned VIM-2 out of the pNOR 2001 vector provided by Dr. Patrice Nordmann (South Paris University, Paris, France) into a pET28a vector and purified the protein as previously described.^{453,465}

2.2.2.7 GC-1

Transformation

The cloning of GC-1 into the high expression plasmid pCS100 was performed and published by Dr. M. Nukaga prior to it being obtained by the Dmitrienko lab.²¹⁹ The recommended *E. coli* strain for

purification from this plasmid was AS266-51 which is an *ampC* deficient C600 with a mutant *ampD* to prevent AmpC contamination of the GC-1.^{219,466} When transformations of GC-1 containing pCS100 were attempted into competent *E. coli* AS266-51, colonies formed on 50 µg/mL chloramphenicol LB agar plates; however, activity was not observed upon growth and induction in LB broth. In later trials, a side by side transformation of 5 µL of pCS100-GC-1 into *E. coli* AS266-51, *E. coli* BL21 DE3, and *E. coli* BL21 PLYS was performed by incubating the plasmid with CaCl₂ competent cells for 30 min on ice before heat shocking at 42 °C for 45 sec. Cells were returned to ice before the addition of 950 µL of LB. Cells were allowed to recover for 1 hr at 37 °C. Transformants were then plated on LB agar supplemented with 50 µg/mL chloramphenicol and incubated at 37 °C overnight. It was determined from induction of small scale liquid cultures that BL21 DE3 was the best strain for growing GC-1 despite the potential for a minor AmpC contaminant.

Growth of Liquid Cultures for GC-1 Overexpression

A single colony of pCS100-GC-1 transformed *E. coli* BL21 DE3 was used to inoculate 70 mL TB broth supplemented with 50 µg/mL chloramphenicol which was incubated at 37 °C shaking at 225 rpm overnight. Six flasks with a 4 L capacity containing 1 L of TB broth supplemented with 50 µg/mL chloramphenicol were then inoculated with 10 mL each of the overnight culture which were incubated at 37 °C shaking at 190 rpm until they reached an optical density at 600 nm of approximately 0.6. As each flask reached the desired optical density, it was induced with 1 mM IPTG and returned to incubator overnight. Cells were harvested by centrifugation at 6000 rpm for 20 min at 4 °C in a JA-10 rotor yielding 54.6 g of pellet. The activity of both the supernatant and a crude lysis of the pellet (using 0.1 mg/mL lysozyme incubated for 10 min at room temperature) were determined using a nitrocefin based activity assay as described in 2.2.2.2. It was determined that the majority of the GC-1 activity was in the supernatant.

Fractionation by Ammonium Sulfate

Solid ammonium sulfate was dissolved in the supernatant to a final concentration of 70% (w/v) at room temperature then stirred at 4 °C for 2 days. The precipitated proteins were extracted by centrifugation at 13500 xg for 60 min at 4 °C in a JA-10 rotor. The extracted proteins, including GC-1, were then slowly resuspended at 100 rpm in 8 mL of 50 mM NaPi pH 7.0 per gram of pellet at 4 °C. Any remaining precipitated proteins were extracted by centrifugation at 13500 xg for 60 min at 4 °C then discarded after the presence of GC-1 in the supernatant was confirmed using the nitrocefin

assay described above. The supernatant (230 mL) was dialyzed against 50 mM NaPi pH 7.0 at 4 °C until the ammonium sulfate concentration was calculated to be below acceptable limits for ion exchange.

Ion Exchange Chromatography

The dialyzed protein solution was diluted in an equal volume of 50 mM MES pH 5.0 then the pH was adjusted to approximately 5.0 with 6 N HCl. The acidified protein was then filtered through a 0.45 µm filter to ensure no particulates remained in the solution. A POROS CM-Sepharose column mounted on a BioCad Sprint Perfusion Chromatography system was equilibrated in 50 mM MES pH 5.0 then loaded at 3 mL/min with the acidified protein ensuring the flow through did not have β-lactamase activity. The column was then washed with 3 column volumes of 50 mM MES pH 5.0 at 3 mL/min followed by 1 column volume each of 50 mM MES, 30 mM NaCl pH 5.0 and 50 mM MES, 50 mM NaCl pH 5.0 at 5 mL/min. A final wash was performed with 2.5 column volumes of 50 mM MES, 100 mM NaCl pH 5.0. GC-1 was eluted from the column using a salt gradient from 50 mM MES, 100 mM NaCl pH 5.0 to 50 mM MES, 500 mM NaCl pH 5.0 over 4 column volumes at 5 mL/min. Fractions containing the highest GC-1 activity by the nitrocefin assay were pooled and concentrated using Amicon Ultra-15 membrane filters with a 10 kDa molecular weight cutoff. An equal volume of glycerol was added to the concentrated GC-1 for storage at -20 °C.

Size Exclusion Chromatography

Dr. Geneviève Labbé performed the size exclusion chromatography to increase the purity of the GC-1 preparations by first dialyzing the glycerol stock into 50 mM MES, 0.2 M NaCl pH 5.5. The dialyzed GC-1 was then concentrated using a Pall Macrosep Advance Centrifugal device with a 10 kDa molecular weight cutoff down to 1.5 mL (2 mL after filter was rinsed). The concentrated GC-1 solution was centrifuged at 14 000 rpm for 5 min to remove dust and particulates before injecting it onto a Superdex 200 26/60 size exclusion column mounted on an AKTA Explorer HPLC system. GC-1 was eluted using isocratic 50 mM MES, 0.2 M NaCl, pH 5.5 at 2 mL/min. Collected fractions with the highest β-lactamase activity by nitrocefin assay were pooled and concentrated using another Pall Macrosep Advance Centrifugal device with a 10 kDa molecular weight cutoff. Concentrated GC-1 was diluted with an equal volume of glycerol for storage at -20 °C.

2.2.2.8 OXA-48

The purification of OXA-48 was performed primarily by Alicia Tjahjadi as part of her undergraduate thesis project under the co-supervision of Dr. Geneviève Labbé and myself.

Transformation

Cloning of codon-optimized OXA-48 with a 3C Protease cleavable N-6His tag into pOPIN vector F without expression of the signal sequence was performed by Dr. Spencer's lab and given to the Dmitrienko lab as a generous gift. The OXA-48 containing plasmid was transformed into 50 μ L of CaCl_2 competent *E. coli* BL21 DE3 cells by incubating them together on ice for 30 min before heat shocking them at 42 °C for 45 sec then resting them on ice for 2 min. Transformants were allowed to recover in 950 μ L of LB for 2 hr at 37 °C and then were plated on LB agar supplemented with 100 μ g/mL ampicillin which was incubated at 37 °C overnight.

Growth of Liquid Cultures for OXA-48 Expression

A single colony from the plate of OXA-48 transformants was used to inoculate 50 mL of LB broth supplemented with 100 μ g/mL ampicillin in a 250 mL flask and incubated overnight at 37 °C, shaking at 250 rpm. Two flasks with a 4 L capacity containing 1 L of LB media supplemented with 100 μ g/mL ampicillin were each inoculated with 20 mL of overnight culture and incubated at 37 °C, shaking at 225 rpm. Once an OD_{600} of approximately 0.6 was reached, expression of OXA-48 was induced with 1 mM IPTG and incubated at 25 °C, shaking at 225 rpm overnight. Cells were harvested by centrifugation at 3000 \times g for 20 min at 4 °C. Cell pellets (11.4 g total) were resuspended in 40 mL of OXA-48 Lysis buffer (50 mM Tris-HCl, 300 mM NaCl, 20 mM imidazole, 10 % (v/v) glycerol, 0.2 % (v/v) NP-40, 0.02 % (v/v) 1-thioglycerol, pH 8.0) then lysed using a large probe on a Heat Systems Ultrasonic processor W-255 sonicator set to 50 % cycle and 50 % power 5 times for 30 sec each with a 1 min rest on ice between bursts. Cellular debris was separated from the lysate by centrifugation at 48 000 \times g for 60 min at 4 °C and the supernatant was retained.

Affinity Chromatography

OXA-48 chromatography was performed in two runs each with the lysate of a different flask. Imidazole was added to each lysate to a final concentration of 20 mM before being loaded at 2 mL/min onto HisPur™ Ni-NTA Superflow Agarose (Thermo Scientific) in an Omnifit column housing mounted on a BioCad Sprint Perfusion Chromatography system that had been equilibrated

with OXA-48 Chelating buffer (50 mM Tris-HCl, 300 mM NaCl, 20 mM imidazole, 10 % (v/v) glycerol, 0.01 % (v/v) 1-thioglycerol, pH 8.0). The column with OXA-48 bound was washed at 3 mL/min with OXA-48 Chelating buffer then at 4 mL/min with 90 % OXA-48 Chelating buffer and 10 % OXA-48 Elution buffer (50 mM Tris-HCl, 300 mM NaCl, 150 mM imidazole, 10 % (v/v) glycerol, 0.01 % (v/v) 1-thioglycerol, pH 8.0) over a total of 55-80 mL. His-tagged OXA-48 was eluted from the column with 100 % OXA-48 Elution buffer while 10 mL fractions were collected until no activity was detected in fractions by nitrocefin assay. Fractions containing the highest OXA-48 activity were dialyzed into OXA-48 Storage buffer (50 mM Tris-HCl, 150 mM NaCl, 10 mM EDTA, 20 % (v/v) glycerol, pH 8.0).

Cleavage of His-tag

The most active fraction from the two days (day 1 fraction 2) was chosen for tag cleavage. His-tagged OXA-48 and His-tagged 3C Protease were both dialyzed at 4 °C using SpectraPor dialysis membranes with a molecular weight cutoff of 8-10 kDa into Dialysis buffer (50 mM Tris-HCl, 150 mM NaCl, pH 8.0). The dialyzed OXA-48 was incubated with 1 mg of 3C Protease per 100 mg of OXA-48 at 4 °C overnight to allow complete cleavage of the N-terminal tag. The protein mixture was loaded onto Ni-NTA Superflow Agarose (Thermo Scientific) in an Omnifit column housing mounted on a BioCad Sprint Perfusion Chromatography system that had been equilibrated with Dialysis buffer at 4 mL/min. OXA-48 was collected in the flow through over 4 fractions then the 3C Protease was eluted from the column with Protease Elution buffer (50 mM Tris-HCl, 300 mM NaCl, 150 mM imidazole, pH 8.0). Pure OXA-48 with the His-tag cleaved was dialyzed as above, then stored at -20 °C in 50 % glycerol.

2.2.3 Characterization of Chromogenic Substrates

Chromogenic β -lactams: nitrocefin, UW-57, UW-58, and UW-154, were synthesized as an E/Z mixture by Dr. Ahmed Ghavami as previously described, and their structures (Figure 2.3) and purity were confirmed by ¹H NMR, ¹³C NMR, and ESI-MS.⁴⁵³ Powders of these substrates were dissolved in DMSO as a necessary step to isomerize completely to the E isomer to a final concentration of 40 mM and stored at -20 °C. If it was suspected that stocks had started to degrade (usually after years in the freezer or if the colour changed), they were checked by UPLC or kinetic comparison to previous data.

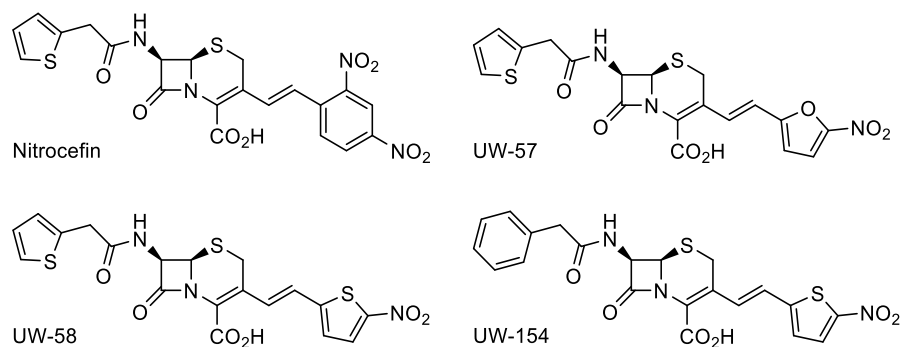


Figure 2.3 Chromogenic β -lactamase substrates synthesized by the Dmitrienko group.

2.2.3.1 Molar Extinction Coefficient Determination

Substrates were diluted to 100 μM in 50 mM HEPES pH 7.2 supplemented with 50 $\mu\text{g/ml}$ BSA, 0.01 % Triton X-100, and 100 μM ZnCl_2 . One sample of this was read directly while the other was completely hydrolyzed using 90 nM VIM-2 for 10 min. Spectral scans were performed using a Cary 50 spectrophotometer in quartz cuvettes from 250-750 nm in triplicate. The wavelength corresponding to the greatest difference between the absorbance of the product and the substrate was determined. A range of substrate concentrations from 1 μM to 100 μM were prepared in 50 mM HEPES pH 7.2 supplemented with 50 $\mu\text{g/mL}$ BSA and 0.01 % Triton X-100. Hydrolyzed substrates were made by incubating with 27 nM VIM-2 until fully hydrolyzed. Greiner 96-well plates were loaded with 200 μL volumes of both hydrolyzed and unhydrolyzed substrates then read at the wavelength to be used for kinetics (NC, 482 nm; UW-57, 520 nm; UW-58, 534 nm; UW-154, 533 nm).

2.2.3.2 Substrate and Product Stability

Substrates were prepared as in 2.2.3.1 and the stability of both substrate and product were assessed by taking scans from 325-750 nm (NC, UW-57, UW-58) in a SpectraMax 190 plate reader or from 250-750 nm in a Cary 50 spectrophotometer at 0 hr, 3 hr, 24 hr, and 96 hr. The 96-well plate containing 200 μL samples of NC, UW-57, and UW-58 substrate and product was lidded and sealed with Parafilm between reads to minimize evaporation.

2.2.4 Biochemical Characterization

The stability of β -lactamases to DMSO is a critical piece of information since most inhibitors and substrates require DMSO as a cosolvent. As such, an upper limit for the total DMSO concentration allowed was determined for all β -lactamases except SFH-1 which was assumed to behave similarly to other MBLs. β -Lactamases were also routinely characterized with chromogenic substrates upon purification or arrival. Kinetic characterization of KPC-2, IMP-1, NDM-1, SPM-1, VIM-2, L1, and GC-1 with NC and the UW substrates were performed by Dr. Genevieve Labbe.⁴⁵³

2.2.4.1 DMSO Stability

The stability of all of the SBLs used in his work (CTX-M-15, KPC-2, GC-1, OXA-23, and OXA-48) and most of the MBLs (IMP-1, NDM-1, SPM-1, VIM-1, VIM-2, and L1) in DMSO supplemented buffer was assessed to give an upper limit to the allowed DMSO concentration in substrate assays as well as later inhibition assays. The enzyme and substrate concentrations used in this assay are detailed in Table 2.1. Class A, B, and C β -lactamases were prepared in 50 mM HEPES pH 7.2 supplemented with 50 μ g/mL BSA and 0.01 % Triton X-100 then incubated with varying DMSO concentrations from 0.05-9.5 % for 10 min at 30 °C. Class D β -lactamases were prepared in 100 mM NaPi, 2.1 mg/mL NaHCO₃, pH 7.0 supplemented with 50 μ g/mL BSA and 0.01 % Triton X-100 then incubated with DMSO concentrations from 0.2-9.5% as described above. The assay was initiated in a 96-well plate by adding 190 μ L of this mixture to 10 μ L of nitrocefin then shaken for 5 sec prior to monitoring the absorbance at 482 nm every 7 sec for 5 min and the initial rate was determined.

Table 2.1 Enzyme and substrate concentrations used for DMSO stability studies.

β -lactamase	Class	Enzyme Concentration	NC Concentration (μ M)
CTX-M-15	A	140 pM	20
KPC-2	A	190 pM	8
IMP-1	B1	170 pM	3.5
NDM-1	B1	570 pM	1
SPM-1	B1	7.5 nM	1
VIM-1	B1	1.5 nM	20
VIM-2	B1	290 pM	15
L1	B3	580 pM	5
GC-1	C	380 pM	15
OXA-23	D	570 pM	50
OXA-48	D	72 pM	80

2.2.4.2 Kinetic Parameter Determination

CTX-M-15

The determination of kinetic parameters for CTX-M-15 was performed for both the tagged and cleaved versions of the protein in both HEPES and phosphate buffers. CTX-M-15 (tagged: 44 pM, tag cleaved: 152 pM) was prepared in 50 mM HEPES pH 7.2 or 100 mM NaPi pH 7.2 supplemented with 50 µg/mL BSA and 0.01 % Triton X-100 then incubated for 10 min at 30 °C in a 96-well plate. The reaction was initiated by addition of CTX-M-15 mix to 16 concentrations of substrate (500 µM – 1 µM) in triplicate then shaking for 5 sec before monitoring the absorbance every 6-7 sec for 5 min (NC: 482 nm, UW-57: 520 nm, UW-58: 534 nm, UW-154: 533 nm) and determining initial rates. Rates were converted into molar units using Beer's Law and molar extinction coefficients for the hydrolysis of each substrate determined in 2.2.3.1 (NC: 11 470 M⁻¹cm⁻¹, UW-57: 10 630 M⁻¹cm⁻¹, UW-58: 12 420 M⁻¹cm⁻¹, UW-154: 10 870 M⁻¹cm⁻¹) then fitted to equations for Michaelis-Menten kinetics (Equation 2.1) or substrate inhibition (Equation 2.2) as appropriate where *v* is the rate of product formation and [S] is the concentration of substrate.⁴⁶⁷

Equation 2.1

$$v = \frac{V_{max}[S]}{K_M + [S]}$$

Equation 2.2

$$v = \frac{V_{max}[S]}{K_M + [S] \left(1 + \frac{[S]}{K_I}\right)}$$

VIM-1

Kinetic parameters for VIM-1 were determined using methods similar to that of CTX-M-15 using 50 mM HEPES pH 7.2, a tagged VIM-1 final concentration of 1.6 nM for NC and 640 pM for the UW substrates and a substrate concentration range from 500 µM to 0.5 µM.

SFH-1

Kinetic parameters for SFH-1 were determined using methods similar to that of CTX-M-15 using 50 mM HEPES pH 7.2, SFH-1 final concentrations of 9 nM (nitrocefin) and 1.8 nM (UW substrates), and a substrate concentration range from 500 µM to 0.5 µM.

OXA-23

Kinetic parameters for OXA-23 were determined using methods similar to that of CTX-M-15 using 100 mM NaPi, 2 mg/mL NaHCO₃, pH 7.0; OXA-23 final concentrations of 600 pM (nitrocefin), 1.2 nM (UW-57, UW-154), and 3 nM (UW-58); and a substrate concentration range from 500 - 0.5 μM.

OXA-48

Kinetic parameters for OXA-48 were determined using methods similar to that of CTX-M-15 using 100 mM NaPi, 2 mg/mL NaHCO₃, pH 7.0; OXA-48 final concentrations of 87 pM (nitrocefin), 347 pM (UW-57), 173 pM (UW-58, UW-154); and a substrate concentration range from 500 μM to 5 μM.

2.3 Results

2.3.1 Metallo-β-Lactamase Protein Sequence Alignment

Alignments of the protein sequences of NDM-1, IMP-1, and VIM-2 with other variants from each family was done using a variety of web-based programs on phylogeny.fr. This was not done for SPM-1 or L1 as they are no other MBL variants in their families.

2.3.1.1 NDM Family Alignment

The amino acid sequence of the NDM family of MBLs is highly conserved resulting in a phylogenetic tree where branches generally indicate a single amino acid change as seen in Figure 2.4.

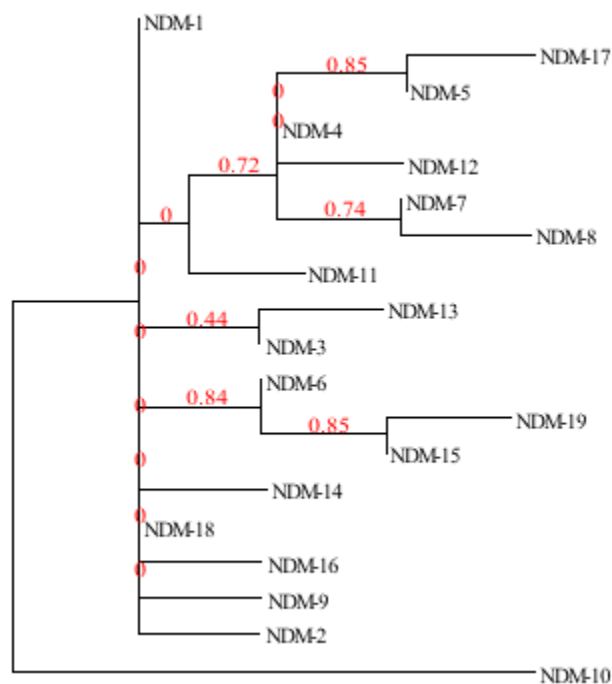


Figure 2.4 Phylogenetic tree of NDM Variants generated using phylogeny.fr and TreeDyn.

Most of the 19 variants within the NDM family are within 1-2 amino acids of NDM-1 with the exception of NDM-10 and NDM-18 which differ by 5 amino acids. A full list of the amino acid changes in the variants relative to NDM-1 can be found in Table 2.2.

The complete sequence alignment for NDM-1 and all of its variants can be found in Appendix E. The most common mutation found among the variants is the M154L mutation which is present in 9 of the 19 variants. Mutation of D130 to either G or N is also fairly common. Other mutations were either unique to a variant or were only found in a small subset of the variants.

Table 2.2 Amino acid differences between NDM-1 and other NDM variants.

NDM Variant	Mutation Relative to NDM-1 numbering
NDM-2	P28A
NDM-3	D95N
NDM-4	M154L
NDM-5	V88L, M154L
NDM-6	A230V
NDM-7	D130N, M154L
NDM-8	D130G, M154L
NDM-9	E152K
NDM-10	R32S, G36D, G69S, A74T, G200R
NDM-11	M154V
NDM-12	M154L, G222D
NDM-13	D95N, M154L
NDM-14	D130G
NDM-15	M154L, A230V
NDM-16	R264H
NDM-17	V88L, M154L, E170K
NDM-18	D48_L49insQRFGD
NDM-19	D130N, M154L, A230V

2.3.1.2 VIM Family Alignment

Whereas NDM family contains only 19 variants including NDM-1, the VIM family contains 55 variants making it likely that there will be more than just 1 or 2 amino acids difference between variants. As seen in the phylogenetic tree in Figure 2.5, there are two main branches of the tree; those that are VIM-1 like, and those that are VIM-2 like. There are 25 amino acids different between VIM-1 and VIM-2: F2L, L4V, L5I, K7S, L12M, I16V, I19V, F25H, V27G, D28E, S29P, S37N, V145A, S192N, I200V, Y201H, R205S, I223V, Q228K, Q234E, F235V, K250Q, T253A, T260K, V265A. Within the two groupings, variation is fairly consistent with only a few amino acids differing between variants in that group. It is worth noting that VIM-7 is widely divergent from both the VIM-1 like and VIM-2 like variants. The complete sequence alignment as well as a table summarizing the amino acid changes of the VIM variants relative to VIM-2 can be found in Appendix E.

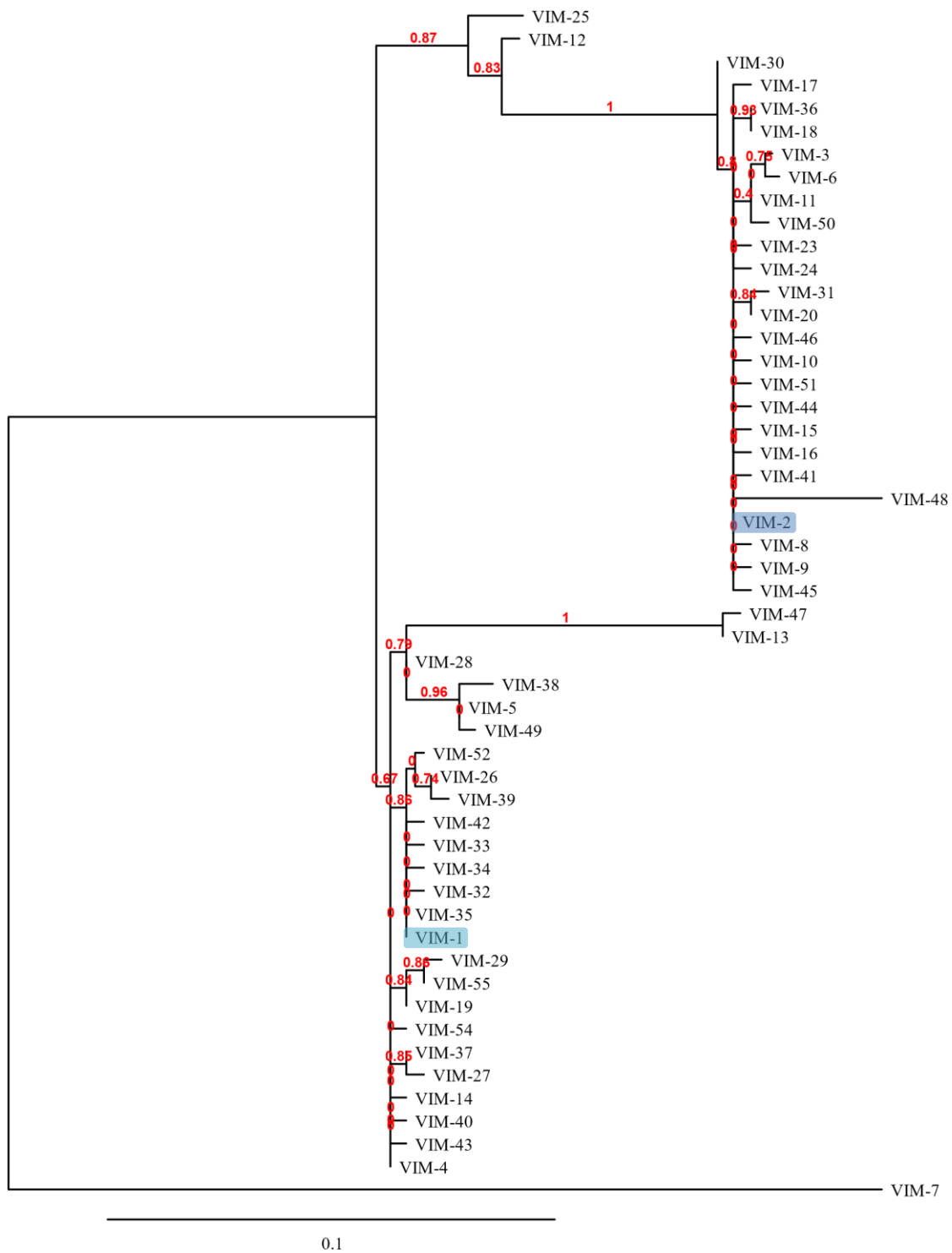


Figure 2.5 Phylogenetic Tree of VIM variants generated by phylogeny.fr and TreeDyn.

2.3.1.3 IMP Family Alignment

The IMP family is the largest of the MBL families with 70 assigned variants. Of these 70 variants, IMP-36, IMP-39, IMP-50, and IMP-65 do not have protein sequences in the NCBI database and IMP-47 has the same amino acid sequence as IMP-8, so IMP-47 was left out of the phylogenetic analysis. The phylogenetic tree generated from this analysis, seen in Figure 2.6, is much more branched than that of the NDM variants or the VIM variants, indicative of the wide sequence variety in this family. The small subset of IMP variants found near IMP-1 on the phylogenetic tree are very similar; however, at the extremities of the tree, variants can differ by over 50 amino acids from IMP-1. The full protein sequence alignment and a table summarizing the amino acid changes relative to IMP-1 can be found in Appendix E.

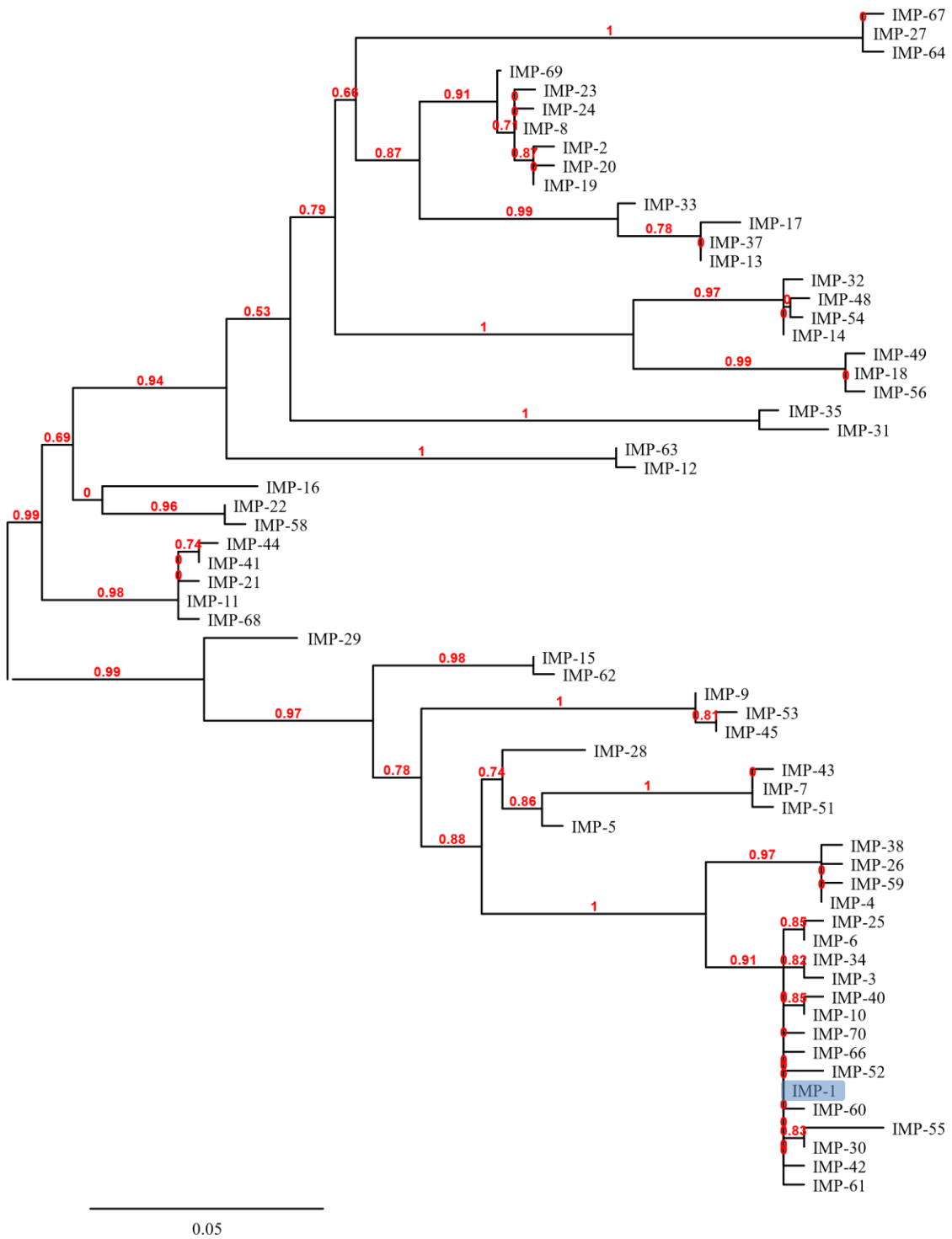


Figure 2.6 Phylogenetic tree of IMP family variants generated by phylogeny.fr and TreeDyn.

The analysis of the relationships between NDM-1, IMP-1, VIM-2, and their respective variants indicates that there is little sequence similarity between MBL families. The NDM variants are all closely related differing by only a few amino acids between NDM-1 and any given NDM variant. Due to both its sequence similarity and clinical significance NDM-1 should be a suitable representative of this family. The VIM family contains two major groupings: VIM-1-like and VIM-2-like. One variant from each these groupings should be represented in screening to check if both branches respond similarly to substrates and inhibitors - VIM-1 and VIM-2 were selected. The amount of variability in the IMP family makes it unreasonable to test representatives of each branch of the phylogenetic tree, so IMP-1 was used as it is among the most prevalent in clinical isolates and is readily available.²⁷⁶

2.3.2 Protein Purification

2.3.2.1 CTX-M-15 Purification

His tagged CTX-M-15 was purified by affinity chromatography before tag cleavage with thrombin. This was an efficient purification in which 12 % of the active protein from the crude was collected in fractions that were used for concentration and cleavage (Table 2.3). The reduction of CTX-M-15 from the 829 mg present in the lysate to the 34 mg eluted from the Ni-NTA column can be explained though its use in method development and its presence in fractions that were not pooled. The apparent loss of CTX-M-15 from the thrombin cleavage is due to only a small portion of the protein having undergone tag cleavage. The remainder of the tagged CTX-M-15 was stored at -20 °C in glycerol for possible His-tag cleavage in the future.

Table 2.3 CTX-M-15 purification table

	Total activity ($\mu\text{mol}/\text{min}$)	% Yield	Total Protein (mg)	Specific activity ($\mu\text{mol}/\text{min}/\text{mg}$)	Fold Purification
Lysate	14000	100	829	17.1	1
Ni-NTA	1700	12	34	49.4	2.9
Concentration	1600	11	34	45.7	2.7
Thrombin Cleavage	56	0.4	0.78	71.6	4.2

2.3.2.2 KPC-2 Purification

The cloning of KPC-2 into a plasmid to introduce a His-tag was futile as the tag was removed during cellular processing along with the signal peptide. The active flow through from the Poros 20HQ column was not formally assayed with NC, run on SDS PAGE, nor aliquoted for future checks. As a result of this lack of testing, it is unknown whether or not this step contributed to purification; although, it is likely that it is responsible for the removal of some anionic proteins. This in conjunction with the purification by the Poros 20S column resulted in > 95 % pure protein by SDS PAGE (Figure 2.7).

Table 2.4 KPC-2 purification table.

	Total activity ($\mu\text{mol}/\text{min}$)	% Yield	Total Protein (mg)	Specific activity ($\mu\text{mol}/\text{min}/\text{mg}$)	Fold Purification
Lysate	54	100	4.4	12	1
Poros 20HQ - 20S	0.25	0.46	0.40	0.62	0.05

2.3.2.3 VIM-1 Purification

VIM-1 was not overexpressed well in *E. coli* BL21 DE3 cells; however, what protein was expressed was found predominantly in the media since the signal peptide was included in the construct. The media was loaded onto a Ni-NTA affinity column and VIM-1 eluted across 3 fractions, one of which was further concentrated yielding 0.5 mg VIM-1 (Table 2.5). Potentially much more VIM-1 could have been purified from the remaining 1.8 L of media; however, the amount that was produced was adequate for the present study.

Table 2.5 VIM-1 purification table

	Total activity ($\mu\text{mol}/\text{min}$)	% Yield	Total Protein (mg)	Specific activity ($\mu\text{mol}/\text{min}/\text{mg}$)	Fold Purification
Media Supernatant	38.9	100	92	0.42	1
Ni-NTA	0.84	2.2	0.56	0.84	3.5
Concentration	0.61	1.6	0.51	0.61	2.8

2.3.2.4 GC-1 Purification

Early testing of the lysate fractions (media, periplasm, and cytosol) determined that most of the GC-1 was exported into the media when it was overexpressed. Since the GC-1 construct did not

include an affinity tag, a 70% ammonium sulfate cut was used to precipitate GC-1 which was then resolubilized, removing 200 mg of various proteins (Table 2.6). This mixture was then purified by ion exchange and cleaned by size exclusion chromatography yielding 2.5 mg of pure GC-1.

Table 2.6 GC-1 purification table.

	Total activity ($\mu\text{mol}/\text{min}$)	% Yield	Total Protein (mg)	Specific activity ($\mu\text{mol}/\text{min}/\text{mg}$)	Fold Purification
Media Supernatant	65319	100	660	99	1
Ammonium Sulfate Soluble Fraction	26024	39.8	460	57	0.6
CM Sepharose	11962	18.3	9.2	1293	13
Sephadex 200	1859	2.8	2.5	774	7.5

Early attempts at purification of KPC-2, IMP-1, and VIM-2 were performed using classical purification techniques such as those used in this GC-1 purification. Each of those purifications failed with all of the protein being lost on either the ion exchange or size exclusion columns. Considering this early experience, it came as a surprise that this purification proceeded relatively well, yielding 2.5 mg of pure GC-1. The good yield of GC-1 as compared to those earlier purifications is likely because the GC-1 purification was performed using an FPLC system while the others were performed using gravity columns.

2.3.2.5 OXA-48 Purification

OXA-48 was overexpressed well and was contained within the cells since no signal peptide was present in the construct. A lack of characterization at the time of purification necessitated the sample of frozen lysate being tested 3 years after the purification was completed. It is probable that this delay skewed the results since the target protein has been exposed to proteolytic enzymes for an extended period. For this reason, the non-physical values for % yield (2.5 million %) and fold purification (270 000 fold) were not included in Table 2.7.

Table 2.7 OXA-48 purification table.

	Total activity ($\mu\text{mol}/\text{min}$)	Total Protein (mg)	Specific activity ($\mu\text{mol}/\text{min}/\text{mg}$)
Lysate	0.34*	350	0.00097*
Ni-NTA	16700	52	180
His-tag cleavage	8300	32	260

*3 year delay in analysis of this sample. Proteolytic degradation is likely.

2.3.2.6 SDS PAGE of Purified β -Lactamases

A summary SDS-PAGE gel of all pure β -lactamases used in this thesis is presented in Figure 2.7 with the enzymes purified in this laboratory on the left side of the gel and any gifted enzymes on the right side of the gel. The β -lactamases purified at U Waterloo: KPC-2, VIM-1, VIM-2, and OXA-48, were determined to be >95 % pure by SDS-PAGE as is evident by the presence of only a single band in each well. CTX-M-15 and GC-1 samples appear to have minor contaminants, the CTX-M-15 contaminant is likely His-tagged CTX-M-15. Many of the β -lactamases received from other researchers: NDM-1, SPM-1, SFH-1, L1, and OXA-23 were also determined to be >95 % pure. Some small contaminant bands are evident in the IMP-1 sample and can likely be attributed to HRV 3C protease and IMP-1 with an uncleaved His-tag that were not successfully removed from the sample.

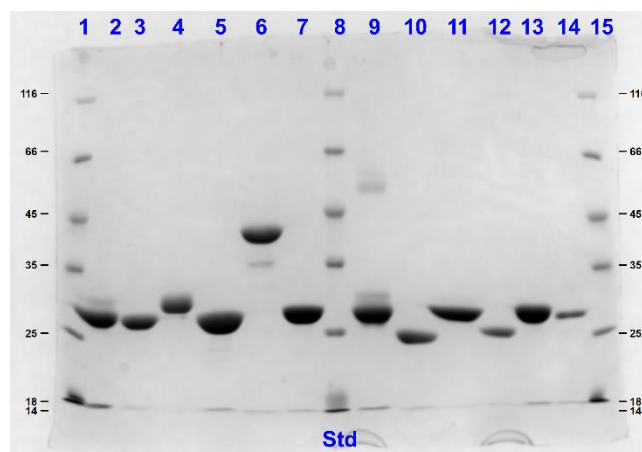


Figure 2.7 SDS-PAGE of pure β -lactamases. 1 LMW Marker, 2 CTX-M-15, 3 KPC-2, 4 VIM-1, 5 VIM-2, 6 GC-1, 7 OXA-48, 8 LMW Marker, 9 IMP-1, 10 NDM-1, 11 SPM-1, 12 SFH-1, 13 L1, 14 OXA-23, 15 LMW Marker.

2.3.2.7 Confirmation of β -Lactamase Identity by Mass Spectrometry

The masses of proteins purified in this laboratory were confirmed by ESI mass spectrometry. In addition, samples of NDM-1, SPM-1, and L1 were tested. This was used to confirm the successful removal of the His-tags from CTX-M-15 and OXA-48 using thrombin and 3C protease respectively. By the same logic, this confirms that the His tag was cleaved from KPC-2 during cellular processing and was not present during purification.

Table 2.8 Masses of pure β -lactamases as predicted using ExPASy ProtParam and determined by mass spectroscopy

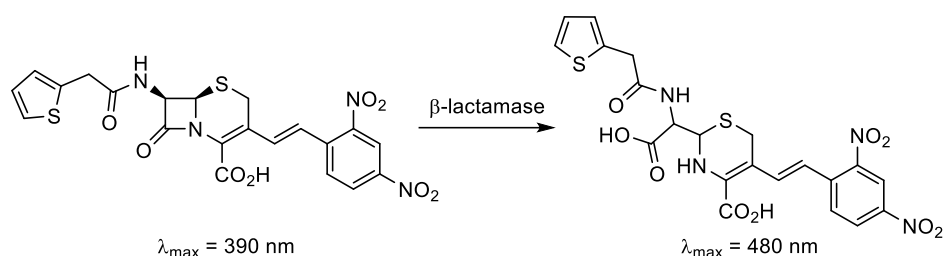
β -Lactamase	Predicted Denatured Mass (Da)	Mass Determined by Mass Spectrometry (Da)
CTX-M-15	28 407	28 406
KPC-2	28 720	28 719
NDM-1	24 318	24 317
VIM-2	25 515	25 515
SPM-1	27 884	27 883
L1	28 706	28 703
GC-1	39 573	39 572
OXA-48	28 301	28 300

Some of the β -lactamases provided by other labs were also analyzed by ESI mass spectrometry as either preliminary experiments for other work or to determine the specifics of the sample sequence given to us. The mass of NDM-1 was determined because the sample provided to us was denoted as Δ 36 NDM-1 which implied that the first 36 amino acids were truncated; however, that did not match any constructs published by that group. Upon determination of the mass, it was confirmed that the first 41 amino acids including the signal peptide were excluded from the construct, consistent with the published construct.³¹⁷

In addition to the masses presented in Table 2.8, the native mass of SPM-1 was also determined to be 28 009 Da (theoretical: 28 015 Da)⁴⁶⁸ which is consistent with 2 Zn ions in the active site. This was performed in ammonium acetate buffer instead of 1:1 H₂O:MeOH 0.1 % formic acid.

2.3.3 Characterization of Chromogenic Substrates

The colour change observed in the chromogenic β -lactams is produced by the hydrolysis of the β -lactam ring by β -lactamases as shown in Scheme 2.2



Scheme 2.2 Hydrolysis of nitroceftriaxone by β -lactamases.

Hydrolyzed and unhydrolyzed versions of the 4 substrates used in this work were plated at various concentrations on a 96-well plate to illustrate the colour change (Figure 2.8). Nitroceftriaxone shows a characteristic change from yellow to red, UW-57 goes from yellow to red/brown, and both UW-58 and UW-154 turn from yellow to purple. This colour change can be exploited for kinetic analysis of β -lactamases capable of hydrolyzing cephalosporins (ESBLs, Class C SBLs, and MBLs).

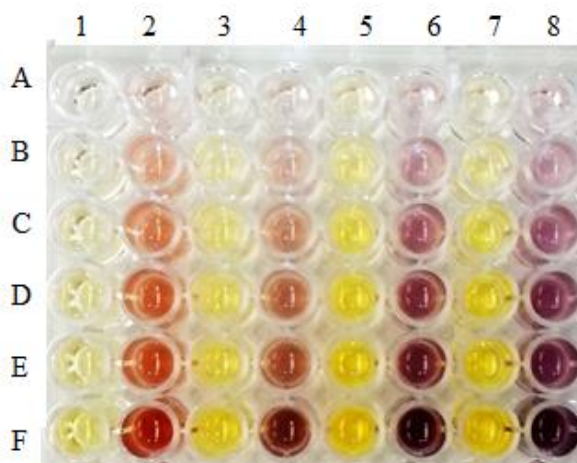


Figure 2.8 Visual appearance of 200 μ L of increasing concentrations of unhydrolyzed and hydrolyzed chromogenic substrates synthesized by the Dmitrienko lab (A: 10 μ M, B: 25 μ M, C: 50 μ M, D: 75 μ M, E: 100 μ M, F: 200 μ M). 1: unhydrolyzed NC, 2: hydrolyzed NC, 3: unhydrolyzed UW-57, 4: hydrolyzed UW-57, 5: unhydrolyzed UW-58, 6: hydrolyzed UW-58, 7: unhydrolyzed UW-154, 8: hydrolyzed UW-154.

At the same concentrations, both the unhydrolyzed and hydrolyzed forms of the UW substrates are more readily detectable visually. Additionally, the colour change of the UW substrates is more

distinctive since they are on opposite sides of the colour wheel instead of going to a neighbouring colour (red-orange).

2.3.3.1 Molar Extinction Coefficient

The wavelength at which the greatest difference between substrate and product curves occurred, λ_{\max} , was determined using spectral scans of both the unhydrolyzed and hydrolyzed versions of the substrates produced by the Dmitrienko lab (Figure 2.9). The λ_{\max} is the optimal wavelength for kinetic analysis as it is where the highest sensitivity occurs. The λ_{\max} was determined to be 482 nm for NC, 520 nm for UW-57, 534 nm for UW-58, and 533 nm for UW-154.

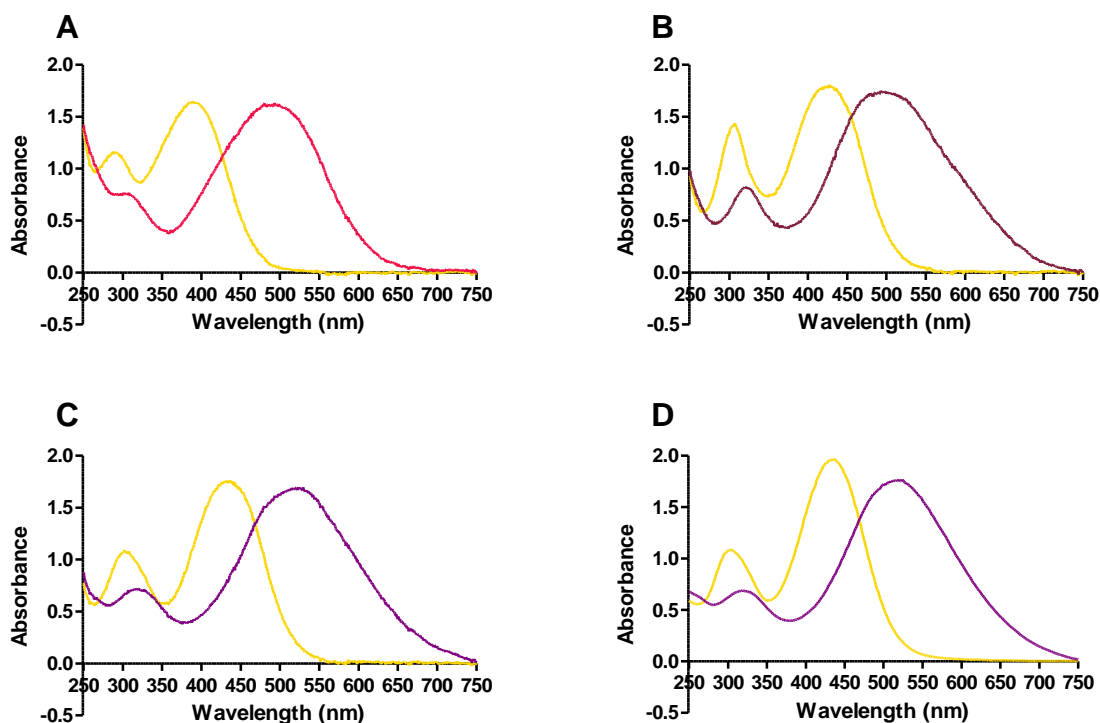


Figure 2.9 Spectral scans of chromogenic substrates before and after hydrolysis with the unhydrolyzed represented by a yellow and the hydrolyzed represented in red/purple for nitrocefin (A), UW-57 (B), UW-58 (C), and UW-154 (D) at 100 μ M. This figure was generated using GraphPad Prism v. 5.03.

Estimates for the molar extinction coefficients for the product can be determined from these scans: NC $\epsilon_{482} = 15\,990\text{ M}^{-1}\text{cm}^{-1}$, UW-57 $\epsilon_{520} = 16\,520\text{ M}^{-1}\text{cm}^{-1}$, UW-58 $\epsilon_{534} = 16\,590\text{ M}^{-1}\text{cm}^{-1}$, and UW-154 $\epsilon_{533} = 17\,140\text{ M}^{-1}\text{cm}^{-1}$; however, it is more accurate to determine the molar extinction coefficients from several different concentrations of substrate. In order to simplify further calculations, the molar extinction coefficient of a 200 μL volume in a standard flat bottom 96-well plate (Greiner Bio One) was determined and used for future calculations as well as the molar extinction coefficient in conventional units as listed in Table 2.9. For the purposes of this work, it is most appropriate to use the difference between molar extinction coefficient of the product and substrate, $\Delta\epsilon$. The differences between the estimates and the calculated extinction coefficients illustrate the inaccuracy of single point determinations and may have been exacerbated by these being from different batches of different ages.

Table 2.9 Molar extinction coefficients for UW substrates

Pathlength	Substrate	Molar extinction coefficient ($\text{M}^{-1}\text{well}^{-1}$)		
		Substrate	Product	Difference
200 μL in Costar 655101 96-well plate (0.571 cm)	NC	679 ± 8	7230 ± 50	6550 ± 50
	UW-57	350 ± 10	6420 ± 30	6070 ± 40
	UW-58	392 ± 5	7490 ± 19	7090 ± 20
	UW-154	533 ± 2	6740 ± 20	6200 ± 20
1 cm	Molar extinction coefficient ($\text{M}^{-1}\text{cm}^{-1}$)			
	NC	1190 ± 10	$12\,660 \pm 80$	$11\,470 \pm 90$
	UW-57	620 ± 20	$11\,240 \pm 50$	$10\,630 \pm 80$
	UW-58	686 ± 8	$13\,110 \pm 30$	$12\,420 \pm 40$
	UW-154	933 ± 3	$11\,800 \pm 30$	$10\,870 \pm 30$

2.3.3.2 Substrate and Product Stability

The stability of both the unhydrolyzed and hydrolyzed versions of each substrate was assessed using spectral scans at 0 hr, 3 hr, 24 hr, and 96 hr (Figure 2.10). The unhydrolyzed versions of the substrates tend to be stable within the time frame of a day of assays and start to degrade within 24 hr. The apparent hydrolysis of the substrates at 96 hr can be observed for NC, UW-57, and UW-58. The products of the substrate hydrolysis are much less stable than the unhydrolyzed substrate often showing a significant decrease in maximal absorbance at only 3 hr (with the exception of nitrocefin).

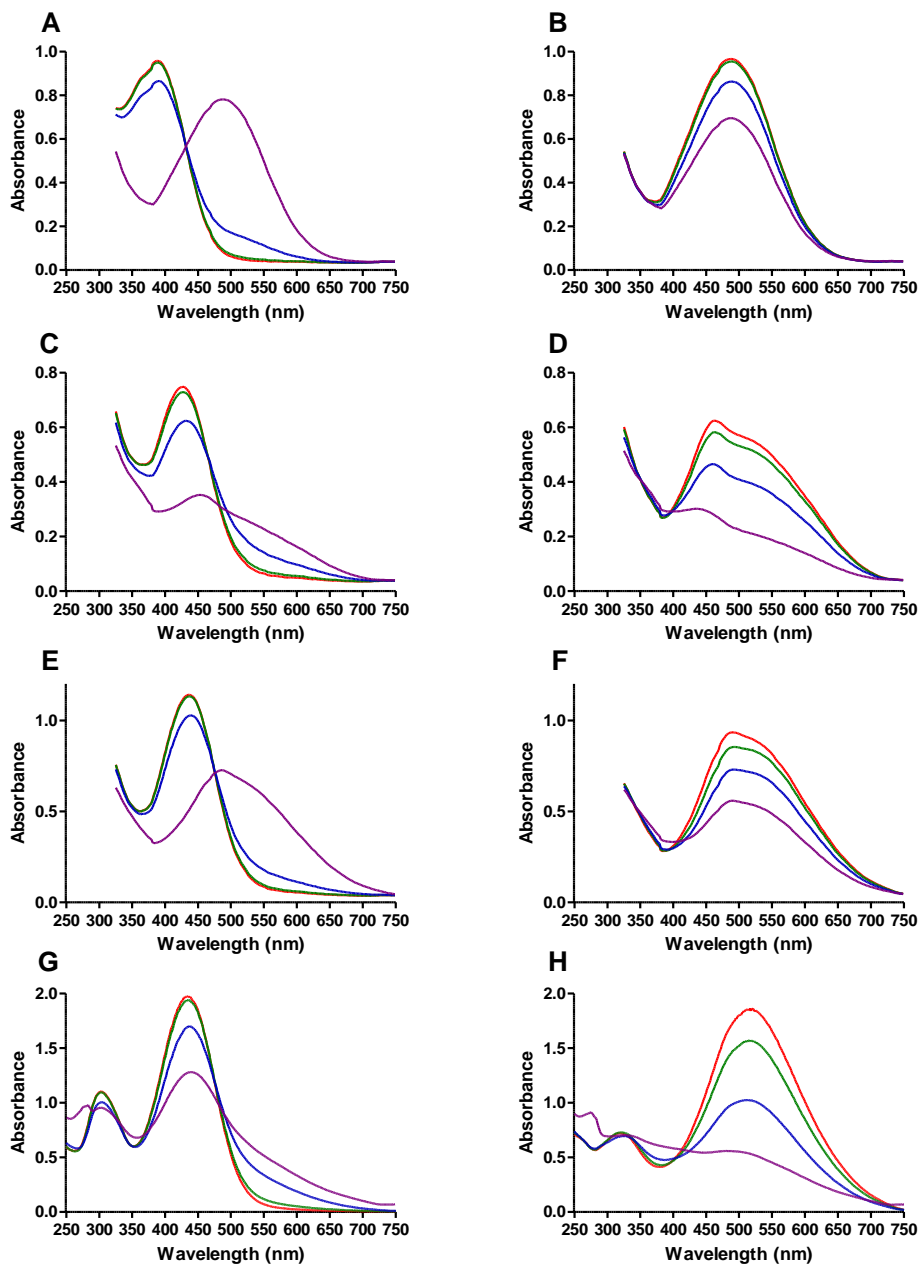


Figure 2.10 Stability spectra of 100 μM chromogenic substrates before and after hydrolysis. NC (A: unhydrolyzed, B: hydrolyzed), UW-57 (C: unhydrolyzed, D: hydrolyzed), UW-58 (E: unhydrolyzed, F: hydrolyzed), and UW-154 (G: unhydrolyzed, H: hydrolyzed) at 0 hr (red), 3 hr (green), 24 hr (blue), 96 hr (purple). This figure was generated using GraphPad Prism v. 5.03.

2.3.4 Biochemical Characterization

2.3.4.1 DMSO Stability

The relative activity of β -lactamases incubated for 10 min in various concentrations of DMSO is presented in Figure 2.11 with stability being defined as a <10 % reduction in activity relative to a no DMSO added control (0.05 % - 0.2 % DMSO present in NC). Of the SBLs, CTX-M-15, OXA-23, and OXA-48 are only stable up to 2 % DMSO while KPC-2 and GC-1 are stable up to 5 % DMSO. VIM-1 is the least DMSO stable of the MBLs, dipping below the acceptable activity reduction after only 1 % DMSO. The other MBLs are much more stable with SPM-1 and VIM-2 being stable up to 2.5 % DMSO, IMP-1 and L1 being stable up to 5 % DMSO, and NDM-1 appearing to be activated in the presence of DMSO. This suggests that in most cases, the presence of 2 % DMSO is tolerated well by β -lactamases.

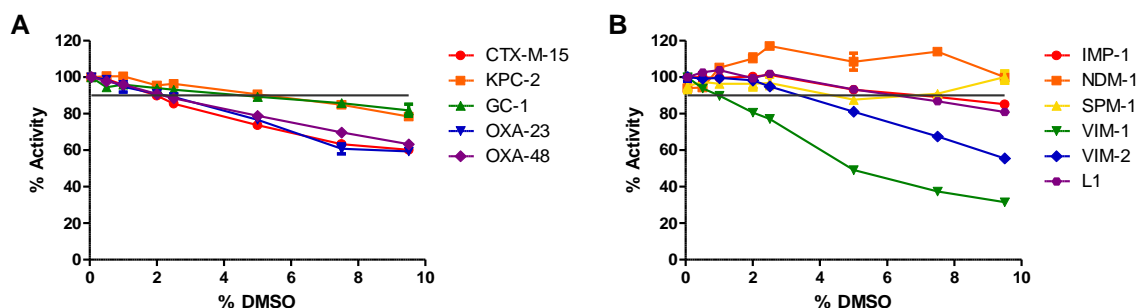


Figure 2.11 DMSO sensitivity of β -lactamases separated into (A) SBLs and (B) MBLs with a cutoff line at 10 % activity reduction. This figure was generated using GraphPad Prism v. 5.03.

2.3.4.2 Determination of Kinetic Parameters

The determination of kinetic parameters was done by non-linear regression of the Michaelis-Menten plots fitting to either Michaelis-Menten (Equation 2.1) or substrate inhibition (Equation 2.2) equations as appropriate. The hydrolysis of NC and UW substrates in 50 mM HEPES pH 7.2 and 100 mM NaPi pH 7.2 by both tagged and cleaved CTX-M-15 is presented in Figure 2.12. These graphs show that the tagged CTX-M-15 is more prone to substrate/product inhibition in both buffer systems as seen by the reduction in rate of hydrolysis at high substrate concentrations. Substrate/product

inhibition is also observed when the His-tag cleaved CTX-M-15 but only in the HEPES buffer system. The concentration of DMSO in these experiments was kept constant.

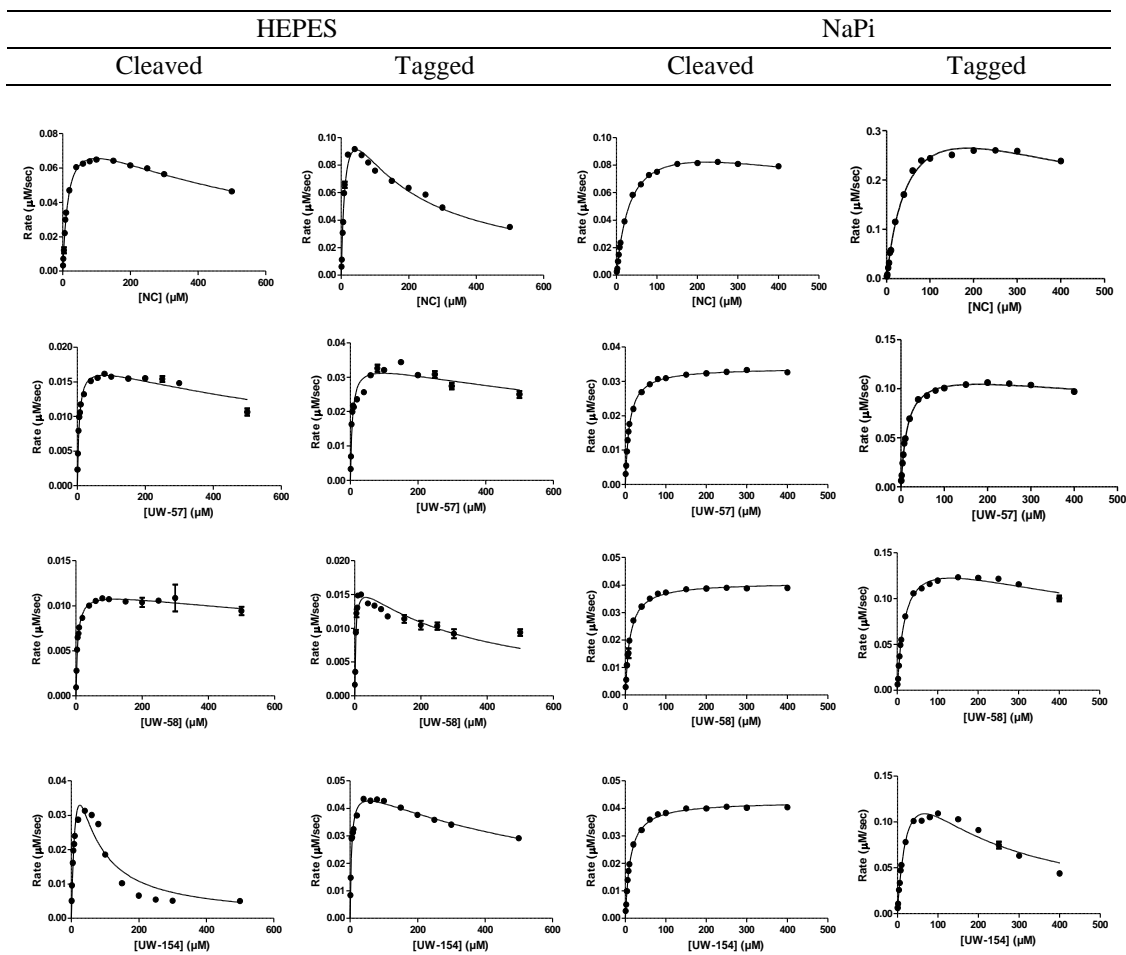


Figure 2.12 Michaelis-Menten plots of CTX-M-15 kinetic parameter determination. Each point represents three replicate measurements, error bars are often smaller than the markers. This figure was generated using GraphPad Prism v. 5.03.

The kinetic parameters determined by the non-linear regression of the graphs in Figure 2.12 can be found in Table 2.10. It is evident that while substrate/product inhibition in HEPES is a slight problem for CTX-M-15 with the tag cleaved, the K_I is at least 10x greater than the K_M for all substrates except UW-154 where they are both about 25 μM . Overall, the K_M and k_{cat} for NC is about 3 times greater

than those for the UW substrates (particularly UW-57 and UW-58) and the k_{cat}/K_M is similar for all substrates within a given set of conditions.

Table 2.10 Kinetic parameters of CTX-M-15 with and without its His-tag against NC and UW substrates.

CTX-M-15 Preparation	Buffer	Substrate	K_M (μM)	K_I (μM)	k_{cat} (s^{-1})	k_{cat}/K_M ($\mu\text{M}^{-1}\text{s}^{-1}$)
Cleaved	HEPES	NC	17.3 ± 0.8	580 ± 40	580 ± 10	33 ± 2
		UW-57	5.6 ± 0.4	1110 ± 140	120 ± 2	21 ± 1
		UW-58	5.8 ± 0.6	2400 ± 800	78 ± 2	13 ± 1
		UW-154	24 ± 8	25 ± 8	640 ± 150	30 ± 10
	NaPi	NC	35.7 ± 0.9	1400 ± 90	716 ± 8	20.1 ± 0.5
		UW-57	10.0 ± 0.2		223.6 ± 0.7	22.4 ± 0.3
		UW-58	11.2 ± 0.3		270 ± 2	24.1 ± 0.7
		UW-154	12.1 ± 0.2		280 ± 1	23.2 ± 0.5
Tagged	HEPES	NC	12 ± 1	150 ± 20	3270 ± 150	250 ± 30
		UW-57	5.9 ± 0.6	1600 ± 400	790 ± 30	130 ± 20
		UW-58	3.5 ± 0.6	330 ± 60	400 ± 20	110 ± 20
		UW-154	4.3 ± 0.2	730 ± 60	1120 ± 20	260 ± 20
	NaPi	NC	57 ± 4	600 ± 70	9700 ± 400	170 ± 10
		UW-57	15.4 ± 0.5	2100 ± 200	2780 ± 30	181 ± 6
		UW-58	18.8 ± 0.8	930 ± 80	3580 ± 70	190 ± 9
		UW-154	30 ± 3	150 ± 20	4660 ± 290	160 ± 20

Combinations without a K_I value were fitted to Equation 2.1 rather than Equation 2.2.

The kinetic parameters of all other β -lactamases used in this thesis have also been determined for NC and the UW substrates. Many of these experiments were published by Dr. Geneviève Labbé using the β -lactamase preparations described above and have been included in Table 2.11.⁴⁵³ Michaelis-Menten plots for the β -lactamases not included in the publication by Ghavami et al. are presented in Figure 2.13 and show typical Michaelis-Menten behaviour with the exception of OXA-48 and VIM-1 which display substrate/product inhibition.

The kinetic parameters for the SBLs used in this thesis against NC and UW substrates are listed in Table 2.11. Generally, KPC-2 and GC-1 β -lactamases have the lowest K_M values for NC and the highest K_M values for UW-154, a trend that is mirrored in the k_{cat} values. This K_M trend does not hold for Class D β -lactamases which have significantly higher K_M values for NC than any other tested substrate by 3 – 4 fold. The k_{cat} values for the Class D SBLs scale with the K_M values as seen in KPC-2 and GC-1. Unlike the other SBLs, GC-1 is susceptible to substrate/product inhibition.

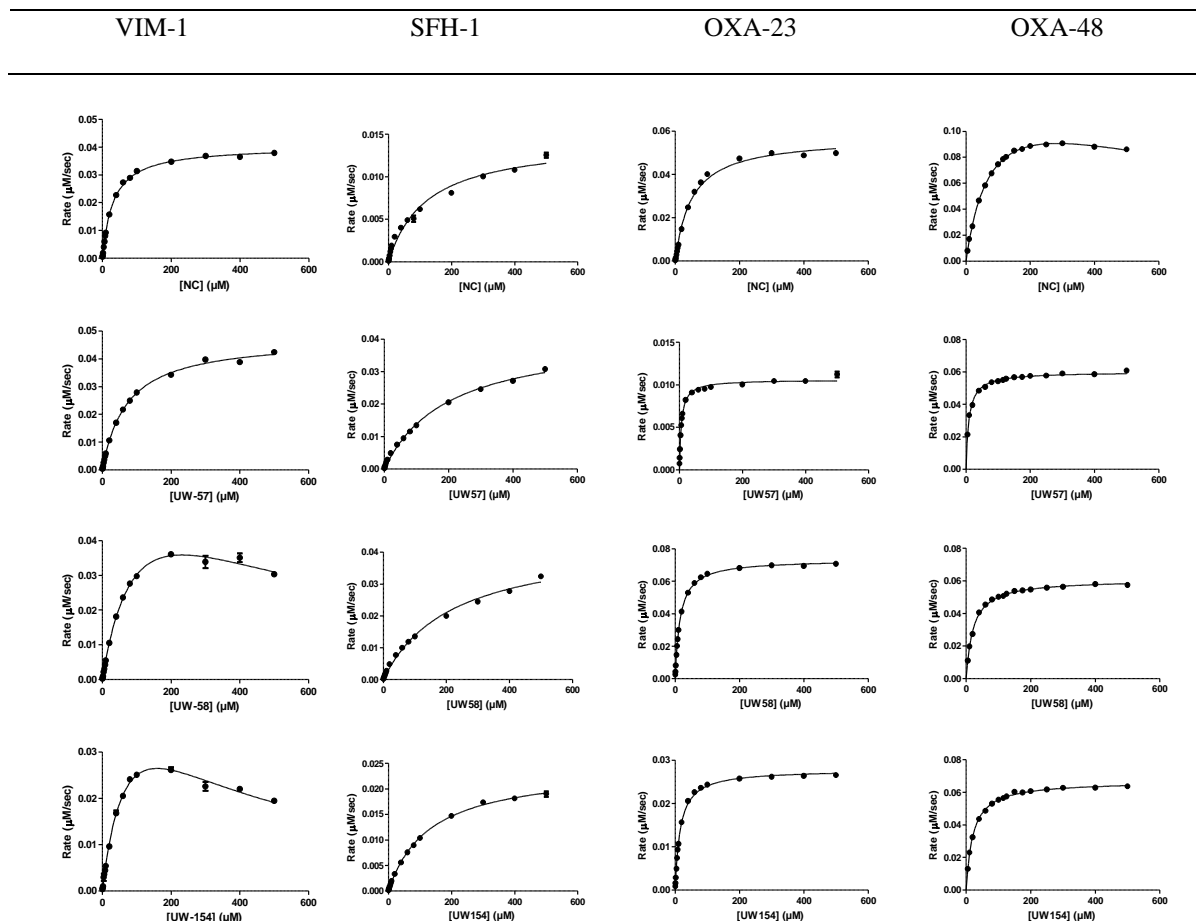


Figure 2.13 Michaelis-Menten plots of VIM-1, SFH-1, OXA-23, and OXA-48 kinetic parameter determination. Each point represents three replicate measurements, error bars are often smaller than the markers. This figure was generated using GraphPad Prism v. 5.03.

The K_I values for this inhibition tend to be at least 10x greater than the K_M values (except for UW-57 where K_I is only about 4x larger than the K_M) so they should not be problematic for kinetic experiments performed at K_M concentrations of substrate. The catalytic efficiencies (k_{cat}/K_M) of all substrates tend to be fairly consistent for each SBL.

The kinetic parameters for the MBLs with NC and the UW substrates (Table 2.12) tend to follow the same trend seen for the SBLs. The K_M values for all substrates tend to be fairly consistent and any

variation is generally mirrored in the k_{cat} values leading to consistent catalytic efficiencies. The only exceptions to this are the NC values for SPM-1, SFH-1, and L1 in which the K_M is slightly (1.1 to 1.5-fold) smaller than it is for other substrates and the k_{cat} is significantly (5 to 10-fold) smaller leading to much lower catalytic efficiencies.

Table 2.11 Kinetic parameters of serine- β -lactamases (except CTX-M-15) against NC and UW substrates.

Enzyme	Class	Substrate	K_M (μM)	K_I (μM)	k_{cat} (s^{-1})	k_{cat}/K_M ($\mu\text{M}^{-1}\text{s}^{-1}$)
KPC-2 ^a	A	NC	8.1 ± 0.2		520 ± 3	64 ± 2
		UW-57	12.6 ± 0.2		463 ± 2	36.8 ± 0.6
		UW-58	14.1 ± 0.3		607 ± 3	43.1 ± 0.9
		UW-154	20.9 ± 0.5		799 ± 7	38 ± 1
GC-1 ^a	C	NC	15.4 ± 0.8	390 ± 20	920 ± 20	60 ± 4
		UW-57	35 ± 4	130 ± 20	1700 ± 100	49 ± 6
		UW-58	20.3 ± 0.7	390 ± 20	1460 ± 30	72 ± 3
		UW-154	35 ± 2	270 ± 30	2200 ± 90	63 ± 4
OXA-23	D	NC	51 ± 2		95 ± 1	1.86 ± 0.08
		UW-57	6.3 ± 0.2		8.85 ± 0.06	1.41 ± 0.05
		UW-58	15.2 ± 0.2		24.44 ± 0.07	1.60 ± 0.02
		UW-154	15.7 ± 0.3		23.2 ± 0.1	1.48 ± 0.03
OXA-48	D	NC	82 ± 2	980 ± 50	1650 ± 20	20.0 ± 0.6
		UW-57	9.2 ± 0.2		242.8 ± 0.8	26.3 ± 0.7
		UW-58	21.5 ± 0.5		351 ± 2	16.3 ± 0.4
		UW-154	20.5 ± 0.4		3787 ± 1	18.8 ± 0.4

^aThese assays were performed by Dr. Geneviève Labbé and were reported by Ghavami et al.⁴⁵³

Combinations without a K_I value were fitted to Equation 2.1 rather than Equation 2.2.

As was seen for the SBLs, some enzymes are subject to substrate/product inhibition; in this case VIM-1, SPM-1 and NDM-1. For SPM-1 and NDM-1, the K_M s are extremely low and the K_I values for the inhibition are around 100x higher. This substrate/product inhibition should not be a problem for inhibition kinetics performed near K_M but should be kept in mind for those performed in excess substrate (usually only 10x K_M). This consideration is irrelevant for NDM-1 as it is only inhibited by UW-57 and inhibition kinetics were performed with NC. For VIM-1, only UW-58 and UW-154 display significant substrate/product inhibition, which is not a problem for kinetic assays performed with NC.

Table 2.12 Kinetic parameters of metallo- β -lactamases with NC and UW substrates

Enzyme	Class	Substrate	K_M (μM)	K_I (μM)	k_{cat} (s^{-1})	k_{cat}/K_M ($\mu\text{M}^{-1}\text{s}^{-1}$)
IMP-1 ^a	B1	NC	3.5 ± 0.2		236 ± 3	67 ± 4
		UW-57	2.5 ± 0.1		229 ± 2	92 ± 4
		UW-58	3.0 ± 0.1		235 ± 2	78 ± 3
		UW-154	6.8 ± 0.2		576 ± 5	85 ± 3
NDM-1 ^a	B1	NC	0.88 ± 0.06		43.7 ± 0.5	50 ± 3
		UW-57	1.43 ± 0.09	1300 ± 100	120 ± 2	84 ± 5
		UW-58	2.15 ± 0.09		185 ± 1	86 ± 4
		UW-154	2.6 ± 0.1		237 ± 2	91 ± 4
SPM-1 ^a	B1	NC	1.2 ± 0.1	630 ± 90	4.9 ± 0.1	4.1 ± 0.4
		UW-57	1.5 ± 0.1	270 ± 20	25.8 ± 0.5	17 ± 1
		UW-58	2.3 ± 0.2	210 ± 20	51 ± 1	22 ± 2
		UW-154	2.6 ± 0.2	130 ± 10	58 ± 2	22 ± 2
VIM-1	B1	NC	31.5 ± 0.6		25.2 ± 0.1	0.80 ± 0.02
		UW-57	71 ± 2		74.3 ± 0.6	1.04 ± 0.03
		UW-58	120 ± 10	450 ± 70	113 ± 9	1.0 ± 0.1
		UW-154	90 ± 9	280 ± 30	88 ± 6	1.0 ± 0.1
VIM-2 ^a	B1	NC	13.9 ± 0.3		471 ± 3	33.9 ± 0.8
		UW-57	12.5 ± 0.5		369 ± 4	30 ± 1
		UW-58	15.1 ± 0.3		529 ± 3	35.0 ± 0.7
		UW-154	17.5 ± 0.9		590 ± 10	34 ± 2
SFH-1	B2	NC	120 ± 10		1.60 ± 0.05	0.013 ± 0.001
		UW-57	200 ± 10		23.2 ± 0.5	0.115 ± 0.006
		UW-58	220 ± 10		24.5 ± 0.6	0.112 ± 0.007
		UW-154	132 ± 4		13 ± 1	0.10 ± 0.01
L1 ^a	B3	NC	5.5 ± 0.5		69 ± 1	13 ± 1
		UW-57	8.5 ± 0.1		279 ± 1	32.8 ± 0.4
		UW-58	15.2 ± 0.4		388 ± 3	25.5 ± 0.7
		UW-154	16.7 ± 0.6		425 ± 6	25 ± 1

^aThese assays were performed by Dr. Geneviève Labbé and were reported by Ghavami et al.⁴⁵³

Combinations without a K_I value were fitted to Equation 2.1 rather than Equation 2.2.

The kinetic parameters determined in this chapter, particularly the K_M s, will be used to inform the design of the experiments in future chapters.

2.4 Discussion

The phylogenetic analysis of NDM variants showed that they are all closely related to NDM-1, often only differing by 1 or 2 amino acids. Each of the amino acids that differ across the NDM variants have been highlighted in green in the NDM-1 structure in Figure 2.14.

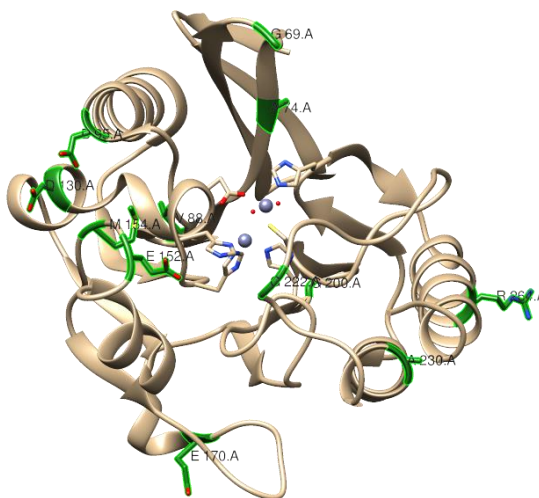


Figure 2.14 NDM-1 crystal structure with residues that are changed among the variants highlighted in green. This figure was generated using UCSF Chimera v. 1.12 from protein databank file 3SPU Chain A.

Of the mutable residues, G222 and E152 are the closest to the active site (within 7 Å of Zn1) and are most likely to cause a difference in substrate hydrolysis or inhibition. The E152 mutation has been studied in NDM-9 and results in a 3-fold increase in the affinity (K_M) and 2-fold increase in hydrolytic activity (k_{cat}) for meropenem while decreasing the affinity for nitrocefin 6-fold and its hydrolytic activity 2-fold relative to NDM-1.⁴⁶⁹ The G222 mutation, which is located on the mobile loop that comes over the active site, was studied in NDM-12 which also contains an M154 mutation. In the NDM-12 variant, the affinity of meropenem is largely unchanged relative to NDM-1 but the hydrolytic activity is decreased 3-fold. In microbial experiments, this showed little difference in MICs against transformed *E. coli* DH5 α ; often only 1 two-fold dilution different for a varied collection of β -lactams which is often considered to be within standard error for this type of experiment.⁴⁷⁰ M154 is also quite close to the active site (within 10 Å of Zn1) and is the most prevalent mutation being found

in 10 of the 19 NDM variants. A study of 4 variants with the M154 mutation (NDM-4, NDM-5, NDM-7, and NDM-8) concluded that this mutation does not have significant effects on the kinetics except that substrate inhibition becomes apparent at high concentrations of nitrocefin.⁴⁷¹ The small changes in kinetic parameters that result from these mutations as well as their physical location suggests that they should not significantly affect the binding of inhibitors. Generally, these variants are similar enough that if a representative of the family (NDM-1) is susceptible to an inhibitor, then all variants should be susceptible to a similar extent.

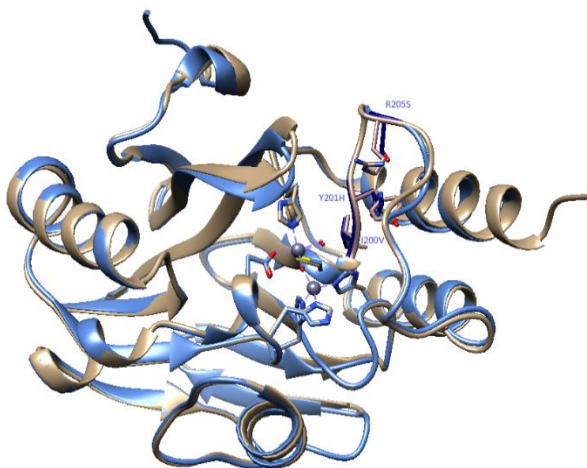


Figure 2.15 Overlay of VIM-1 and VIM-2 crystal structures with variable residues within 10 Å of the Zn atoms highlighted in a darker colour and labelled relative to VIM-2. This figure was generated using UCSF Chimera v. 1.12 from the following protein databank files: VIM-1 (blue, PDB: 5N5G), VIM-2 (tan, PDB: 4BZ3).

The phylogenetic tree in Figure 2.5 shows that the VIM variants can be split into two major and three minor groups: VIM-1-like and VIM-2-like being the major groups, and VIM-12-like, VIM-13-like, and VIM-7 being the minor groups. Many of the mutations that occur in this family occur in the signal peptide region (1-20 aa) and are not present in the mature protein. The mutations between VIM-2 and VIM-1 within 10 Å of the Zn atoms, I200V, Y201H, and R205S, have been highlighted in Figure 2.15. A crystal structure of VIM-1 bound to hydrolyzed meropenem (PDB: 5N5I) has also been obtained and of the three mutations listed above, only S205 falls within 5 Å of the hydrolysis product. In VIM-2, when this is an Arg residue, the polarity of the amino acid is reversed and comes much closer to the amide oxygen on the side chain of meropenem. This would change the kinetics of

meropenem hydrolysis between VIM-1 and VIM-2 as one has favourable contacts with the product and the other has unfavourable contacts.

A comparison of substrate and inhibition kinetics between VIM-2 and four VIM-1 like variants (VIM-1, VIM-4, VIM-5, and VIM-38) was reported by Makena et al. and determined that these variants behave similarly with various substrates but differ greatly in their behaviour with isoquinoline-based metal chelators.⁴⁷² This similarity between the substrate kinetics of VIM-1 and VIM-2 was also observed in this lab where their K_M values for nitrocefin are relatively close (31 μM and 13.9 μM ⁴⁵³ respectively). From an epidemiological standpoint, VIM-1 is by far the most prevalent VIM variant in clinical isolates although VIM-2 is also found in multiple isolates.²⁷⁸ VIM-1 is woefully understudied as a protein with crystal structures having been released very recently and two publications with original kinetic data (one of which uses VIM-1 with an uncleaved C-terminal His-tag).^{464,472} Conversely, VIM-2 is extensively studied and is often the go-to VIM for studies with MBLs. The observation by Makena that they do not necessarily behave in a similar manner with inhibitors in addition to the structural observations, suggest that VIM-1 should be included in initial screens of inhibitors to determine whether or not VIM-2 alone will be an adequate representative of the VIM family for the inhibitors in this study.⁴⁷²

On first inspection of the phylogenetic tree in Figure 2.6, the IMP variants do not appear to have any major groupings like the VIM family with the exception of the grouping around IMP-1. A 2014 analysis of the diversity of IMP variants identified 5 main branches of the phylogenetic tree; however only 42 IMP variants were identified at that time, and there are now 70 identified IMP variants and the phylogenetic tree has increased in complexity.⁴⁷³ A study by Matsumura et al. on the global epidemiology of IMP producing clinical isolates showed that IMP-1 and IMP-4 (which only has 10 amino acids different from IMP-1) are the most prevalent IMP variants.²⁷⁶ Purification and characterization of an adequate number of IMP variants was beyond the scope of the present study and so characterization of substrates and inhibitors were limited to IMP-1 due to its clinical significance and availability.

None of the purifications in this chapter were the same as one another. Of the proteins purified in this work, the yield of final usable protein was greatest for OXA-48 which yielded 32 mg of pure protein from 2 L of liquid culture once the tag was cleaved. A similar yield of CTX-M-15 could be achieved as there is 34 mg of concentrated tagged protein; however, as a result of the limited supply

of thrombin at the time of this investigation, only a small portion of the protein was subjected to tag cleavage. Other His-tagged β -lactamases did not give high yields for various reasons: VIM-1 did not overexpress well in the cells and only a small portion of the available culture was used in purification, and KPC-2 did not bind to the Ni-NTA column leading us to believe that the His-tag was cleaved in the cells, a hypothesis later confirmed by ESI-MS. GC-1, the only β -lactamase that was never tagged, yielded 2.5 mg of pure protein after ammonium sulfate precipitation, ion exchange, and size exclusion chromatography. The SDS-PAGE presented in Figure 2.7 confirms the purity of each β -lactamase used in this thesis, and the masses in Table 2.8 confirm their identity. Each of these preparations yielded an adequate amount of protein for the kinetics presented in this thesis although the tagged purifications (like CTX-M-15) were by far preferred to untagged purifications (like GC-1) due to the ease of the purification.

The four substrates produced in this laboratory (NC, UW-57, UW-58, and UW-154) were deemed adequate for the study of the β -lactamases used in this work as they each demonstrate a maximal difference between the substrate and product spectra in the visible range, making them conducive to use in polystyrene 96-well plates. These substrates also proved to be stable within the time constraints of a normal day of assays (as long as 3 hr at room temperature) and the relative instability of the product should not interfere with assays as most are only run for 5-10 min. To minimize any possible deterioration of the substrate, they will be kept on ice after dilution until they are ready to be used.

While each of the substrates can be hydrolyzed by all of the β -lactamases used in this thesis, some are better than others in specific cases. Most assays presented in this thesis will be run using nitrocefin as the substrate due to its widespread use in the literature, facilitating comparison. The exception to this is SFH-1 which behaves similarly with UW-57 and UW-58 but has a k_{cat} 15-fold lower than NC which translates into more SFH-1 being required to achieve readable rates with NC. Due to the extremely limited supply of SFH-1 and the amount of it required for any given assay, it will be assayed with UW-58 for inhibition studies.

It was important to establish how tolerant the various β -lactamases are to DMSO since the majority of the inhibitors used in this work are soluble in DMSO. The cutoff for stability was set at 10 % activity reduction since that is considered in the literature to be the acceptable error for enzyme kinetics and has been used as a cutoff in similar experiments.⁴⁷⁴⁻⁴⁷⁶ All β -lactamases were stable up to at least 2% DMSO with the exception of VIM-1 which was only stable up to 1 % DMSO. This will

be considered the upper limit of DMSO concentration even though some β -lactamases are stable at DMSO concentrations much higher than 2 %.

As can be seen in Table 2.13, the values for various kinetic parameters with nitrocefin vary widely in the literature for SBLs. CTX-M-15 and KPC-2 are widely studied Class A β -lactamases in enzymatic assays and the K_M determined in our lab fits within the expected range for KPC-2 but is 2-fold lower than any of the literature K_M s for CTX-M-15. Conversely, our k_{cat} for CTX-M-15 is consistent with literature values while our k_{cat} for KPC-2 is about 10x those found in the literature. The class D SBLs, OXA-23 and OXA-48 are generally studied with meropenem as opposed to nitrocefin; however, our values for K_M fall within the expected variance based on the spread seen in the literature for Class A SBLs. The k_{cat} for OXA-23 obtained in this study is much lower than the literature value (93 s^{-1} and 1500 s^{-1} respectively) but considering the literature value is for a OXA-23-MBP fusion protein, differences are expected.⁴⁷⁷ The two literature values for the OXA-48 K_M vary four fold and our value falls halfway between them, although the reported k_{cat} values range from 143 s^{-1} to 1610 s^{-1} .^{241,478} GC-1 has been previously studied with cephalothin, cefuroxime, ceftazidime, benzylpenicillin, ampicillin, and aztreonam; however, studies with nitrocefin have only been performed by members of the Dmitrienko lab, so there is no literature value for comparison.^{219,479}

Table 2.13 Literature values for serine- β -lactamase kinetic parameters with nitrocefin.

Enzyme	Class	K_M (μM)	k_{cat} (s^{-1})	k_{cat}/K_M ($\mu\text{M}^{-1}\text{s}^{-1}$)	Source
CTX-M-15	A	35	582	16.6	Faheem ⁴⁸⁰
		47	190	4	Ourghanlian ⁴⁸¹
		88	7619	86	Maryam ⁴⁸²
		17	570	33	this study
KPC-2	A	24	78	3.3	Yigit ²⁰⁴
		11	42	3.9	Ourghanlian ⁴⁸¹
		5	30	6.0	Papp-Wallace ⁴⁸³
		6	52	8.7	Papp-Wallace ⁴⁸⁴
		8.1	520	64	Ghavami ⁴⁵³ (this group)
GC-1	C	15.4	920	60	Ghavami ⁴⁵³ (this group)
OXA-23	D	109	1500	13.8	Torol ⁴⁷⁷
		51	93	1.83	this study
OXA-48	D	120	940	7.7	Docquier ²⁴¹
		36	143	4	Stojanoski ⁴⁷⁸
		82	1610	19.6	this study

Similar to the SBLs, the literature values for the kinetic parameters of MBLs with nitrocefin vary widely. The K_M and k_{cat} values obtained by members of the Dmitrienko lab for NDM-1, VIM-2, and L1 are consistent with literature values. The literature values for NDM-1 vary by more than an order of magnitude, likely because its K_M approaches the lower limit for detection of NC by spectrophotometry (rates cannot be determined for NC concentrations below 0.5 μM). The K_M of IMP-1 from the Dmitrienko lab is approximately 2-16-fold lower than literature values although, the k_{cat} is fairly consistent.

Table 2.14 Literature values for metallo- β -lactamase kinetic parameters with nitrocefin.

Enzyme	Class	K_M (μM)	k_{cat} (s^{-1})	k_{cat}/K_M ($\mu\text{M}^{-1}\text{s}^{-1}$)	Source
IMP-1	B1	20	467	23	Yamaguchi ³⁰²
		12	276	23	Siemann ⁴²⁰
		27	63	2.3	Laraki ⁴⁰³
		8.2	13.	16	Moali ⁴⁸⁵
		55.7	2794	50	van Berkel ³¹⁷
		3.5	236	67	Ghavami ⁴⁵³ (this group)
NDM-1	B1	3	12.5	4.2	Kim ⁴⁸⁶
		1.3	15	12	Thomas ⁴⁸⁷
		8.8	25.3	2.9	van Berkel ³¹⁷
		1.1	16	15	Yang ⁴⁸⁸
		3.7	2.6	0.69	Yang ⁴⁸⁸
		11	65	5.9	Makena ⁴⁷¹
		0.9	43.7	50	Ghavami ⁴⁵³ (this group)
SPM-1	B1	4	0.5	0.1	Murphy ⁴⁸⁹
		16	0.7	0.04	van Berkel ³¹⁷
		1.2	4.9	4.1	Ghavami ⁴⁵³ (this group)
VIM-1	B1	15	130	8.7	Makena ⁴⁷²
		17	95	5.6	Franceschini ⁴⁶⁴
		31	25	1.0	this study
VIM-2	B1	13.8	206	15	Marchiaro ⁴⁹⁰
		18	770	43	Docquier ⁴⁰⁴
		7.2	226	31	van Berkel ³¹⁷
		50	510	10	Makena ⁴⁷²
		13.9	471	34	Ghavami ⁴⁵³ (this group)
SFH-1	B2	106	0.06	0.00057	Fonseca ⁴⁹¹
		120	1.57	0.013	this study
L1	B3	4	41	10	Crowder ⁴⁹²
		5.5	69	13	Ghavami ⁴⁵³ (this group)

SPM-1 also gave a lower K_M when compared to literature values as well as a higher k_{cat} leading to catalytic efficiency that is as much as 100 x greater than literature (4.1 vs 0.04).³¹⁷ The obtained K_M of SFH-1 is consistent with literature value (120 μM and 106 μM respectively); however, we obtained a much higher k_{cat} value.⁴⁹¹ Despite our determination of a high k_{cat} for SFH-1, it is still too low for efficient use in kinetic assays using NC which is why UW-58 was used as it has a higher k_{cat} .

The VIM-1 purified in this laboratory was found to exhibit stability issues in certain storage conditions, one of the least stable conditions was used for this determination and likely contributed to the discrepancy between the kinetic parameters determined here and the literature. A Michaelis-Menten parameter determination was performed for NC with the ideal storage condition and gave values consistent to the literature (K_M 18.6 μM , k_{cat} 48 s^{-1} , k_{cat}/K_M 2.6 $\text{s}^{-1}\mu\text{M}^{-1}$) however, this was done with 2 technical replicates with only 7 concentrations of NC. This suggests that any further studies performed with VIM-1 should pay closer attention to the stability problem with this MBL.

The values for the various kinetic parameters obtained in this laboratory (either in this study or in Ghavami 2015)⁴⁵³ will be used to inform later experiments as they are most representative of the conditions and constructs used.

2.5 Future Work

As it currently stands, all of the chromogenic substrates in the literature are cephalosporins which limits their usefulness since not all β -lactamases are capable of hydrolyzing cephalosporins. A chromogenic version of a penicillin and a carbapenem could be used in conjugation with one of the cephalosporins as a diagnostic tool to visually determine if a bacterial strain is resistant to any or all of these β -lactam subclasses. This could additionally make kinetics more affordable for β -lactamases that do not hydrolyze cephalosporins well such as SFH-1, OXA-23, OXA-48, and some non-ESBL class A and C β -lactamases since lower concentrations would likely be used for assays performed at K_M concentrations. Development of chromogenic substrates based on other β -lactam scaffolds would also require acquisition or purification of more class A and C β -lactamases: ideally AmpC, P99, CMY-2, and L2 since they are present in the resistant clinical isolates in our collection.

Chapter 3

Inhibition of Metallo- β -Lactamases by Phosphonomethyl Pyridine Carboxylates

3.1 Introduction

The objective of this chapter is to assess the inhibitory potency of pyridine-based inhibitors of metallo- β -lactamases and the potential applications of this inhibition in combination therapy. Previous studies in collaboration with this laboratory concerning the inhibition of bacterial and fungal Class II fructose-1,6-bisphosphate aldolase demonstrated that 6-phosphonomethyl-pyridine-2-carboxylates (PMPCs) are moderately inhibitory (IC_{50} 57-130 μ M).⁴⁹³ Early docking studies suggested that these compounds may also be inhibitory towards MBLs, a hypothesis which was bolstered by literature reports of picolinic acid derivatives and phosphonates inhibiting MBLs.

Dipicolinic acid (DPA) has been used for decades in the identification and characterization of β -lactamases as MBLs, the logic being that if a β -lactamase was inactivated by a metal-binding agent such as DPA, it must be an MBL.⁴⁹⁴ The characterization of IMP-1 and VIM-1 at the turn of the millennium with multiple chelators showed that DPA is one of the more effective inactivators of these MBLs. Upon further exploration of this inactivation, the authors determined that DPA forms a transient ternary complex with the metal-containing enzyme.^{403,464} A few years later, a study was performed on IMP-1 to assess the efficacy of a wide range of chelators and to explore the potential activity of its monozinc form. The most potent IMP-1 chelator from this study, DPA, was shown to be able to extract one of the zinc ions from the IMP-1 active site only when applied in large excess for 10-24 hours. When treated for only 3 hours, 87% of the di-zinc form of IMP-1 remained, suggesting that metal ion removal is slow and the inhibition observed at short incubation times is not the result of Zn extraction.⁴⁰⁰ When SPM-1 was characterized in 2003, it was determined that DPA bound preferentially to one of the Zn ions over the other, unlike IMP-1 and VIM-1 whose kinetics suggest equal affinity for both Zn ions.^{403,464,489} Later structural studies on SPM-1 determined that it is structurally a B1/B2 hybrid, which, with the earlier observation suggest that different subclasses of MBLs may react differently with DPA.^{287,489}

The many reports of MBL inhibition or inactivation by DPA inspired development of DPA based inhibitors. Horsfall et al. studied the inhibitory potency of other pyridinedicarboxylic acids (PDCA) such as 2,3-PDCA, 2,4-PDCA, 2,5-PDCA, and 3,4-PDCA in addition to the standard 2,6-PDCA (DPA) and picolinic acid (PA) against MBLs from all three subclasses using imipenem as a reporter substrate. They found that the Class B2 MBL, CphA, was most potently inhibited by these compounds after 30 minutes of pre-incubation at room temperature, but the inhibition was generally weak (uninhibited by 100 μM 2,3-PDCA, 2,5-PDCA, and 3,4 PDCA and 8 %, 12%, and 38% residual activity when inhibited by 100 μM of PA, DPA, and 2,4-PDCA respectively). Additionally, they determined that inhibition of CphA by these compounds was pH dependent and occurred through a competitive mechanism.⁴¹⁰ Thioacid and thioester derivatives of DPA have also been found to be inhibitory towards Class B3 MBLs, CcrA and L1, but not SBLs.⁴³⁹ This will be explored in more detail in Chapter 4. The most in depth work on the inhibitory action of DPA analogs was reported by Chen et al. in 2017 after the present study of MBL inhibition by PMPCs was completed and details the synthesis of 47 DPA analogs as well as their inhibitory potency against NDM-1. The most potent inhibitor from this study (compound 2 in Figure 3.1) gave in IC_{50} for NDM-1 of 0.08 μM was also a good inhibitor for IMP-1 and VIM-2 with IC_{50} s of 0.24 μM and 0.21 μM respectively.⁴⁹⁵

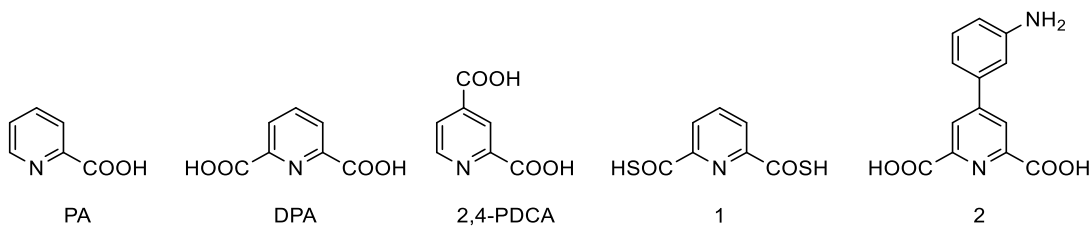


Figure 3.1 MBL inhibitors based off the DPA core structure. 2,4-PDCA,⁴¹⁰ 1,⁴³⁹ and 2⁴⁹⁵ are the most potent novel inhibitors from their respective publications.

The known phosphonate β -lactamase inhibitors are primarily mechanism based SBL inhibitors. The first of these, the phosphonate monoesters such as compound 3 from Figure 3.3, was reported in 1991 by the Pratt group at Wesleyan as an inhibitor of three Class A SBLs: PC1, BC1, and a TEM-type.³⁷⁷ This inhibitor series was then found to also inhibit the Class C SBL P99 and a crystal structure of it bound to the active site of PC1 was generated.^{378,379} The PC1 crystal structure confirmed the hypotheses that the phosphonate monoesters inactivate SBLs by forming a covalent

bond between the phosphorous atom and the catalytic serine residue (Ser70) and that inhibitor potency is dependent upon leaving group stability.³⁷⁹

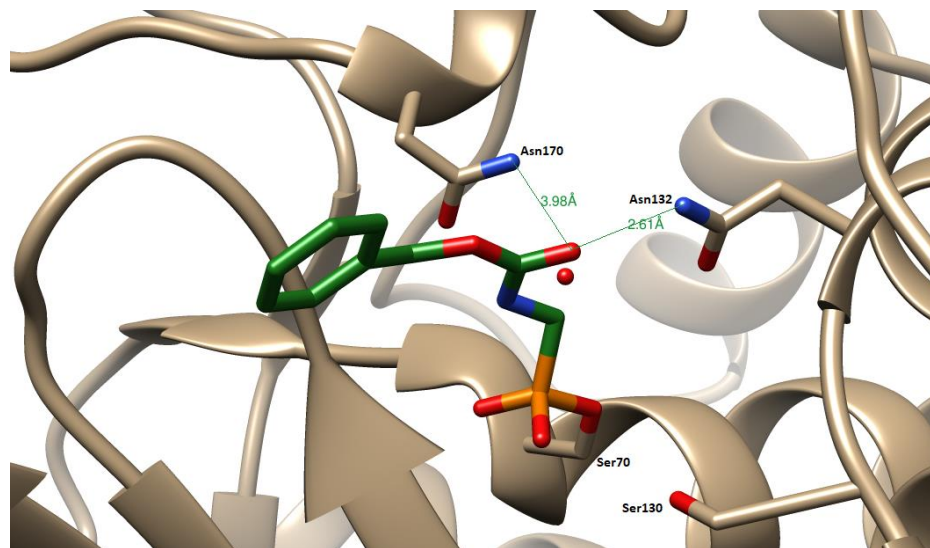


Figure 3.2 PC1 from *S. aureus* covalently inactivated by a phosphonate monoester (compound 3 from Figure 3.3). This figure was generated using UCSF Chimera v. 1.12 from the protein databank file 1BLH.³⁷⁹

More analogs of the phosphonate monoesters were generated to explore the requirements of the part of the molecule that bonds to the serine residue, yielding compound 4 from Figure 3.3. Compound 4 was found to be 20 fold more potent against the TEM-type SBL, 20 fold less potent against P99, and maintain similar potency with PC1.³⁸⁰ Once it was thoroughly established that phosphonates could be SBL inhibitors, two publications probed the possibility of phosphates as SBL inhibitors. Compounds such as compound 7 from Figure 3.3 were found to inhibit OXA-1, P99, and a TEM-type with a suggested mechanism that differs from the phosphonate monoesters: the serine OH attacks the carbon of the ester rather than the phosphorous atom.^{385,386} Further studies also identified bicyclic and monocyclic phosph(on)ates as inhibitors of P99, a TEM-type SBL, OXA-1, and OXA-10 with the bicyclics acting by a mechanism similar to the phosphates expect with the rings being reformed upon reversal, and the monocyclics undergoing a two-step mechanism.³⁸¹⁻³⁸⁴

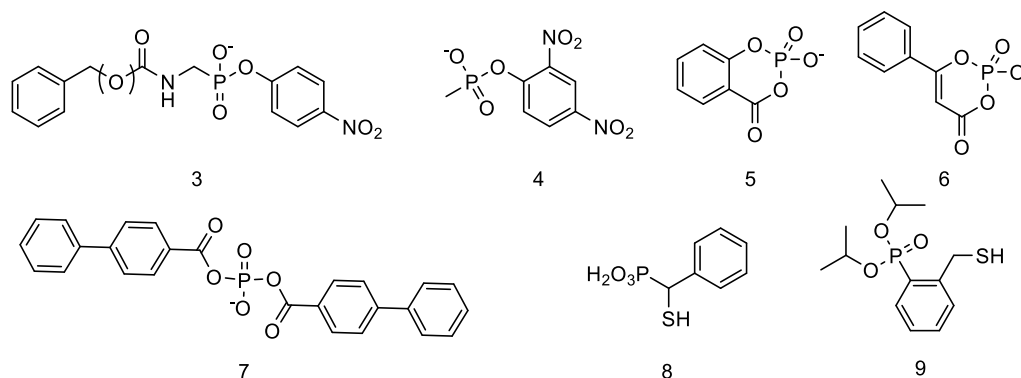


Figure 3.3 Phosph(on)ate based inhibitors of β -lactamases. The SBL inhibitors 3^{377,378}, 4³⁸⁰, 5³⁸¹, 6³⁸³, and 7^{385,386} are the most potent inhibitors from their respective publications. Compounds 8 and 9 are phosphonate based MBL inhibitors.⁴²⁴

The only series of phosphonate inhibitors of MBLs published to date (with the exception of those studied in this chapter) are the mercaptophosphonates, the most potent of which is compound 8 from Figure 3.3. These compounds act as competitive inhibitors of representatives from all three subclasses of MBL: VIM-4 (B1), CphA (B2), and L1(B3), being most potent against the monozinc MBL, CphA. This study also determined two crystal structures of CphA, one of compound 8 bound to CphA and one of compound 9 bound to CphA. Compound 8 was found to bind to the active site with 2 of the phosphonate oxygens interacting with the zinc ion while compound 9 bound such that the thiol was interacting with the zinc ion.⁴²⁴ This illustrates that when two moieties, a phosphonate and a thiol, are competing to interact with zinc, the two contacts made by the phosphonate oxygens are collectively stronger than the single contact from the thiol.

3.2 Methods

Materials used in this chapter were the same as those listed in Chapter 2 unless otherwise stated.

3.2.1 Enzyme Kinetics

3.2.1.1 Inhibitor Screening

A library of PMPCs was made by organic chemists in the Dmitrienko group, primarily by Dr. Anthony Krismanich, and their structures and purity were confirmed by ¹H NMR, ¹³C NMR, and MS. A table containing the structures, molecular weights, laboratory codes, and common acronyms of

these compounds can be found in Appendix A, an abridged figure can be found in Figure 3.4. PMPC-3 and PMPC-4 were prepared as racemic mixtures and were tested as such. Synthetic picolinate derivatives, were prepared as 100 mM stocks in DMSO with the exception of: PMP and DPMP which were prepared as 50 mM stocks in 50 mM HEPES pH 7.2. Commercial picolinate derivatives, DPA, PA, and 6-MPA (Sigma), were prepared in DMSO, the same as synthetic picolinate derivatives. All inhibitor stocks were stored at -20 °C and were remade when necessary.

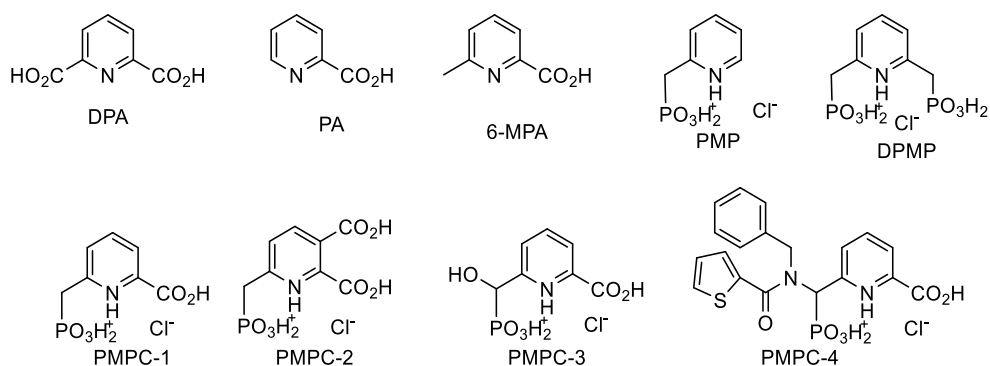


Figure 3.4 Structures of picolinic acid derivatives used in this chapter.

Enzyme stocks for class A, B, and C β -lactamases were prepared in 50 mM HEPES pH 7.2 supplemented with 50 μ g/mL BSA and 0.01 % Triton X-100 while the stocks for class D enzymes were prepared in 100 mM NaPi, 2.1 mg/mL NaHCO₃, pH 7.0 supplemented with 50 μ g/mL BSA and 0.01 % Triton X-100. Enzyme specific conditions are listed in Table 3.1; the total DMSO concentration was kept below 2 %.

Enzyme stocks were pre-incubated with a small selection of inhibitor concentrations from 1 mM, 500 μ M, 100 μ M, 10 μ M, and 1 μ M in addition to the appropriate DMSO control in triplicate for 10 min at 30 °C in flat bottomed microplates. After pre-incubation, inhibited enzyme stock was added to nitrocefin/UW-58 concentrations at or near the K_M to a final volume of 200 μ L and was monitored at 482 nm (NC) or 534 nm (UW-58) every 5-7 sec for 5 min (30 min for SFH-1) using a SpectraMax 190 plate reader (Molecular Devices, Sunnyvale, CA). The initial rate of each reaction was determined using SoftMax 6.0 software (Molecular Devices, Sunnyvale, CA) over a minimum of 5 points. Percent inhibition was calculated relative to a control containing the same concentration of DMSO.

Table 3.1 Kinetic parameters and conditions for PMPC inhibitor screening.

Enzyme	Molecular class	Substrate	K _M (μM)	Enzyme Conc. in assay	[Substrate] in assay (μM)
KPC-2	A	NC	8.1 ± 0.2 ⁴⁵³	211 pM	8
GC-1	C	NC	15.4 ± 0.8 ⁴⁵³	41 pM	15
OXA-48	D	NC	81 ± 2	79 pM	80
IMP-1	B1	NC	3.5 ± 0.2 ⁴⁵³	186 pM	3.5
NDM-1	B1	NC	0.88 ± 0.06 ⁴⁵³	620 pM	1
SPM-1	B1	NC	1.2 ± 0.1 ⁴⁵³	8.17 nM	1
VIM-1	B1	NC	19 ± 1	1.15 nM	15
VIM-2	B1	NC	13.9 ± 0.3 ⁴⁵³	313 pM	15
SFH-1	B2	UW-58	220 ± 10	1.86 nM	100
L1	B3	NC	5.5 ± 0.5 ⁴⁵³	637 pM	5

3.2.1.2 IC₅₀ Determination

A more thorough analysis of inhibition was performed for enzyme/inhibitor concentrations that showed at least 50 % inhibition at 100 μM. Assays were performed as described in 3.2.1.1 using 7 or 14 different concentrations of inhibitor. Inhibitor concentrations were determined using data from the inhibitor screen ensuring both plateaus and the hill of the plot were well defined. Each measurement was performed on 3-4 separate days unless otherwise indicated. Initial rates were normalized then fitted to Equation 3.1 using GraphPad Prism version 5.00 for Windows (GraphPad Software, San Diego, CA) by non-linear least squares regression.

Equation 3.1

$$y = \frac{100}{1 + 10^{(\log IC_{50} - [I]) \cdot s}}$$

Where y is the normalized initial rate, [I] is the log of the inhibitor concentration, and s is the Hill slope. Measurements and uncertainties from each day were averaged using the statistical method described in Appendix B.

3.2.1.3 Determination of Inhibition Constant, K_I

Assays to determine the K_I for the most potent enzyme/inhibitor combinations were performed in 50 mM HEPES pH 7.2 supplemented with 50 μg/mL BSA and 0.01 % Triton X-100 in 96-well flat

bottomed microplates at a final volume of 200 μL . Enzyme mixture was added to nitrocefin ($\gg K_M$) containing dilutions of inhibitor as determined from IC_{50} experiments in triplicate; specific conditions can be found in Table 3.2. Assay was monitored at 482 nm every 6 sec for 10 min at 30 $^\circ\text{C}$ in a SpectraMax 190 plate reader (Molecular Devices, Sunnyvale, CA).

Table 3.2 Conditions of time-dependent K_I determination.

Enzyme	[Enzyme] in assay	[NC] in assay
IMP-1	60 pM	25 μM
NDM-1	600 pM	15 μM
VIM-2	39.2 pM	100 μM
L1	308 pM	50 μM

Progress curves were fitted to Equation 3.2 by non-linear regression using GraphPad Prism version 5.00 for Windows (GraphPad Software, San Diego, CA) to determine k_{obs} , the apparent first-order rate constant at steady state, for each inhibitor concentration.^{496,497}

Equation 3.2
$$[P]_t = v_s t + \frac{(v_o - v_s)(1 - e^{-k_{\text{obs}}t})}{k_{\text{obs}}} + C$$

Where $[P]_t$ is the concentration of product at time t , v_o is the initial rate, v_s is the steady state rate, and C is a constant used to mitigate any background absorbance. The values of k_{obs} were then plotted against their respective concentration of inhibitor $[I]$ to determine which mechanism described in Scheme 3.1 this data fits. The resulting linear plot defined by Equation 3.3 suggests that the data fits Scheme 3.1A.

Equation 3.3
$$k_{\text{obs}} = k_{-o} \left(1 + \frac{[I]}{K_I^{\text{app}}} \right)$$

Where k_{-o} is the dissociation rate constant of EI, the enzyme:inhibitor complex, and K_I^{app} is the apparent inhibition constant. The value of K_I^{app} can be determined by dividing the value of the y-intercept, k_{-o} , by the value of the slope, k_{-o}/K_I^{app} . K_I was then determined using the value of K_I^{app} and Equation 3.4.

Equation 3.4
$$K_I^{\text{app}} = K_I \left(1 + \frac{[S]}{K_M} \right)$$

Finally, k_{on} and k_{off} , the association and dissociation rate constants of EI can be determined using Equation 3.5, where $k_{off} = k_{-o}$ from Equation 3.3.

Equation 3.5
$$K_I = \frac{k_{off}}{k_{on}}$$

3.2.2 Microbial Experiments

3.2.2.1 Bacterial Strains

Detailed information regarding the clinical isolates and control strains used in this study can be found in Appendix C. The *Pseudomonas putida* strain expressing VIM-2 (UWB24), *Escherichia coli* strain expressing both CTX-M-15 and NDM-1 (UWB75), *Pseudomonas aeruginosa* strain expressing VIM-2 (UWB78), and *E. coli* strain expressing both CTX-M-15 and IMP-1 (UWB93), were obtained from the collection of clinical isolates at Calgary Laboratory Services, Calgary, Alberta and were provided by Dr. Johann Pitout and Dr. Dylan Pillai. A *Klebsiella pneumoniae* strain expressing NDM-1 (UWB116), was provided by Dr. Allison McGeer from Mount Sinai Hospital in Toronto, Ontario.

3.2.2.2 Minimum Inhibitory Concentration (MIC) Determination

MIC values for meropenem with the bacterial strains in 3.2.2.1 were assayed by broth microdilution several times in cation adjusted Mueller Hinton broth (MHB) (Sigma) according to the Clinical Laboratory Standards Institute (CLSI) guidelines.⁴⁹⁸ Overnight cultures in MHB were grown shaking at 225 rpm and 37 °C then diluted to approximately 0.5 McFarland as measured by OD₆₀₀. The 0.5 McFarland culture was diluted 100-fold in MHB, making the inoculum. Microtiter plates containing media and two-fold dilutions of meropenem were inoculated with equal volumes of inoculum to a final volume of 200 µL. The growth control (100 µL) that was diluted 1000-fold was plated on Mueller Hinton agar (MHA). Microtiter plates were shaken for 10 sec before being incubated overnight at 37 °C in humid conditions; agar plates were also incubated overnight at 37 °C. MICs were determined by measuring the OD₆₀₀ using a Powerwave XS2 (BioTek) plate reader with an absorbance of 0.07 considered the breakpoint for growth then confirmed visually.

3.2.2.3 Potentiation of β -lactam Antibiotics by PMPCs

Potentiation experiments were performed using the method described in 3.2.2.2 with a gradient of two-fold dilutions of inhibitor, dissolved in DMSO, in the microtiter plates perpendicular to the meropenem gradient.

3.3 Results

3.3.1 Enzyme Kinetics

3.3.1.1 Inhibitor Screening

The inhibitors used in this chapter were first screened against all of the purified β -lactamases available in the Dmitrienko lab to test for inhibition as well as to give a rough estimate of the IC_{50} . To maximize the possibility of seeing inhibition, the inhibitors were preincubated with the enzyme for 10 minutes prior to being added to nitrocefin at concentrations near K_M . These screens were performed in the presence of Triton X-100 to reduce the probability of observing inhibition as a result of aggregation.

The data shown in Table 3.3 indicates that DPA, all of the PMPCs, and DPMP are reasonably potent inhibitors of both B1 and B3 MBLs. The representative B2 MBL, SFH-1, was not inhibited to the same degree by the PMPCs as the other MBLs but its response to DPA was consistent. The PMPCs that significantly inhibited SFH-1 were PMPC-3 and PMPC-4 which both reduced its activity by just over 50 % at 10 μ M. NDM-1 also demonstrated comparable sensitivity with PMPC-3 and PMPC-4. Other MBLs were most potently inhibited by PMPC-4 with VIM-1, and VIM-2 being inhibited by more than 50 % at 1 μ M. PMPC-1 is consistently a more potent inhibitor than DPA, and PMPC-2 is comparable to it against NDM-1, SPM-1, VIM-1, SFH-1, and L1. With IMP-1 and VIM-2, PMPC-2 is less effective at 10 μ M than PMPC-1 was, suggesting that the carboxylate at the 3 position of the pyridine ring may interfere with binding for some MBLs. PA, 6-MPA, and PMP are poor inhibitors that only show activity at the highest concentrations and therefore do not warrant further study. The IC_{50} of PA with VIM-2 will be determined to get an idea of how this compares in more detailed experiments.

Table 3.3 Screening of PMPCs and related commercial compounds against MBLs

		% Inhibition						
		IMP-1	NDM-1	SPM-1	VIM-1	VIM-2	SFH-1	L1
DPA	100 μ M	93.0	91.2	81.1	72.9	97.9	91.9	92.2
	10 μ M	46.1	82.7	30.0	52.4	84.3	59.7	62.2
	1 μ M	17.4	32.3	18.8	-14.5	9.9	4.4	-2.7
PA	100 μ M	19.7	46.4	44.1	37.4	74.6		46.4
	10 μ M	16.5	37.7	18.1	-12.6	26.4		12.5
	1 μ M	17.2	25.9	22.1	-19.9	8.2		-0.6
6-MPA	100 μ M	20.5	32.7	18.0	-11.7	8.5		8.0
	10 μ M	25.9	36.4	14.2	-3.5	4.7		-5.0
	1 μ M	-13.7	7.0	8.5	-9.5	2.4		-3.7
PMPC-1	100 μ M	98.4	99.0	81.7	87.5	101.2	61.6	77.4
	10 μ M	66.2	97.6	26.1	76.2	93.7	41.7	90.8
	1 μ M	2.3	53.4	25.1	39.9	24.7	22.0	32.0
PMPC-2	100 μ M	89.0	101.6	84.0	79.3	97.2	57.7	105.5
	10 μ M	12.4	91.6	41.4	86.4	39.5	40.6	82.3
	1 μ M	0.4	61.5	19.0	42.8	11.9	26.1	24.0
PMPC-3	100 μ M	95.9	101.3	88.7	87.5	96.1	85.2	90.9
	10 μ M	63.6	108.2	41.2	80.0	78.6	54.0	87.0
	1 μ M	26.1	69.7	26.7	33.9	14.7	37.0	32.1
PMPC-4	100 μ M	96.7	100.2	106.5	103.9	101.1	71.6	100.5
	10 μ M	92.0	103.0	70.3	90.8	99.7	51.1	92.9
	1 μ M	24.6	84.3	21.8	61.3	64.7	35.1	39.6
PMP	1 mM	60.7	45.3	14.9		85.0		40.4
	100 μ M	8.5	-14.3	14.4		32.7		2.0
	10 μ M	-3.1	-8.3	10.0		0.4		-3.6
DPMP	1 mM	96.7	98.6	73.9		99.3		97.5
	100 μ M	54.3	97.3	38.4		88.8	33.6	83.5
	10 μ M	1.0	87.3	16.9		35.0	19.7	33.8

Bolded values are >50 % inhibited.

A selection of SBLs was screened to ascertain whether or not these are metallo-enzyme specific inhibitors. As seen in Table 3.4, these compounds do not inhibit SBLs at concentrations comparable to their inhibition of MBLs.

Table 3.4 Screening of PMPCs and related commercial compounds against SBLs.

		% Inhibition		
		KPC-2	GC-1	OXA-48
DPA	500 μ M	28.1	6.5	0.7
	100 μ M	-5.0	-16.4	
	10 μ M	-8.1	-13.7	
PA	500 μ M	10.3	1.3	2.3
	100 μ M	-2.4	-7.9	
	10 μ M	-12.1	-12.9	
6-MPA	500 μ M	12.3	-1.4	1.1
	100 μ M	-6.4	-11.2	
	10 μ M	-5.7	-3.7	
PMPC-1	500 μ M	33.2	25.1	0.6
	100 μ M	4.6	-3.9	
	10 μ M	1.0	-5.2	
PMPC-2	500 μ M	14.5	42.8	1.6
	100 μ M	6.0	1.1	
	10 μ M	-1.1	-14.1	
PMPC-3	500 μ M	13.9	34.8	3.2
	100 μ M	3.8	4.2	
	10 μ M	-4.6	-6.3	
PMPC-4	500 μ M	56.7	47.2	4.8
	100 μ M	19.4	14.3	
	10 μ M	-4.6	0.7	
PMP	1 mM	24.0	17.7	
	500 μ M	12.2	9.7	-2.4
DPMP	1 mM	22.2	25.9	
	500 μ M	19.6	16.1	-2.1

Some inhibition can be detected at 500 μ M for KPC-2 and GC-1, with the greatest effect being observed with PMPC-4 (57 % and 47 % inhibition respectively). The inhibition of SBLs by PMPCs was not considered potent enough to warrant further study.

3.3.1.2 IC₅₀ Determination

A more in-depth screen of MBL inhibition by PMPCs was performed by determining IC₅₀s when the inhibitor was preincubated with enzyme for 10 min prior to addition to nitrocefin. Trends in the efficacy of inhibitors for each enzyme can best be demonstrated by the dose response curves in Figure 3.5. Generally, DPMP (and PA and PMP where applicable) are the poorest inhibitors as seen by their curves being shifted to the right of the others. Little difference can be seen between PMPC-1, PMPC-3, and PMPC-4 against most enzymes, although PMPC-4 is notably more potent than the others against VIM-2. Of the PMPCs, PMPC-2 is the least potent, falling well to the right of the curves of other PMPCs for IMP-1, VIM-1, and VIM-2.

In most cases, the curve shape and Hill slope is fairly consistent for the different inhibitors against any given enzyme with the exception of DPA with SFH-1 and DPMP with both SPM-1 for which the Hill slopes are much higher. This difference may be indicative of inhibitor binding to multiple sites or non-specific inhibition.⁴⁹⁹

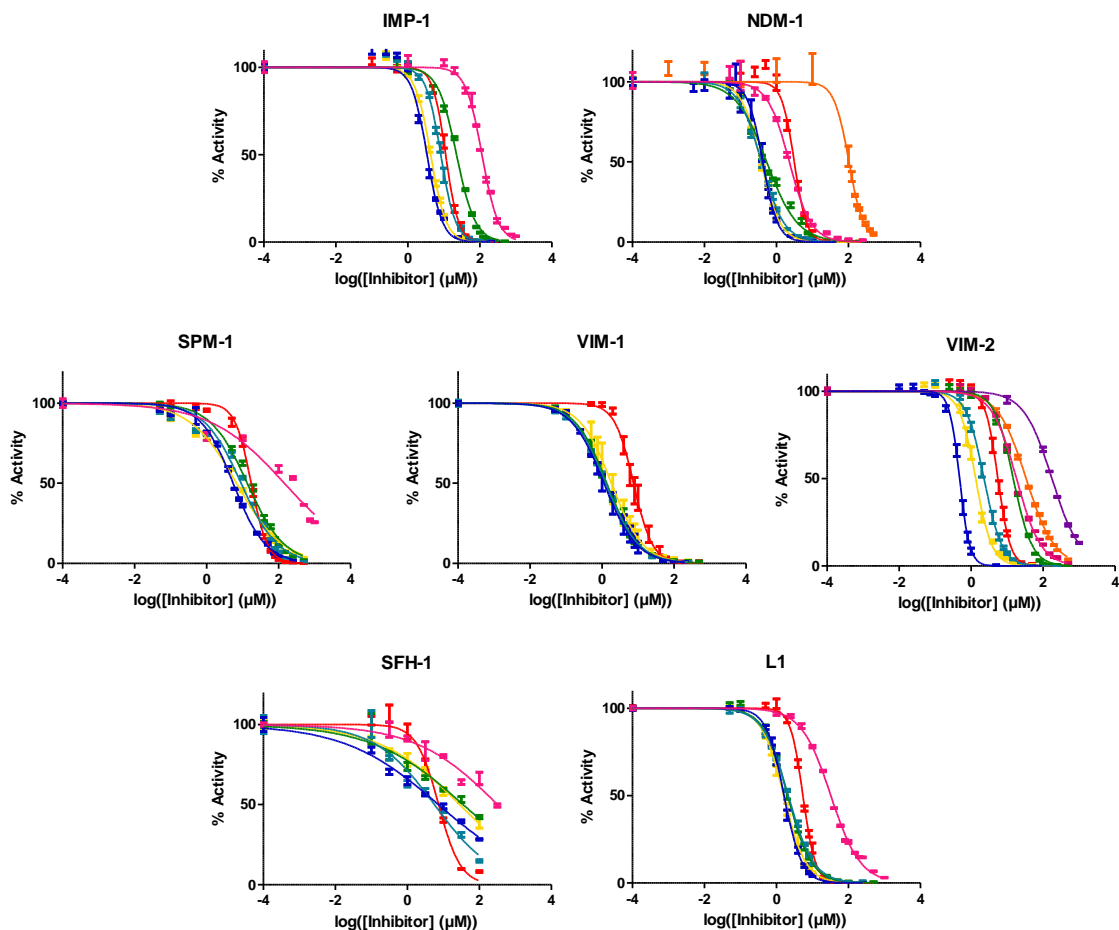


Figure 3.5 Dose response curves of MBLs with PMPCs and related compounds. The enzyme/inhibitor combinations in Table 3.5 are presented here with the inhibitors represented as follows: DPA (—), PA (—), PMPC-1 (—), PMPC-2 (—), PMPC-3 (—), PMPC-4 (—), PMP (—), and DPMP (—). The graphs in this figure were generated using GraphPad Prism v. 5.03.

The data in Table 3.5 is a numeric representation of the graphs in Figure 3.5 which allows for comparison between enzymes. From this it can be seen that NDM-1 is the MBL that is most susceptible to inhibition by PMPCs with IC_{50} values of 0.31 μ M to 0.55 μ M for the PMPCs, all of which are lower than the IC_{50} values for any other enzyme/inhibitor combination. SPM-1 and SFH-1 are poorly inhibited relative to the other MBLs with SFH-1 being less susceptible to inhibition than SPM-1. The B1 MBLs are inhibited most potently by PMPC-4 with PMPC-1 being less than 2-fold less potent than PMPC-4 against all B1 MBLs except VIM-2. Unlike the B1 MBLs, the B2 MBL,

SFH-1, was most potently inhibited by PMPC-3 than PMPC-4 (IC₅₀s of 0.56 μM and 7.3 μM respectively) and PMPC-1 is 5-fold less potent than the most potent inhibitor, PMPC-3. The B3 MBL L1, is very similarly inhibited by all of the PMPCs such that the 95% confidence intervals for each PMPC inhibitor encompasses the IC₅₀ values of all of the other PMPC inhibitors. As was suggested from the screening experiments, PA, PMP, and DPMP are relatively weak inhibitors of MBLs. Using VIM-2 as a model system (since it showed some susceptibility to all inhibitors in screening), PMP is the weakest inhibitor followed by PA, and DPMP with IC₅₀ values of 170 μM, 32 μM, and 18 μM respectively. With IMP-1, VIM-2, and SFH-1, PMPC-2 is a weaker inhibitor than DPA suggesting that this is not necessarily a good compound on which to base further structural optimization.

Table 3.5 IC₅₀'s of PMPCs against MBLs

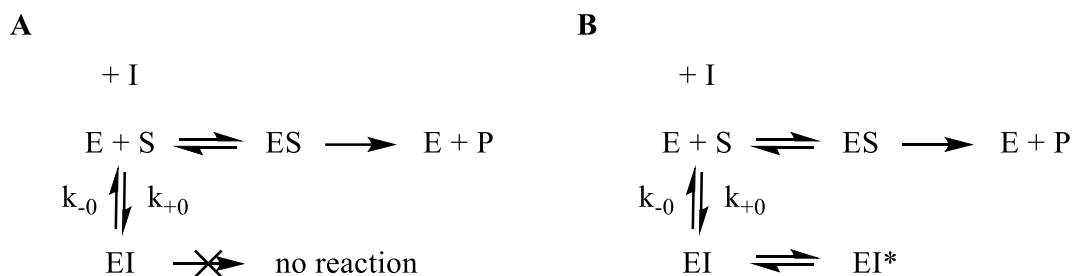
	IC ₅₀ (μM)						
	(95% Confidence Interval)						
	IMP-1	NDM-1	SPM-1	VIM-1	VIM-2	SFH-1	L1
DPA	10 (7-15)	2.6 (2.0-3.4)	18 (11-29)	5.3 * (5.1-5.5)	5.2 (2.9-9.3)	6.4 * (5.5-7.4)	5.2 (4.8-5.7)
PA		101 (50-202)			32 (28-37)		
PMPC-1	3.9 (3.2-4.8)	0.37 (0.25-0.55)	6.8 (5.6-8.3)	0.82 * (0.78-0.85)	1.3 (0.7-2.3)	29 * (21-40)	1.5 (1.0-2.2)
PMPC-2	21 (19-24)	0.55 (0.44-0.59)	13 (8-23)	1.4 * (1.3-1.5)	14.1 (13.6-14.7)	36 * (20-65)	1.9 (1.0-3.4)
PMPC-3	7.2 (5.2-10.1)	0.32 (0.21-0.49)	9.1 (6.1-13.6)	1.27 * (1.21-1.32)	1.9 (1.3-2.9)	5.6 * (3.8-8.1)	2.1 (1.6-2.6)
PMPC-4	2.9 (2.3-3.7)	0.31 (0.20-0.47)	5.4 (4.4-6.5)	0.80 * (0.77-0.83)	0.46 (0.31-0.70)	7.3 * (6.0-9.0)	1.6 (0.9-2.8)
PMP					170 * (150-190)		
DPMP	108 * (103-114)	2.0 * (1.8-2.2)	150 * (100-210)		18 * (17-19)		33 * (31-34)

* From a single experiment of three technical replicates.

From these data, it was determined that the inhibition should be better characterized for enzyme/inhibitor combinations with low IC₅₀ values. The enzyme/inhibitor combinations selected for this analysis were IMP-1, NDM-1, VIM-2, and L1 with the inhibitors DPA, PMPC-1, PMPC-3, and PMPC-4. The stock of purified VIM-1 was extremely limited and still has the C-terminal His tag attached, thus it was excluded from further study.

3.3.1.3 Determination of the Inhibition Constant

Preliminary assays performed without preincubation of the inhibitor with the enzyme showed progress curves that exhibit asymptotes, particularly at high concentrations of inhibitor. This is indicative of time-dependent inhibition (sometimes referred to as slow-binding inhibition), which can be described by either of the mechanisms in Scheme 3.1.⁴⁹⁶ In mechanism A, the inhibitory complex, EI, forms in a single, slow step; whereas in mechanism B, the inhibitory complex forms then isomerizes slowly to the EI* complex.



Scheme 3.1 Enzyme inhibition mechanisms that can exhibit time-dependent inhibition.

Progress curves from either mechanism of time-dependent inhibition can be fit to Equation 3.2, resulting in the coloured fit curves seen in Figure 3.6. From this analysis, the k_{obs} can be determined, and plotted against the concentration of inhibitor, [I], to generate a secondary plot which allows us to distinguish between mechanism A and B. If the inhibition is occurring by mechanism A, the secondary plot has a linear relationship described by Equation 3.3; whereas if the inhibition is occurring by mechanism B, the secondary plot will be hyperbolic.

Plots of the progress curves of IMP-1, NDM-1, VIM-2, and L1 inhibited by PMPC-1 are found in Figure 3.6 and the error bars are representative of the error between the three replicate measurements on the same day. The secondary plots generated from these progress curves for each MBL/inhibitor combination was linear, indicating that these compounds inhibit the MBLs by a one-step mechanism such as mechanism A from Scheme 3.1.

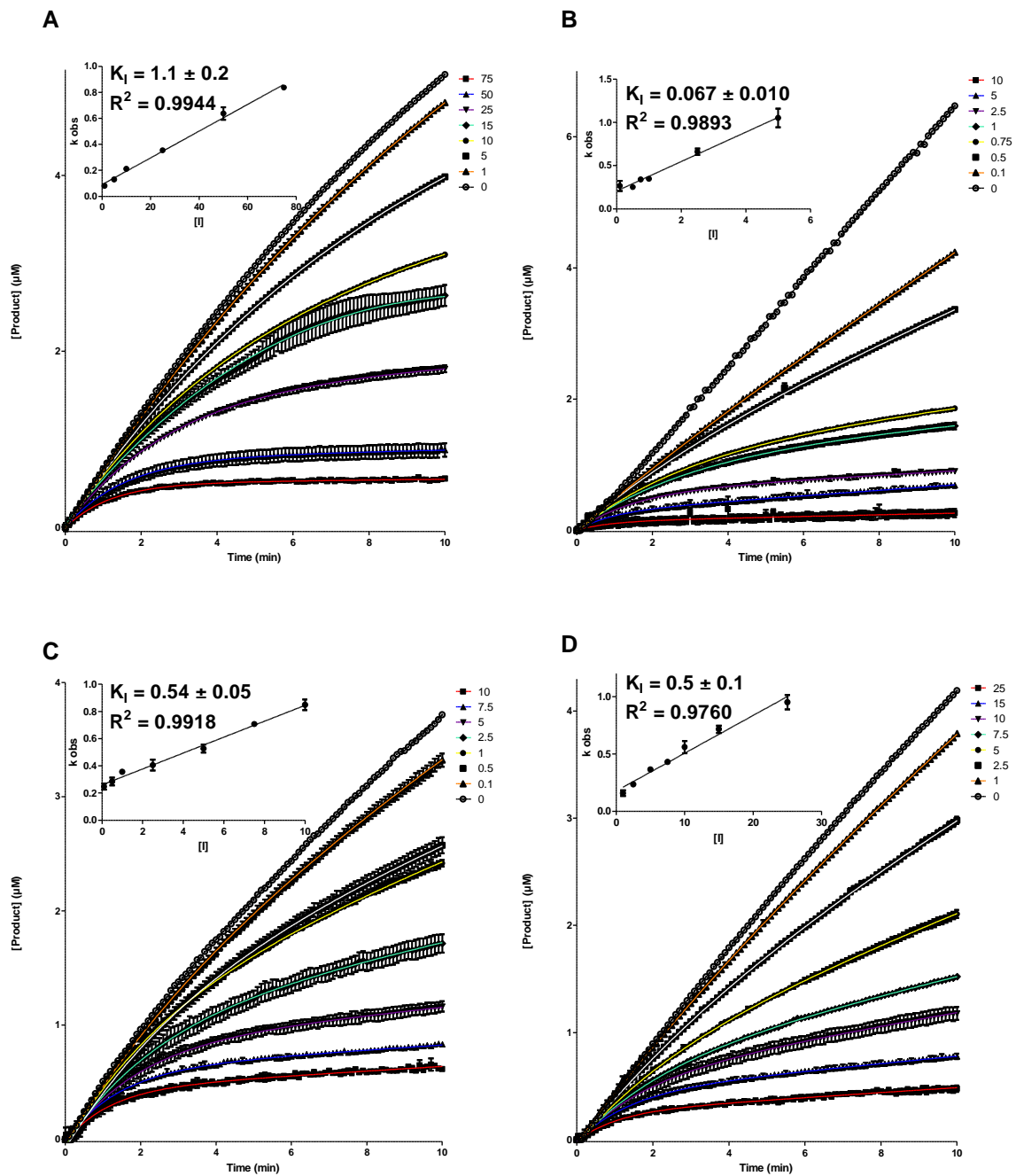


Figure 3.6 Time-dependent K_I graphs for PMPC-1 against representative MBLs : IMP-1 (A), NDM-1 (B), VIM-2 (C), and L1 (D). The graphs in this figure were generated using GraphPad Prism v. 5.03.

The graphs corresponding to those in Figure 3.6 for DPA, PMPC-3, and PMPC-4 can be found in Appendix D.

The K_I values in Table 3.6 were determined from further analysis of the linear regression of the secondary plots. Consistent with the IC_{50} data, PMPC-4 is the most potent inhibitor as it has the lowest K_I for each enzyme; as much as 14.2 times more potent than PMPC-1. The general trends for inhibitor potency within each enzyme system seen in the IC_{50} data also holds up here, although the scaling is not consistent (ie. PMPC-4 was 8-fold more potent than DPA against NDM-1 in terms of IC_{50} values, however the K_I is almost 100-fold lower). The K_I values for PMPC-1 and PMPC-3 are generally similar while the K_I values for DPA are 1.5-49 times greater than those of PMPC-1. Finally, NDM-1 is most sensitive to PMPCs with K_I values from 34 nM to 74 nM.

Table 3.6 K_I of DPA, PMPC-1, -3, and -4 against select MBLs.

	K_I (μ M)			
	DPA	PMPC-1	PMPC-3	PMPC-4
IMP-1	2.8 ± 0.4	1.1 ± 0.2	1.5 ± 0.1	0.4 ± 0.2
NDM-1	3.3 ± 0.6	0.067 ± 0.010	0.074 ± 0.008	0.034 ± 0.006
VIM-2	0.8 ± 0.3	0.54 ± 0.05	0.61 ± 0.04	0.038 ± 0.009
L1	1.1 ± 0.3	0.5 ± 0.1	0.41 ± 0.10	0.4 ± 0.1

The first order rate constant for the dissociation of the EI complex, k_{off} , for each enzyme/inhibitor combination was determined from the y-intercept of the secondary plot. The second order rate constant for the association of the EI complex, k_{on} was calculated from the known values of k_{off} and the K_I ; the results of these analyses are found in Table 3.7.

Table 3.7 On and off rates of metallo- β -lactamase inhibition by PMPCs.

	k_{on} ($M^{-1}sec^{-1}$)			
	DPA	PMPC-1	PMPC-3	PMPC-4
IMP-1	500 ± 100	1400 ± 300	980 ± 90	4000 ± 2000
	0.0014 ± 0.0002	0.0015 ± 0.0002	0.00147 ± 0.00008	0.0014 ± 0.0006
NDM-1	1300 ± 300	$51\ 000 \pm 9000$	$54\ 000 \pm 8000$	$110\ 000 \pm 20\ 000$
	0.0043 ± 0.0003	0.0034 ± 0.0003	0.0040 ± 0.0004	0.0036 ± 0.0002
VIM-2	5000 ± 2000	8000 ± 800	9100 ± 700	$70\ 000 \pm 20\ 000$
	0.004 ± 0.001	0.0043 ± 0.0002	0.0055 ± 0.0002	0.0027 ± 0.0005
L1	1200 ± 400	6000 ± 2000	5000 ± 1000	5000 ± 2000
	0.0013 ± 0.0003	0.0029 ± 0.0005	0.0019 ± 0.0004	0.0020 ± 0.0004

The k_{off} values for the various inhibitors against any one enzyme are fairly consistent, ranging from 0.0013 sec^{-1} to 0.0055 sec^{-1} , while the k_{on} values vary greatly. The k_{on} values for PMPC-4 are 2-7.5-fold larger than the inhibitor with the next highest k_{on} for B1 MBLs. This indicates that the EI complex forms fastest with PMPC-4, and the k_{off} values show that it dissociates at approximately the same rate as the other inhibitors, resulting in stronger inhibition. This trend does not hold up with L1 which has very similar k_{on} values across the PMPCs ($5000 \text{ M}^{-1}\text{sec}^{-1} - 6000 \text{ M}^{-1}\text{sec}^{-1}$). The lack of increased k_{on} for PMPC-4 with L1 is consistent with the K_i and IC_{50} data which suggests that PMPC-4 does not hold a particular advantage over the other PMPCs against L1, unlike the B1 MBLs.

3.3.2 Potentiation of meropenem against MBL producing Gram negatives

It is one thing to inhibit enzymes *in vitro*, but another thing entirely to penetrate the Gram-negative cell wall and restore antibiotic potency. Five strains MBL producing clinical isolates including two *E. coli* strains, two *Pseudomonas* spp., and a *K. pneumoniae* were selected to determine whether or not the PMPCs could potentiate meropenem activity *in vivo*. Strains UWB93 and UWB75 co-express the SBL CTX-M-15 which does not significantly hydrolyze meropenem and thus should not significantly contribute to the meropenem MIC when the MBL is inhibited.

The Clinical Laboratory Standards Institute (CLSI) defines *Enterobacteriaceae* (*E. coli* and *K. pneumoniae*) as susceptible to meropenem when the MIC is at or below 1 mg/L and as resistant at or above 4 mg/L. *Pseudomonas* spp. are considered susceptible to meropenem at or below 2 mg/L and are resistant at or above 8 mg/L. The data in Table 3.8 indicates that DPA tends to bring the MIC of meropenem into susceptible range with two-fold less inhibitor than PMPCs although it tends to require 16 mg/L DPA or more to achieve susceptibility. PMPC-4 is the least effective of the tested inhibitors against each strain and only brings UWB93 and UWB116 into the susceptible range, others showed a decrease in MIC at high concentrations of PMPC-4, but not enough to be clinically useful. UWB116 is particularly sensitive to potentiation by PMPCs with meropenem MICs entering the susceptible range with only 16-32 mg/L of inhibitor. None of the tested inhibitors had intrinsic antibacterial activity at the concentrations used in this assay.

Table 3.8 Sensitization of MBL producing Gram negatives to meropenem by DPA and PMPCs.

Strain	β -lactamase	Meropenem MIC (mg/L)	Inhibitor	Meropenem MIC (mg/L) in the presence of Inhibitor					
				4	8	16	32	64	128
				mg/L	mg/L	mg/L	mg/L	mg/L	mg/L
<i>E. coli</i> UWB93	IMP-1 CTX-M-15	4	DPA	4	4	2	1	0.25	<0.03
			PMPC-1	4	4	4	2	0.5	0.25
			PMPC-2	4	4	4	4	2	0.5
			PMPC-3	4	4	4	4	2	0.5
			PMPC-4	4	4	4	2	2	0.5
<i>E. coli</i> UWB75	NDM-1 CTX-M-15	128	DPA	128	128	64	16	<0.5	<0.5
			PMPC-1	128	128	64	32	4	<0.5
			PMPC-2	128	128	64	64	16	4
			PMPC-3	128	128	128	64	32	2
			PMPC-4	128	128	128	64	64	8
<i>K. pneumoniae</i> UWB116	NDM-1	32	DPA	16	4	0.5	<0.125	<0.125	<0.125
			PMPC-1	16	8	4	0.25	<0.125	<0.125
			PMPC-2	16	8	2	0.5	<0.125	<0.125
			PMPC-3	8	8	1	<0.125	<0.125	<0.125
			PMPC-4	16	8	2	0.5	<0.125	<0.125
<i>P. putida</i> UWB24	VIM-2	128	DPA	128	128	128	64	4	2
			PMPC-1	128	128	128	64	32	4
			PMPC-2	128	128	128	128	64	32
			PMPC-3	128	128	128	128	64	32
			PMPC-4	128	128	128	128	64	32
<i>P. aeruginosa</i> UWB78	VIM-2	128	DPA	64	64	64	32	8	4
			PMPC-1	128	128	64	64	16	8
			PMPC-2	128	128	128	64	64	16
			PMPC-3	128	128	128	128	64	8
			PMPC-4	128	128	64	64	64	16

Bolded MIC values are susceptible to meropenem according to CLSI guidelines.⁵⁰⁰

Italicized MIC values are intermediate (neither resistant nor susceptible) to meropenem according to CLSI guidelines.⁵⁰⁰

3.4 Discussion

Previous studies have indicated that DPA is an effective inhibitor of both IMP-1 and NDM-1.^{400,495} Due to the structural similarity of DPA and the PMPCs, it was considered likely that the PMPCs would also inhibit MBLs. The initial synthesis of PMPC-1 and PMPC-2 was directed at inhibition of Class II fructose-1,6-bisphosphate aldolase, a metallo-enzyme.⁵⁰¹

The PMPCs and related pyridine compounds are poor inhibitors of SBLs, only inhibiting KPC-2 and GC-1 at the highest tested concentration, 500 μM . In most cases, this inhibition is modest, reducing the activity of these enzymes by 10-40 % relative to the uninhibited control. The only tested compound that managed to elicit a response of greater than 50 % inhibition against SBLs was PMPC-4 which is also the most potent inhibitor against the MBLs.

The MBLs are potentially inhibited by PMPCs, and to a lesser extent by other picolinic acid derivatives depicted in Figure 3.4. Of the commercial picolinic acid derivatives: PA, DPA, and 6-MPA, the most potent inhibitor of MBLs is DPA. The improved activity of DPA over PA indicates that the presence of the carboxylate at the 6-position is beneficial as it decreases the IC_{50} by 6 to greater than 20-fold. A study on the inhibitory activity of commercial picolinate derivatives against MBLs by Horsfall et al. showed that 100 μM DPA was able to reduce the activity of IMP-1 to 2 % relative to an uninhibited control in the absence of added zinc while 100 μM PA was only able to reduce the activity by 31%.⁴¹⁰ In the presence of 100 μM ZnCl_2 , the inhibition of IMP-1 by DPA is substantially diminished (72 % residual activity at 100 μM DPA) suggesting that DPA in solution with Zn^{2+} is being sequestered and is not available for inhibition.⁴¹⁰ The data presented by Horfall et al. is consistent with the data presented in Table 3.3 for DPA in which 7 % activity remains after incubation with 100 μM DPA but is not consistent with the data for PA (80.3 % residual activity at 100 μM PA). The data in Horsfall et al. with VIM-2 and L1 are not comparable as they appear to be run in the presence of 100 μM ZnCl_2 , although this is not explicitly detailed in the Methods section of their paper.⁴¹⁰ Substitution of the carboxylate on DPA at the 6 position with a methyl group completely abolishes activity, suggesting that the presence of a polar group at the 6-position is favourable for inhibition.

The inhibition is further improved when the 6-carboxylate is substituted by a phosphonomethyl group, decreasing the IC_{50} values by another 2.6-7-fold. Substitution of both DPA carboxylates by phosphonomethyl groups as in DPMP leads to a reduction in activity for all MBLs except NDM-1 which has comparable IC_{50} values for DPA and DPMP (2.59 μM and 2.03 μM respectively). Furthermore, if the carboxylate from PMPC-1 is excluded (PMP) the inhibitory activity is completely abolished, emphasizing the importance of the carboxylate at the 2-position.

Within the PMPCs, two substitution sites were explored: the 3-position of the pyridine ring (PMPC-2), and the methylene group of the phosphonate (PMPC-3 and PMPC-4). The addition of a

carboxylate to PMPC-1 at the 3-position of the ring to form PMPC-2 provides no improvement in the inhibition of NDM-1 or L1 and increases the IC_{50} 2-11-fold against IMP-1, SPM-1, and VIM-2. This suggests that the addition of an anionic group to the 3-position of the pyridine ring increases specificity but does not improve the potency of these inhibitors. The addition of either a small polar group (PMPC-3) or large hydrophobic group (PMPC-4) to the methylene group of the PMPC-1 phosphonate did not significantly affect the inhibition in terms of IC_{50} with the exception of the 2.8-fold decrease in the IC_{50} from PMPC-1 (1.29 μ M) to PMPC-4 (0.464 μ M) for VIM-2. It should be noted that PMPC-3 and PMPC-4 were synthesized as racemic mixtures so they may be twice as potent as reported if the binding to the active site is selective for only one enantiomer.

The two VIM variants, VIM-1 and VIM-2, showed similar IC_{50} values for most of the compounds tested. The only compound for which their IC_{50} 's varied significantly was PMPC-2 which is also the only compound in this set that may have two modes of inhibition: one as a PMPC and the other as a phthalate. Phthalates (specifically 3-(4-hydroxypiperidin-1-yl)-aminophthalic acid) are known to inhibit B1 MBLs by coordinating one carboxylate group, which would be equivalent to the carboxylate at the 2 position in PMPCs, with the two active site Zn ions and the other carboxylate (the 3 position in PMPC-2) interacts with Lys161 in IMP-1 (Figure 3.7A). Crystallographic studies done in collaboration with Dr. Jim Spencer (University of Bristol) yielded structures of IMP-1 with PMPC-1 and L1 with PMPC-1 and PMPC-3. In the IMP-1 structure, PMPC-1 coordinates its pyridine nitrogen and carboxylate with Zn2. The carboxylate also hydrogen bonds with Lys161, the phosphonate hydrogen bonds to the bridging water/hydroxide and interacts weakly with Ser80 in IMP-1, and the aromatic ring has an edge-face interaction with Trp28 (Figure 3.7C).^{414,415} The potential for two binding modes for PMPC-2 may explain the discrepancy in the potency trend mentioned above. If PMPC-2 preferentially binds in a manner similar to PMPC-1, it is expected that the IC_{50} would be similar to the other PMPCs as it is for NDM-1, L1, and VIM-1 since they should be making the same contacts. If PMPC-2 preferentially binds in a manner similar to the phthalates, this may result in significantly different IC_{50} as seen with IMP-1, SPM-1, and VIM-2 since the contacts made in the active site are completely different. This dichotomy greatly complicates the kinetics as inhibition may be a result of multiple binding modes, each with differing affinities.

It has been shown that the K_D of Zn2 depends heavily on pH and while these two K_{DS} were not determined at the same pH, the K_D of IMP-1 was determined at a range of pHs (4.33-5.61) and decreases as pH increases.³⁰² This suggests that if the trend holds, 0.7 μ M may be an over estimation of the K_D of Zn2 in IMP-1 at pH 7 which may explain why it retains its Zn while L1 does not in the crystallization experiments with PMPC-1. Additionally, the K_D values were determined for the proteins in solution, and they may be significantly different with respect to one another in the crystalline state. The replacement of Zn2 in L1 by the phosphonate group of the PMPCs results in a very strong interaction between one of the phosphonate oxygens and Zn1 (1.8 Å). This interaction is notably stronger than the interactions between Zn1 and the three His residues that coordinate it to the active site (2.1 Å average). Additionally, the two PMPCs, PMPC-1 and PMPC-3 bind to L1 in the same manner, overlaying on each other almost perfectly as seen in Figure 3.8B.

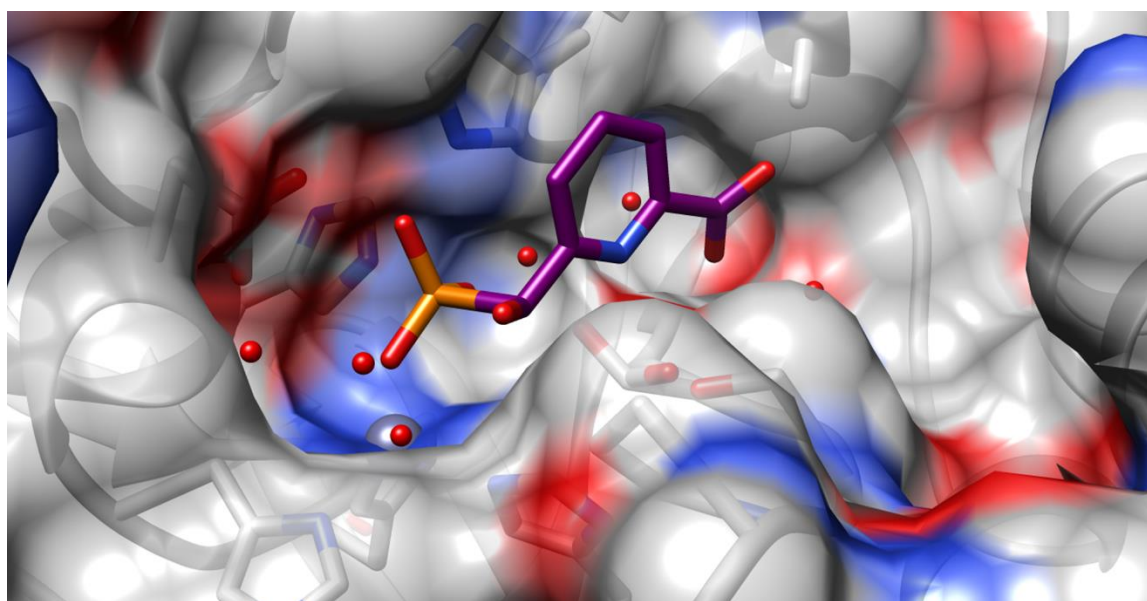


Figure 3.9 Binding of the S-enantiomer of PMPC-3 to the active site of L1. This figure was generated using Chimera v. 1.12 from the protein databank file 5HH6.

Unlike PMPC-1 which has no stereocenters, the C6 methine group of PMPC-3 is chiral and was synthesized as a racemic mixture. The crystal structure of L1 with PMPC-3 bound shows that the binding of PMPC-3 to the active site is stereospecific for the S-enantiomer. By mapping the protein surface, as in Figure 3.9, it can be seen that the 6'-hydroxyl group points towards the opening of the

active site and that the R-enantiomer would likely have unfavourable contacts with the protein surface. The relative openness of this part of the binding pocket indicates that large substituents such as that of PMPC-4 would be well tolerated but their binding would also be stereospecific. Due to the stereoselectivity of the L1 active site, it is probable that the IC_{50} and K_I values for PMPC-3 and PMPC-4 should be half that which was detailed above. It is uncertain whether or not the other MBLs require the same enantiomer as L1 for inhibition by PMPC-3 and PMPC-4.

In the case of binding of PMPC-4 to IMP-1, it is clear from qualitative modelling that the bulky N-thienoyl-N-benzyl group can only be accommodated in the binding site if the stereochemistry is of the R configuration. This is due to the prediction of very bad contacts with the zinc ions and the bridging hydroxide ion if the stereochemistry is of the S configuration. Thus, it is reasonable to suggest that only the R-isomer of PMPC-4 contributes to inhibition and that the effective IC_{50} and K_I values with IMP-1 should be half what is reported above.

In the case of PMPC-3, the hydroxyl group in the S-isomer makes close contacts with the bridging hydroxide as well as with the aspartate carboxylate that is a ligand to Zn^{2+} . These may however be tolerated since they may involve hydrogen bonding interactions. In the R-isomer, no contacts are predicted between the hydroxyl group and the protein. Thus it is possible that both stereoisomers contribute to the observed enzyme inhibition.

In early experiments performed with no pre-incubation with the inhibitors (DPA, PMPC-1, PMPC-3, and PMPC-4) and three B1 MBLs (IMP-1, NDM-1, and VIM-2) and one B3 MBL (L1) exhibited burst kinetics wherein there is an initial fast rate and a slower steady state rate (Figure 3.10). The burst kinetics are most evident in mid-range inhibitor concentrations of the progress curves in Figure 3.6 and are not caused by substrate depletion as only 10 % or less of the substrate is consumed at the end of a 10 min assay. This, in conjunction with the observation that IC_{50} 's taken at different preincubation times stabilize at 10 min (data not shown), indicates that DPA and the PMPCs inhibit MBLs by a time dependent mechanism rather than classical competitive inhibition.

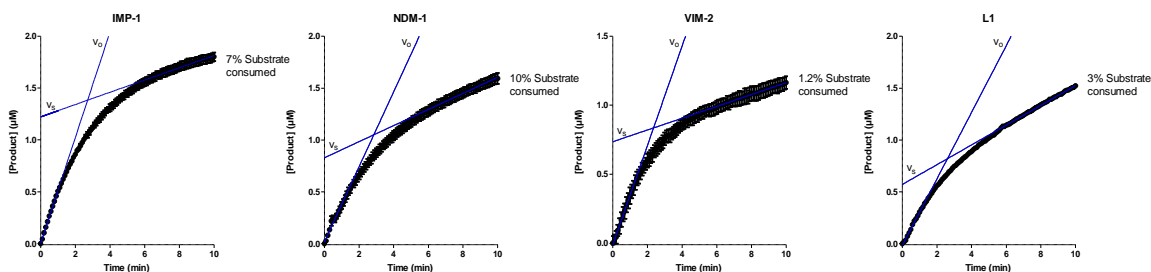


Figure 3.10 Fits of initial and steady state rates on representative progress curves of MBLs inhibited by PMPC-1 (25 μM for IMP-1, 1 μM for NDM-1, 5 μM for VIM-2, and 7.5 μM for L1). The graphs in this figure were generated using GraphPad Prism v. 5.03.

Time dependent kinetics can be the result of either slow-binding or slow-tight-binding. The possibility of slow-tight-binding inhibition was excluded since the concentrations of inhibitor required to see inhibition are in great excess relative to the concentration of the MBL being inhibited.⁴⁹⁶ Secondary plots of the rate of change between the initial rate, v_o and the steady state rate, v_s , denoted as k_{obs} , and the concentration of inhibitor were used to determine that inhibition occurs through the formation of an EI complex, and that that complex does not isomerize further. Determination of the inhibition constant, K_i , showed that PMPC-1, PMPC-3, and PMPC-4 were similarly potent against IMP-1, VIM-2, and L1 with PMPC-4 being the most potent. NDM-1 is the most susceptible to inhibition by the PMPC's with K_i values ranging from 34-74 nM. The K_i values for DPA against each of the MBLs is larger than those of the PMPCs by 1.3-45-fold indicating that the PMPCs are more effective inhibitors of MBLs than DPA.

Slow binding inhibitors exhibit lower rates of association (k_{on}) than classical inhibitors which tend to have association rates of 10^6 - $10^8 \text{ M}^{-1}\text{sec}^{-1}$ and in order to be effective inhibitors, the dissociation rates (k_{off}) must be even slower.⁴⁹⁶ The dissociation rates determined for DPA, PMPC-1, PMPC-3, and PMPC-4 are very consistent across the MBLs as they all tend to be on the order of 10^{-3} sec^{-1} . Since the dissociation rates are so consistent, any differences in the efficacy of an inhibitor is predicated by the association rate, which can vary by a hundred-fold for different inhibitors against the same enzyme. The k_{on} are highest for NDM-1 and approach being fast enough for classical kinetics with PMPC-4 ($10^6 \text{ M}^{-1}\text{sec}^{-1}$). This is consistent with the structural characteristics of NDM-1 in that it has the largest and most open active site allowing it to bind larger inhibitors faster than enzymes with tighter active site like IMP-1 which has the slowest association rates for every

inhibitor. In most cases, PMPC-4 has the fastest k_{on} which may be due to the hydrophobic group on the C6-methine carbon since it will contribute to a lower extent of hydration of the phosphonate group.

The benefits of PMPC-4 for inhibiting MBLs does not translate into improved sensitization of MBL producers to meropenem most likely since it may not cross the outer membrane as well as the smaller compounds DPA and PMPC-1. The two VIM-2 producing *Pseudomonas* strains, UWB24 and UWB78, are very resistant to sensitization by DPA and the PMPCs. Although MIC reduction was observed with each of the tested compounds against these two strains, only one of them could be brought into the susceptible range and it required 128 mg/L DPA to do it. Sensitization of the two *E. coli* strains, UWB93 and UWB75, was most effective for DPA which made them susceptible at 32 mg/L and 64 mg/L respectively. PMPC-1 was not far behind requiring only 2-fold more compound to make the strains susceptible to meropenem while other PMPCs required at least another 2-fold more compound. The most susceptible strain was the *K. pneumoniae* strain UWB116 which could be sensitized to the susceptible range by only 16 mg/L of either DPA or PMPC-3 and 32 mg/L of all other PMPC compounds.

Overall, the PMPCs are potent inhibitors of class B1 and B3 MBLs with little to no inhibitory activity against any class of SBL. This inhibition occurs by a time-dependent, one-step, competitive mechanism in which the rate of dissociation of the EI complex is fairly consistent and the affinity of the inhibitor for the MBL active site is determined largely by the rate of association, k_{on} . SAR studies suggest that negatively charged groups at both the 2 and 6 positions of the pyridine ring are required for inhibition, and the PMPC configuration at these positions is more potent than the dicarboxylate or diphosphonomethyl configurations. Modification of the methylene group in the PMPCs was tolerated well and resulted in increased affinity. Of the compounds with modifications of the methylene group, PMPC-4 is the most potent inhibitor despite it being a racemic mixture; however, this potency does not translate in microbial growth inhibition experiments as PMPC-4 was only able to sensitize two of the 5 tested Gram negatives into the susceptible range although MIC reduction was seen for all 5 strains. DPA and PMPC-1 are the two most effective compounds in sensitizing the bacteria likely due to their size and polarity; this charge/size consideration should be taken into account for development of future PMPC analogs.

3.5 Future Work

One of the possible explanations for the discrepancy between the kinetic results and the crystallography with respect to the replacement of Zn²⁺ in L1 is that it may be due to the zinc ion affinities differing in the crystalline state in comparison to the solution state. To establish whether or not the zinc ion is abstracted in solution state, mass spectrometry experiments will be attempted. Preliminary studies on SPM-1 have demonstrated that the dizinc form of the enzyme can be detected as the primary species by ESI-MS under non-denaturing conditions. It is likely that L1 could also be detected by native ESI-MS as the dizinc enzyme. If L1 retains 2 Zn ions when treated with PMPCs prior to analysis by ESI-MS, then the replacement is a crystallographic artifact; however, a mono-Zn L1 by this method does not confirm the crystal structure as the interaction of the Zn may have been weakened enough by the PMPC to allow it to dissociate in the MS. If a mono-Zn spectrum was obtained, further studies using ICP-MS, as described by King et al., would be required to determine if Zn²⁺ is actually being removed from the active site.⁴⁰¹

Experiments performed in this chapter used racemic mixtures of PMPC-3 and PMPC-4; however, the crystal structure of L1 with PMPC-3 demonstrated stereoselectivity for the S-enantiomer. It should be noted that the stereoselectivity of the crystalline form of the enzyme may not be representative of the stereoselectivity of the solution state enzyme. As such, enantiomerically pure (both R and S) samples of PMPC-3 and PMPC-4 should be synthesized as tested with the MBLs to determine if the S-enantiomer is the active inhibitor for all of them as well as how potent the pure stock is. Once the issue of the stereochemistry at the C6-methylene group is sorted out, new analogs in the PMPC series can be rationally developed using the crystal structures of IMP-1 and L1 with PMPCs bound.

The crystal structure of PMPC-1 bound to IMP-1 suggests a number of strategies for enhancing the affinity of the PMPCs for MBL active sites. As indicated in Figure 3.11C, a substituent on C3 would extend out of the active site so substituents that would increase the uptake into cells could be attached here. The results with PMPC-2 demonstrate that the addition of an anionic group to this position is disadvantageous; however, addition of an ether linker to either an amine or a siderophore may be tolerated.

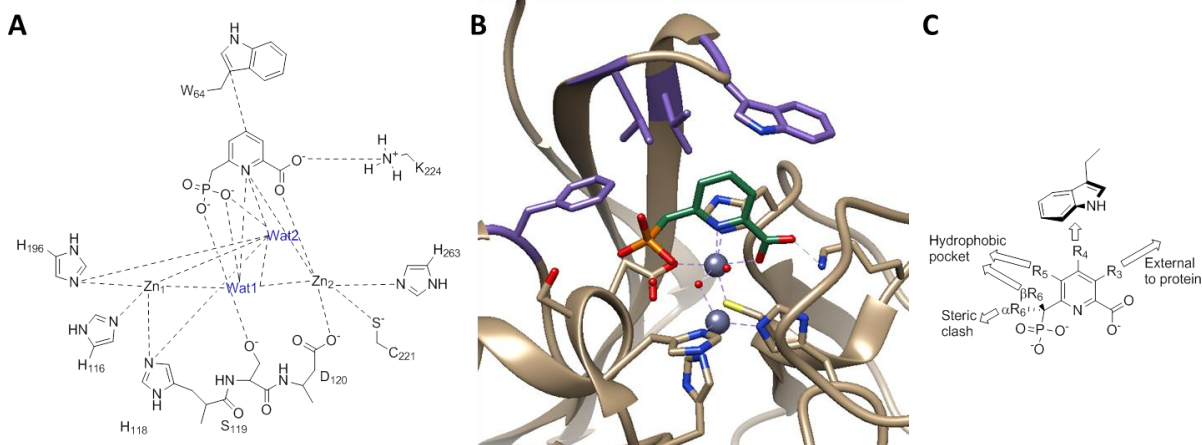


Figure 3.11 Binding of PMPC-1 to the active site of IMP-1, highlighting opportunities for development of future PMPCs. (A) Schematic of the binding interactions involved in PMPC-1 binding to IMP-1. (B) The hydrophobic pocket of IMP-1 highlighted in purple. (C) Positions on the PMPC core that could be modified to optimize binding to B1 MBLs. This figure was generated using Chimera v. 1.12 from the protein databank file 5HH4.

Substituents at C4 and in the α -orientation on the C6 methine would not be well tolerated due to steric clashes with Trp64 and the zinc ions/ligands respectively. Hydrophobic substitutions on C5 or in the β -orientation on the C6 methine would point towards the hydrophobic pocket highlighted in purple in Figure 3.11B. This hydrophobic pocket is well conserved within the B1 MBLs, so these hydrophobic groups would improve inhibition against more than just IMP-1.

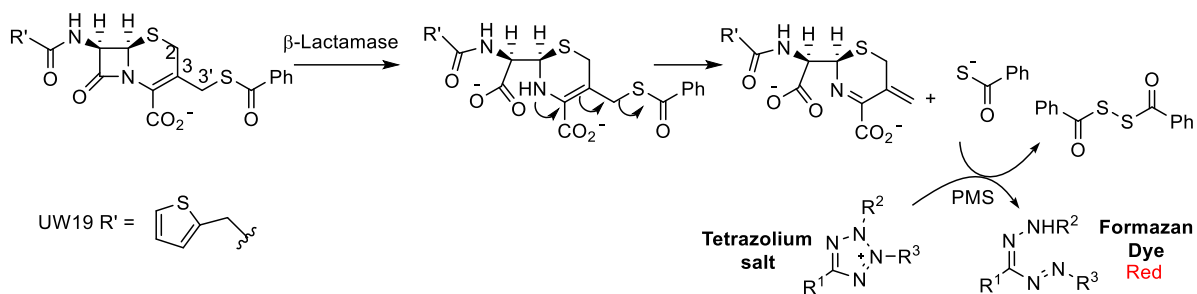
Chapter 4

Thioacids and 3'-Acylthio-Cephalosporins as B3 Inhibitors

4.1 Introduction

Cephalosporins such as cefotaxime and ceftazidime account for 12% of all antibiotic prescriptions in Canada and are considered highly important by the WHO.^{9,16,17} Over the past few decades, cephalosporin resistance has become increasingly prevalent to the point where early generation cephalosporins are no longer prescribed for Gram negative infections.⁴⁴ The first report of an ESBL-producer was in 1983 in Germany which was followed by reports of ESBL-producers around the world in the late-80's.^{503,504} Resistance to extended spectrum cephalosporins (generations 3-5) in Canadian hospitals has been monitored since 1995 by the Canadian Nosocomial Infection Surveillance Program and it was determined that 116 ESBL producers in 12 Canadian hospitals in a one year period (Sept 1999- Sept 2000).⁵⁰⁵ Shortly thereafter, a study in Calgary showed that ESBLs were becoming increasingly prevalent in community acquired infections.⁵⁰⁶ The most prevalent ESBLs are CTX-M-15-like, SHV-type, and KPC-type, although MBLs such as NDM-1 are increasing in prevalence.^{17,507} Recently avibactam (see Figure 1.13), an inhibitor effective against SBLs, has been approved by the FDA which (at least temporarily) solves that part of the ESBL problem.⁵⁰⁸

In a collaboration between the Dmitrienko lab and Panbio Inc. in Australia discussed in 2.1 several strategies to develop a novel chromogenic β -lactamase substrate including one strategy that involved the release of a thioacid as described in Scheme 4.1 were explored. In this strategy, a 3'-acylthiocephalosporin is hydrolyzed by a β -lactamase, followed by a rearrangement that expels a thioacid which in turn, reacts with a tetrazolium salt in the presence of 1-methoxy phenazine methosulfate (PMS) to form a red formazan dye.



Scheme 4.1 Formazan dye strategy for a chromogenic cephalosporin.

The formazan dye strategy was not successful in making a chromogenic cephalosporin, since the 3'-acylthiocephalosporins were poor substrates for β -lactamases. As part of their characterization, early compounds in this series, including UW-19 (Scheme 4.1), were found to protect meropenem from hydrolysis by metallo- β -lactamases. In the enzyme assays depicted in Figure 4.1, co-administration of UW-19 with meropenem extended the half-life of meropenem three-fold while another compound in this series, AK075, extended its half-life 5.5-fold. To confirm whether or not this was a characteristic of cephalosporins, ceftiofur and moxalactam were tested for comparable activity and were determined that they do not protect meropenem. This interesting and potentially advantageous behaviour inspired a synthetic effort that resulted in over 70 novel cephalosporins which were assessed based on their synergy with meropenem in microbiological experiments. While some experiments were performed to elucidate the reason that these cephalosporins protected meropenem, the work was not completed as it coincided with a personnel turnover in the Dmitrienko lab.

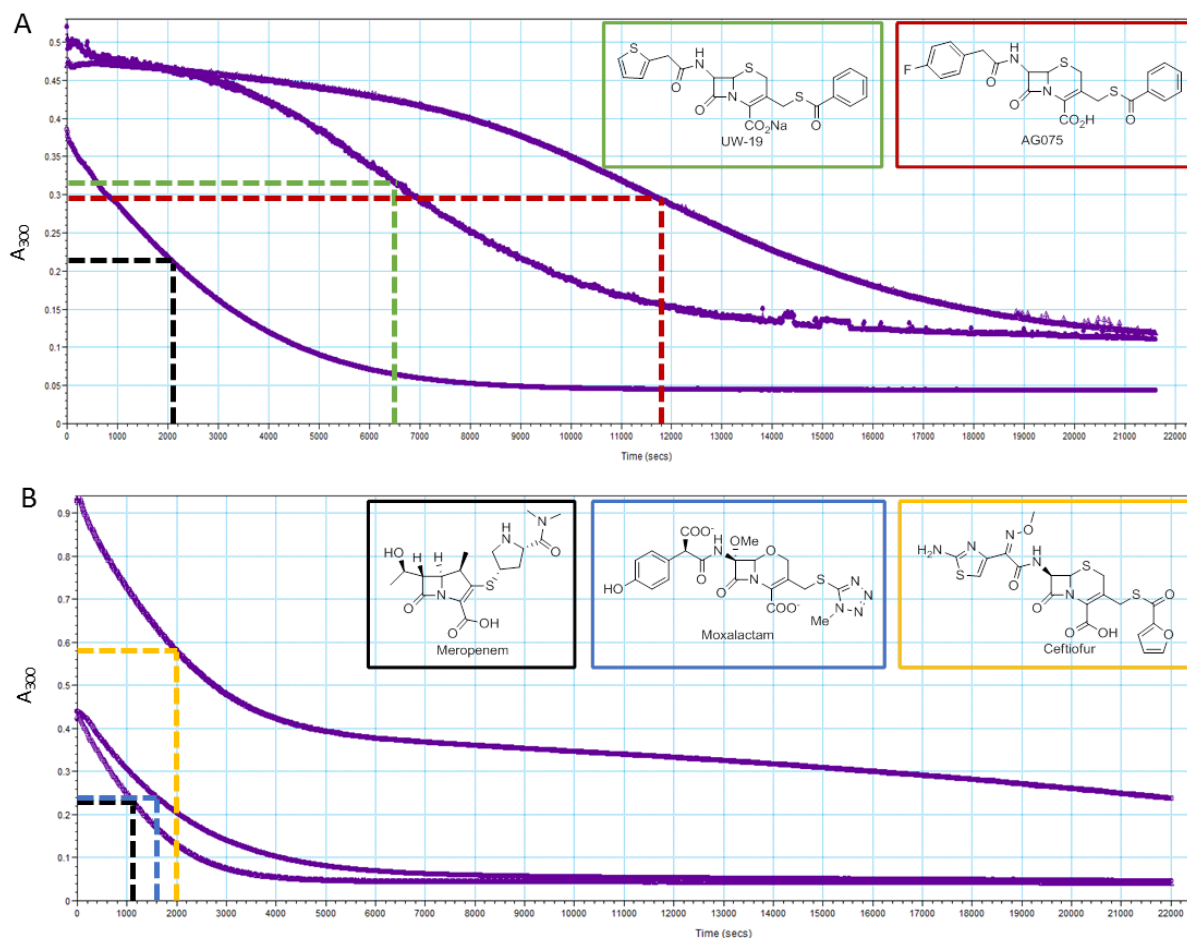


Figure 4.1 Protection of meropenem hydrolysis by synthetic and commercial cephalosporins. The novel cephalosporins UW-19 and AG075 protect meropenem from hydrolysis by IMP-1, extending its half-life 3-fold and 5.5-fold respectively (A). The commercial cephalosporin ceftiofur and oxacephamycin moxalactam are not capable of conferring the same protection to meropenem (B).

The mechanism presented in Scheme 4.1 suggests that after the cephalosporin is hydrolyzed by a β -lactamase, the hydrolysis product expels an aromatic thioacid as its conjugate base. There are a number of examples in the literature of thiols and thioesters being potent inhibitors of MBLs as reviewed by McGeary et al.³⁹⁷ but relatively few examples of the interaction of thioacids with MBLs. Tsang et al. have reported that the thioacid formed upon hydrolysis of an 8-thioxo-cephalosporin is an inhibitor of BcII a B1 MBL that seldom arises in clinical samples (Figure 4.2).⁵⁰⁹

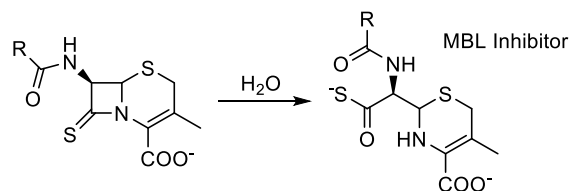


Figure 4.2 Generation of a MBL inhibitor from 8-thioxo-cephalosporins. ⁵⁰⁹

More recently, researchers at Pfizer Global R&D reported using a high throughput bioassay to screen 19,366 natural product extracts including those from actinomycete cultures to identify two potent inhibitors of the Class B1 MBL CcrA (from *Bacterioides fragilis*) and the Class B3 MBL L1 from (*S. maltophilia*) PMTC and PDTC.⁴³⁹

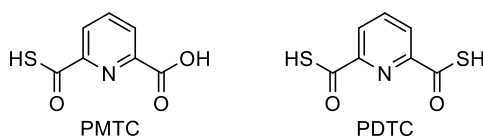


Figure 4.3 Potent inhibitors of CcrA and L1 determined from natural product screen. ⁴³⁹

The goals of the research described in this Chapter were as follows:

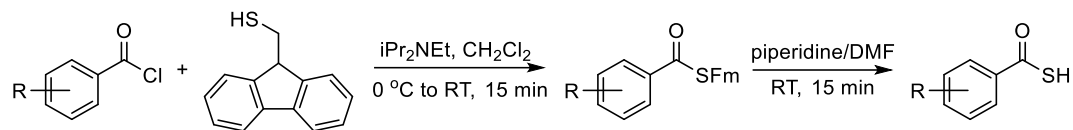
- 1) Estimate the potential of aromatic thiocids as inhibitors of MBLs
- 2) Determine the potency of PMTC and PDTC as inhibitors of clinically important MBLs
- 3) Gain insights in to the mechanism of inhibition of MBLs by 3'-acylthiocephalosporins
- 4) Gain insights into the potency and mechanism of a 3'-acylthiocephalosporin, UW-123 (Table 4.2), that has significant activity as a stand-alone antibiotic against MBL-producing clinical isolates.

4.2 Methods

Materials used in this chapter were the same as those listed in Chapter 2 unless otherwise stated. Thiobenzoic acid (TBA) is the only inhibitor that was not synthesized in this lab but was purchased from Sigma.

4.2.1 Synthetic Thioacids and 3'-acylthiocephalosporins

A library of thioacids was synthesized by Dr. Ahmed Desoky and Dr. Glenn Abbott in the Dmitrienko group using a new synthetic method shown in Scheme 4.2, and their structures and purity were confirmed by ¹HNMR, ¹³CNMR, and ESI-MS.



Scheme 4.2 Abridged method for thioacid synthesis.

A table containing the structures, molecular weights, laboratory codes, and common acronyms of these compounds can be found in Appendix A, an abridged depiction can be found in Table 4.1.

Table 4.1 Structures of phenyl thioacids presented in this chapter

	R ₁	R ₂	R ₃	R ₄	R ₅
TBA	H	H	H	H	H
TA-1	H	H	Br	H	H
TA-2	H	OMe	H	H	H
TA-3	Cl	H	Cl	H	H
TA-4	Cl	H	Cl	H	Cl
TA-5	H	NO ₂	H	H	H
TA-6	H	NO ₂	H	NO ₂	H
TA-7	H	H	NHAc	H	H
TA-8	H	H	NHBoc	H	H

Samples of PMTC, PDTC, and I-PDTC, a benzene variant of PDTC, were synthesized using the same strategy.

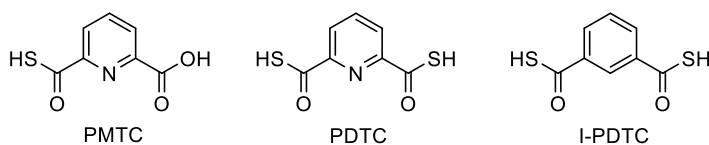
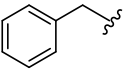
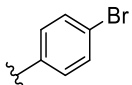
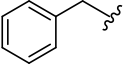
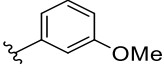
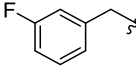
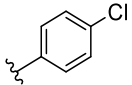
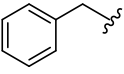
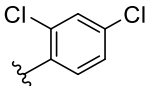
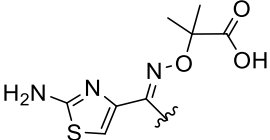
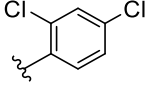
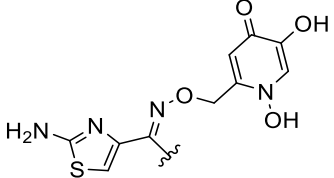
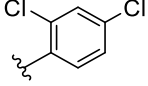


Figure 4.4 Structure of pyridine based thioacids and related compounds presented in this chapter.

The primary goal for the study of the thioacids was to determine whether or not they are inhibitory towards β -lactamases when released from a cephalosporin. While it is useful to know the *in vitro* inhibitory properties of the thioacids, ultimately, the potency of the cephalosporin against β -lactamase producing bacteria is more important. In order to assess this potency, a series of 3'-

acylthiocephalosporins were made by Dr. Desoky and other organic chemists in the Dmitrienko group. In total, over 70 compounds in this series were made. Only a small subset of these compounds are presented in this work. The 3'-acylthiocephalosporins presented in this work, found in Table 4.2, were all made by Dr. Ahmed Desoky and their structures have been confirmed using the methods described for the compounds in Table 4.1.

Table 4.2 Structures of cephalosporins presented in this chapter

	R ₁	R ₂
TE-1		
TE-2		
TE-3		
TE-4		
TE-5		
UW-123		

The R₁ sidechains for TE-5 and UW-123 were chosen to optimize uptake into Gram negative bacteria. For TE-5, the R₁ sidechain is the same as that from ceftazidime – a highly successful antibiotic against clinically important Gram negative pathogens.⁹ The R₁ sidechain of UW-123 is a catechol siderophore mimic intended to increase uptake into *Pseudomonas* strains through Fe³⁺ uptake porins. This sidechain has also been used in BAL30072, a monobactam in Phase 3 clinical trials for treatment of Gram negative infections, especially *Pseudomonas aeruginosa*.⁵¹⁰ Catechol-type siderophores such as enterobactin and pyoverdine are known to facilitate iron uptake in *E. coli*,

K. pneumoniae, and *P. aeruginosa* which suggests that these siderophore mimics may increase uptake in other bacterial pathogens as well as in *Pseudomonas*.⁵¹¹

4.2.2 β -Lactamase Enzyme Kinetics

4.2.2.1 Thioacid Solubility

Thioacids were dissolved in DMSO using a combination of vortexing and sonicating to make 100 mM, 50 mM, or 25 mM stocks. The stock concentration was chosen for each thioacid was the highest concentration where all solid appeared to dissolve. Upon freezing, these stocks precipitated and the resulting solid would not dissolve back into the DMSO so they were used as fine suspensions. To test whether or not the solubility of these compounds could be improved by deprotonation of the thioacid, 5 mM solutions of TA-1 were prepared from the precipitated freezer stocks in the presence of 0, 1, and 6 molar equivalents of NaOH. Each of the solutions was then diluted to 50 μ M in DMSO and to 100 μ M in 50 mM HEPES pH 7.2 the latter is intended to mimic kinetic assay conditions. The pH of each of the prepared solutions of TA-1 was determined using colorpHast[®] pH 0-14 indicator strips (EM-Reagents, Gibbstown, NJ).

4.2.2.2 Inhibitor Screening

The assays in this section were performed as described in 3.2.1.1 for CTX-M-15, KPC-2, GC-1, OXA-48, IMP-1, NDM-1, SPM-1, VIM-2, and L1 with the following stipulations:

The phenyl thioacids were screened against L1 in the presence and absence of one molar equivalent of NaOH to assess differences and determine the best conditions to be used with other β -lactamases. Screening of the other β -lactamases against the synthetic phenyl thioacids (TA-1 – TA-8) listed in Table 4.1 was carried out in the presence of NaOH. Later studies with the inhibitors presented in Figure 4.4 were also carried out with one molar equivalent of NaOH to assist in complete dissolution.

4.2.2.3 IC₅₀ Determination

The assays in this section with PMTC, PDTC, and I-PDTC were performed as described in 3.2.1.2 with the most concentrated stock being prepared with one molar equivalent of NaOH.

4.2.3 Antimicrobial Susceptibility

4.2.3.1 Bacterial Strains

Detailed information regarding bacterial strains can be found in Appendix C. The bacterial strains used by Merck are part of their collections.

4.2.3.2 MIC Determination

MICs were determined using methods described in 3.2.2.2. Some compounds were prepared as DMSO stocks, in which case the final concentration of DMSO was 1.25 %. Commercial antibiotics that were used for comparison: meropenem (Mero) (A. G. Scientific, San Diego, CA), imipenem (Imi), ceftazidime (CAZ) (Sigma), cephotoxim (CTX) (Sigma). Later experiments with UW-123 were performed in the presence and absence of a serine- β -lactamase inhibitor. In the case of the experiments performed in the Dmitrienko lab, this inhibitor was either BLI-489 or avibactam (Figure 4.5), in the Merck panels, it was an undisclosed inhibitor from the same functional class as avibactam.

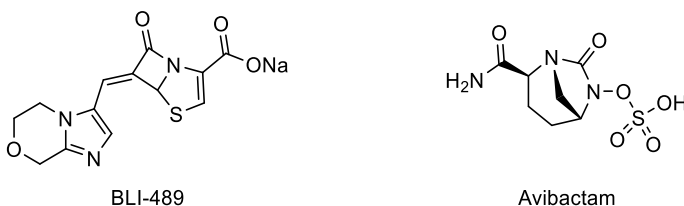


Figure 4.5 Serine- β -lactamase inhibitors used in microbiological experiments in the Dmitrienko lab. ^{337,512}

4.2.3.3 Checkerboard Synergy Assay

Checkerboard synergy assays were performed against meropenem as described in 3.2.2.3 with final DMSO concentrations of 1.67 %. To ensure complete dissolution of the thioacids, one molar equivalent of NaOH was added to the initial DMSO stock. Some compounds precipitated in MH media, in these cases, after growing overnight at 37 °C in a 96-well plate, 10 μ L from each well was spotted onto MH agar then incubated overnight to assess the viability of any remaining bacteria. By comparing the minimum bactericidal concentrations (MBCs) generated by spot plate for meropenem and the same MICs measured by OD₆₀₀, correlation between the two techniques was established.

Fractional inhibitory concentrations (FICs) were determined using Equation 4.1 with the caveat that if one compound does not have an MIC in the range of the experiment, it is assumed to be the next dilution above the limit.

Equation 4.1
$$FIC = \frac{\text{lowest MIC } X_{\text{combined}}}{MIC X_{\text{alone}}} + \frac{\text{lowest MIC } Y_{\text{combined}}}{MIC Y_{\text{alone}}}$$

The determined FIC values indicate what type of relationship exists between the two compounds as listed in Table 4.3.

Table 4.3 Relationships indicated by FIC

FIC	Relationship
≤ 0.5	Synergistic
$0.5 < FIC \leq 1$	Additive
$1 < FIC < 2$	Indifferent
≥ 2	Antagonistic

4.2.4 Mode of Action

The experiments performed in this section were adapted from Moya et al. and Page et al.^{116,513}

4.2.4.1 Time-Kill Kinetics

The UW-123 used in these experiments was from a different stock than the one used in the MIC experiments above. An MIC was determined for the strain being used and was found to be different from the one above. These experiments were set up using the MIC of this stock: 1 mg/L.

4.2.4.1.1 Monitoring by Optical Density

MH agar plates were streaked with a wild type *E. coli* (UWB59) and incubated at 37 °C overnight then stored at 4 °C. Single colonies were used to inoculate 1 mL of MH broth which was shaken at 250 rpm overnight at 37 °C. O/N cultures of *E. coli* (UWB59) were diluted 1/100 in MH broth and grown to an OD₆₀₀ of approximately 0.2 in an incubator at 37 °C and 250 rpm. Dilutions of antibiotic were prepared at 4x, 2x, 1x, 0.5x, 0.25x, and 0x MIC in MH with 1.25% DMSO. Cultures were then added to 96 well plates by a 1/20 dilution with the antibiotic preparations. Plates were shaken in the plate reader for 10 sec on low speed then read at 600 nm every hour for 8 hours and again at 24 hours then incubated at 37 °C between reads. Same day experiments were performed in quadruplicates with

only MH in the wells on the edge of the plate. Three separate day replicates were performed. Normalization of data was performed by subtracting the absorbance of the sterility control from that of the wells with bacteria and antibiotic at that concentration and time to eliminate background effects.

4.2.4.1.2 Monitoring by Colony Forming Units

The setup of this experiment was similar to that detailed in 4.2.4.1.1 except that the growth component of the assay was performed in snap cap tubes with a final volume of 1 mL instead of in a microplate with a 200 μ L final volume using only 2x, 1x, 0.5x, 0.25x, and 0x MIC. The tubes were shaken at 250 rpm for the duration of their incubation at 37 °C with aliquots taken at 0 hr, 0.5 hr, 1 hr, 2 hr, 4 hr, 8 hr, and 24 hr. Aliquots were immediately diluted and plated on MH agar then incubated at 37 °C overnight. Several dilutions were plated for each time and concentration combination to ensure at least one readable plate was obtained, totaling 119 agar plates. Due to the amount of supplies required to perform this experiment, only a single replicate was performed.

4.2.4.2 Phase Contrast Microscopy

The setup of this experiment was similar to that of 4.2.4.1.1 with the 1/100 dilution of cultures being made in both MH broth and MH broth supplemented with 0.3 M sucrose. Likewise, dilutions of antibiotic (128 mg/L – 0.0625 mg/L) were also made in MH broth in the presence and absence of 0.3 M sucrose. After 2 hr of incubation at 37 °C in a microplate, 100 μ L was taken from each well and pelleted at 5000 rpm for 5 min in an Eppendorf 5415 C centrifuge and the supernatant was decanted. The pellets were kept on ice until about 0.5 μ L of the pellet (resuspended in the small amount of retained supernatant) was visualized under oil immersion at 1000x magnification on a Zeiss Axioskop 2 plus phase contrast microscope.

4.2.4.3 Penicillin Binding Protein Competitive Binding Assay

4.2.4.3.1 Preparation of PBP Containing Membrane Fragments

P. aeruginosa Membrane Fragments

Procedures for PBP membrane preparation and Bocillin binding assay were adapted from Moyá et al.¹¹⁶ *P. aeruginosa* PA01 cells were obtained from Dr. Stephen Seah of the University of Guelph and designated UWB96. An overnight culture of PA01 cells was prepared by inoculating two tubes

containing 2 mL Luria Bertani (LB) broth with scrapings from a glycerol stock and shaking them at 250 rpm, 37 °C, overnight (16-20 hr). The 4 mL of PA01 overnight culture were used to inoculate 500 mL LB broth which was then incubated at 37 °C, shaking at 185 rpm until the OD₆₀₀ reached 1 (~5 hr). Cells were then centrifuged in a JA-10 rotor at 4400 xg for 10 min at 4 °C and the supernatant was discarded. The pellets were washed in 150 mL of Buffer A (20 mM KH₂PO₄, 140 mM NaCl, pH 7.5) then centrifuged again at 4400 xg for 10 min at 4 °C and the supernatant was discarded. The cells in the pellet were then lysed using a large probe on a Heat Systems Ultrasonic processor W-255 sonicator set to 50 % cycle and 50 % power 5 times for 30 sec each with 1 min rest on ice between bursts. The lysate was then centrifuged in a JA-25.5 rotor at 12 000 xg for 10 min at 4 °C and the supernatant and pellets were retained separately and frozen on dry ice then stored at -80 °C. The supernatant was thawed and transferred into 10 mL Oak Ridge polypropylene tubes with a nylon screw cap for use in a T-1270 rotor of a Sorvall WX100 Ultra centrifuge. Samples were centrifuged at 150 000 xg for 1 h at 4 °C and the supernatant was discarded. The pellets were resuspended in 1 mL Buffer A and pooled. Total membrane protein concentration was determined by Bradford assay as described in 2.2. The *P. aeruginosa* PBP membrane preparation was then aliquoted, frozen on dry ice, and stored at -80 °C.

E. coli Membrane Fragments

A similar but modified procedure was used for the isolation of membrane fragments from *E. coli* (ATCC 25922, UWB 102). An overnight culture of *E. coli* cells was prepared by inoculating 5 mL of LB broth with scrapings from a glycerol stock and shaking them at 200 rpm, 37 °C, overnight (16-20 hr). The 5 mL of *E. coli* overnight culture was used to inoculate 1 L LB broth which was then incubated at 37 °C, shaking at 200 rpm until the densely grown. Cells were then centrifuged in a f10 4x1000 LEX rotor in a Sorvall RC 6+ centrifuge at 4400 xg for 10 min at 4 °C and the supernatant was discarded. The pellets were washed in 150 mL of Buffer B (20 mM NaH₂PO₄, 140 mM NaCl, pH 7.5) then centrifuged again at 4400 xg for 10 min at 4 °C and the supernatant was discarded. The cells in the pellet were resuspended in 40 mL of Buffer B, then lysed using a small probe on a Microson Ultrasonic Cell Disruptor set to 5 power, 5 times for 30 sec each at 4 °C with 1 min rest on ice between bursts. The lysate was then centrifuged in a f13 14x50cy rotor at 12 000 xg for 5 min at 4 °C and the pellets were retained separately and frozen on dry ice then stored at -80 °C. The supernatant was transferred into 70 mL Beckman polypropylene tubes with an aluminum screw cap for use in a Type 45 Ti rotor of a Beckman-Coulter Class S Optima L-90K Ultracentrifuge. Samples were

centrifuged at 134 032 xg (34 000 rpm) for 1 h at 4 °C with maximum acceleration and slow deceleration then the supernatant was discarded. The pellets were resuspended in 1 mL Buffer B then aliquoted and flash frozen on dry ice to be stored at -80 °C. Upon testing this preparation, it was too dilute to quantify PBP 2 or 3 – the following procedural additions were to generate a more concentrated stock. The retained pellet from the sonication was thawed and suspended in another 40 mL Buffer B then lysed more completely using a large probe on a Heat Systems Ultrasonic processor W-255 sonicator set to 50 % cycle and 50 % power 5 times for 30 sec each with 1 min rest on ice between bursts. The lysate was then centrifuged in an f13 14x50cy rotor at 10 000 xg for 5 min at 4 °C. The supernatant was decanted into 70 mL Beckman polypropylene tubes with an aluminum screw cap and balanced against a pooled solution of the previous aliquots, with Buffer B. Both samples were centrifuged at 134 032 xg (34 000 rpm) for 1 h at 4 °C with maximum acceleration and slow deceleration in a Type 45 Ti rotor. Each pellet was resuspended in 20 mL of Buffer B, then they were pooled together and centrifuged again at 134 032 xg for 1 h at 4 °C with maximum acceleration and slow deceleration in a Type 45 Ti rotor. The pellet was then soaked in 500 µL of Buffer B overnight at 4 °C to allow complete resuspension before aliquoting and freezing on dry ice for storage at -80 °C. Total membrane protein concentration was determined by Bradford assay as described in 2.2.

4.2.4.3.2 PBP Competitive Binding Assay

Two-fold dilutions of UW-123 ranging from 128 mg/L to 0.0039 mg/L were prepared in Buffer B (20 mM NaPi, 140 mM NaCl, pH 7.5) and DMSO such that the final concentration of DMSO in each sample was 1.28 % while aliquots of the PBP membrane preparation were thawed on ice. The PBP membrane preparation (10 µL) was incubated with a 3x concentrated stock of UW-123 (5 µL) for 30 min at 37 °C after vortexing. In a darkened room, 5 µL of the fluorescent penicillin, Bocillin (Thermo), was added and returned to the incubator for 30 min at 37 °C after vortexing. Samples were prepared for SDS-PAGE by adding 5 µL of 5x SDS-PAGE Buffer to each sample, vortexing, and boiling for 3 min before spinning down any condensation. Each sample (20 µL) as well as 5 µL of low molecular weight marker was loaded onto two 10 % SDS-PAGE gel which were run at 80 V in the dark until the blue dye front had reached the bottom of the gel. Gels were uncased directly onto a Phoros (BioRad, Hercules, CA) gel reading system and visualized at $\lambda_{ex}= 488$ nm and $\lambda_{em}= 530$ nm. Band densities were determined using Image Lab software (BioRad, Hercules, CA) and were normalized and fitted to Equation 3.1 using GraphPad Prism 5.00 for Windows (GraphPad Software, San Diego, CA) with the added constraint that the bottom plateau is set to 0 since it is not well

defined. Gels were then stained with Coomassie Blue R-250 (BioRad, Hercules, CA) containing stain overnight then destained with 50 % methanol, 10 % acetic acid in water. Coomassie stained gels were visualized on a Gel Doc EZ Imager (BioRad, Hercules, CA).

4.3 Results

Preliminary studies aimed at probing the mechanism of MBL inhibition by 3'-acylthiocephalosporins were carried out by Dr. Laura Marrone in this research group. She discovered that, for UW-19, the IC_{50} for inhibition of nitrocefin hydrolysis by IMP-1 was 3.1 μ M. Following this, a complete hydrolysis of UW-19 was carried out using the SBL KPC-2 and the hydrolysis product was separated from the enzyme. The hydrolysis product, at 60 μ M was found to cause 48% reduction in the catalytic activity of IMP-1. In a separate experiment, thiobenzoate itself (TBA) at 60 μ M was found to reduce the catalytic activity of IMP-1 by 56%. Thus, neither thiobenzoate alone nor the hydrolysis products, presumed to be TBA and the cephalosporin-derived elimination product (shown in Scheme 4.1) were sufficiently effective as inhibitors to explain the inhibitory potency of UW-19.

This led to the proposal the the inhibition by UW-19 was likely a consequence of tight binding of the intact cephalosporin (low K_M , estimated to be 0.07 μ M) followed by slow release of the cephalosporin-derived elimination product from the active site resulting in a low k_{cat} .⁵¹⁴

4.3.1 Released Phenyl Thioacids as β -Lactamase Inhibitors

In an effort to ascertain if the inhibitory activity of 3'-acylthiocephalosporins could be altered by substitutions on the thioacids, a selection of phenyl thioacids were tested for their inhibitory activity towards β -lactamases. These compounds are not very soluble directly in either DMSO or water at pHs that can be readily withstood by the β -lactamases, necessitating the addition of NaOH.

To determine if the addition of NaOH would cause a significant pH change in the stocks and assays, the pH of 5 mM and 50 μ M DMSO stocks of TA-1 were determined when prepared with one and six molar equivalents of NaOH and without. As demonstrated in Table 4.4, when 5 mM TA-1 was prepared without NaOH, it was neutral (pH 7) whereas the TA-1 that was prepared with 1 equivalent of NaOH was slightly basic (pH 8). When an excess of NaOH was used in TA-1 stock preparation, the solution becomes more basic (pH 9). Upon 100-fold dilution in DMSO without additional NaOH, each of these stocks became pH 9.

Table 4.4 pH of DMSO stocks of TA-1 when prepared with and without NaOH.

[TA-1] (mM)	equivalents of NaOH	pH
5	0	7
5	1	8
5	6	9
0.05	0	9
0.05	1	9
0.05	6	9

It was important to know if the addition of NaOH would change the conditions of the kinetic assays. To this end, the 5 mM stocks of TA-1 prepared with 0, 1, and 6 equivalents of NaOH were diluted 50-fold in 50 mM HEPES pH 7.2 as they would be in kinetic assays. Once diluted, both solutions of 100 μ M TA-1 were pH 7 confirming that the addition of NaOH to the thioacid stock does not change the pH of the kinetic assays. This experiment was not repeated for 50 μ M stocks, although the results of the 100 μ M TA-1 prepared with excess NaOH suggest that the HEPES will be able to buffer the 50 μ M stocks as well.

4.3.1.1 Inhibitor Screening

A very preliminary screen suggested that the Class B3 MBL L1 would be the most susceptible of our β -lactamases to inhibition by thioacids, so it was chosen as the test system to determine whether or not stocks should be prepared with NaOH. A range of concentrations (100 μ M, 10 μ M, and 1 μ M) of each thioacid listed in Table 4.1 were screened for inhibition of L1 when the stocks were prepared without NaOH and with 1 molar equivalent of NaOH (Table 4.5).

Table 4.5 Phenyl thioacid screening against L1 when prepared in the presence and absence of NaOH (presented as % inhibition).

[TA]	0 equivalents NaOH			1 equivalent NaOH		
	100 μ M	10 μ M	1 μ M	100 μ M	10 μ M	1 μ M
TBA	-14.2	24.1	19.7	86.1	40.4	12.1
TA-1	25.4	42.4	36.6	91.2	61.4	13.4
TA-2	26.6	10.0	18.2	5.7	45.4	23.3
TA-3	13.9	20.8	10.3	91.7	51.1	8.1
TA-4	-18.9	-18.1	-12.2	19.6	0.4	-3.0
TA-5	68.4	50.5	23.8	86.9	70.0	17.5
TA-6	67.4	44.4	16.7	91.5	72.8	15.5
TA-7	1.7	3.3	6.0	-4.7	8.9	3.9
TA-8	16.6	8.5	3.0	34.9	6.7	1.8

Bolded values indicate >50 % inhibition.

The data in Table 4.5 suggest that phenyl thioacids are more inhibitory when prepared in the presence of 1 molar equivalent of NaOH. Regardless of whether or not the stocks were made with NaOH, thioacids containing nitro group(s), TA-5 and TA-6, are the most potent L1 inhibitors. These were the only compounds to reduce the activity of L1 by more than 50% when NaOH was not used to aide in dissolution, and to elicit >70% inhibition at 10 μ M when NaOH was used. The other phenyl thioacids that significantly inhibited L1 were TA-1 which had a bromine at C4, and TA-3 which has chlorines at both C2 and C4.

Inspection of the data collected without the addition of NaOH shows unusual trends for some thioacids: TBA, TA-1, TA-3, and TA-7 are more inhibitory at 10 μ M than they are at 100 μ M. It is probable that while the solutions are clear and the no scatter is observed in the absorbance, these thioacids may be forming colloids at 100 μ M, reducing their availability for the L1 active site. The only case of this when the thioacids were treated with NaOH is TA-2 which has an OMe group at C3. Studies on other β -lactamases were carried out using phenyl thioacid stocks that have been prepared using NaOH since it did not display as much atypical behavior (colloid formation) and was more potently inhibitory.

Table 4.6 Phenyl thioacid inhibitor screening against SBLs

Inhibitor	Concentration	% Inhibition			
		CTX-M-15	KPC-2	GC-1	OXA-48
TA-1	100 μ M	-2.8	-1.5	13.0	2.3
	10 μ M	-2.9	-5.6	3.6	1.0
	1 μ M	1.1	1.7	0.9	0.6
TA-2	100 μ M	-0.5	-3.2	84.0	-10.2
	10 μ M	2.2	-9.3	19.4	-1.7
	1 μ M	-2.8	-0.8	2.9	-1.4
TA-3	100 μ M	1.0	-0.9	56.9	1.9
	10 μ M	1.3	3.3	16.5	2.0
	1 μ M	0.7	1.9	0.4	1.4
TA-4	100 μ M	10.0	-3.2	4.7	1.1
	10 μ M	10.1	-12.2	1.7	2.4
	1 μ M	1.7	-4.8	3.0	-5.1
TA-5	100 μ M	-1.8	-5.9	51.6	2.5
	10 μ M	1.3	-5.2	18.2	-1.5
	1 μ M	-1.5	0.0	1.6	-2.5
TA-6	100 μ M	-2.6	-15.1	40.8	3.0
	10 μ M	-2.6	-11.3	9.4	1.1
	1 μ M	-0.3	-2.7	-4.8	0.9
TA-7	100 μ M	7.2	-5.3	61.2	2.9
	10 μ M	6.0	-18.3	63.4	1.5
	1 μ M	-2.8	-0.7	17.6	4.4
TA-8	100 μ M	8.8	0.6	10.6	1.5
	10 μ M	5.4	-4.2	3.9	-0.1
	1 μ M	1.5	-4.4	3.8	-0.8

Bolded values indicate >50 % inhibition.

The SBLs used in this screen were generally not inhibited by the thioacids with the exception of GC-1 as seen in Table 4.6. GC-1 was found to be most susceptible to inhibition by TA-7 which has a NHAc group at C4 and slightly susceptible to TA-2, TA-3, and TA-5 which have a C3 OMe, a C2 and C4 Cl, and a C3 NO₂ respectively. The SBLs commonly found in the clinical isolates used in this study, CTX-M-15, KPC-2, and OXA-48, show no response with their perceived deviation from 0 % inhibition being accounted for by experimental variability and scatter.

Table 4.7 Phenyl thioacid inhibitor screening against MBLs.

Inhibitor	Concentration	% Inhibition				
		IMP-1	NDM-1	SPM-1	VIM-2	L1
TA-1	100 μ M	33.0	-21.5	27.0	13.5	91.2
	10 μ M	6.9	-13.6	-1.1	3.5	61.4
	1 μ M	3.9	-4.7	0.8	2.1	13.4
TA-2	100 μ M	32.8	22.8	38.4	12.1	5.7
	10 μ M	1.4	12.1	4.7	-4.9	45.4
	1 μ M	7.2	16.7	4.8	-2.0	23.3
TA-3	100 μ M	18.3	-13.5	-1.7	8.7	91.7
	10 μ M	8.3	-5.0	-5.0	4.7	51.1
	1 μ M	-3.6	-4.0	-2.7	0.4	8.1
TA-4	100 μ M	0.5	-11.5	-3.3	-7.7	19.6
	10 μ M	2.7	-7.7	-2.5	-8.9	0.4
	1 μ M	4.4	2.0	7.0	-5.7	-3.0
TA-5	100 μ M	49.9	-0.6	19.9	37.5	86.9
	10 μ M	9.9	-5.2	18.2	11.3	70.0
	1 μ M	0.8	-7.4	-9.2	3.2	17.5
TA-6	100 μ M	78.8	5.0	35.9	61.4	91.5
	10 μ M	19.9	-13.4	-1.0	3.5	72.8
	1 μ M	6.0	-10.1	-2.5	-2.3	15.5
TA-7	100 μ M	38.2	53.6	29.0	17.3	-4.7
	10 μ M	19.6	69.2	37.9	19.4	8.9
	1 μ M	7.2	18.7	8.4	8.9	3.9
TA-8	100 μ M	2.7	6.2	-1.6	-1.8	34.9
	10 μ M	-0.1	-5.8	1.6	-3.7	6.7
	1 μ M	1.6	-1.2	9.8	0.5	1.8

Bolded values indicate >50 % inhibition.

The phenyl thioacids were also screened against MBLs as potential inhibitors using similar methods. The data in Table 4.7 shows that the B1 MBLs are slightly more inhibited than the SBLs at the highest concentrations of phenyl thioacids. IMP-1 and VIM-2 were 78.8% and 61.4 % inhibited by TA-6 (3,5-dinitro) respectively, consistent with L1 which is also inhibited most potently by TA-6. NDM-1 was only inhibited by more than 50% by TA-7 (4-NHAc) which is more consistent with GC-1 than L1 which was uninhibited by this thioacid. Throughout Table 4.7 there are examples of the B1 MBLs starting to show slight inhibition (~30%) at 100 μ M with TA-1, TA-2, TA-5, TA-6, and TA-7. While it is encouraging that these can be inhibited by phenyl thioacids, the inhibition is too weak to be clinically relevant. In addition to those presented below, the Class B2 MBL SFH-1 was screened with TA-1 and was not significantly inhibited up to 316 μ M.

4.3.1.2 Meropenem potentiation by phenyl thioacids

The most potent L1 inhibitors (TA-1, TA-5, and TA-6) were assayed for potentiation of meropenem against 10 *S. maltophilia* strains. Of these strains, 7 are known to produce both the Class B3 MBL L1 and the Class A SBL L2, 2 produce only L2, and one has not been sequenced to identify coded β -lactamases. These compounds were not found to be soluble in MH broth at 1.25 % (TA-1, TA-5) or 1.67% (TA-6) DMSO, necessitating spotting 10 μ L from each well onto MH agar to distinguish between growth and precipitate as depicted in Figure 4.6.

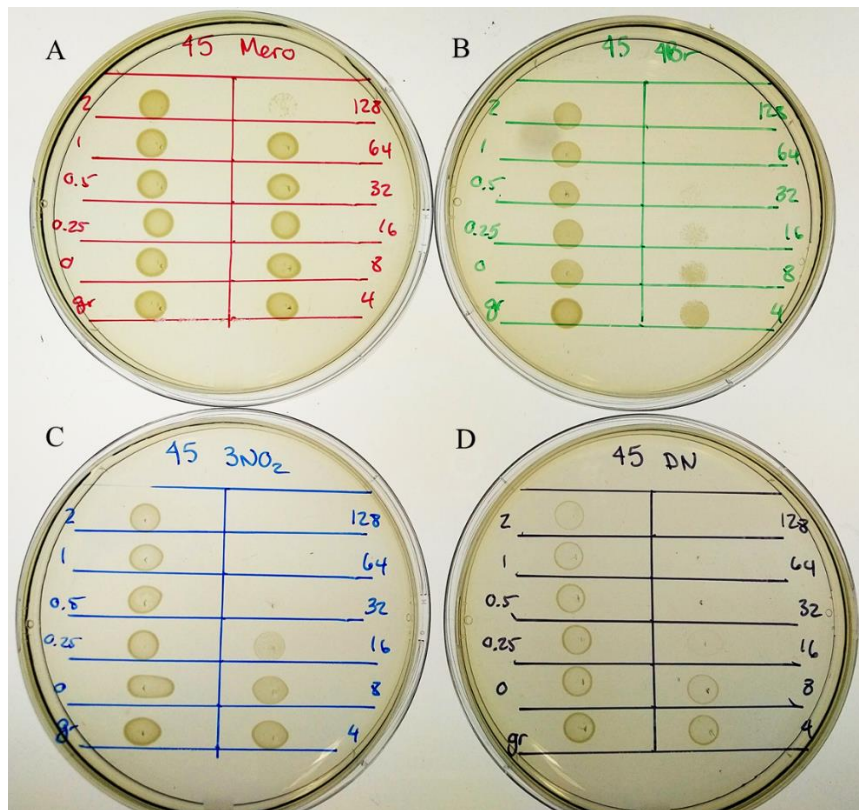


Figure 4.6 MH agar spot plates of thioacid potentiation of meropenem against L1 and L2 producing *S. maltophilia* (UWB 45) for 128 mg/L TA-1 (B), TA-5 (C), or TA-6 (D). Plate A is the unsupplemented control. The values along the perimeter of the agar plates indicate the concentration of meropenem in the sample starting from 128 mg/L in the upper right corner progressing downwards then left in 2-fold serial dilutions to 0.25 mg/L. The sample labelled “0” is the inhibitor and the sample labelled “gr” is the growth control which contains neither meropenem nor thioacid.

Prior to spotting on MH agar, MICs were determined using the standard combination of OD₆₀₀ and visual inspection. The MIC values for meropenem from this analysis served as a control to determine whether or not the agar spotting (MBC) was representative of the MICs determined by standard methods. Using UWB45 as an example, the MIC for meropenem alone was determined to be 128 mg/L using standard methods and the agar spot plate showed an MBC of 128 mg/L, validating that the spot plates are representative of meropenem MICs in solution. The plates in Figure 4.6 demonstrate that TA-1 is able to reduce the MBC of meropenem against UWB45 from 128 mg/L to 64 mg/L, TA-5 reduces the MBC to 32 mg/L, and TA-6 reduces the MBC to 16 mg/L. The potentiation of meropenem by these phenyl thioacids was also determined against other *S. maltophilia* strains (Table 4.8).

Of the 10 *S. maltophilia* strains assayed in this section, three (UWB26, 29, and 44) did not grow due to problems with the inoculum. The remaining strains had good agreement between their meropenem MIC and MBC. UWB46 and UWB48 had a 2-fold difference between these measurements likely due to the OD₆₀₀ measurement not guaranteeing that there is no growth in solution, just that is not turbid enough to be above to cutoff absorbance of 0.07, so growth could be reflected on the agar plate but not the OD₆₀₀ reading. Atypical growth was observed and noted for seven samples in which growth was observed as colonies rather than a homogeneous spot which may be a result of resistant mutants or very few viable cells in that sample.

Table 4.8 Potentiation of meropenem against *S. maltophilia* strains by TA-1, TA-5, and TA-6 as determined using agar spot plate technique.

UWB	β-lactamase	Mero MIC (mg/L)	Meropenem MBC (mg/L)			
			Mero control	128 mg/L TA-1	128 mg/L TA-5	128 mg/L TA-6
33	L1, L2	4	8	1	1*	2*
34	L1, L2	>32	>32	32*	>32*	>32*
39	L1, L2	256	256	128*	256	128
45	L1, L2	128	128	64	32	16
46	L1, L2	64	128	32	64	128
48	L2	128	>128	64*	>128	>128
49	L2	>32	>32	>32	>32	>32

*colonies at the highest meropenem concentration with growth

Strains that produce only L2 (UWB48 and 49) were largely unaffected by the presence of the phenyl thioacids. The exception to this is when UWB48 was treated with 128 mg/L TA-1 and the

MIC of meropenem was reduced at least 4-fold. For most of the L1-producing strains, TA-1 was the most effective phenyl thioacid in potentiating meropenem yielding at least a 2-fold reduction in MBC. The most susceptible strain to potentiation was UWB 33 whose meropenem MBC was reduced 8-fold in the presence of TA-1 and TA-5, and 4-fold in the presence of TA-6. While the potentiation of meropenem by these compounds may be underwhelming in comparison to that of the PMPCs described in Chapter 3, this assay requires the phenyl thioacids to cross the outer membrane and find its target without getting diverted by other potential targets. The intended application of these thioacids would involve them being delivered to their targets as part of a 3'-acylthiocephalosporin and released upon hydrolysis, reducing the likelihood of off target interactions and potentially increasing their potency.

4.3.1.3 MICs of 3'-acylthiocephalosprins against *Stenotrophomonas maltophilia*

To assess the intended thioacid delivery system, the 3'-acylthiocephalosprins, and the impact of substitutions on the thioacid leaving group *in vivo*, a selection of 3'-acylthiocephalosporins with a simple phenylacetyl or 3-fluorophenylacetyl on the C7-amido nitrogen group and a variety of thioacid leaving groups at C3'' were used in this study. While the most potent thioacids were the 3-nitro (TA-5) and 3,5-dinitro (TA-6) substituted phenyl thioacids, cephalosporins with these groups on the right-hand side were not available at the time of testing. Two *S. maltophilia* strains that are known not to produce L1 but produce the other β -lactamase present in each of these strains, L2, was used as a control. Three commercial β -lactams were also tested, meropenem (Mero), ceftazidime (CAZ), and cefotaxime (CTX), to give a relative measure of the potency of the novel cephalosporins. The only β -lactam for which there is a CLSI guideline for resistance is ceftazidime which is seldom used as a therapy for *S. maltophilia* infections due to their nearly ubiquitous expression of cephalosporinases.^{500,515-517}

Table 4.9 MICs of 3'-acylthiocephalosporins and control β -lactams against β -lactamase producing strains of *S. maltophilia*.

UWB	β -Lactamases	MIC (mg/L)								
		Mero	CAZ	CTX	TE-1	TE-2	TE-3	TE-4	TE-5	UW-123
26	L1, L2	256	256	256	>128	>128	>128	>128	64	16
29	NS	64	32	128	64	>128	128	64	8	4
33	L1, L2	4	<i>16</i>	8	64	128	>128	128	4	32
34	L1, L2	8	8	<i>16</i>	64	128	128	64	4	2
39	L1, L2	128	128	256	128	>128	>128	128	<i>16</i>	<i>16</i>
43	L1, L2	32	<i>16</i>	<i>16</i>	32	128	64	32	4	0.5
44	L1, L2	< 1	< 1	< 1	128	64	64	32	2	0.25
45	L1, L2	64	64	128	32	>128	>128	128	<i>16</i>	4
46	L1, L2	32	4	32	64	128	128	64	4	2
48	L2	64	< 1	<i>16</i>	128	>128	>128	>128	8	1
49	L2	<i>16</i>	2	<i>16</i>	64	128	128	64	4	2

NS – not sequenced, the presence of β -lactamases is unknown

Bolded MIC values are susceptible to β -lactams according to CLSI guidelines.⁵⁰⁰

Italicized MIC values are intermediate (neither resistant nor susceptible) to β -lactams according to CLSI guidelines.⁵⁰⁰

The simple 3'-acylthiocephalosporins, TA-1 – 4 are generally poor antibiotics for *S. maltophilia* strains with MICs no lower than 32 mg/L. Of these compounds, TE-1 and TE-4 are the most potent against this panel although studies with other bacterial strains and variable right-hand side groups have distinguished the 2,4-dichloro substitution pattern as the most potent as a standalone antibiotic. Through optimization of the group on the left-hand side, the potency of these compounds was improved from TE-4, though TE-5, to UW-123. TE-5 is more potent than meropenem against 9 of the 11 *S. maltophilia* strains in Table 4.9 and UW-123 is generally 2 to 4-fold more potent than TE-5 and is only less potent than meropenem against one strain, UWB33.

In addition to being poor antibiotics against *S. maltophilia* strains, the early 3'-acylthiocephalosporins, TE-1 through TE-4, were ineffective at potentiating meropenem beyond a 2-fold MIC improvement as seen in Table 4.10. Although little potentiation of meropenem by these compounds is observed in terms of MIC reduction, the combination of the two antibiotics did significantly decrease the density of the cultures in the wells. This was particularly evident towards the higher ends of both the cephalosporin and meropenem concentration ranges. The discrepancies between the meropenem MICs reported in Table 4.9 and those in Table 4.10 are likely due to more bacteria being present in the inoculum when the latter was prepared. Ideally, there should be 500 000

CFU/mL in the inoculum and while the colony counts for the experiment described in Table 4.10 (UWB26: 850 000 CFU/mL, UWB45: 320 000 CFU/mL, and UW49: 830 000 CFU/mL), they were not considered out of range, nor were those for the experiment in Table 4.9 (UWB26: 590 000 CFU/mL, UWB45: 260 000 CFU/mL, and UWB49: 190 000 CFU/mL). For most organisms, minor differences like this in the colony counts do not significantly impact the MICs; however, the *S. maltophilia* strains in this lab have been found to be difficult in this respect in the past.

Table 4.10 Potentiation of meropenem by 3'-acylthiocephaloporins (Ceph) against β -lactamase producing strains of *S. maltophilia*.

Strain	β -lactamase	Ceph	Ceph MIC (mg/L)	Meropenem MIC (mg/L) in the presence of Ceph						
				0 mg/L	4 mg/L	8 mg/L	16 mg/L	32 mg/L	64 mg/L	128 mg/L
UWB 26	L1, L2	TE-1	>128	512	512	512	512	512	256	256
		TE-2	>128	512	512	512	512	512	256	256
		TE-3	>128	512	256	256	256	256	256	256
		TE-4	>128	512	512	512	512	512	256	256
UWB 45	L1, L2	TE-1	>128	128	128	128	128	128	64	64
		TE-2	>128	128	128	128	128	128	128	128
		TE-3	>128	128	128	128	128	128	128	64
		TE-4	>128	128	128	128	128	128	128	64
UWB 49	L2	TE-1	>128	>64	>64	>64	>64	>64	>64	64
		TE-2	>128	>64	>64	>64	>64	>64	>64	>64
		TE-3	>128	>64	>64	>64	>64	>64	>64	>64
		TE-4	>128	>64	>64	>64	>64	>64	>64	64

Bolded values indicate potentiation relative to meropenem control.

Optimization of the 3'-acylthiocephalosporins involved over 70 novel cephalosporins in pursuit of an MBL resistant β -lactam antibiotic that could be co-administered with meropenem. These compounds were screened using a meropenem synergy assay with MBL producing Gram negative pathogens. From this significant synthetic and microbiological effort, one compound distinguished itself for its potency as a standalone antibiotic against not only *S. maltophilia*, but other MBL producers as well and its moderate synergistic activity with meropenem: UW-123.

4.3.2 MICs of UW-123

In order to assess UW-123's potential as a standalone antibiotic, several MIC panels were performed in the presence and absence of an SBL inhibitor by both our lab and Merck.

4.3.2.1 UW panel of Bacterial Strains

Table 4.11 MICs of UW-123 in the presence and absence of 4 mg/L BLI-489 against select bacteria from the UW collection.

Bacterial Strain	UWB	MBL	SBL	MIC (mg/L)			
				UW-123		CAZ	Mero
				with BLI	no BLI		
<i>A. baumannii</i>	94		OXA-23	8	>128	>128	32
	95		OXA-23	8	>128	>128	32
<i>E. coli</i>	59			0.25	0.125	0.125	0.125
	57		CMY-2	0.125	2	32	<0.06
	75	NDM-1	CTX-M-15	>128	>128	>128	128
	91	NDM-1		>128	>128	>128	>128
<i>K. pneumoniae</i>	60			4	4	0.5	<0.06
	11		KPC-2	32	>128	>128	32
	16		KPC-3	64	>128	>128	32
	88		KPC-2, SHV-12	64	>128	>128	>128
	87		CTX-M-15, OXA-48	16	32	128	2
	86		OXA-48	2	4	8	16
	56		CMY-2	8	8	32	0.06
	82	VIM-1		32	32	>128	64
	83	VIM-1		64	128	>128	128
<i>P. aeruginosa</i>	62			8	8	2	1
	25	IMP-7		>128	>128	>128	>128
	31	IMP-5		2	4	32	64
	78	VIM-2		4	4	32	64
<i>S. maltophilia</i>	26	L1	L2	2	2	16	>128

The antibiotic potency of UW-123 relative to ceftazidime (CAZ) and meropenem was first assessed with 20 strains from the UW bacterial collection. These 20 strains were selected for their expression of an assortment of β -lactamases, both MBL and SBL, as well as a few wild types for comparison. For the purposes of antibiotic development, an MIC of 32 mg/L or higher (red) is not useful while an MIC of 4 mg/L or less (green) in combination with a β -lactamase inhibitor is considered susceptible.^{500,518}

Some of the bacterial strains tested for antibiotic susceptibility are completely resistant to all of the tested antibiotics regardless of whether or not an SBL inhibitor was co-administered such as UWB25, 75, 91 while others such as UWB11, 16, 82, 83, and 88 showed a response to the presence of SBL inhibitor but did not fall below 32 mg/L. The wild types (UWB59, 60, 62) did not show reduction of

the UW-123 MIC in the presence of the SBL inhibitor, confirming that it is a true wild type and does not produce an SBL. Conversely, all of the strains that produce only SBLs (except UWB56) showed improved UW-123 MICs in the presence of the SBL inhibitor. This improvement can be as much as 16-fold as it as for UWB57 whose MIC dropped from 2 mg/L to 0.125 mg/L with the addition of 4 mg/L BLI-489. The strains that produced MBLs were much more sensitive to UW-123 than they were to either ceftazidime and meropenem with the most pronounced difference being against the IMP-5 and VIM-2 producing strains of *P. aeruginosa* (UWB31, 78). This effect could be a result of UW-123 being insensitive to MBLs or turning over very slowly in MBLs and thus losing less antibiotic to hydrolysis by MBL than other β -lactams. Unlike strains that produced IMP and VIM β -lactamases, those that produced NDM-1 were not anymore susceptible to UW-123 than they were to ceftazidime or meropenem which may be a result of the MICs being out of range or NDM-1 being insensitive to UW-123.

To determine whether or not UW-123 could also be potentiated by the clinical SBL inhibitor avibactam, three MBL producing strains (UWB75, 78, and 93) were assayed with both UW-123 and ceftazidime against various concentrations of avibactam. The strains were chosen because they are the most β -lactam resistant strains for each NDM, IMP, and VIM producers in the UW collection. The standard administration of avibactam in microbiological assays is 4 mg/L; however, higher concentrations can be assayed to explore the possibility of better synergy at higher concentrations.

Table 4.12 MICs of UW-123 against select strains from UW collection and its potentiation by avibactam.

Bacterial Strain	UWB	MBL	SBL	Antibiotic	Cephalosporin MIC (mg/L)		
					0 mg/L Avi	4 mg/L Avi	8 mg/L Avi
<i>E. coli</i>	75	NDM-1	CTX-M-15	UW-123	>128	128	64
				CAZ	>1024	>1024	>1024
	93	IMP-1	CTX-M-15	UW-123	>128	64	64
				CAZ	1024	512	256
<i>P. aeruginosa</i>	78	VIM-2	UW-123	4	8	8	
			CAZ	128	128	128	

Two of the MBL producers co-express CTX-M-15, a common SBL in clinical pathogens. The strains that produced the SBL showed improved sensitivity to UW-123 when co-administered with 4 mg/L of avibactam and administration of 8 mg/L avibactam did not offer a significant advantage over 4 mg/L as demonstrated in Table 4.12. The strain that only produced an MBL did not show significant change in the MIC in response to the administration of either concentration of avibactam. This is consistent with the previous result that BLI-489 does not potentiate UW-123 against VIM-2 producing *P. aeruginosa* (UWB78). As was also seen in Table 4.11, UW-123 is consistently much more potent than ceftazidime against these MBL producers regardless of whether or not an SBL inhibitor was co-administered.

4.3.2.2 Merck panel of Bacterial Strains

UW-123 was found to be superior to both meropenem and ceftazidime against the MBL producing strains from the UW collection but required an SBL inhibitor to improve potency against strains that express SBLs. The UW collection does not have a lot of variation within each of the MBL families, so a sample of UW-123 was sent to Merck for testing against IMP, NDM, and VIM producing strains. The Merck testing was performed on 25 MBL producing strains each of the families mentioned above using ceftazidime and imipenem as comparators. The BLI used in these experiments was not disclosed but is known to be a DBO like avibactam but is not the DBO that they were pursuing for FDA approval.

IMP producing strains

Many of the IMP producing strains in the Merck panel were not sequenced at high enough resolution at the time of these assays to determine the specific variant with the exception of the five *K. pneumoniae* strains that produce IMP-26. The lack of specific typing to the IMPs also suggests that the screening may have missed any SBLs in many of these strains. Contrary to expectations, a few of the IMP producing strains in Table 4.13 demonstrate an antagonistic relationship between the BLI and UW-123.

Table 4.13 MICs of UW-123 in the presence and absence of an undisclosed avibactam-like inhibitor against a Merck panel of IMP producers.

Bacterial strain	Identifier	MBL	SBL	MIC (mg/L)			
				UW-123		CAZ	Imi
				with BLI*	no BLI		
<i>C. freundii</i>	CL 5724	IMP		32	2	128	2
<i>K. pneumoniae</i>	MB 9713	IMP		16	>32	>128	8
	MB 9248	IMP-26	CTX-M-15	16	>32	>128	1
	MB 9249	IMP-26	CTX-M-15	16	>32	>128	2
	MB 9245	IMP-26		16	32	>128	2
	MB 9247	IMP-26		32	32	>128	2
	MB 9721	IMP-26		4	>32	>128	2
<i>P. aeruginosa</i>	CL 5673	IMP	AmpC-ind	4	1	>128	128
	CL 5730	IMP	AmpC-ind	2	2	>128	32
	CL 5679	IMP		8	8	>128	32
	CL 5727	IMP		16	16	>128	4
	CL 5728	IMP		16	16	>128	>128
	CL 5729	IMP		16	16	>128	64
	CL 5732	IMP		8	8	>128	8
	CL 5733	IMP		>32	>32	>128	128
	CL 5734	IMP		8	4	>128	8
	CL 5737	IMP		>32	>32	>128	128
	CL 5742	IMP		32	>32	128	32
	MB 9708	IMP		2	4	64	16
	CL 5745	IMP		16	8	>128	16
	<i>P. putida</i>	MB 9707	IMP		>32	>32	>128
<i>S. marcescens</i>	CL 5725	IMP		>32	>32	>128	>128
	CL 5726	IMP		>32	>32	>128	>128
	CL 5738	IMP		8	2	>128	4
	CL 5741	IMP		16	16	>128	16

Previous experiments with UW-123 in combination with an SBL inhibitor showed no more than a 2-fold increase in MIC when compared to UW-123 alone which is considered within the allowed uncertainty of the experiment. The Merck strains, on the other hand, exhibit as much as a 16-fold increase in MIC when UW-123 is in combination with the BLI suggesting that there must be an unfavourable interaction between the two compounds against certain bacterial strains. Additional information was not provided as to whether or not this is a common observation with those strains.

As was also seen in Table 4.11, UW-123 seems to be better than ceftazidime against every strain; however, when comparing to imipenem, the advantages of UW-123 shine through against *P.*

aeruginosa. Approximately two thirds of the *P. aeruginosa* strains were more susceptible to UW-123 than imipenem, even without the addition of the BLI which did little to nothing for this subset. The IMP producing strains of *K. pneumoniae* tend to be more sensitive to imipenem than UW-123 as well as more responsive to the BLI than the *P. aeruginosa* strains. The addition of BLI brought the MICs of UW-123 nearer to those of imipenem for most *K. pneumoniae* strains. The tested strains of *S. marcescens* were similarly susceptible to UW-123 and imipenem which is in and of itself encouraging that a cephalosporin can be equally potent as a carbapenem.

NDM producing strains

The only NDM variant represented in the NDM panel from Merck is NDM-1 because it is by far the most clinically important variant (and was at the time of this panel the only one found in clinical isolates). Many of the NDM producing strains co-express at least one SBL, necessitating the use of the SBL inhibitor since UW-123 is known to be susceptible to SBLs. This increases the complexity of the problem since none of the clinically available classes of SBL inhibitors actually inhibit all SBLs. The most common SBLs in this panel, CTX-M-15 and CMY-2, have been previously found to be susceptible to avibactam, and should be similarly susceptible to other inhibitors of that class.^{361,519}

The data in Table 4.14 suggest that UW-123 is not as effective against NDM-1 producers as it was against IMP producers: imipenem is much more effective against most of the strains in this panel than UW-123 regardless of whether or not the BLI is present. This is consistent with the observation from Table 4.11 that UW-123 was completely ineffective against NDM-1 producers. Both NDM-1 producing *E. coli* strains used in the UW panel gave out of range or top of range MICs for each of the tested antibiotics which prevented meaningful conclusions from being drawn; however, the overwhelming result from the Merck panel is that NDM-1 producing strains of *E. coli* are much more susceptible to carbapenems than to UW-123.

Table 4.14 MICs of UW-123 in the presence and absence of an undisclosed avibactam-like inhibitor against a Merck panel of NDM-1 producers.

Bacterial strain	Identifier	MBL	SBL	MIC (mg/L)			
				UW-123		CAZ	Imi
				with BLI*	no BLI		
<i>A. baumannii</i>	CLB 3003A	NDM-1		>32	>32	>128	128
<i>E. coli</i>	CLB 30022	NDM-1	CMY-2	16	16	>128	2
	CLB 30048	NDM-1	CTX-M-15	32	>32	>128	>128
	CLB 30005	NDM-1	CTX-M-15, CMY-2	32	>32	>128	8
	CLB 30009	NDM-1	CTX-M-15, CMY-2	32	>32	>128	8
	CLB 30016	NDM-1	CTX-M-15, CMY-2	>32	>32	>128	8
	CLB 30026	NDM-1	CTX-M-15, CMY-2	>32	>32	>128	8
	CLB 30028	NDM-1	CTX-M-15, CMY-2	>32	>32	>128	16
	CLB 30042	NDM-1	CTX-M-15, CMY-2	32	>32	>128	8
	CLB 30008	NDM-1		16	16	>128	8
<i>E. cloacae</i>	CLB 30004	NDM-1	CTX-M-15, ACT/MIR	>32	>32	>128	4
	CLB 30018	NDM-1	CTX-M-15, ACT/MIR	>32	>32	>128	4
	CLB 30030	NDM-1	CTX-M-15, ACT/MIR, OXA-181	2	>32	>128	16
	CLB 30031	NDM-1	CTX-M-15, ACT/MIR, OXA-181	2	>32	>128	16
	MB 9867	NDM-1	TEM-1, CTX-M-15	4	>32	>128	4
<i>K. pneumoniae</i>	CLB 30046	NDM-1	CMY-2	32	32	>128	16
	CLB 30039	NDM-1	CTX-M-15	>32	>32	>128	16
	CLB 30001	NDM-1	CTX-M-15, CMY-2	16	>32	>128	16
	CLB 30006	NDM-1	CTX-M-15, CMY-2, DHA	>32	>32	>128	64
	CLB 30012	NDM-1	CTX-M-15, DHA-1	32	>32	>128	8
	CLB 30019	NDM-1	CTX-M-15, DHA-1	32	>32	>128	8
	CLB 30010	NDM-1	DHA-1	16	16	>128	8
	CLB 30034	NDM-1	SHV-12, CTX-M-15	32	32	>128	8
	CLB 30011	NDM-1	SHV-2A, DHA-1	32	>32	>128	2
<i>M. morgani</i>	CLB 30047	NDM-1	DHA-1	16	>32	>128	8

The only subset that yielded promising results from the NDM Merck panel was the *E. cloacae* strains: three of the five strains showed a reduction in the MIC of UW-123 in the presence of BLI that made it similarly potent to imipenem. This suggests that it may not be NDM-1 that is causing the lack

of sensitivity to UW-123 but rather other features of pathogenic *Enterobacteriaceae* that are preventing it from reaching its target. This trend was also observed in the UW panel as well as the IMP panel in which clinical isolates of *K. pneumoniae* and *E. coli* are much less susceptible to UW-123 than other strains, even in the presence of a BLI.

VIM producing strains

Table 4.15 MICs of UW-123 in the presence and absence of an undisclosed avibactam-like inhibitor against a Merck panel of VIM producers.

Bacterial strain	Identifier	MBL	SBL	MIC (mg/L)			
				UW-123		CAZ	Imi
				with BLI*	no BLI		
<i>C. freundii</i>	MB 9163	VIM-1		4	16	>128	2
	MB 9864	VIM-32	CMY-81	32	32	>128	8
<i>E. cloacae</i>	MB 9787	VIM-1	ACT/MIR	4	1	>128	4
	MB 9158	VIM-1		8	8	>128	4
	MB 9160	VIM-1		0.125	2	>128	4
	MB 9178	VIM-5		>32	>32	>128	4
<i>K. pneumoniae</i>	MB 9773	VIM-1	KPC-2	4	16	>128	64
	MB 9151	VIM-1		0.5	0.5	>128	64
	MB 9152	VIM-1		1	2	>128	16
	MB 9153	VIM-1		1	8	>128	32
	MB 9155	VIM-1		16	8	>128	32
	MB 9156	VIM-1		1	1	>128	64
	MB 9159	VIM-1		0.5	0.5	>128	64
	MB 9161	VIM-1		4	32	>128	32
	MB 9166	VIM-1		2	4	>128	2
	MB 9171	VIM-26		1	0.5	>128	32
	MB 9172	VIM-26		0.25	1	>128	64
	MB 9175	VIM-27		8	16	>128	64
	MB 9177	VIM-5		4	>32	>128	16
	<i>P. aeruginosa</i>	MB 9732	VIM		8	8	64
MB 9758		VIM		>32	>32	>128	>128
MB 9344		VIM-2		16	16	16	16
MB 9345		VIM-2		4	4	16	128
MB 9346		VIM-2		32	>32	64	>128
MB 9347		VIM-2		16	16	128	>128

The Merck panel of VIM producers includes at least 6 VIM variants and 3 of the strains also express an SBL. Despite the lack of SBLs in these strains, 11 strains responded to the BLI and reduced the MIC of UW-123. The VIM panel was the most susceptible of the Merck panels to UW-123 with 10 of the 25 strains having MICs of 4 mg/L or less without BLI and 16 of 25 with BLI as seen in Table 4.15. This is a distinct improvement over the 6 of 25 IMP producers with UW-123 MICs of 4 mg/L or lower. Similar to other panels, ceftazidime was ineffective against almost all strains making any response to UW-123 a vast improvement over other cephalosporins.

The *K. pneumoniae* strains from the IMP and NDM panels were less susceptible to UW-123 than imipenem both in the presence and absence of the BLI. In the VIM panel, only two of the 13 *K. pneumoniae* strains were less susceptible to UW-123 than imipenem in the absence of BLI while the addition of BLI brings the MIC of UW-123 to or lower than that of imipenem for all of them. Likewise, all of the *P. aeruginosa* strains in the VIM panel were more or equally susceptible to UW-123 than both ceftazidime and imipenem regardless of whether or not it was assayed with the BLI.

4.3.3 Bacterial Synergy of UW-123 with Meropenem

Compounds in this series were developed to be co-administered with a carbapenem as a protective agent against MBLs. UW-123 was the best antibiotic from this series; however, early synergy screening assays with meropenem were often out of range.

Table 4.16 Synergy of UW-123 and meropenem against select strains from the UW collection.

Strain	β -lactamase	UW-123 MIC (mg/L)	Meropenem MIC (mg/L) in the presence of UW-123							FIC*
			0 mg/L	1 mg/L	2 mg/L	4 mg/L	8 mg/L	16 mg/L	32 mg/L	
<i>K. pneumoniae</i> UWB11	KPC-3	>32	64	32	32	64	32	32	64	0.27
<i>K. pneumoniae</i> UWB16	KPC-2	>32	128	32	32	32	32	32	32	0.28
<i>E. coli</i> UWB75	NDM-1 CTX-M-15	>32	128	128	128	128	128	64	64	0.75
<i>P. aeruginosa</i> UWB31	VIM-2	8	64	32	32	16	-	-	-	0.13
<i>P. aeruginosa</i> UWB78	VIM-2	4	64	32	16	-	-	-	-	0.35
<i>S. maltophilia</i> UWB26	L1, L2	2	128	128	64	32	-	-	-	0.25

*Synergistic (FIC \leq 0.5), Additive (0.5 < FIC \leq 1), Indifferent (1 < FIC < 2), Antagonistic (FIC \geq 2)

The synergy of UW-123 and meropenem was assayed against 6 β -lactamase producing strains using a microplate checkerboard synergy assay. UW-123 was able to potentiate meropenem against *K. pneumoniae* and *P. aeruginosa* strains at even the lowest concentrations (1 mg/L) as seen in Table 4.16. For the chosen *E. coli* and *S. maltophilia* strains, higher concentrations of UW-123 were required to decrease the MIC of meropenem against those bacteria. This combination of antibiotics demonstrates synergy against the *S. maltophilia* strain but not the *E. coli* against which they are additive. It is possible that not all *E. coli* strains will be resistant to synergistic effects of these two antibiotics as UWB75 among the most resistant strains in our collection.

4.3.4 Mode of Action Studies of UW-123

To get a better understanding of how UW-123 works as an antibiotic, a series of experiments were performed to establish whether or not it is lethal to cells, what (if any) morphological changes occur in response to treatment, and the specific target(s) and potency against common pathogens.

4.3.4.1 Time Kill Curves

β -Lactam antibiotics are widely accepted to be bactericidal as treatment with therapeutic concentrations results in cell lysis. Studies have shown that this bactericidal activity is concentration dependent such that lower concentrations of β -lactam are bacteriostatic if only one critical PBP is inhibited while higher concentrations are bactericidal as a result of inhibition of multiple PBPs.^{520,521} In this work, time-kill curves for UW-123 were first generated by OD₆₀₀ to establish the expected behavior at specific timepoints then by CFU to determine viability. The time-kill curve produced by reading the culture density, depicted in Figure 4.7A shows a reproducible “bump” in the curve at around 3 hr corresponding to morphological change. This method of assaying growth in the presence of antibiotic is good as a starting point for comparing different classes of antibiotics (data not shown) but gives little insight into the viability of the cells in the culture

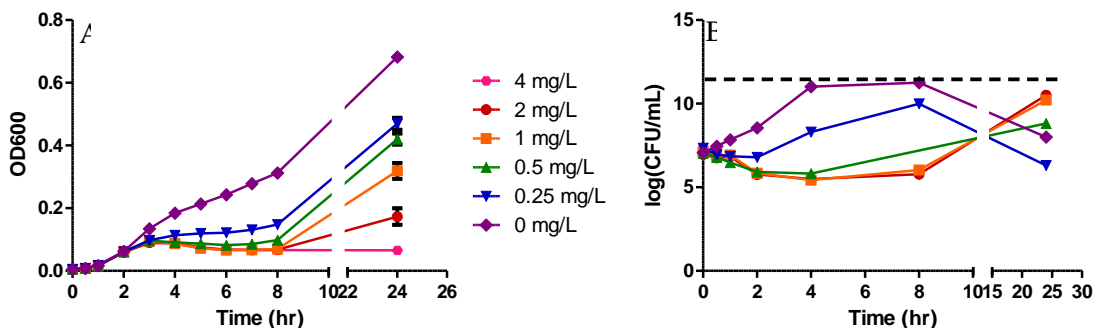


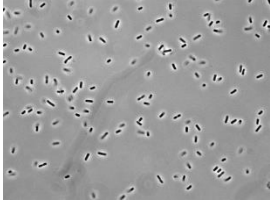
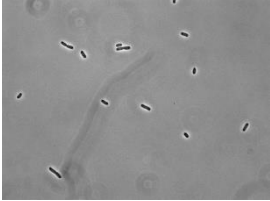
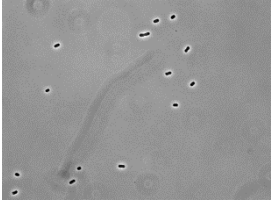
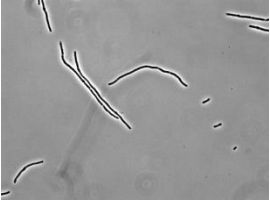
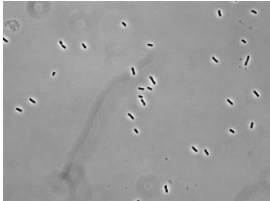

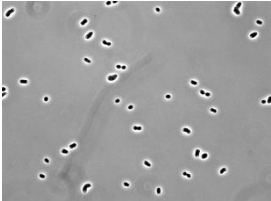

Figure 4.7 UW-123 time kill curves against wild type *E. coli* (UWB 59) monitored by (A) OD₆₀₀ and (B) CFUs. The graphs in this figure were generated using GraphPad Prism v. 5.03.

Plating UW-123 treated cultures at various timepoints on MH agar gives insight into cell viability after antibiotic treatment. Bactericidal activity is defined as a 3-log unit reduction in the number of viable cells relative to the starting timepoint of the untreated control. The experiment in Figure 4.7B started with 10^7 viable cells per mL of liquid culture. At 4 hours, the number of viable cells in 1 mL of culture had fallen to its minimal value of $10^{5.5}$ when treated with either 1 or 2 mg/L UW-123 (1x and 2x MIC respectively), a 1.5 log unit reduction. This suggests that higher concentrations of UW-123 would be required to induce a bactericidal effect and that at these concentrations, UW-123 behaves as a bacteriostatic antibiotic. Later experiments performed with other β -lactam antibiotics showed that bactericidal activity occurs at 4x MIC and greater (data not shown).

4.3.4.2 Morphology

Inhibition of certain HMM PBPs results in characteristic morphological changes which can be observed by phase contrast microscopy. The OD₆₀₀ measurement of the time-kill curves of many antibiotics suggested that most morphological changes occurred at 2-3 hr after treatment as indicated by a transient “bump” in the curves. This prompted the decision to stop the growth at 2 hr and determine the morphology of the cells by phase contrast microscopy. This form of microscopy was chosen over fluorescence or traditional light microscopy because it does not require staining or fixing of the bacteria and it has been used to determine bacterial morphologies in the literature.^{117,513,522} A DMSO control was performed to ensure that any morphological changes were the result of the antibiotic rather than the solvent. Additionally, aztreonam and meropenem were tested as controls for known *E. coli* PBP 3 and PBP 2 inhibitors respectively.

Table 4.17 Sucrose stabilized, β -lactam treated *E. coli* under 1000x magnification by phase contrast microscopy.

Control	Aztreonam	Meropenem	UW-123
			
Untreated	0.0078 mg/L	0.00195 mg/L	0.25 mg/L
			
DMSO	0.03125 mg/L	0.0078 mg/L	1 mg/L

Cell density should not be considered in analysis of these microscopy images; samples were not prepared quantitatively.

The treatment of cells with 1.25 % DMSO did not induce significant morphological changes – Table 4.17 illustrates that some cells may have elongated slightly which that may be within normal variation when compared to the untreated control. As expected, inhibition of PBP 3 in *E. coli* by aztreonam induced filamentation at concentrations above the MIC (0.0156 mg/L) but not below the MIC. Some elongation can be observed below the MIC but is minimal compared to the filamentation above the MIC. Inhibition of PBP 2 in *E. coli* by meropenem induced the expected spheroplasting of the cells. The addition of 0.3 M sucrose to the MH broth is supposed to stabilize osmotically unstable spheroplasts.⁵²² When *E. coli* cells were treated with 0.0156 mg/L meropenem in the presence and absence of sucrose, the sucrose free media yielded many spheroplasted cells while the sucrose media yielded only cellular debris (data not shown).

UW-123 induced filamentation at all assayed concentrations (128 mg/L – 0.0625 mg/L); however, normal morphology cells can be observed in samples treated with 0.25 mg/L or less UW-123 as seen in Table 4.17. Contrary to the effect of sucrose on meropenem treated cells, UW-123 treated cells

grown in the presence of sucrose were much more stable at concentrations in excess of the MIC such as 128 mg/L, maintaining the groups of filaments observed for 1 mg/L in Table 4.17 as opposed to the only one cell could be found in the culture treated with 128 mg/L UW-123 in the absence of sucrose (data not shown). The formation of filaments by treatment with UW-123 suggests that UW-123 primarily inhibits subclass B3 PBPs, specifically PBP 3 in *E. coli*.

4.3.4.3 Competition of UW-123 with Bocillin for PBP Binding

To confirm the hypothesis that UW-123 acts as an inhibitor of subclass B3 PBPs, membrane fragments from two wild-type Gram negative organisms, *E. coli* and *P. aeruginosa*, were isolated. The wild-type *E. coli* strain used in this experiment is an ATCC control strain, unlike the one used above and was acquired after the previous experiments were performed. Membrane fragments from this particular *E. coli* strain were required for work not presented in this thesis and some of which was used to assay UW-123. In addition to *E. coli*, membrane fragments from *P. aeruginosa* were isolated due to the marked increase in potency of UW-123 over ceftazidime and meropenem against *P. aeruginosa* strains from our lab.

P. aeruginosa PBPs

Variable concentrations of the isolated membrane fragments from *P. aeruginosa* were assayed using the SDS-PAGE Bocillin assay described in 4.2.4.3.2 to determine the optimal concentration of fragment to use in the assay (data not shown). Multiple SDS-PAGE gels of varying acrylamide contents (10%, 12.5%, and 15%) were also tested to ensure optimal separation. The optimal conditions for this assay were determined to be 1.4 mg/mL protein per well, run on a 10% SDS-PAGE gel. Using these conditions, the membrane fragments were first incubated with UW-123, allowing adequate time for the covalent bonds to form, then Bocillin was added and incubated for the same amount of time allowing selective labelling of uninhibited PBPs. Identification of PBPs used the R_f values of the bands from gel A and the Coomassie stained LMW marker.

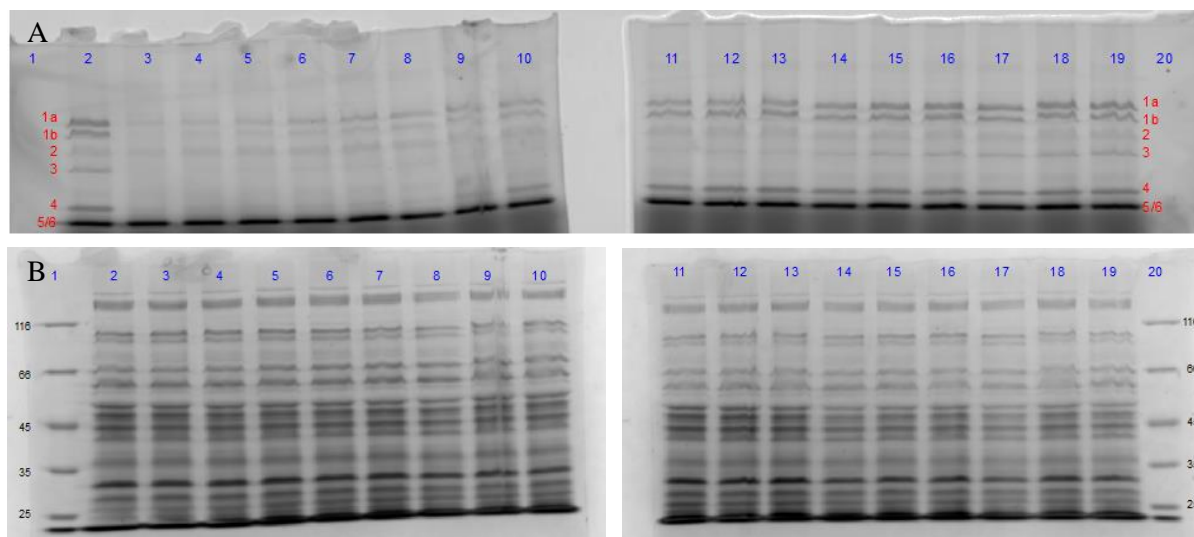


Figure 4.8 SDS-PAGE of UW-123 bound to *P. aeruginosa* PBPs competing with Bocillin. Gel A is the Bocillin fluorescent read, Gel B is the Coomassie stained read. The lanes correspond to the following concentrations of UW-123: 2) 0 mg/L; 3) 128 mg/L; 4) 64 mg/L; 5) 32 mg/L; 6) 16 mg/L; 7) 8 mg/L; 8) 4 mg/L; 9) 2 mg/L – streak in the lane thus discluded; 10) 1 mg/L; 11) 0.5 mg/L; 12) 0.25 mg/L; 13) 0.125 mg/L; 14) 0.0625 mg/L; 15) 0.0313 mg/L; 16) 0.0156 mg/L; 17) 0.0078 mg/L; 18) 0.0039 mg/L; 19) 0 mg/L. Lanes 1 and 20 contained low molecular weight marker.

The visualization of the fluorescence is dependent upon the covalent binding of Bocillin to the various PBPs, and a decrease in intensity of any band relative to the control is indicative of UW-123 competing for the active site of that PBP. As can be seen in Figure 4.8A, UW-123 binds to *P. aeruginosa* PBP 1a and PBP 3 at low concentrations and PBP 1b and PBP 4 at slightly higher concentrations. Graphing the relative intensities of the bands gives a clearer picture of the binding (Figure 4.9).

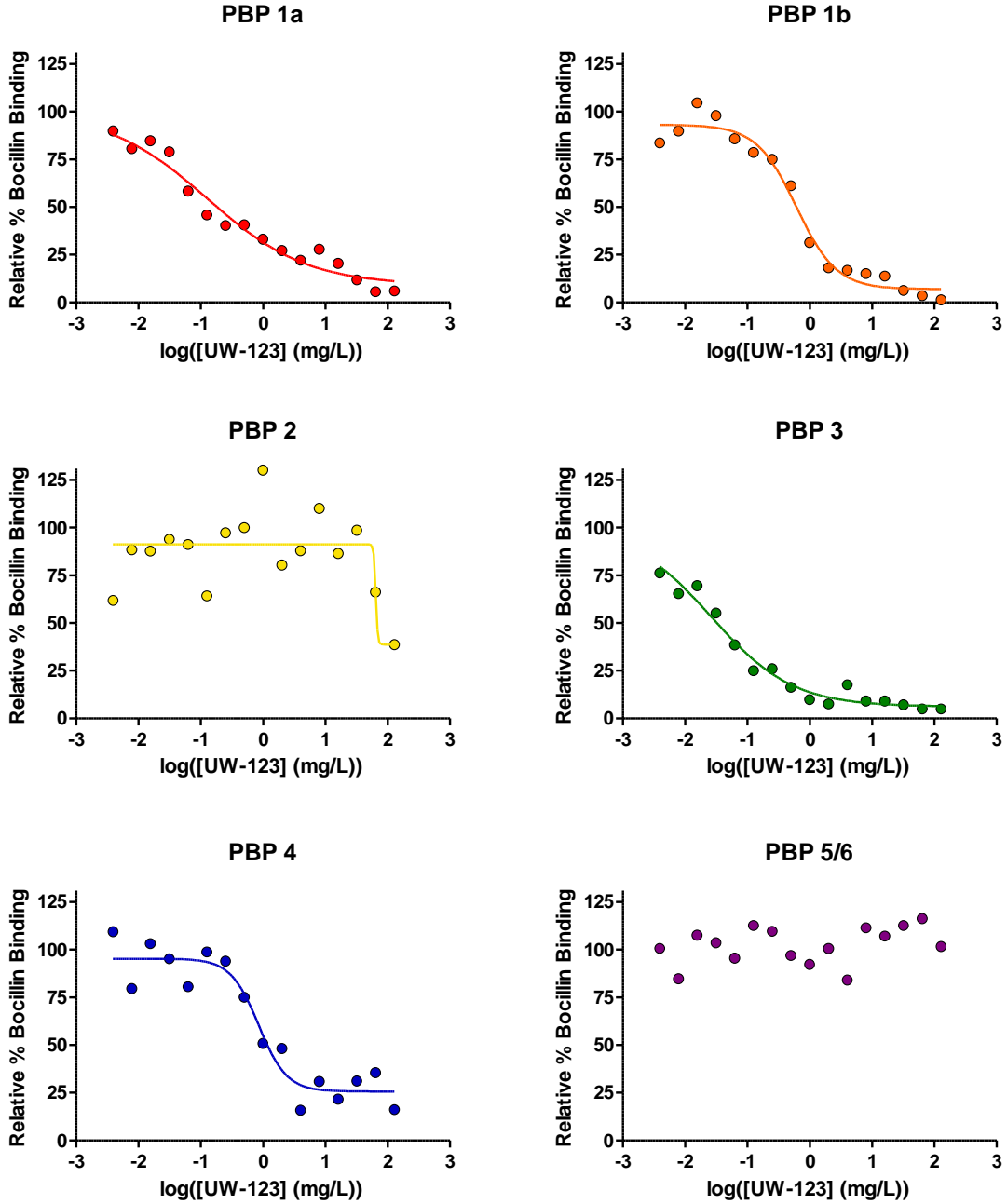


Figure 4.9 Dose response curves of the relative competitive binding of UW-123 to PBPs from *P. aeruginosa* with Bocillin. The graphs in this figure were generated using GraphPad Prism v. 5.03.

The weak intensity of PBP2 in the gels resulted in a high degree of uncertainty in the measurement of the band densities resulting in scatter and poor curve fitting (Figure 4.9). Looking at the gel in Figure 4.8A, it is evident that PBP2 was not inhibited by UW-123 since the corresponding band appears to be only slightly weaker in intensity when treated with 128 mg/L UW-123 (well 2) than when treated with no UW-123 (well 1). The curve fitting of PBPs 1a, 1b, 3, and 4 was good, although PBP 1a and PBP 3 required constraints for the upper plateau since it was not well defined. The fitting of the dose response curves from Figure 4.9 yielded the IC₅₀s presented in Table 4.18.

Table 4.18 IC₅₀s of the competitive binding of UW-123 to PBPs from *P. aeruginosa* with Bocillin.

PBP	IC ₅₀ (mg/L)
1a	0.13 ± 0.05
1b	0.6 ± 0.1
2	NI
3	0.027 ± 0.005
4	0.8 ± 0.3
5/6	NI

NI – Not significantly inhibited

As expected, the most potently inhibited PBP was the subclass B3 PBP 3 with an IC₅₀ of 0.027 mg/L. The other PBPs were an order of magnitude less potently inhibited than PBP 3 with IC₅₀s ranging from 0.13 mg/L to 0.8 mg/L indicating that the antibiotic potency is primarily due to PBP 3 inhibition in *P. aeruginosa*.

E. coli PBPs

In the same manner as for the *P. aeruginosa* PBP assay, the optimal conditions for the *E. coli* PBP assay were determined to be 0.32 mg/mL protein per well, run on a 10% SDS-PAGE gel. Unlike the *P. aeruginosa* PBPs, PBP 1a and 1b could not be resolved for *E. coli*. Close inspection of the gels in Figure 4.10A shows two bands at this position; however, they did not migrate uniformly and cannot be isolated from one another for band density analysis. Additionally, the signal for PBP 5/6 is so intense that it may impact the readings for PBP 4 since these two bands are not well resolved. It should be noted that the visualization in Figure 4.10A has been optimized for PBP 2 and PBP 3 - the high fluorescence signal at the bottom of the gel was minimized when quantifying PBP 5/6.

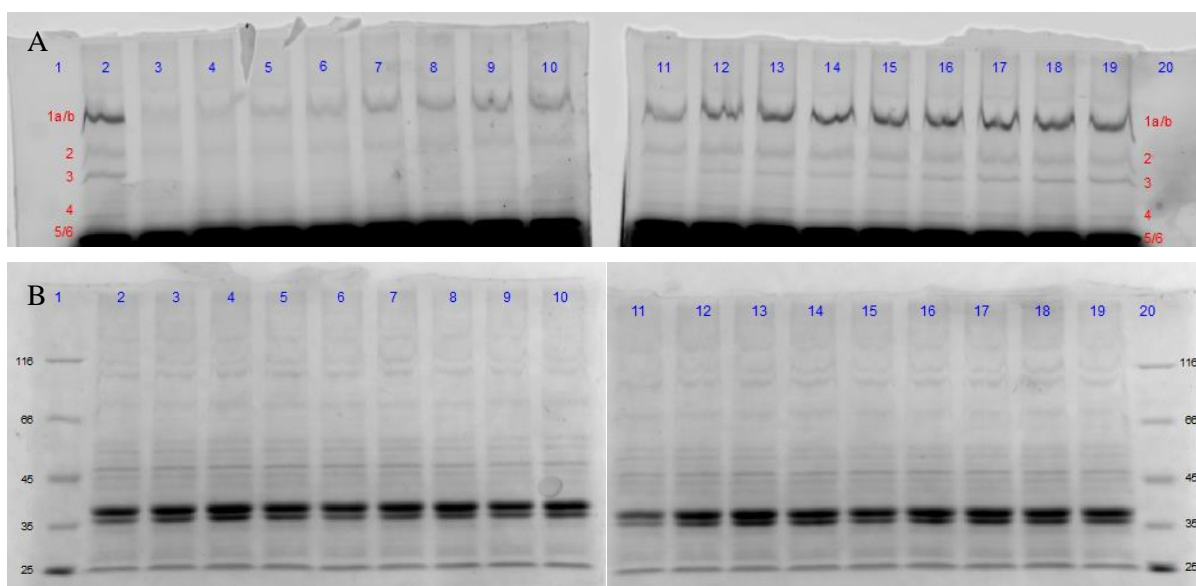


Figure 4.10 SDS-PAGE of UW-123 bound to *E. coli* PBPs competing with Bocillin. Gel A is the Bocillin fluorescent read, Gel B is the Coomassie stained read. The lanes correspond to the following concentrations of UW-123: 2) 0 mg/L; 3) 128 mg/L; 4) 64 mg/L; 5) 32 mg/L; 6) 16 mg/L; 7) 8 mg/L; 8) 4 mg/L; 9) 2 mg/L; 10) 1 mg/L; 11) 0.5 mg/L – water entered sample during boiling; 12) 0.25 mg/L; 13) 0.125 mg/L; 14) 0.0625 mg/L; 15) 0.0313 mg/L; 16) 0.0156 mg/L; 17) 0.0078 mg/L; 18) 0.0039 mg/L; 19) 0 mg/L. Lanes 1 and 20 contained low molecular weight marker.

As above, the visualization of the fluorescence is indicative of covalently bound Bocillin in the active sites of the various PBPs, and a decrease in intensity of any band relative to the control is indicative of UW-123 competing for the active site of that PBP. As can be seen in Figure 4.10A, UW-123 binds to *E. coli* PBP 3 at low concentrations and PBP 1a/b and PBP 2 at higher concentrations. Graphing the relative intensities of the bands gives a clearer picture of the binding (Figure 4.11).

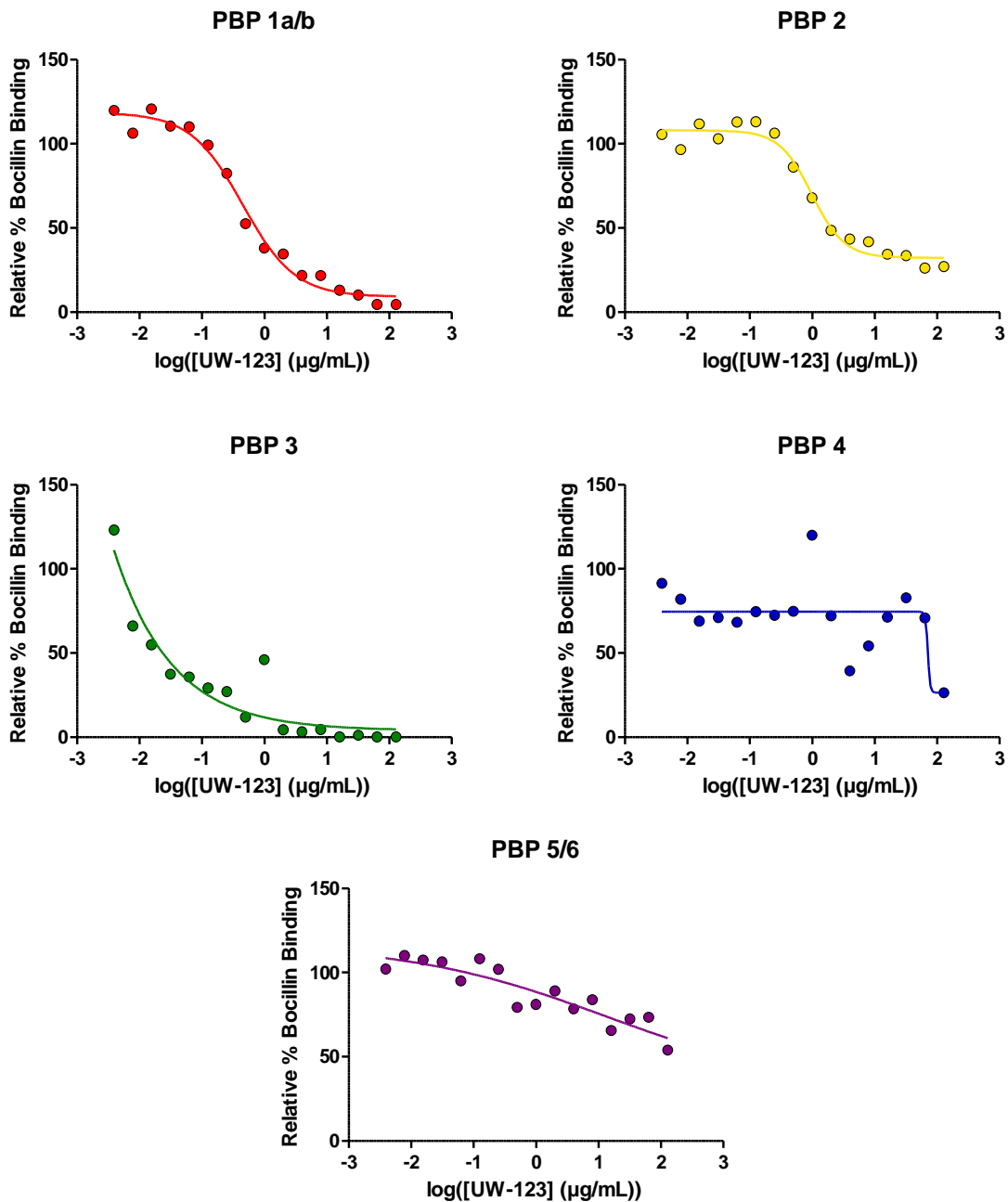


Figure 4.11 Dose response curves of the relative competitive binding of UW-123 to PBPs from *E. coli* with Bocillin. The graphs in this figure were generated using GraphPad Prism v. 5.03.

The affinity of UW-123 for the active sites of PBP 1a/b and PBP 2 appear to be similar with both curves having midpoints between 0.1 and 1 mg/L. PBP 3 was much more susceptible to inhibition by UW-123 with only the lowest assayed concentration (0.0039 mg/L) representing the upper plateau.

As was expected, there is a lot of scatter in the PBP 4 data; however, visual inspection of the gel confirms that the band intensity is consistent throughout most of the wells, only decreasing at the highest UW-123 concentrations. Likewise, little inhibition of PBP 5/6 was observed, although the intensity of these bands steadily decreased with increasing UW-123.

The dose-response plots in Figure 4.11 were fitted using nonlinear regression to determine the IC₅₀s presented in Table 4.19. The curves for PBP 4 and PBP 5/6 did not go low enough (PBP 4 and PBP 5/6 were not inhibited enough) to determine an IC₅₀ with certainty.

Table 4.19 IC₅₀s of the competitive binding of UW-123 to PBPs from *E. coli* with Bocillin.

PBP	IC ₅₀ (mg/L)
1a/b	0.45 ± 0.08
2	1.0 ± 0.2
3	0.02 ± 0.01 [†]
4	NI
5/6	NI

NI – Not significantly inhibited

[†]Top of curve not well defined, constrained to 110 (comparable to top of curve for 1a/b and 2)

As the morphological data suggested, PBP 3 is the most potently inhibited *E. coli* PBP and its level of inhibition is comparable to that of PBP 3 from *P. aeruginosa* – both 0.02-0.03 mg/L. Likewise, the inhibition of PBP 1 a/b from *E. coli* is close to the average inhibition of the Class A PBPs from *P. aeruginosa* (0.45 mg/L and 0.37 mg/L respectively). Unlike *P. aeruginosa*, significant inhibition of PBP 2 from *E. coli* was observed, although it is weaker than the inhibition of PBP 3 and the Class A PBPs.

4.3.5 Pyridine thioacids – a more potent alternative to phenyl thioacids

Phenyl thioacids are at best moderate inhibitors of MBLs, by increasing the potency of the released thioacid inhibitor the efficacy of these cephalosporins could be further improved against MBL producing strains. From Chapter 3, we know that pyridine rings with negatively charged groups at the 2 and 6 positions are potent inhibitors of all subclasses of MBLs. Additionally, Roll et al. have demonstrated that pyridine thiocarboxylates (also referred to as pyridine thioacids) are potent inhibitors of B3 MBLs; however, their analysis did not include other MBL subclasses.⁴³⁹ This section explores the potential inhibitory activity of two pyridine thiocarboxylates, PMTC and PDTC, and the

benzene derivative of PDTC, I-PDTC (structures depicted in Figure 4.4) against a variety of β -lactamases.

4.3.5.1 Inhibitor Screening

Like the phenyl thioacids, the pyridine thiocarboxylates required the addition of NaOH to the stocks to ensure complete dissolution - this was most pronounced for I-PDTC. These compounds were first screened for SBL inhibition to establish whether or not they are universal β -lactamase inhibitors. As expected, CTX-M-15, KPC-2, and OXA-48 are not inhibited by any of the tested compounds as seen in Table 4.20. Some mild inhibition of CTX-M-15 was observed with I-PDTC at 100 μ M, but this is not enough inhibition to warrant further study.

Table 4.20 Pyridine thioacid inhibitor screening against SBLs.

Inhibitor	Concentration	% Inhibition			
		CTX-M-15	KPC-2	GC-1	OXA-48
PMTC	100 μ M	-0.3	-2.1	54.3	-0.4
	10 μ M	1.2	-2.9	44.1	-0.9
	1 μ M	-0.5	-1.2	5.6	0.3
PDTC	100 μ M	3.8	3.0	69.5	1.2
	10 μ M	-3.1	-3.0	37.6	-1.1
	1 μ M	-2.1	-2.8	1.4	1.1
I-PDTC	100 μ M	37.1	-5.1	85.4	6.4
	10 μ M	2.2	-3.4	50.2	-1.5
	1 μ M	-1.1	-0.5	6.3	-2.4

Bolded values are >50 % inhibited.

As was also observed for the phenyl thioacids in Table 4.6, GC-1 is the only SBL that is significantly susceptible to inhibition by this subset of thioacids. The data in Table 4.20 shows that I-PDTC is the most potent inhibitor of GC-1 from this series, suggesting that the pyridine core is not necessary or beneficial for GC-1 inhibition. GC-1 is also indifferent to the number of thiocarbonyl groups on the molecule as evidenced by the negligible difference between the inhibitory potency of PMTC and PDTC.

Although the pyridine core was not advantageous for GC-1 inhibition, it yielded very potent MBL inhibition as demonstrated in Table 4.21. The most potent inhibitor in this series appears to be PMTC which completely inhibits IMP-1, NDM-1, and VIM-2 at all assayed concentrations and demonstrated >50% inhibition at all concentrations for SFH-1 and L1. PDTC is slightly less effective, inhibiting

most MBLs by about 73 % at 1 μM as opposed to the >95% seen with most B1 MBLs at 1 μM PMTC. SPM-1 is less potently inhibited than other B1 MBLs, demonstrating complete inhibition at 10 μM PMTC and only 42% inhibition at 1 μM while the other B1 MBLs are still completely inhibited at 1 μM .

Table 4.21 Pyridine thiocarboxylate inhibitor screening against MBLs

Inhibitor	Concentration	% Inhibition					
		IMP-1	NDM-1	SPM-1	VIM-2	SFH-1	L1
PMTC	100 μM	99.8	99.2	99.5	99.9	96.7	99.7
	10 μM	99.9	100.0	99.5	99.9	96.1	99.9
	1 μM	97.3	96.8	42.5	99.6	62.4	84.2
PDTC	100 μM	98.6	94.1	101.9	99.9	93.6	100.2
	10 μM	100.0	99.7	90.2	99.8	96.9	99.0
	1 μM	71.5	73.1	45.9	74.5	73.6	78.2
I-PDTC	100 μM	61.8	27.2	54.8	31.8	41.2	61.3
	10 μM	12.7	5.3	0.3	-0.6	13.1	35.1
	1 μM	6.5	7.3	-7.3	-0.6	-4.4	22.7

Bolded values are >50 % inhibited.

The inhibitor with a benzene core, I-PDTC, only inhibits MBLs at the highest assayed concentrations. The drastic drop in inhibitory potency from PDTC to I-PDTC suggests that the pyridine core is essential of potent inhibition.

4.3.5.2 IC₅₀ Determination

A wider range of PMTC and PDTC concentrations were assayed with GC-1, the B1 MBLs, and L1 to give a more accurate measure of inhibition. These assays were performed with three technical replicates but was only performed once to allow enough material for bacterial studies. The dose response curves generated from these experiments are shown in Figure 4.12.

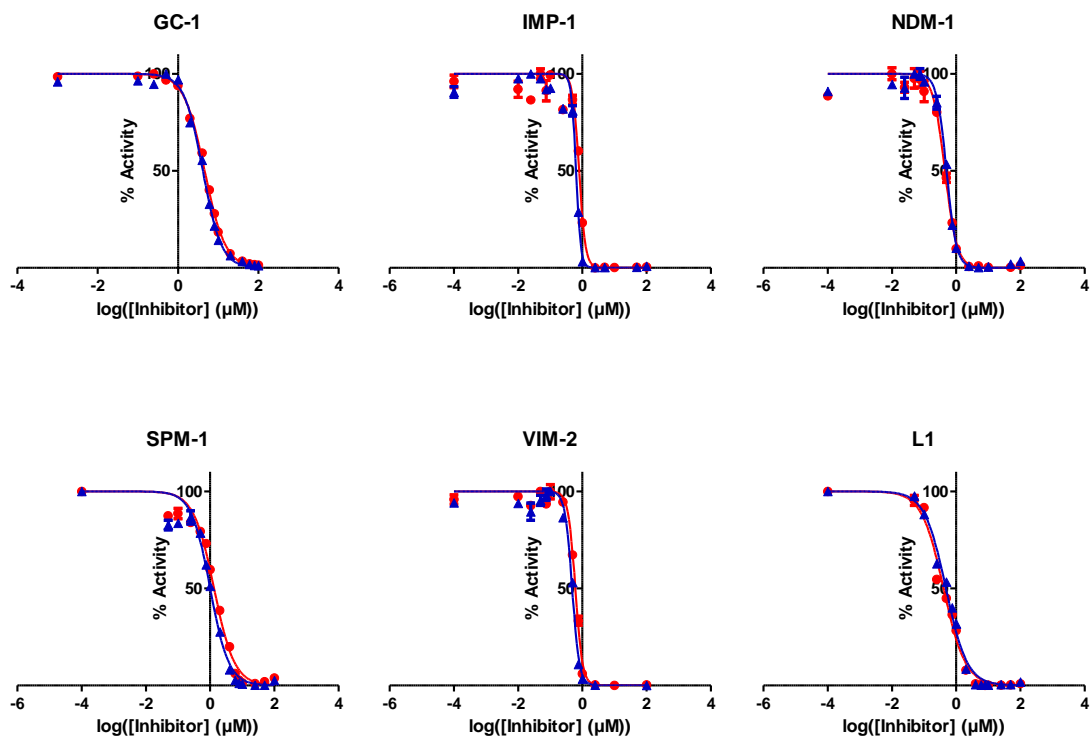


Figure 4.12 Dose response curves of MBLs and GC-1 inhibited by PMTC and PDTC (red and blue respectively). The graphs in this figure were generated using GraphPad Prism v. 5.03.

It is evident from the dose response curves in Figure 4.12 that PMTC and PDTC are very similarly potent inhibitors against all assayed enzymes as the curves are overlapping throughout the vertical portion of the curve. This steepness of this region is well conserved for each enzyme; however, there is a distinct difference between enzymes. The curves for IMP-1 and VIM-2 are much steeper (Hill slope >4) than SPM-1 and L1 (Hill slope ~ 1.3) with NDM-1 and GC-1 having intermediate slopes which may be indicative of differing inhibition mechanisms for the different enzymes.⁴⁹⁹

Fitting of these dose response curves to Equation 3.1 yielded the IC_{50} values listed in Table 4.22. These data confirm that PMTC and PDTC have similar potency with IC_{50} values differing by no more than 25% (SPM-1). It is probable that with more repeats of this experiment, the IC_{50} values for PMTC and PDTC will fall within the uncertainty of one another. Despite the differences observed in the steepness of the dose response curves, the pyridine thiocarboxylates exhibit consistent potency across the MBLs with IC_{50} values ranging from 0.41 μM to 0.79 μM for the assayed MBLs with the

exception of SPM-1 which was slightly less susceptible to inhibition. A dose response curve was also generated for SFH-1; however, the assayed concentrations were not low enough to obtain the upper plateau region. The estimates for the IC₅₀ of these compounds against SFH-1 are consistent with those of the majority of the MBLs (0.70 μM and 0.47 μM for PMTC and PDTC respectively).

Table 4.22 IC₅₀s of pyridine thiocarboxylates against class B and C β-lactamases.

β-lactamase	Class	IC ₅₀ (μM)	
		PMTC	PDTC
GC-1	C	4.61 ± 0.08	4.2 ± 0.1
IMP-1	B1	0.79 ± 0.02	0.63 ± 0.02
NDM-1	B1	0.45 ± 0.02	0.50 ± 0.02
SPM-1	B1	1.33 ± 0.06	1.01 ± 0.06
VIM-2	B1	0.60 ± 0.01	0.48 ± 0.02
L1	B3	0.41 ± 0.02	0.48 ± 0.02

In addition to being potent MBL inhibitors, PMTC and PDTC are inhibitors of GC-1, albeit a 10-fold less potent than against MBLs. Despite the reduced potency against GC-1 relative to the MBLs, PMTC and PDTC are similarly potent against GC-1 with IC₅₀s of 4.61 μM and 4.2 μM respectively. This inhibition broadens the spectrum of targets from solely MBLs to MBLs and some SBLs. To further explore the potential of the pyridine thiocarboxylates as β-lactamase inhibitors, they were assayed as an adjuvant to potentiate meropenem against β-lactam resistant pathogens.

4.3.5.3 Potentiation of meropenem by pyridine thiocarboxylates

The potentiation of meropenem was assayed using a microplate checkerboard assay with two-fold dilutions of meropenem along the long axis of the plate and two-fold dilutions of the inhibitor along the short axis. The addition of sodium hydroxide to stock solutions of pyridine thiocarboxylates was required for complete dissolution prior to dilution in MH broth. A small amount of precipitate was observed in the wells corresponding to the highest concentration of the inhibitors after overnight growth. Spotting on agar plates was not used to differentiate between growth and precipitate in these assays because comparison to other wells containing the same concentration of inhibitor allowed for visual differentiation.

Each of the strains in Table 4.23 demonstrate potentiation of meropenem by the pyridine thiocarboxylates at the highest assayed concentrations as evidenced by a 4-fold or greater reduction in

the MIC. The most susceptible strain was the IMP-1 and CTX-M-15 producing *E. coli*, UWB 93, which was reduced to intermediate inhibition by only 4 mg/L PDTC and 8 mg/L PMTC. This strain was made completely susceptible to meropenem (MIC of 1 mg/L or less) in the presence of 16 mg/L PDTC and 64 mg/L PMTC. Most other strains were only brought into intermediate or susceptible range but the highest concentrations of adjuvant. This is a significant accomplishment for UWB 75 and UWB 24 which have meropenem MICs of 128 mg/L and require a 32 to 64-fold reduction of their MIC to enter the intermediate range.

Table 4.23 Sensitization of MBL producing Gram negatives to meropenem by pyridine thiocarboxylates.

Strain	β -lactamase	Meropenem MIC (mg/L)	Inhibitor	Meropenem MIC (mg/L) in the presence of Inhibitor					
				4 mg/L	8 mg/L	16 mg/L	32 mg/L	64 mg/L	128 mg/L
<i>E. coli</i> UWB93	IMP-1	4	PMTC	4	2	2	2	0.5	0.25
	CTX-M-15		PDTC	2	2	1	0.25	0.25	0.125
<i>E. coli</i> UWB75	NDM-1	128	PMTC	128	64	64	64	8	4
	CTX-M-15		PDTC	64	64	64	16	4	2
<i>K. pneumoniae</i> UWB116	NDM-1	32	PMTC	16	16	8	8	2	0.25
			PDTC	16	16	8	8	2	0.25
			I-PDTC	32	16	16	16	16	8
<i>P. putida</i> UWB24	VIM-2	128	PMTC	128	128	128	128	64	4
			PDTC	128	128	128	64	4	2
<i>P. aeruginosa</i> UWB78	VIM-2	128	PMTC	128	128	128	128	32	32
			PDTC	128	128	128	64	32	32

Bolded MIC values are susceptible to β -lactams according to CLSI guidelines.⁵⁰⁰

Italicized MIC values are intermediate (neither resistant nor susceptible) to β -lactams according to CLSI guidelines.⁵⁰⁰

The most effective compound at potentiating meropenem is PDTC which elicits the same MIC reductions with at least 2-fold less compound for most bacterial strains. The only strain where the two pyridine thiocarboxylates are equivalent was UWB 116, this was also the only strain for which I-PDTC was assayed. The benzene core of I-PDTC abolishes much of the potency of PDTC, such that PDTC elicits a 32-fold greater reduction in MIC than I-PDTC at 128 mg/L. Additionally, I-PDTC does not reduce the MIC of meropenem against UWB 116 enough to bring it into intermediate resistance.

4.4 Discussion

4.4.1 Phenyl Thioacid Inhibitors of B3 MBLs

The phenyl thioacids proved to be moderate inhibitors of L1 but inhibited few other β -lactamases. This inhibition was improved substantially when the most concentrated DMSO stock of the inhibitor was prepared in the presence of one molar equivalent of NaOH. Upon addition of the NaOH, it is assumed that the thiocarboxylate group is deprotonated. Although the initial DMSO solution did not seem to contain precipitate, it is possible that the aromatic thioacids are in an aggregated state and that deprotonation breaks up the aggregate resulting in a higher effective concentration of the conjugate base of the thioacid to act as an inhibitor.

The phenyl thioacids with halogen substituents on the aromatic ring TA-1, TA-3, and TA-4 demonstrated decreased potency at high concentrations when prepared in the absence of NaOH. Preliminary dose response curves of these compounds under the same conditions gave unusual “U-shaped” curves (data not shown). Most of the literature regarding U-shaped dose response curves involves hormesis, the overcompensation of cells or organisms in response to deviation from homeostasis, which does not apply to *in vitro* enzyme assays.⁵²³ In this case, it is likely that the U-shaped dose response curves are indicative of the halogenated phenyl thioacids forming aggregates or colloids at high concentrations resulting in reduced availability of the free inhibitor for binding to the enzyme active site.⁵²⁴

The most potent set of phenyl thioacid inhibitors of L1 were those with one or more nitro group on the phenyl ring, TA-5 (at C3) and TA-6 (at C3 and C5), while the second most potent set of inhibitors has a halogen at C4, TA-1 (Br at C4) and TA-3 (Cl at C2 and C4). TA-4 which has an additional chlorine at C6 is a poor inhibitor. It is not clear if this effect is steric or electronic. TA-2 which has a methoxy group (inductively electron withdrawing but pi-electron donating) at C3 is a poor inhibitor of L1. This suggests that it is beneficial to have π -electron withdrawing groups (e.g. NO₂) meta to the thioester rather than a π -electron donating groups (e.g. OMe).

Upon testing with a broader panel of MBLs, TA-6 which has nitro groups at C3 and C5 had the greatest breadth of inhibitory activity as it inhibited IMP-1 and VIM-2 by more than 50% at 100 μ M and showed limited activity with SPM-1. Other trends seen with L1 do not hold up: TA-2 and TA-7 are more potent against the B1 MBLs than both TA-1 and TA-3, suggesting that the hydrophobic

substituent is preferred over the halogens in these MBLs. This may be the result of the C3 substituent weakly interacting with the loop that closes over the B1 active sites. NDM-1 does not behave the same way as other B1 MBLs with these inhibitors, it is only significantly inhibited by TA-7 which may be a result having a much more flexible loop than IMP-1 or VIM-2.

Unlike the PMPCs, the phenyl thioacids are capable of inhibiting at least one of the SBLs, GC-1, although the Class A and Class D SBLs were not affected. The mode of inhibition of GC-1 by aromatic thioacids is unclear.

In bacterial studies, the phenyl thioacids were able to potentiate meropenem against L1 producing strains of *S. maltophilia*. Most strains were more potentiated by TA-1 than either of the phenyl thioacids with nitro substituents. This is contrary to the observation that the nitro substituents improved the inhibitory potency of the phenyl thioacids in enzyme kinetic assays and suggests that TA-1 may cross the outer membrane better than TA-5 or -6 or it may have fewer off-target interactions. Since meropenem is a bactericidal antibiotic, the MBCs were reflective of the MICs with no more than a 2-fold difference between the MIC and MBC of meropenem. This suggests that since the thioacids are not antibiotics themselves and should not disrupt the ability of meropenem to kill bacteria, the MBC reduction would also be reflected in the MICs if they were readable. The only point in the MBC experiment where it becomes uncertain whether or not they are reflective of MICs is when the growth spots are only colonies. Due to the low count of viable bacteria in these spots, it is likely that these wells would not have reached the growth cutoff. This is most pronounced against UWB 33 which had only colonies in many of the spots as seen in Figure 4.13.

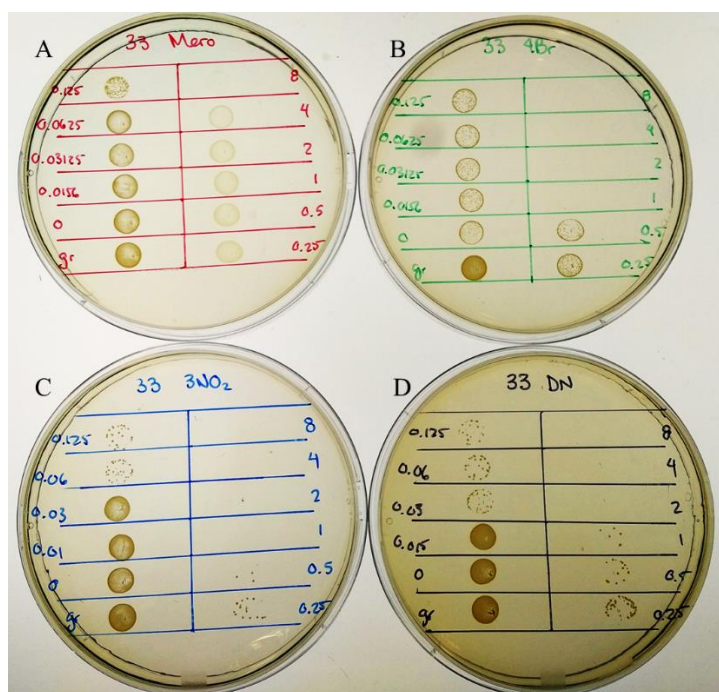


Figure 4.13 Spot plates of UWB 33 on MH agar to determine the MBCs of thioacid potentiated meropenem when treated with no adjuvant (A), 128 mg/L TA-1 (B), 128 mg/L TA-5 (C), and 128 mg/L TA-6.

The inhibition of L1 by the phenyl thioacids may be the result of the thiocarboxylate sulfur atom replacing the catalytically essential hydroxide ion that is normally shared as a ligand by the two Zn^{2+} ions in the active site. This behavior, depicted in Figure 4.14, has been previously demonstrated for the sulfur atom of numerous thiols including D-captopril, N-(3-mercaptopropanoyl)-D-alanine, and the bisthiazolidine derivatives but a crystal structure of a thioacid in the L1 active site has never been acquired.^{255,425,429}

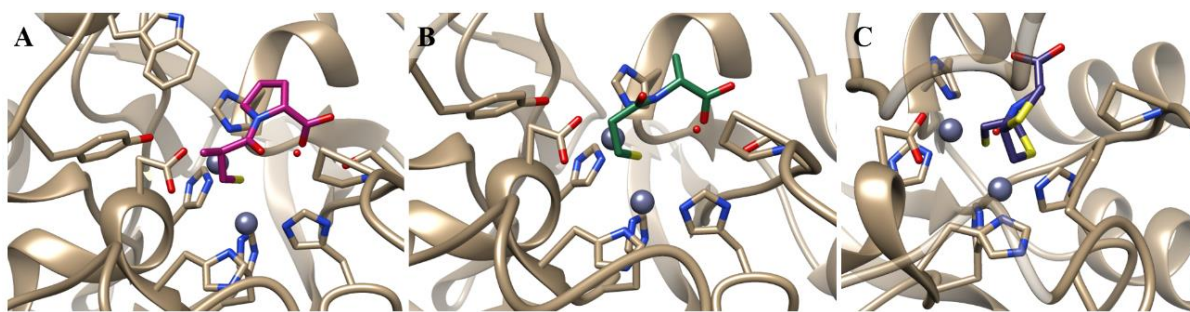


Figure 4.14 Binding of thiols to the L1 active site : D-captopril (PDB: 2FU8), N-mercaptopropanoyl-D-alanine (PDB: 2QDT), bisthiazolidine (PDB: 5EVB). This figure was generated from the aforementioned protein databank files using Chimera v. 1.12.

4.4.2 3'-Acylthiocephalosporins as delivery systems for phenyl thioacid inhibitors of L1

Precipitation of an adjuvant is not ideal for assays since the true accessible concentration of the compound is unknown. The challenges of determining the potentiation of meropenem by the phenyl thioacids would be a problem for potential drug development; however, the intended application of these compounds is through a 3'-acylthiocephalosporin. Unlike the phenyl thioacids, the synthetic cephalosporins were completely soluble, and use of a cephalosporin as a delivery system ensures that the thioacid is released at its target. The release of the thioacid at its target circumvents any solubility problems, reduces the potential for off-target reactions, and the thioacid should be in the active, deprotonated form. Simple 3'-acylthiocephalosporins with leaving groups at C3' similar to the thioacids discussed above were less effective at potentiating meropenem against *S. maltophilia* strains than the thioacid alone. This suggests that these cephalosporins may be having difficulty crossing the outer membrane or that they are poor substrates that are not being turned over enough to release an adequate amount of inhibitor.

S. maltophilia is known to be a highly antibiotic resistant pathogen with low outer membrane permeability, efficient efflux mechanisms, and chromosomally encoded β -lactamases (L1 and L2).^{525–527} This resistance is particularly prevalent for β -lactams due to the chromosomally encoded β -lactamases such that only 26.5% of *S. maltophilia* isolates from a Greek hospital were susceptible to either ceftazidime and treatment with β -lactams is only recommended when the patient exhibits adverse effect to other antibiotics such as trimethoprim/sulfamethoxazole.^{515,517} This is what makes

the antimicrobial potency of TE-5 and UW-123 against β -lactamase producing strains of *S. maltophilia* interesting: *S. maltophilia* strains that co-produce L1 and L2 have been widely reported to be immune to β -lactam monotherapy (with sporadic reports of limited ceftazidime efficacy).^{279,526-534}

4.4.3 UW-123

The most potent standalone antibiotic to come from the extensive medicinal chemistry effort of developing the 3'-acylthiocephalosporins was UW-123. The increased potency of this compound relative to the other 3'-acylthiocephalosporins is most likely a result of more efficient uptake into the bacteria due to the siderophore mimic in the amido sidechain on the C7 nitrogen. In assays where UW-123 was not co-administered with any other antibiotic or adjuvant, it was shown to be less effective against strains that express extended spectrum SBLs. This is, in part, due to these enzymes being excellent at hydrolyzing cephalosporins, but more importantly, it is due to the phenyl thioacids not being inhibitory towards Class A and Class D SBLs. The vast majority of bacterial strains in the Dmitrienko lab inventory that produce SBLs produce either Class A or Class D ESBLs, so efficacy of UW-123 against strains producing Class C SBLs, particularly Class C ESBLs, was not established.

4.4.3.1 Efficacy of UW-123 against bacterial pathogens

In the UW panel, UW-123 was more potent than either ceftazidime or meropenem against strains that produce only MBLs due to the inhibition of the MBL by the released thioacid inhibitor. The only case where this was not true was against strains that produce NDM-1. These strains, UWB 75 and 91, are highly resistant to all β -lactam antibiotics and require potent inhibition of NDM-1 for sensitization as demonstrated by the PMPCs in Table 3.8. Since the phenyl thioacids were not inhibitory towards B1 MBLs *in vitro*, least of all NDM-1, it is probable that they are also not inhibitory *in vivo*, leading to the insensitivity of these strains to UW-123.

The insensitivity of NDM-1 producers was also observed in the Merck panel of NDM-1 producers in Table 4.14 in which UW-123 was less potent than either ceftazidime or imipenem against all strains in the absence of BLI. While many of the NDM-1 producing strains demonstrated a reduction in UW-123 MIC in the presence of BLI consistent with the widespread SBL co-expression, only 3 of the strains were sensitized enough to be considered susceptible. Unlike NDM-1 producers which were not susceptible ($\text{MIC} \leq 4 \text{ mg/L}$) to UW-123 alone, both the IMP and VIM producing strains from the Merck panels had 6 and 9 strains that were susceptible to UW-123 without the aid of a BLI.

The VIM panel was the most susceptible of the Merck panels to UW-123 and was also the most responsive to the addition of the BLI, increasing the number of susceptible strains from 9 to 15 of 25 upon its addition (Table 4.15). This demonstrates that the VIM-producing strains in the UW panel in Table 4.12 are not necessarily representative of all VIM-producers as the *K. pneumoniae* VIM-1 strains (UWB 82 and 83) were highly resistant to UW-123 while the VIM-2 producing *P. aeruginosa* (UWB 78) was only moderately susceptible. Although the Merck panel of VIM-producers contained at least 6 VIM variants, these were heavily weighted towards VIM-1-like variants with only 4-6 of the 25 strains being from the VIM-2 branch of the family. Unfortunately, all of the potential strains that produce a VIM-2-like variant were *P. aeruginosa* strains with no VIM-1-like variants being represented in this organism so although the VIM-2 strains were less susceptible to UW-123, it is not certain whether that is a characteristic of *P. aeruginosa* or the VIM-2-like variants.

Across both the NDM and VIM panels from Merck, the BLI performed as expected, reducing the MIC of UW-123 against a few of the strains. In the VIM panel, there was an occasional discrepancy in which UW-123 became less effective in the presence of the BLI, although this only happened in 3 of the 25 strains and only one of those was actually a significant (increase of ≥ 4 -fold in MIC). The IMP-1 panel had more of these anomalies with 5 of the 25 strains demonstrating this behavior and three of those being a significant decrease in efficacy. It is possible that this BLI has off-target interactions in some strains (such as inducing the expression of an SBL or efflux pump) that increase the resistance of the cell to UW-123 or β -lactams in general.

In assays with a small set of β -lactamase-producing bacteria from the Dmitrienko lab collection, UW-123 was found to behave synergistically with meropenem against most strains (Table 4.16). The only strain against which they did not show synergy was UWB75, and *E. coli* that produces both NDM-1 and CTX-M-15. This is consistent with the results from the Merck panel of NDM-1-producers, suggesting that UW-123 is highly susceptible to NDM-1 and does not reach its target in the cell in high concentrations.

4.4.3.2 Mode of action of UW-123

At the assayed concentrations, UW-123 is a bacteriostatic antibiotic at concentrations as high as 2x MIC that induces filamentation in *E. coli* cells. Other literature cephalosporins such as CXA-101 and ceftazidime have also been found to be bacteriostatic at 2x MIC, approaching but not attaining a 3-log unit reduction at 8 hr.¹¹⁶ In those studies, a bactericidal load of antibiotic was achieved at 8 hour

incubation with 4x MIC and only slightly surpassed the 3-log unit cutoff. This, in addition to the observation that when the killing curve is collected using OD measurements, the 4x MIC sample has much less growth at 24 hr than the 2x MIC sample (Figure 4.7) suggests that going to higher concentrations in the agar plate count experiments would likely yield a set of conditions under which UW-123 is bactericidal.

The morphological changes associated with inhibition of PBP 2 and PBP 3 in *E. coli* were confirmed using meropenem and aztreonam respectively. These experiments were carried out in the presence of 0.3M sucrose to increase the likelihood of observing delicate morphologies through osmotic stabilization. Consistent with the literature, inhibition of PBP 2 by meropenem created spheroplasts and inhibition of PBP 3 by aztreonam induced filamentation (Table 4.17).⁵³⁵ Cephalosporins, such as ceftazidime, have also been known to induce filamentation through PBP 3 inhibition.⁵³⁵ The filamentation of *E. coli* cells in the presence of UW-123 is indicative of a β -lactam antibiotic that inhibits subclass B3 PBPs such as PBP 3 in *E. coli*.

Studies to quantify the binding of UW-123 to the PBPs of *E. coli* and *P. aeruginosa* confirmed that UW-123 inhibits the B3 PBP, PBP3, most potently in each organism.

4.5 Future Work

The success of UW-123 as a more potent cephalosporin against MBL producing Gram negative pathogens suggests that this is an area of study that warrants further pursuit.

The data presented in section 4.3.1.1 suggest that the phenyl thioacids are moderate inhibitors of L1 and have some inhibitory activity against IMP-1 and VIM-2. The kinetic studies in this section operated under the assumption that NaOH only deprotonates the thioacid and does not cause any side reactions in DMSO. A thorough literature search has not yielded any studies that have been carried out under these conditions. To confirm whether or not the addition of NaOH is just deprotonating or changing the structure of the phenyl thioacids, structural studies (such as ¹HNMR or MS) would need to be performed on the reaction mixture over time as a decrease in colour intensity is observed.

The proposed mechanism for the 3'-acylthiocephalosporins suggests that upon hydrolysis, a rearrangement occurs that results in the release of a thioacid, a phenomenon that has yet to be confirmed. Reaction mixtures of either base hydrolyzed or enzyme hydrolyzed 3'-acylthiocephalosporin could be analyzed by ESI-MS to determine whether or not the thioacid is

released. This study could also be used to determine whether or not the enzyme active site contributes to the rearrangement. If a thioacid is released, further studies kinetic studies to better quantify the inhibition (IC_{50}) and to determine the mechanism by which inhibition occurs would be warranted.

Much like the phenyl thioacids, there is more kinetics work to be done with the pyridine thioacids: additional replicates of the IC_{50} s should be done to establish reproducibility and mechanistic studies should be pursued. Additionally, the Dmitrienko group has acquired an expression plasmid for His-tagged AmpC which should be used to generate pure AmpC protein and tested for inhibition with PMTC and PDTC to determine whether or not the inhibition of GC-1 is characteristic of Class C SBLs or if it is GC-1 specific.

The the pyridine thioacids were found to be potent β -lactamase inhibitors; however, they pose both solubility and reactivity problems in a clinical setting. Delivery of these compounds, particularly the dithioacid, PDTC, using a cephalosporin has been considered with a bis-PDTC-cephalosporin (Figure 4.15) having been synthesized.

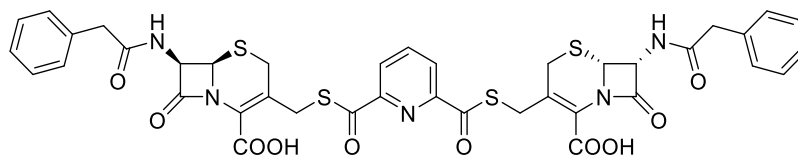


Figure 4.15 Bis-PDTC-cephalosporin

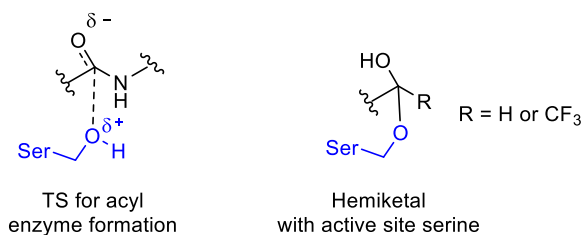
Some preliminary experiments have been conducted with this compound and it was found to be ineffective alone and in combination with avibactam (only for UWB 75, 93) against 5 MBL producing Gram negatives (UWB: 24, 26, 75, 78, 93). For each of these, the MIC of the bis-PDTC-cephalosporin was >128 mg/L alone and came down to 128 mg/L when in combination with 4 mg/L avibactam against UWB 93. It is likely that this compound is too large to adequately penetrate the outer cell membrane of Gram negative bacteria since it is 860 Da. Another strategy for delivery of these compounds may need to be considered such as attempting to deliver only the monothioacid, PMTC, which displays similar potency *in vitro* and only requires protection on one thioacid.

Chapter 5

Other β -Lactamase Inhibitors

5.1 Introduction

In the late 1960's and early 1970's a number of reports appeared in the literature concerning the inhibition of serine proteases by electrophilic carbonyl compounds such as aldehydes and trifluoromethylketones.⁵³⁶⁻⁵³⁸ It was argued the such inhibitors formed hemiacetal or hemiketal adducts with the enzyme active site serine hydroxyl group and that such adducts interacted particularly favourably with the enzyme active site since they were mimics of either the tetrahedral intermediate involved in the catalytic mechanism or mimics of the structurally related transition state involved in forming them. (Scheme 5.1) Hence, such compounds were referred to as transition state analogues.⁵³⁹⁻⁵⁴¹



Scheme 5.1 Comparison of hemiketal formation with TS and intermediate in acyl enzyme mechanism.

Inspired by these observations, this laboratory as well as several other academic and industrial research laboratories explored the concept of creating cyclobutanones that mimic β -lactam antibiotics as potential inhibitors of β -lactamases as well as potential antibiotics that bind to penicillin binding proteins (PBPs), in the late 1970's to mid 1980's (Figure 5.1).^{389,390,542-545}

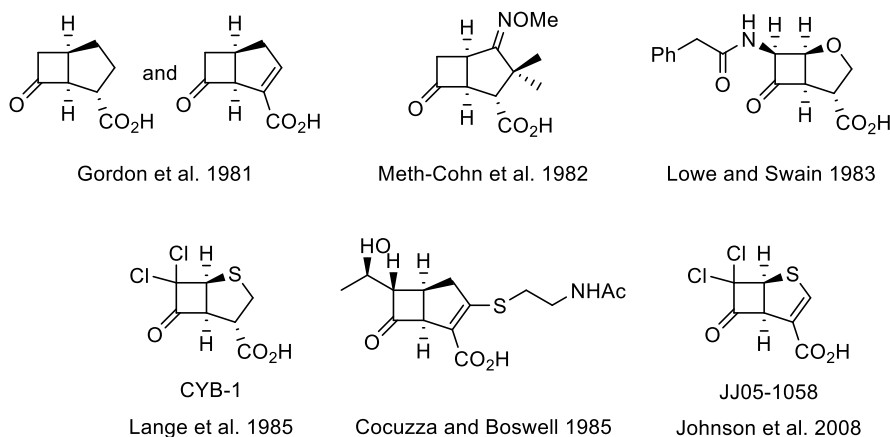


Figure 5.1 Examples of cyclobutanone mimics of β -lactam antibiotics.^{389,542–546}

In this group, racemic CYB-1: (1*S*,4*S*,5*S*)-7,7-dichloro-6-oxo-2-thiabicyclo[3.2.0]heptane-4-carboxylic acid (Figure 5.1) was prepared and tested as a potential inhibitor of the Class A SBL Bc-I from *Bacillus cereus*. This compound exhibited no SBL inhibition at concentrations up to 1 mM. Likewise, the cyclobutanones prepared in this context by others were not potent inhibitors of Class A SBLs nor good antibiotics. Since at that time potent SBL inhibitors such as clavulanic acid and penicillanic acid sulfones such as sulbactam (Figure 1.11) were coming into clinical use, all research concerning the cyclobutanones as SBL inhibitors was abandoned.

With the emergence of clinically important bacteria that produce new SBLs exhibiting carbapenemase activity and that are poorly inhibited by clavulanate and the penicillanic acid sulfones, as well as the carbapenem-hydrolyzing MBLs in the late 90's, this laboratory began to revisit the cyclobutanones as potential inhibitors of both the SBLs and the MBLs. Computational, spectroscopic and crystallographic studies in this group led to the realization that the cyclobutanone-type penicillin mimic **A** (Figure 5.2) had a strong preference for an endo conformation of the five-membered ring which forces the essential carboxylate group into a pseudo-axial orientation that is not favourable for binding to the active sites of β -lactamases.⁵⁴⁶

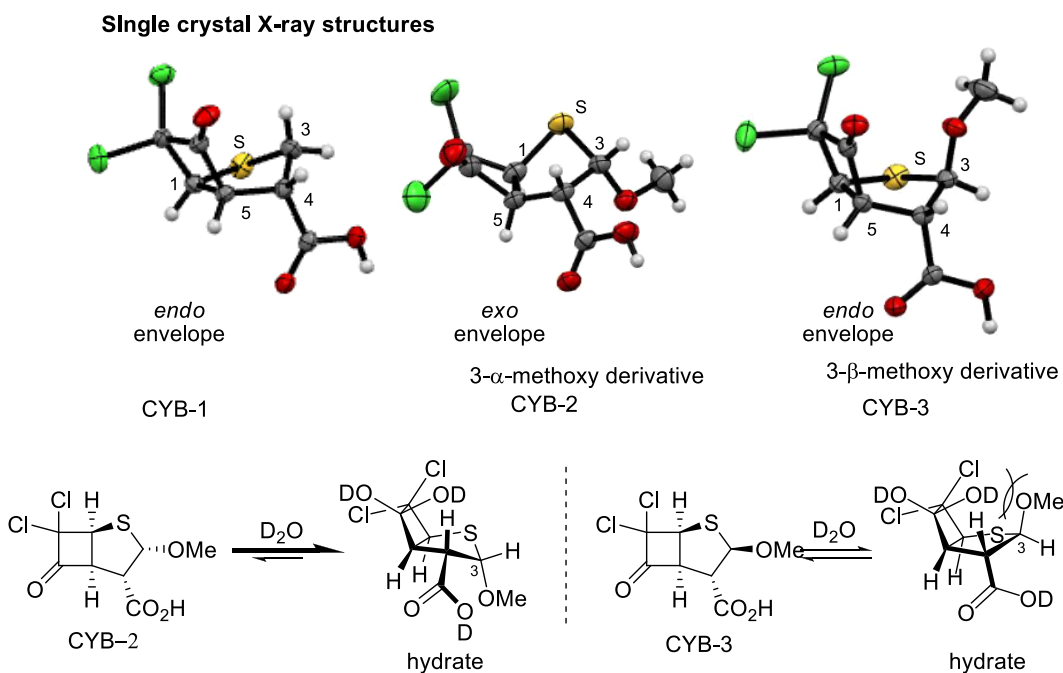
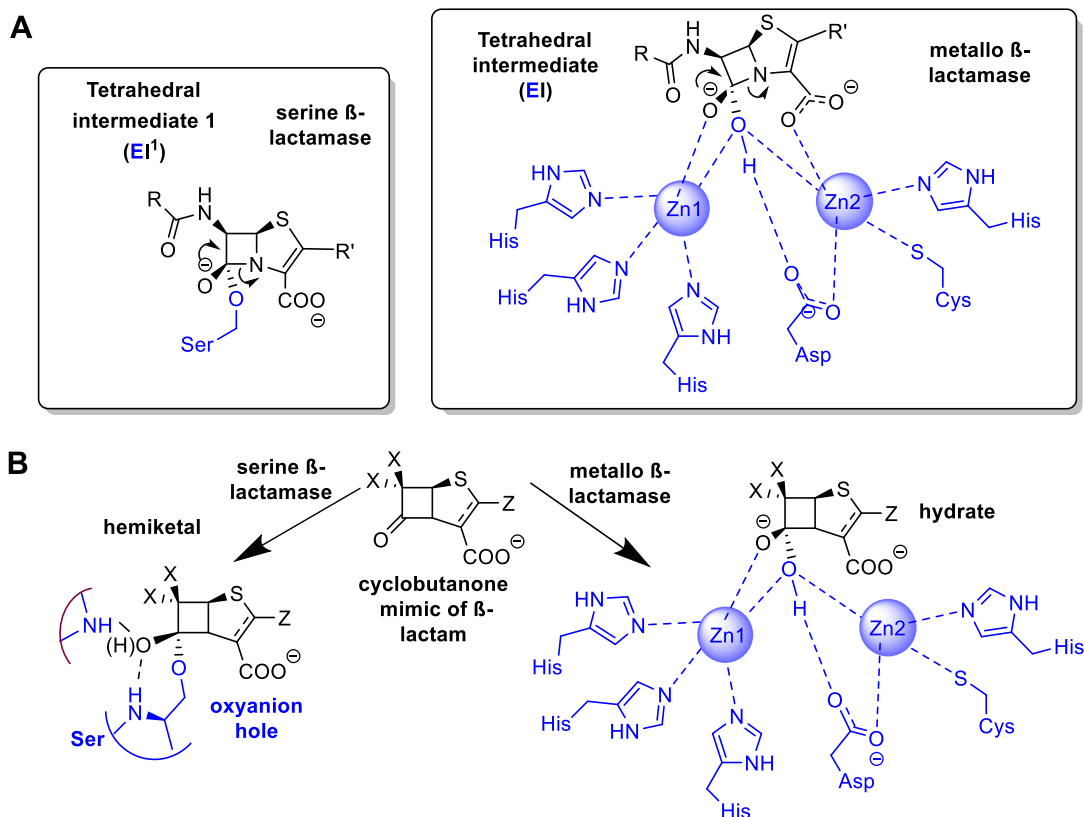


Figure 5.2 Conformations of C3-substituted cyclobutanones and the steric interactions of the hydrates. The colour-coded (Cl = green, S = yellow, O = red, C = grey, H = white) ball-and-stick ORTEP plots were generated using Mercury 3.7 software and are based on atomic coordinates from original X-ray crystallographic data generated by Dr. Abdeljalil Assoud in the Department of Chemistry X-ray crystallographic laboratory at the University of Waterloo.

It was also discovered that the preferred conformation of the five-membered ring could be controlled by introduction of a heteroatom in the α -orientation (Figure 5.2) which creates an anomeric effect between the heteroatom and the sulfur lone pairs of electrons leading to a preference for the *exo*-conformation and a spatial orientation of the carboxylate group that is more favourable for binding to β -lactamases. The compounds incorporating two chlorine atoms at C7, the C=O of the cyclobutanone were found to be prone to exist predominantly as a hydrate in water and as a hemiketal in methanol. This tendency was especially pronounced for those compounds that possess a heteroatom in the α -orientation adjacent to the sulfur atom (Figure 5.2).

It was envisaged that SBL inhibition would occur via hemiketal formation with the active site serine hydroxyl group of SBLs and MBL inhibition might arise through binding to the zinc ions as a hydrate as shown below in Scheme 5.2B.



Scheme 5.2 Parallels between the binding of penems and cyclobutanones to SBLs and MBLs. Proposed binding modes of tetrahedral intermediates in the β -lactamase-catalyzed hydrolysis of a penem (A) and the potential for cyclobutanones as broad-spectrum SBL and MBL inhibitors.

In a collaborative study with the protein X-ray crystallography group of Natalie Strynadka at UBC it was possible to demonstrate the formation of a hemiketal linkage with the active site serine hydroxyl group of the Class D SBL OXA-10 (Figure 5.3A) It was also possible to demonstrate that the cyclobutanone CYB-2 and the unsaturated cyclobutanone JJ05-1058 (Figure 5.1) exhibit significant inhibition of SBLs of Classes A, C and D and the MBL IMP-1.³⁹¹

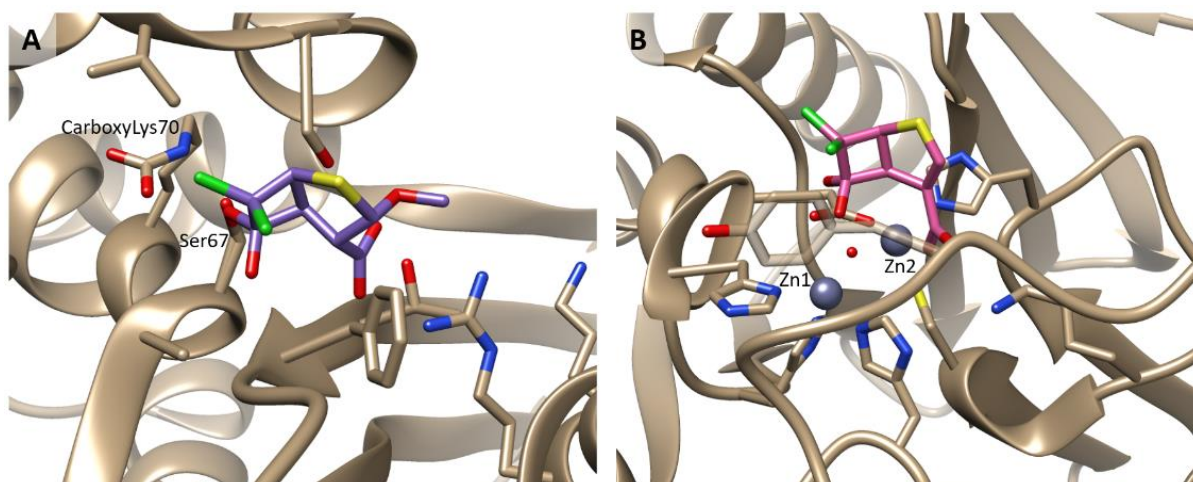


Figure 5.3 X-Ray crystal structures of cyclobutanones bound to β -lactamases. (A) CYB-2 bound to OXA-10 as a serine hemiketal. (B) JJ05-1058 bound to the B1 MBL SPM-1 as a hydrate. This figure was generated using Chimera v. 1.12 from the protein databank files 3LCE and 5NDB respectively)^{391,392}

More recently, in a collaborative study with colleagues Christopher Schofield at the University of Oxford and James Spencer at the University of Bristol in the UK, this group has been able to show that the unsaturated cyclobutanone JJ05-1058 binds in its hydrated form to the active site of the Class B1 MBL SPM-1 with the hydroxide ion that bridges between the two zinc ions retained rather than being displaced by one of the oxygen groups of the hydrate as had been speculated in earlier studies in this group (Figure 5.3B).³⁹²

The goal of the present study of cyclobutanone-type β -lactamase inhibitors was to expand the understanding of the spectrum of activity of the unsaturated cyclobutanone-type inhibitor JJ05-1058 as an inhibitor of clinically important SBLs and MBLs as well as to gain some initial insight into the possibility of binding to PBPs which might suggest possible antibacterial activity.

5.2 Methods.

5.2.1 β -Lactamase Enzyme Kinetics

One of the most active cyclobutanone analogues from the Johnson 2010 paper seen in Figure 5.1 was tested against a wider array of β -lactamases. Solid JJ05-1058 (compound 5)³⁹¹ was provided by

chemists in the Dmitrienko lab, and the structure was confirmed using ^1H NMR, ^{13}C NMR, and ESI-MS. The solid was dissolved in DMSO to make a 50 mM stock which was stored at $-20\text{ }^\circ\text{C}$.

Since previous work has been done on these compounds, screening of numerous cyclobutanone analogs was forgone and JJ05-1058 was directly used for IC_{50} determinations. All β -lactamases used in this thesis were tested using the conditions detailed in Table 5.1. Enzyme stocks for class A, B, and C β -lactamases were prepared in 50 mM HEPES pH 7.2 supplemented with 50 $\mu\text{g}/\text{mL}$ BSA and 0.01 % Triton X-100 whereas the stocks for class D enzymes were prepared in 100 mM NaPi, 2.1 mg/mL NaHCO_3 , pH 7.0 supplemented with 50 $\mu\text{g}/\text{mL}$ BSA and 0.01 % Triton X-100.

Table 5.1 Kinetic parameters and conditions for inhibitor screening.

Enzyme	Molecular class	Substrate	K_M (μM)	Enzyme Conc. in assay	[Substrate] in assay (μM)
CTX-M-15	A	NC	17.3 ± 0.8	150 pM	20
KPC-2	A	NC	8.1 ± 0.2^{453}	211 pM	8
IMP-1	B1	NC	3.5 ± 0.2^{453}	186 pM	3.5
NDM-1	B1	NC	0.88 ± 0.06^{453}	620 pM	1
SPM-1	B1	NC	1.2 ± 0.1^{453}	8.17 nM	1
VIM-1	B1	NC	19 ± 1	16.4 nM	30
VIM-2	B1	NC	13.9 ± 0.3^{453}	313 pM	15
SFH-1	B2	UW-58	220 ± 10	1.86 nM	100
L1	B3	NC	5.5 ± 0.5^{453}	637 pM	5
GC-1	C	NC	15.4 ± 0.8^{453}	41 pM	15
OXA-23	D	NC	51 ± 2	620 pM	100
OXA-48	D	NC	81 ± 2	79 pM	80

Literature work was performed in the absence of detergent, so IC_{50} determinations here were done both in the presence and absence of Triton X-100. Two preincubation times were tested (10 min and 30 min) to compare with other inhibitors using the standard 10 min pre-incubation as well as the literature values which were acquired with 30 min pre-incubation. The enzyme mix was incubated with either control DMSO or 7-14 dilutions of JJ05-1058 made in DMSO in triplicate for 10 or 30 min at $30\text{ }^\circ\text{C}$ in flat bottomed 96-well plates (Greiner, Monroe, NC) prior to addition to nitrocefin or UW-58 as appropriate to initiate the reaction. The reaction was shaken for 5 sec then monitored at 482 nm (NC) or 534 nm (UW-58) every 5-7 sec for 5 min (30 min for SFH-1) using a SpectraMax 190 (Molecular Devices, Sunnyvale, CA). Initial rates were determined using SoftMax 6.0

(Molecular Devices, Sunnyvale, CA) then normalized and fitted to Equation 3.1 using GraphPad Prism version 5.00 for Windows (GraphPad Software, San Diego, CA) by non-linear least squares regression. The concentration of DMSO present in the final assay mixture was kept under 2 % which set an upper limit for JJ05-1058 concentrations at 1000 μ M. Due to this upper limit, the plateau at the high inhibitor concentration end was not always present or well defined.

5.2.2 Penicillin Binding Protein Binding Assay

Preparation of PBP Containing Membrane Fragments

Procedures for PBP membrane preparation and Bocillin binding assay were adapted from Moyá et al.¹¹⁶ *P. aeruginosa* PA01 cells were obtained from Dr. Stephen Seah of the University of Guelph. An overnight culture of PA01 cells was prepared by inoculating two tubes containing 2 mL Luria Bertani (LB) broth with scrapings from a glycerol stock and shaking them at 250 rpm, 37 °C, overnight (16-20 hr). The 4 mL of PA01 overnight culture were used to inoculate 500 mL LB broth which was then incubated at 37 °C, shaking at 185 rpm until the OD₆₀₀ reached 1 (~5 hr). Cells were then centrifuged in a JA-10 rotor at 4400 xg for 10 min at 4 °C and the supernatant was discarded. The pellets were washed in 150 mL of Buffer A (20 mM KH₂PO₄, 140 mM NaCl, pH 7.5) then centrifuged again at 4400 xg for 10 min at 4 °C and the supernatant was discarded. The cells in the pellet were then lysed using a large probe on a Heat Systems Ultrasonic processor W-255 sonicator set to 50 % cycle and 50 % power 5 times for 30 sec each with 1 min rest on ice between bursts. The lysate was then centrifuged in a JA-25.5 rotor at 12 000 xg for 10 min at 4 °C and the supernatant and pellets were retained separately and frozen on dry ice then stored at -80 °C. The supernatant was thawed and transferred into Oak Ridge polypropylene tubes with a nylon screw cap for use in a T-1270 rotor of a Sorvall WX100 Ultra centrifuge. Samples were centrifuged at 150 000 xg for 1 h at 4 °C and the supernatant was discarded. The pellets were resuspended in 1 mL Buffer A and pooled. Total membrane protein concentration was determined by Bradford assay as described in 2.2. The *P. aeruginosa* PBP membrane preparation was then aliquoted, frozen on dry ice, and stored at -80 °C.

PBP Competitive Binding Assay

Two-fold dilutions of JJ05-1058 ranging from 128 mg/L to 0.0039 mg/L were prepared in Buffer B (20 mM NaPi, 140 mM NaCl, pH 7.5) and DMSO such that the final concentration of DMSO in each sample was 1.28 % while aliquots of the PBP membrane preparation were thawed on ice. The PBP membrane preparation (10 μ L) was incubated with a 3x concentrated stock of JJ05-1058 (5 μ L) for 30

min at 37 °C after vortexing. In a darkened room, 5 µL of the fluorescent penicillin, Bocillin, was added and returned to the incubator for 30 min at 37 °C after vortexing. Samples were prepared for SDS-PAGE by adding 5 µL of 5x SDS-PAGE Buffer to each sample, vortexing, boiling for 3 min before spinning down any condensation. Each sample (20 µL) as well as 5 µL of low molecular weight marker was loaded onto a 10 % SDS-PAGE gel which were run at 80 V in the dark until the blue dye front had reached the bottom of the gel. Gels were uncased directly onto a Pharos (BioRad, Hercules, CA) gel reading system and visualized at $\lambda_{\text{ex}}= 488 \text{ nm}$ and $\lambda_{\text{em}}= 530 \text{ nm}$. Band densities were determined using Image Lab software (BioRad, Hercules, CA) and were normalized and fitted to Equation 3.1 using GraphPad Prism 5.00 for Windows (GraphPad Software, San Diego, CA) with the added constraint that the bottom plateau is set to 0 since it is not well defined. Gels were then stained with Coomassie Blue R-250 (BioRad, Hercules, CA) containing stain overnight then destained with 50 % methanol, 10 % acetic acid in water. Coomassie stained gels were visualized on a Gel Doc EZ Imager (BioRad, Hercules, CA).

5.3 Results

5.3.1 Inhibition of β -Lactamases

The cyclobutanone JJ05-1058, was screened against 12 β -lactamases for inhibitory activity using a standardized IC_{50} assay. The effects of pre-incubation time and presence of detergent are best demonstrated by the graphs used to determine the IC_{50} s in Figure 5.4 for the SBLs and Figure 5.5 for the MBLs.

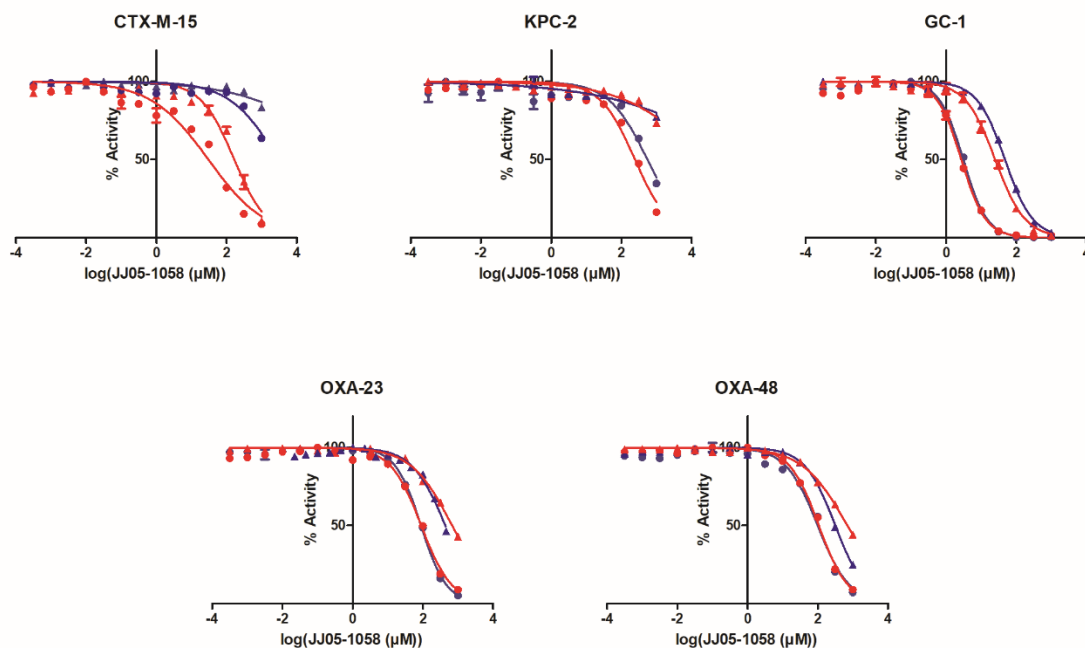


Figure 5.4 Inhibition of SBLs by JJ05-1058. Assays performed in the presence of 0.01 % Triton X-100 are displayed in blue while those performed in the absence of Triton X-100 are displayed in red; preincubation times of 10 min (▲) and 30 min (●) are shown. The graphs in this figure were generated using GraphPad Prism v. 5.03.

From the graphs in Figure 5.4 it can be seen that the inhibition of KPC-2, GC-1, OXA-23, and OXA-48 by JJ05-1058 depends heavily on pre-incubation time with longer incubation times resulting in more potent inhibition whereas the presence or absence of detergent makes little difference. This trend is indicative of slow-binding that requires more than 10 min to achieve steady state. From these data, it cannot be conclusively stated whether or not steady state has even been achieved after 30 min pre-incubation. CTX-M-15 shows a similar trend as the other SBLs with respect to longer incubation times resulting in more inhibition but also shows a significant dependence on detergent which was not observed in other SBLs. In the presence of 0.01 % Triton X-100 (blue curves), inhibition is only observed at the highest concentrations for CTX-M-15, but by excluding Triton X-100 from the mix, the IC_{50} was brought within the tested concentration range.

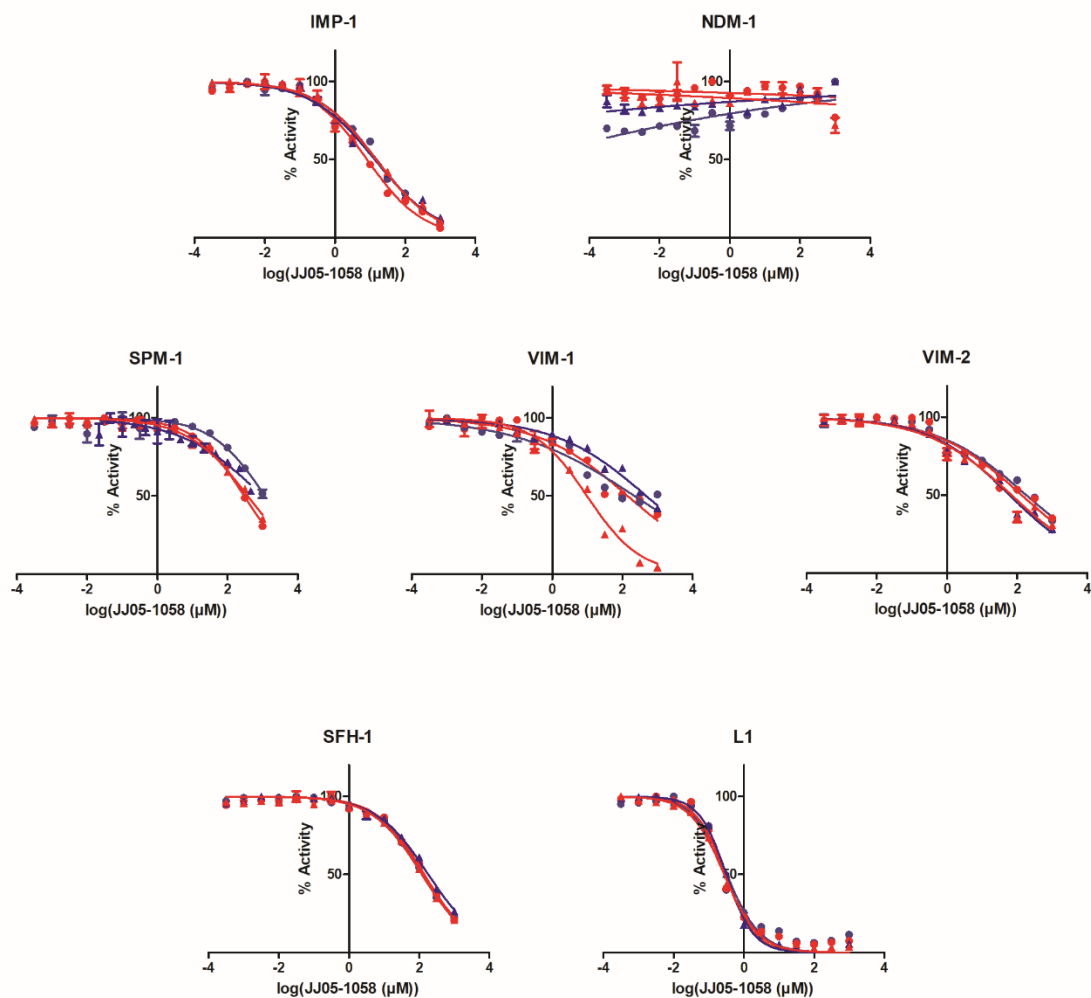


Figure 5.5 Inhibition of MBLs by JJ05-1058. Assays performed in the presence of 0.01 % Triton X-100 are displayed in blue while those performed in the absence of Triton X-100 are displayed in red; preincubation times of 10 min (▲) and 30 min (●) are shown. The graphs in this figure were generated using GraphPad Prism v. 5.03.

Unlike the SBLs, the inhibition of the MBLs by JJ05-1058 is largely unchanged regardless of both pre-incubation time and detergent. The major outlier in this group appears to be NDM-1 which is not inhibited by JJ05-1058 under any conditions, even at the highest concentrations. The values of the IC₅₀s determined from the graphs above are listed in Table 5.2.

Table 5.2 IC₅₀ of β -Lactamases with JJ05-1058 with variable pre-incubation times and detergent concentrations.

β -Lactamase	Class	IC ₅₀ (μ M)			
		0.01% Triton X-100		no Triton X-100	
		10 min	30 min	10 min	30 min
CTX-M-15	A	NI	>1000	170 \pm 40	31 \pm 10
KPC-2	A	NI	560 \pm 210	NI	250 \pm 50
IMP-1	B1	14 \pm 3	15 \pm 3	15 \pm 3	8.2 \pm 2.1
NDM-1	B1	NI	NI	NI	NI
SPM-1	B1	990 \pm 960	1200 \pm 800	380 \pm 80	300 \pm 50
VIM-1	B1	480 \pm 140	220 \pm 150	10 \pm 3	210 \pm 70
VIM-2	B1	60 \pm 20	180 \pm 70	70 \pm 30	140 \pm 60
SFH-1	B2	210 \pm 20	130 \pm 10	120 \pm 20	140 \pm 20
L1	B3	0.32 \pm 0.03	0.33 \pm 0.08	0.28 \pm 0.03	0.29 \pm 0.05
GC-1	C	48 \pm 3	3.1 \pm 0.2	25 \pm 3	2.7 \pm 0.4
OXA-23	D	440 \pm 70	88 \pm 7	680 \pm 70	90 \pm 12
OXA-48	D	320 \pm 30	100 \pm 17	700 \pm 70	108 \pm 9

NI – not inhibited

From the data in Table 5.2, it is evident that L1 is the most potently inhibited by JJ05-1058 of the assayed β -lactamases and that NDM-1 is the least susceptible. IMP-1 is generally 10 times more potently inhibited by JJ05-1058 than other B1 MBLs, and this discrepancy along with the behavior of NDM-1 suggests that broad generalizations about the efficacy of this compound against any one class based on only a few enzymes may be erroneous. With that in mind, the class A enzymes that have been assayed were not very susceptible to inhibition by JJ05-1058 while the class C enzyme, GC-1, was reasonably susceptible although the same may not be true for other class A and C SBLs. The two assayed class D SBLs are very consistent with each other, demonstrating moderate inhibition at 30 min pre-incubation. Many of the larger IC₅₀ values in the table above have error values that greatly exceed 10 %. The relatively large error values are due to a lack of data points defining the lower plateau leading to increased uncertainty in the curve fitting. The lack of points at concentrations exceeding 1000 μ M is due to the solubility limits of JJ05-1058 in 2 % DMSO.

Previously, a trend with respect to incubation time in which inhibition increased with time, was observed from the graphs of SBLs; however, some MBLs (VIM-1 and VIM-2) show an opposite trend. Additionally, a more subtle trend with respect to detergent can be observed in the values of the IC₅₀s. Generally, inhibition of both SBLs and MBLs is improved or not significantly changed when Triton X-100 is left out of the mix with the exception of the Class D SBLs. Both OXA-23 and OXA-

48 have lower IC_{50} values, indicating more potent inhibition by JJ05-1058, when in the presence of 0.01% Triton X-100; however, this effect is most pronounced at 10 min pre-incubation.

5.3.2 Competitive binding to Penicillin binding proteins

The structural similarity of penicillins and cyclobutanones suggest that the cyclobutanones may also bind to the active site of PBPs. This binding was assayed by incubating membrane fragments from *P. aeruginosa* PA01 with JJ05-1058 followed by Bocillin, a fluorescent penicillin. This method is advantageous as it allows selective assaying of an array of related proteins at physiological relative concentrations without purifying 6-7 individual membrane proteins. The gels from this assay are first read using the fluorescence of Bocillin (Figure 5.6A) then stained with Coomassie and read again (Figure 5.6B).

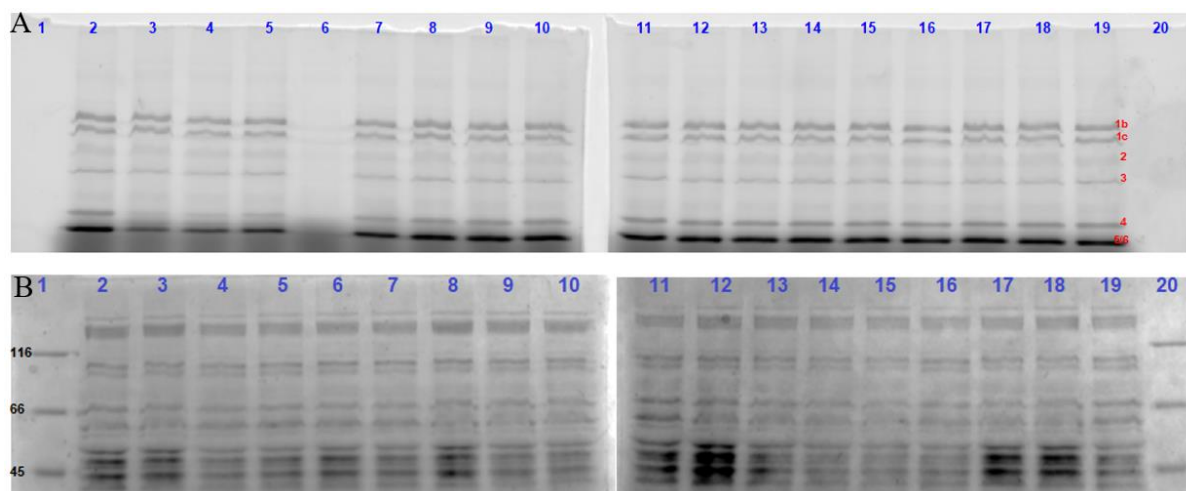


Figure 5.6 SDS-PAGE of JJ05-1058 bound to *P. aeruginosa* PBPs competing with Bocillin. Gel A is the Bocillin fluorescent read, Gel B is the Coomassie stained read. The lanes correspond to the following concentrations of JJ05-1058: 2) 0 mg/L; 3) 128 mg/L; 4) 64 mg/L; 5) 32 mg/L; 6) 16 mg/L – mistake when pipetting Bocillin; 7) 8 mg/L; 8) 4 mg/L; 9) 2 mg/L; 10) 1 mg/L; 11) 0.5 mg/L; 12) 0.25 mg/L; 13) 0.125 mg/L; 14) 0.0625 mg/L; 15) 0.0313 mg/L; 16) 0.0156 mg/L; 17) 0.0078 mg/L; 18) 0.0039 mg/L; 19) 0 mg/L. Lanes 1 and 20 contained low molecular weight marker.

The visualization of the fluorescence shows the Bocillin covalently bound to the various PBPs, and a decrease in intensity of any band relative to the control is indicative of JJ05-1058 competing for the active site of that PBP. As can be seen in Figure 5.6A, JJ05-1058 binds to PBP 4 and PBP 5/6 at high

concentrations. Graphing the relative intensities of the bands gives a clearer picture of the binding (Figure 5.7).

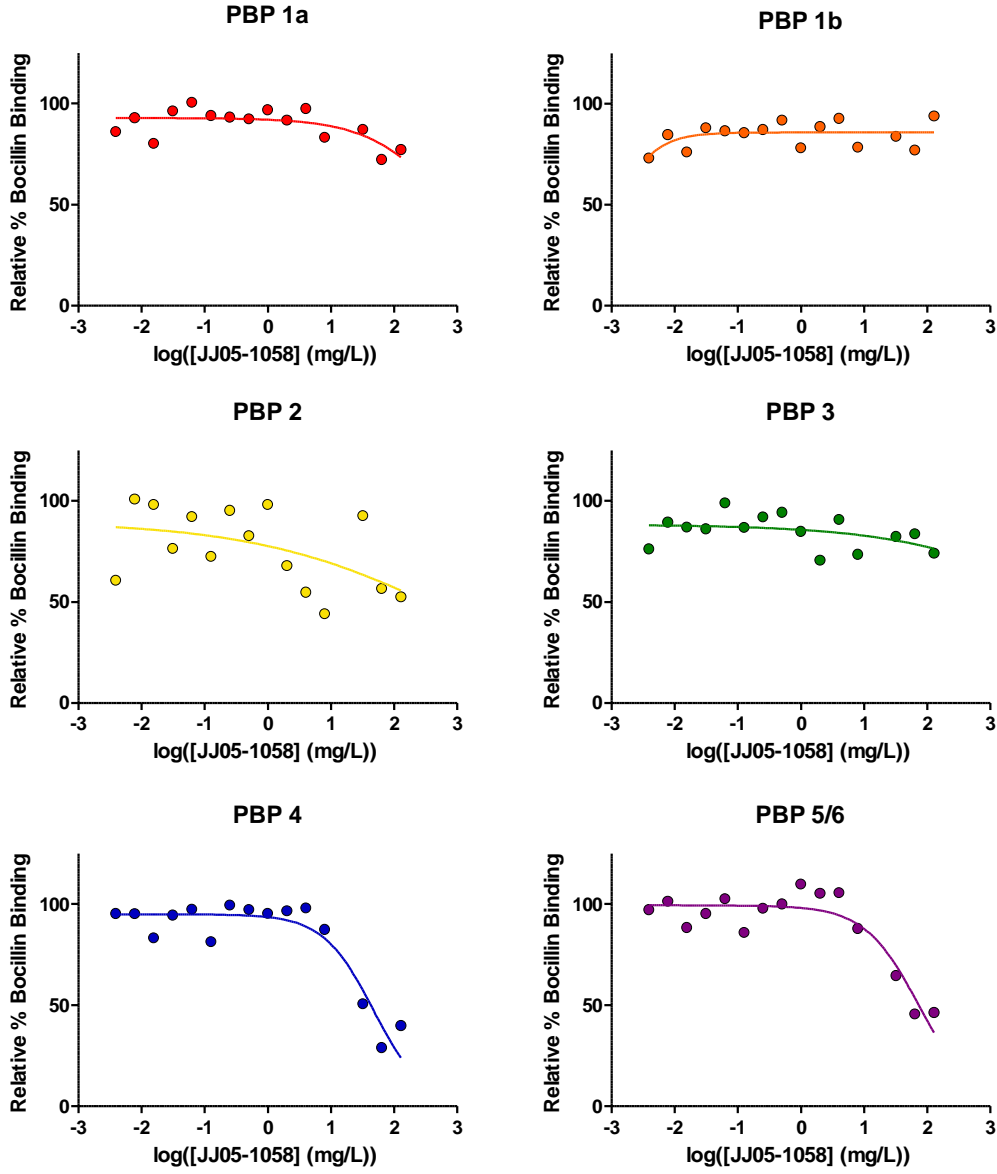


Figure 5.7 JJ05-1058 competition for PBP binding with Bocillin. The graphs in this figure were generated using GraphPad Prism v. 5.03.

Again, the binding of JJ05-1058 to PBP 4 and PBP 5/6 is evident at high concentrations. The large amount of scatter in the graph of PBP 2 (Figure 5.7) is due to the low intensity of the band on the SDS PAGE gel (Figure 5.6A). Upon curve fitting, the IC₅₀ values in Table 5.3 were determined and showed that JJ05-1058 binds best to PBP 4 with an IC₅₀ of 47.3 mg/L.

Table 5.3 IC₅₀s of JJ05-1058 competing with Bocillin for binding to *P. aeruginosa* PBPs.

PBP	1a	1b	2	3	4	5/6
IC ₅₀ (mg/L)	>128	>128	>128	>128	47.3	74.3

When the PBP binding IC₅₀s are converted into molar units, it is 198 μM for PBP 4 and 311 μM for PBP 5/6 making the binding comparable to that of many of the β-lactamases. The PBPs inhibited by JJ05-1058 are all non-essential LMM PBPs, so any potentiation of meropenem observed in bacterial experiments would be the result of β-lactamase inhibition rather than synergistic PBP inhibition.

5.4 Discussion

Three of the IC₅₀s performed using the cyclobutanones were repeats of those presented by Johnson et al.: IMP-1, KPC-2, and GC-1 pre-incubated for 30 min in the absence of Triton X-100.³⁹¹ Comparison of the values determined in this work to the literature are presented in Table 5.4 and shows that the values for GC-1 were reproducible; however, those for KPC-2 and IMP-1 are not. Since the time that these values were initially determined, each of these enzyme stocks has been re-made and the storage conditions have been changed to prolong their lifetime. When the original values were determined, enzyme stocks were being stored on ice at 4 °C in buffer and since then we have changed the storage conditions to -20 °C in 50 % glycerol. Additionally, the KPC-2 and IMP-1 stocks that were used in the Johnson paper were purified from a different expression vector that did not include a His-tag. The slight differences in sequence and storage between the literature and this study should not be significant enough to cause the order of magnitude difference between these IC₅₀ values. It is possible that differences in the preparation and purity of these two batches could cause differences.

Table 5.4 Comparison of literature values for JJ05-1058 IC₅₀s to those presented in this study.

	IC ₅₀ (μM)		
	KPC-2	IMP-1	GC-1
Johnson et al.	26 ± 2	213 ± 21	4.5 ± 0.3
This study	250 ± 50	8.2 ± 2.1	2.7 ± 0.4

The effects of two variables on IC₅₀ were examined in this study: pre-incubation time and presence of detergent. Detergent is generally used in enzyme kinetics to reduce the probability of non-specific inhibition by preventing aggregate formation.⁵⁴⁷⁻⁵⁴⁹ JJ05-1058 inhibition was significantly impaired by the presence of 0.01 % Triton X-100 against CTX-M-15, KPC-2, SPM-1, and to a lesser extent, L1 and GC-1. Inhibition of IMP-1 and VIM-2 was mostly unaffected by the presence or absence Triton X-100 while SFH-1 and VIM-1 were only affected when pre-incubated for 10 min. For SFH-1, the IC₅₀ values suggest that the presence of Triton X-100 slowed the achievement of steady state; however, it is more likely that when incubated for 10 min in the absence of Triton X-100 some non-specific binding occurred. Contrary to expectation, OXA-23 and OXA-48 were slightly more inhibited in the presence of Triton X-100 although with longer pre-incubation, this difference falls within the uncertainty of the values. It is also possible that a slight error occurred in pipetting and that additional replicates could change this observation as it is very slight.

The time variable of JJ05-1058 inhibition produced much more consistent trends: in the majority of cases, longer pre-incubation resulted in more potent inhibition. This observation is indicative of time dependence in which steady-state takes more than 10 min to achieve. IMP-1, SPM-1, SFH-1, and L1 did not demonstrate time dependence beyond the uncertainty of the IC₅₀ values. The VIM β-lactamases did yield higher IC₅₀ values with longer incubation times; however, there is a discrepancy in the control rates between the 10 min and 30 min incubation times in which the 30 min control rates are half again as fast as the 10 min control rates. If the faster turnover is a result of faster off rates (k_{off}), then the inhibitor could also have higher off rates due to the structural similarity between JJ05-1058 and substrates for β-lactamases. A higher off rate would result in a shorter EI complex half-life and consequently higher IC₅₀s.

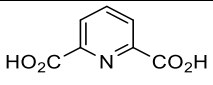
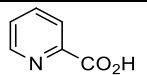
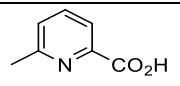
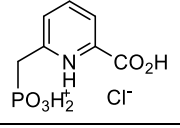
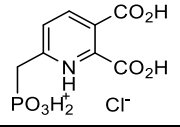
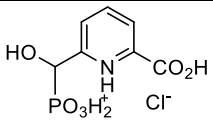
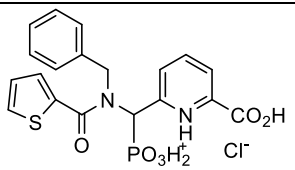
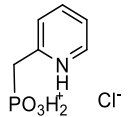
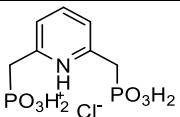
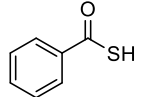
In addition to inhibiting β-lactamases, JJ05-1058 also inhibits low molecular weight PBPs from *P. aeruginosa*. This dual mode of action suggests that compounds of this family should behave synergistically with β-lactam antibiotics to kill β-lactamase producing bacteria.

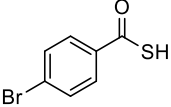
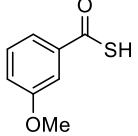
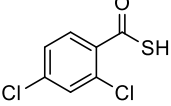
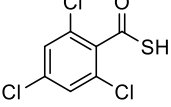
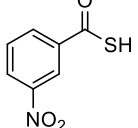
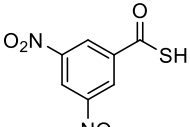
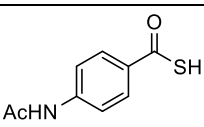
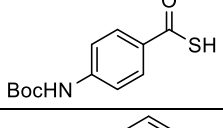
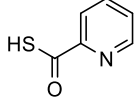
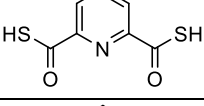
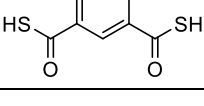
5.5 Future Work

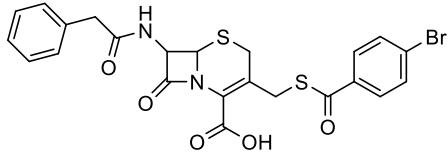
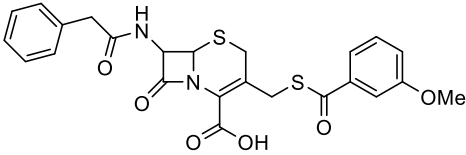
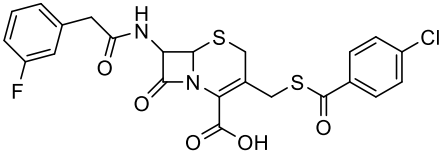
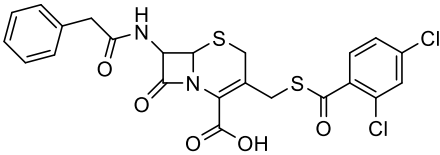
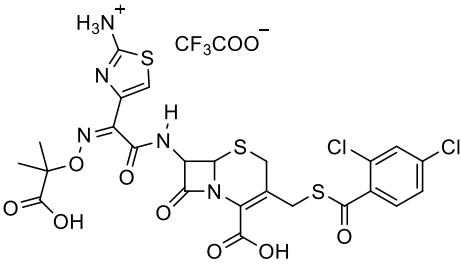
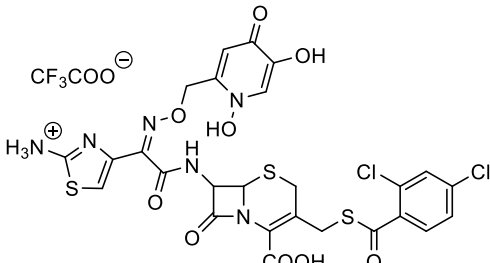
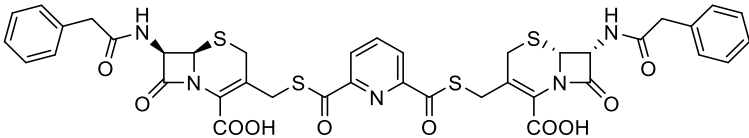
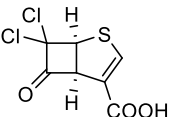
The cyclobutanone JJ05-1058 has been screened against 12 β -lactamases in this study; however, the IC_{50} values presented here are from a single experiment due to time constraints. Additional replicates of the experiments that demonstrated inhibition should be obtained to solidify trends and get more accurate values. Since the data suggests the inhibition of cyclobutanones is time dependent, it should be further characterized using methods similar to those described in 1113.2.1.3. The hypothesis regarding higher off rates for VIM β -lactamases at longer pre-incubation times could be tested by performing the experiment described in 3.2.1.3 using both the 10 min pre-heating described as well as a 30 min pre-heating to ascertain whether or not a difference in k_{off} and $t_{1/2}$ is observed. To date, only the only cyclobutanones that have been synthesized and tested are derived from the core structure of a penicillin.³⁸⁸

Appendix A

Structures of β -Lactamase Inhibitors

Compound Identifier	Structure	Laboratory Codes	Molecular Weight (g/mol)
DPA		Commercial: 2,6-Pyridinedicarboxylic acid	167.12
PA		Commercial: 2-Pyridinecarboxylic acid	123.11
6-MPA		Commercial: 6-Methylpyridine-2-carboxylic acid	137.14
PMPC-1		MB9801-60B AK10025-027 AK12012-025	253.57
PMPC-2		MS-213 AK12012-115	297.58
PMPC-3		AK10025-089	269.57
PMPC-4		AK12012-023B	468.84
PMP		AK12012-162 AK12021-001	209.57
DPMP		AK12021-005	303.57
TBA		Commercial	138.18

TA-1		AD-4Br-TA	217.08
TA-2		AD-3OMe-TA	168.21
TA-3		AD-DCI-TA	207.07
TA-4		AD-TCI-TA	241.51
TA-5		AD-3NO2-TA	183.18
TA-6		AD-DN-TA	228.18
TA-7		AD-4NHAc-TA	195.24
TA-8		AD-4NHBoc-TA	253.32
PMTC		PMTA	139.17
PDTC		PDTA	199.24
I-PDTC		I-PDTA	198.25

TE-1		AD-4Br-TE	547.44
TE-2		AD-3OMe-TE	498.57
TE-3		AD-3F4Cl-TE	520.97
TE-4		AD-2,4DCl-TE	537.43
TE-5		AD-109, AD-10012-109	788.58
UW-123		AD-TA-123, WPI282	841.60
bis-PDTC- ceph			859.96
JJ05-1058		JJ966, JJ930, JJ1058, JJ958, unsat DCCB	239.07

Appendix B

Statistical Methods for IC₅₀ Averages

Since we are working with values that have an associated uncertainty (the standard error), each value should contribute differently to the mean such that values with lower uncertainties are more strongly weighted. In order to do this, a weighted mean is used on the log (IC₅₀) values so as to not change the nature of the relationship between the IC₅₀ and the error.*

$$\bar{p} = \frac{\sum_{i=1}^N p_i * w_i}{\sum_{i=1}^N w_i}$$

Where p_i is a property (in this case, each log(IC₅₀) value) and w_i is the weight as defined by $w_i = \frac{1}{u_i^2}$ where u_i is the log(SE) associated with each log(IC₅₀) value. This makes Eq. 1 the same as the weighted mean equation in the Jones paper (except I used the log values of the IC₅₀ and SE).

In order to deal with the uncertainty of the weighted mean, the relative weights must be calculated

$$\bar{w}_i = \frac{w_i}{\sum_{i=1}^N w_i}$$

From this, the uncertainty of the weighted mean, $u(\bar{p})$ can be determined:

$$u(\bar{p}) = \sqrt{\frac{1}{N-1} \sum_{i=1}^N (p_i - \bar{p})^2 * \bar{w}_i}$$

This gives the SE of the weighted mean, so we can convert this into the 95% confidence interval using the t-table equation:

$$\bar{x} \pm t * u(\bar{p})$$

From this point the values for the mean and the 95% confidence interval that were calculated could be converted back into the conventional form by taking the antilog of the values.⁵⁵⁰

Appendix C

Clinical Isolates and Control Strains

UWB	Organism	Isolate Identifier	Known Resistance	Source
11	<i>K. pneumoniae</i>		KPC-3	Dr. Dylan Pillai
16	<i>K. pneumoniae</i>		KPC-2	Dr. Dylan Pillai
24	<i>P. putida</i>	C10	VIM-2	Dr. Johann Pitout
25	<i>P. aeruginosa</i>	C7	VIM-2	Dr. Johann Pitout
26	<i>S. maltophilia</i>	5563	L1, L2	Dr. Dylan Pillai
27	<i>P. aeruginosa</i>	5564		Dr. Dylan Pillai
28	<i>P. aeruginosa</i>	5566		Dr. Dylan Pillai
29	<i>S. maltophilia</i>	5568		Dr. Dylan Pillai
31	<i>P. aeruginosa</i>	5785	IMP-5 like	Dr. Dylan Pillai
33	<i>S. maltophilia</i>	6069	L1, L2	Dr. Dylan Pillai
34	<i>S. maltophilia</i>	6081	L1, L2	Dr. Dylan Pillai
35	<i>P. aeruginosa</i>	6225		Dr. Dylan Pillai
39	<i>S. maltophilia</i>	6487	L1, L2	Dr. Dylan Pillai
43	<i>S. maltophilia</i>	6773	L1, L2	Dr. Dylan Pillai
44	<i>S. maltophilia</i>	6776	L1, L2	Dr. Dylan Pillai
45	<i>S. maltophilia</i>	6779	L1, L2	Dr. Dylan Pillai
46	<i>S. maltophilia</i>	6781	L1, L2	Dr. Dylan Pillai
48	<i>S. maltophilia</i>	6924	L2	Dr. Dylan Pillai
49	<i>S. maltophilia</i>	6952	L2	Dr. Dylan Pillai
56	<i>K. pneumoniae</i>	A7 AmpC ACC1	CMY-2	Dr. Johann Pitout
57	<i>E. coli</i>	A9 AmpC	CMY-2	Dr. Johann Pitout
59	<i>E. coli</i>	1175		Dr. Karen Pike
60	<i>K. pneumoniae</i>			Dr. Karen Pike
62	<i>P. aeruginosa</i>	27853		ATCC ⁵⁵¹
75	<i>E. coli</i>	MH1	NDM-1, CTX-M-15	Dr. Johann Pitout
78	<i>P. aeruginosa</i>	Vim I-1	VIM-2	Dr. Johann Pitout
82	<i>K. pneumoniae</i>	KpSA01	VIM-1	Dr. Dylan Pillai
83	<i>K. pneumoniae</i>	Kp3VIM	VIM-1	Dr. Dylan Pillai
86	<i>K. pneumoniae</i>	Kp5OXA	OXA-48	Dr. Dylan Pillai
87	<i>K. pneumoniae</i>	Kp9OXA	OXA-48, CTX-M-15	Dr. Dylan Pillai
88	<i>K. pneumoniae</i>	KpCG02	KPC-2, SHV-12	Dr. Dylan Pillai

91	<i>E. coli</i>	MH01	NDM-1, CTX-M type 1	Dr. Dylan Pillai
93	<i>E. coli</i>	Ec7IMP	IMP-1, CTX-M-15	Dr. Dylan Pillai
94	<i>A. baumannii</i>	AB01	OXA-23	Dr. Dylan Pillai
95	<i>A. baumannii</i>	AB02	OXA-23	Dr. Dylan Pillai
96	<i>P. aeruginosa</i>	PA01		Dr. Stephen Seah
102	<i>E. coli</i>	25922		ATCC ⁵⁵²
116	<i>K. pneumoniae</i>	L3142005	NDM-1	Dr. Allison McGeer

Appendix D

K_i Graphs of DPA, PMPC-3, and PMPC-4

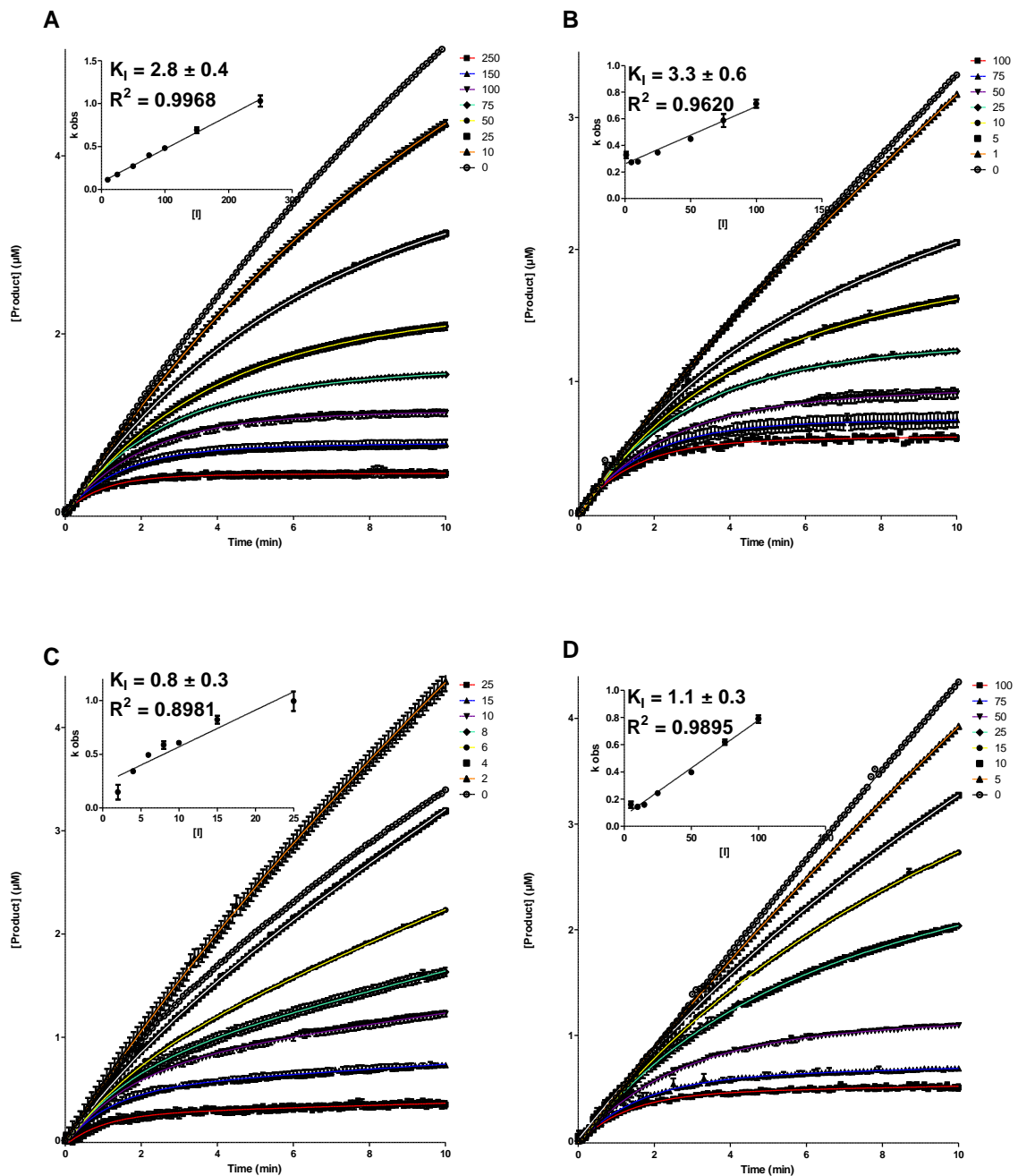


Figure 5.8 Time Dependent K_i graphs for DPA against representative MBLs IMP-1 (A), NDM-1 (B), VIM-2 (C), and L1 (D).

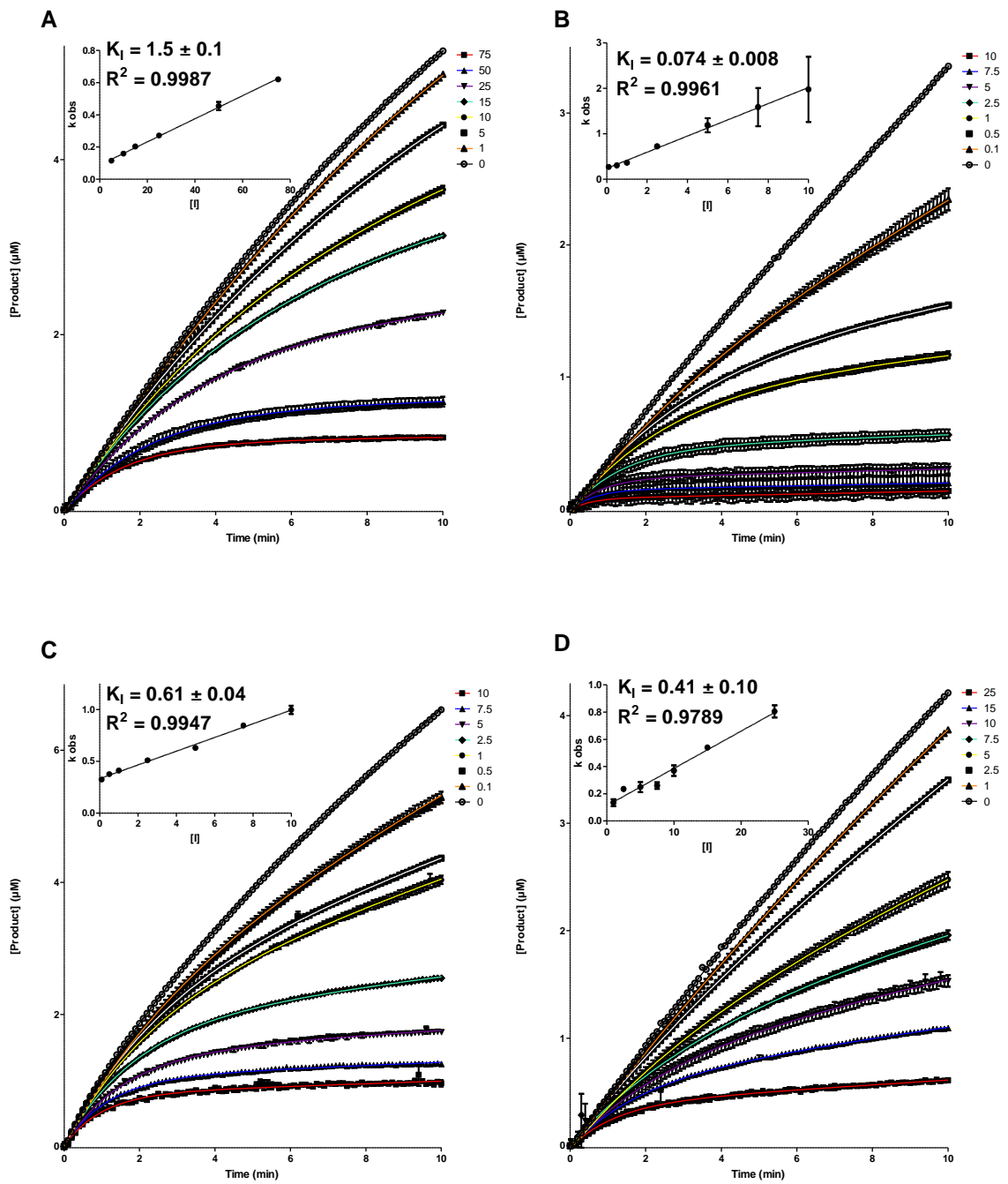


Figure 5.9 Time Dependent K_1 graphs for PMPC-3 against representative MBLs IMP-1 (A), NDM-1 (B), VIM-2 (C), and L1 (D).

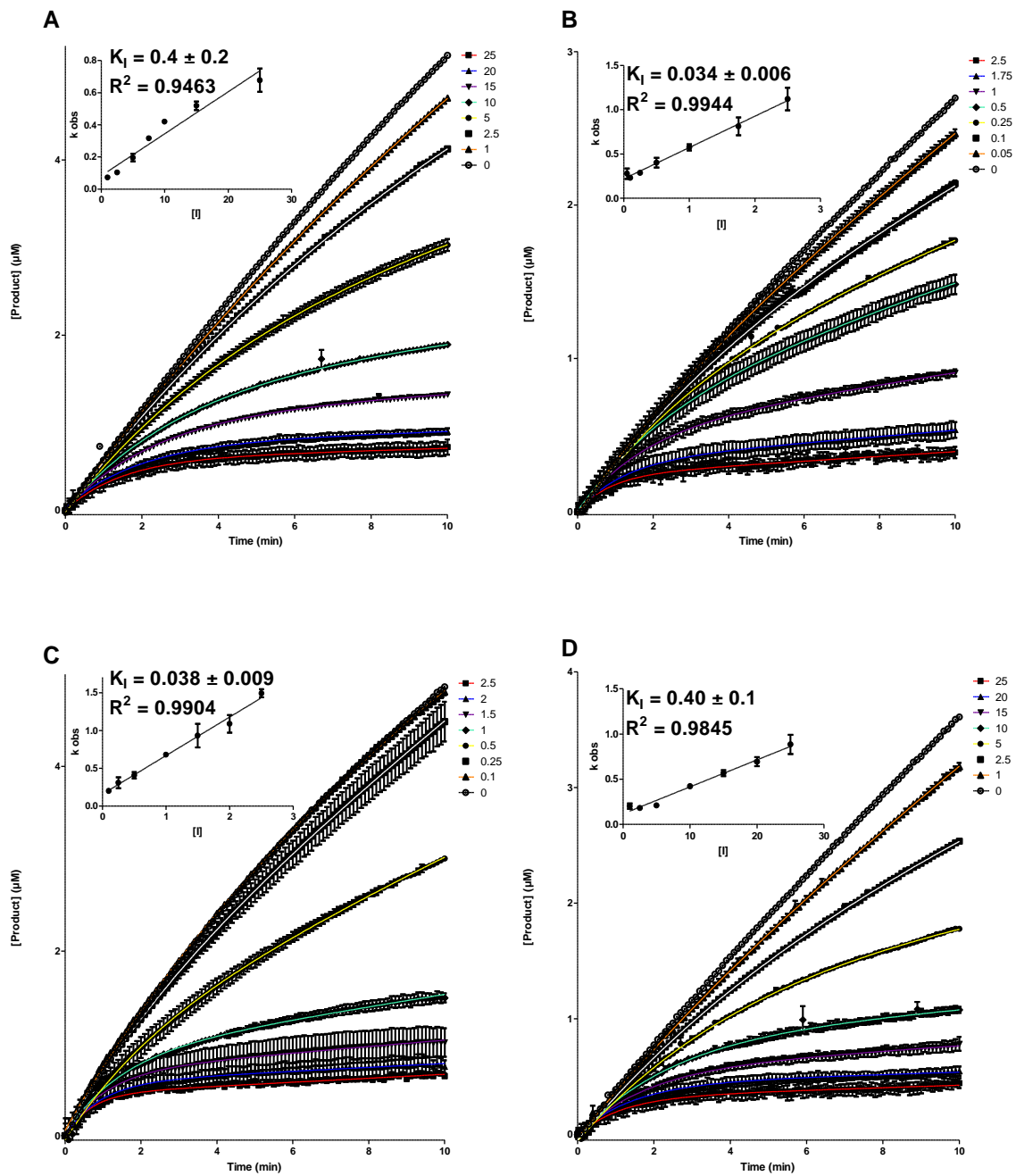
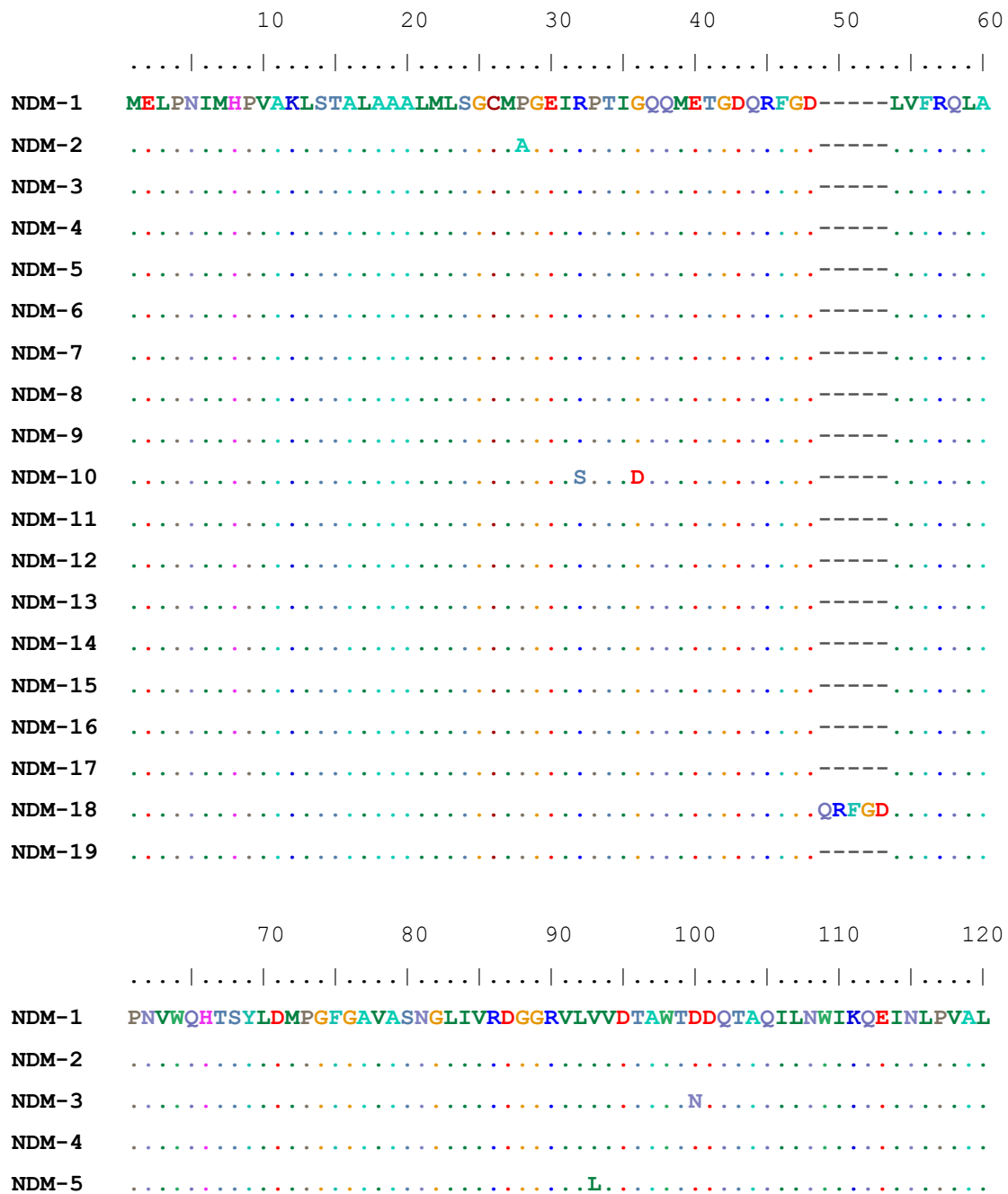


Figure 5.10 Time Dependent K_I graphs for PMPC-4 against representative MBLs IMP-1 (A), NDM-1 (B), VIM-2 (C), and L1 (D).

Appendix E

Protein Sequence Alignments

Alignment of NDM variants relative to NDM-1



NDM-6
 NDM-7
 NDM-8
 NDM-9
 NDM-10S.....T.....
 NDM-11
 NDM-12
 NDM-13N.....
 NDM-14
 NDM-15
 NDM-16
 NDM-17L.....
 NDM-18
 NDM-19

130 140 150 160 170 180

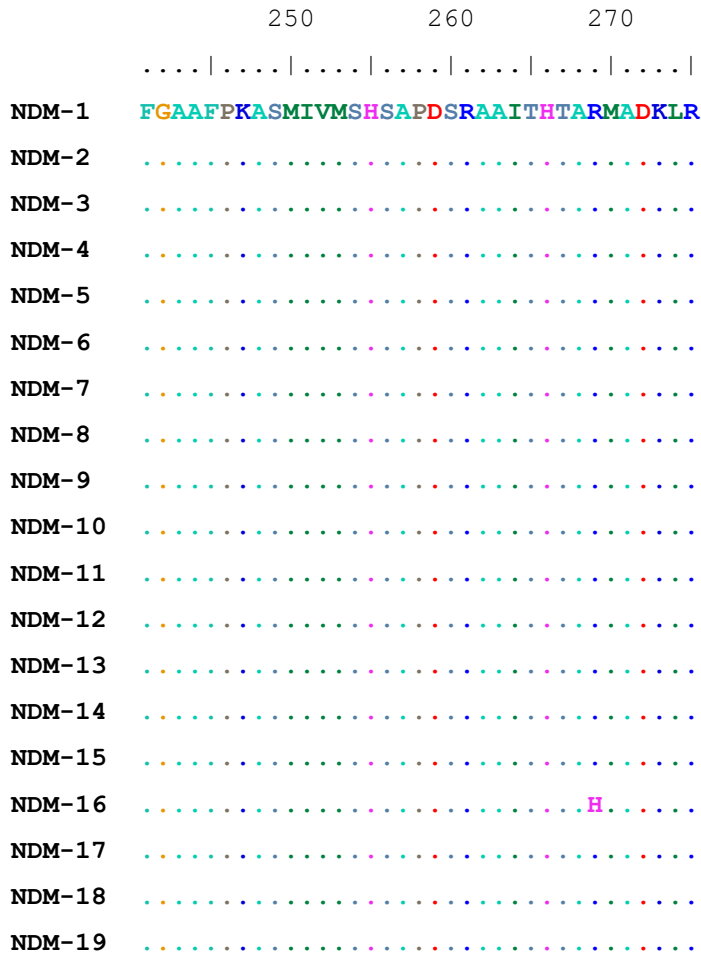
.....|.....|.....|.....|.....|.....|.....|.....|.....|.....|.....|.....|.....|
 NDM-1 AVVTHAHQDKMGGMDALHAAGIATYANALSNQLAPQEGMVAAQHSLTFAANGWVEPATAP
 NDM-2
 NDM-3
 NDM-4L.....
 NDM-5L.....
 NDM-6
 NDM-7N.....L.....
 NDM-8G.....L.....
 NDM-9K.....
 NDM-10
 NDM-11V.....
 NDM-12L.....
 NDM-13L.....
 NDM-14G.....
 NDM-15L.....

NDM-16
 NDM-17L.....K.....
 NDM-18
 NDM-19N.....L.....

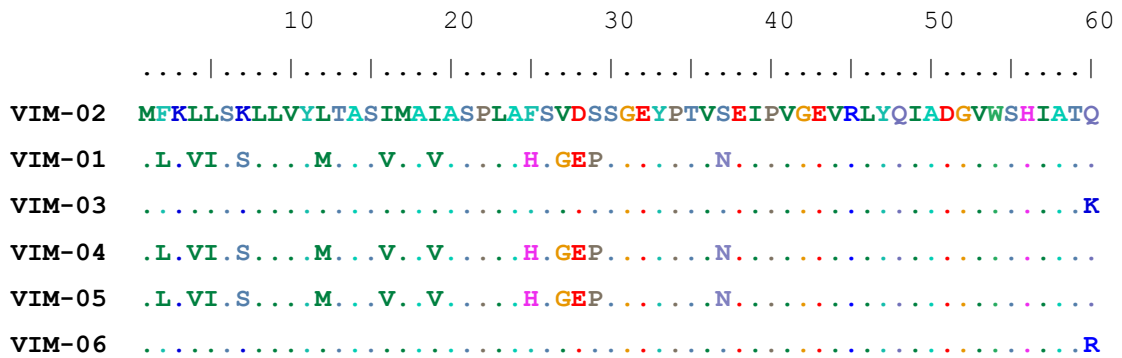
.....190.....200.....210.....220.....230.....240.....

.....|.....|.....|.....|.....|.....|.....|.....|.....|.....|.....|.....|

NDM-1 NFGPLKVFYPGPGHTSDNITVGIIDGTDIAGGCLIKDSKAKSLGNLGDADTEHYAASARA
 NDM-2
 NDM-3
 NDM-4
 NDM-5
 NDM-6V.....
 NDM-7
 NDM-8
 NDM-9
 NDM-10R.....
 NDM-11
 NDM-12D.....
 NDM-13
 NDM-14
 NDM-15V.....
 NDM-16
 NDM-17
 NDM-18
 NDM-19V.....



Alignment of VIM Variants relative to VIM-2



VIM-07 ..Q-IRSF..GIS.FV..VLGSA.Y.AQPG.....DD.....K.G.....
 VIM-08
 VIM-09
 VIM-10
 VIM-11
 VIM-12 ..L.VI.S...M..V..V....H.GEP.....N.....
 VIM-13 ..L.VI.S..F.M..L..V....H.GE.R.....D.....H
 VIM-14 ..L.VI.S...M..V..V....H.GEP.S.....N.....
 VIM-15
 VIM-16L.....
 VIM-17M.....
 VIM-18R
 VIM-19 ..L.VI.S...M..V..V....H.GEP.....N.....
 VIM-20
 VIM-23
 VIM-24
 VIM-25 ..L.VI.S...M..V..V....H.GEP.....N.....
 VIM-26 ..L.VI.S...M..V..V....H.GEP.....N.....
 VIM-27 ..L.VI.S...M..V..V....H.GEP.....N.....S..
 VIM-28 ..L.VI.S...M..V..V....H.GEP.....N.....
 VIM-29 ..L.VI.S...M..V..V....H.GEP.....N.....
 VIM-30N.....
 VIM-31
 VIM-32 ..L.VI.S...M..V..V....H.GEP.....N.....
 VIM-33 ..L.VI.S...M..V..V....H.GEP.....N.....
 VIM-34 ..L.VI.S...M..V..V....H.GEP.....N.....
 VIM-35 ..L.VI.S...M..V..V....H.GEP.....N.....
 VIM-36R
 VIM-37 ..L.VI.S...M..V..V....H.GEP.....N.....S..
 VIM-38 ..L.VI.S.....V..V....H.GEP.....N.....
 VIM-39 ..L.VI.S...M..V..V....H.GEP.....A.N.....
 VIM-40 ..L.VI.S...M..V..V....H.GEP.....N.....
 VIM-41
 VIM-42 ..L.VI.S...M..V..V....H.GEP.....N.....

VIM-43 .L.VI.S...M..V..V...VH.GEP.....N.....
VIM-44
VIM-45I.....
VIM-46 ...F.....A.....
VIM-47 ...VV.S..F.M..L..V...H.GEP.....D.....H
VIM-48
VIM-49 .L.VI.S...M..V..V...H.GEP.....N.....S..
VIM-50
VIM-51
VIM-52 .L.VI.S...M..V..V...H.GEP.....N.....
VIM-54 .L.VI.S...M..V..V...H.GEP.....N.....
VIM-55 .L.VI.S...M..V..V...H.GEP.....N.....

70 80 90 100 110 120

.....|.....|.....|.....|.....|.....|.....|.....|.....|.....|.....|.....|.....|
VIM-02 SFDGAVYPSNGLIVRDGDELLIDTAWGAKNTAALLAEIEKQIGLPVTRAVSTHFHDDR
VIM-01
VIM-03
VIM-04
VIM-05
VIM-06
VIM-07 KLGDT..S.....A.....V.....SI.....
VIM-08
VIM-09
VIM-10
VIM-11
VIM-12
VIM-13 T..V.....T..V.....S.....
VIM-14
VIM-15
VIM-16
VIM-17
VIM-18
VIM-19

VIM-20
VIM-23
VIM-24
VIM-25
VIM-26
VIM-27
VIM-28
VIM-29
VIM-30
VIM-31
VIM-32
VIM-33
VIM-34 I
VIM-35
VIM-36
VIM-37
VIM-38
VIM-39
VIM-40
VIM-41
VIM-42
VIM-43
VIM-44
VIM-45
VIM-46
VIM-47 T . . V T . . V S
VIM-48
VIM-49
VIM-50
VIM-51
VIM-52
VIM-54
VIM-55

	130	140	150	160	170	180
					
VIM-02	GGVDVLR	AAGVATY	ASPSTRRLA	EVEGNEI	PTHSL	EGLSSSGDAVRF
VIM-01			A		
VIM-03				S	
VIM-04			A		
VIM-05	K		A		
VIM-06				S	
VIM-07		T L Q	AA	V A	KA V V
VIM-08		A			
VIM-09		I			
VIM-10					
VIM-11				S	
VIM-12			A		
VIM-13	A		A	V	
VIM-14			A		
VIM-15					
VIM-16					
VIM-17					
VIM-18			---		
VIM-19			A		
VIM-20					
VIM-23					
VIM-24					
VIM-25	K		A		
VIM-26			A		
VIM-27			A		
VIM-28			A		
VIM-29			A		
VIM-30					
VIM-31					
VIM-32			AA		
VIM-33			A		
VIM-34			A		

VIM-35A.....

VIM-36A.....

VIM-37A.....

VIM-38K.....A.....

VIM-39A.....

VIM-40V.A.....

VIM-41A.....

VIM-42A.....

VIM-43A.....

VIM-44A.....

VIM-45A.....

VIM-46A.....

VIM-47A.....A.....V.....

VIM-48A.....

VIM-49K.....A.....

VIM-50S.....

VIM-51A.....

VIM-52A.....

VIM-54A.S.....

VIM-55A.....

190 200 210 220 230 240

.....|.....|.....|.....|.....|.....|.....|.....|.....|.....|.....|.....|.....|

VIM-02 TDNLVVYVPSASVLYGGCAIYELSRTSAGNVADADLAEWPTSIERIQQHYPEAQFVIPGH

VIM-01N.....VH.....S.....V.....K.....EV.....

VIM-03N.....VH.....S.....V.....K.....EV.....

VIM-04N.....VH.....S.....V.....K.....EV.....

VIM-05N.....VLA.....S.....V.....K.....EV.....

VIM-06N.....VLA.....S.....V.....K.....EV.....

VIM-07 G.....AVR.F.....VH.A.E.....N.....AT.K.....R.....EV.....

VIM-08N.....VLA.....S.....V.....K.....EV.....

VIM-09N.....VLA.....S.....V.....K.....EV.....

VIM-10N.....VLA.....S.....V.....K.....EV.....Y.....

VIM-11N.....VLA.....S.....V.....K.....EV.....

VIM-12 N VH S
 VIM-13 N VL G.V EV
 VIM-14 N VH V K EV
 VIM-15 F
 VIM-16
 VIM-17
 VIM-18
 VIM-19 K VH V K EV
 VIM-20 R
 VIM-23 S
 VIM-24 L
 VIM-25 N VLA V K
 VIM-26 N VL S V K EV
 VIM-27 N VH S V K EV
 VIM-28 N VL V K EV
 VIM-29 K VH S V KR EV
 VIM-30
 VIM-31 H R
 VIM-32 N VH S V K EV
 VIM-33 N F VH S V K EV
 VIM-34 N VH S V K EV
 VIM-35 N VH S T V K EV
 VIM-36
 VIM-37 N VH V K EV
 VIM-38 N VLA V K EV
 VIM-39 N VL S V K EV
 VIM-40 N VH V K EV
 VIM-41 N
 VIM-42 N VH S K EV
 VIM-43 N VH V K EV
 VIM-44
 VIM-45
 VIM-46
 VIM-47 N VL G.V EV

VIM-48
VIM-49 N VLA V K EV
VIM-50 L
VIM-51 V
VIM-52 N VR S V K EV
VIM-54 N VH V K EV
VIM-55 K VH V KR EV

250 260 270

.....|.....|.....|.....|.....|.....|..

VIM-02 GLPGGLDLLKHTTNVVKAHTRSVVE-----
VIM-01 Q A K A-----
VIM-03-----
VIM-04 Q A K A-----
VIM-05 Q A T K A-----
VIM-06-----
VIM-07 E Q T KV P A-----
VIM-08-----
VIM-09-----
VIM-10-----
VIM-11-----
VIM-12-----
VIM-13 Q A A-----
VIM-14 Q A K A-----
VIM-15-----
VIM-16-----
VIM-17-----
VIM-18-----
VIM-19 Q A K A-----
VIM-20-----
VIM-23-----
VIM-24-----
VIM-25-----
VIM-26 Q A K A-----

VIM-27Q..A.....K....A.-----
 VIM-28Q..A.....K....A.-----
 VIM-29Q..A.....K....A.-----
 VIM-30-----
 VIM-31-----
 VIM-32Q..A.....K....A.-----
 VIM-33Q..A.....K....A.-----
 VIM-34Q..A.....K....A.-----
 VIM-35Q..A.....K....A.-----
 VIM-36-----
 VIM-37Q..A.....K....A.-----
 VIM-38Q..A...T..K.....-----
 VIM-39Q..A.....K....A.-----
 VIM-40Q..A.....K....A.-----
 VIM-41-----
 VIM-42Q..A.....K....A.-----
 VIM-43Q..A.....K....A.-----
 VIM-44N.....-----
 VIM-45-----
 VIM-46-----
 VIM-47Q..A.....A.-----
 VIM-48---G..AKIGGSQR
 VIM-49Q..A...T..K....A.-----
 VIM-50-----
 VIM-51-----
 VIM-52Q..A.....K....A.-----
 VIM-54Q..A.....K....A.-----
 VIM-55Q..A.....K....A.-----

VIM-1	<i>F2L, L4V, L5I, K7S, L12M, I16V, I19V, F25H, V27G, D28E, S29P, S37N, V145A, S192N, I200V, Y201H, R205S, I223V, Q228K, Q234E, F235V, K250Q, T253A, T260K, V265A</i>
-------	--

VIM-3	Q60K, N148S
VIM-4	<i>F2L, L4V, L5I, K7S, L12M, I16V, I19V, F25H, V27G, D28E, S29P, S37N, VI45A, S192N, I200V, Y201H, I223V, Q228K, Q234E, F235V, K250Q, T253A, T260K, V265A</i>
VIM-5	<i>F2L, L4V, L5I, K7S, L12M, I16V, I19V, F25H, V27G, D28E, S29P, S37N, A128K, VI45A, S192N, I200V, Y201L, E202A, I223V, Q228K, Q234E, F235V, K250Q, T253A, K257T, T260K, V265A</i>
VIM-6	Q60R, N148S
VIM-7	K3Q, L4del, <i>L5I</i> , S6R, <i>K7S</i> , L8F, Y11G, L12I, T13S, S15F, <i>I16V, I19V</i> , A20L, S21G, P22S, L23A, F25Y, V27A, D28Q, <i>S29P</i> , S30G, S37D, E38D, Q48K, A50G, S61K, F62L, D63G, G64D, A65T, P68S, G77A, A93V, A110S, V111I, A135T, S138L, R141Q, <i>VI45A</i> , E146A, I150V, T152A, E156K, G157A, A164V, L172V, T181G, S190A, A191V, S192R, Y195F, <i>I200V, Y201H</i> , L203A, T206E, D215N, T221A, S222T, E224K, H229R, <i>Q234E, F235V</i> , D247E, <i>K250Q</i> , A258T, <i>T260K</i> , N261V, S263P, <i>V265A</i>
VIM-8	T139A
VIM-9	T139I
VIM-10	F235Y
VIM-11	N148S
VIM-12	<i>F2L, L4V, L5I, K7S, L12M, I16V, I19V, F25H, V27G, D28E, S29P, S37N, VI45A, S192N, I200V, Y201H, R205S</i>
VIM-13	<i>F2L, L4V, L5I, K7S</i> , V10F, <i>L12M</i> , I16L, <i>I19V, F25H, V27G, D28E</i> , S30R, A50D, Q60H, S61T, A65V, A89T, A93V, A110S, V125A, <i>VI45A</i> , I150V, <i>S192N, I200V</i> , Y201L, T221G, <i>Q234E, F235V, K250Q, T253A, V265A</i>
VIM-14	<i>F2L, L4V, L5I, K7S, L12M, I16V, I19V, F25H, V27G, D28E, S29P</i> , G31S, <i>S37N, VI45A, S192N, I200V, Y201H, I223V, Q228K, Q234E, F235V, K250Q, T253A, T260K, V265A</i>
VIM-15	Y195F
VIM-16	S55L
VIM-17	I16M
VIM-18	Q60R, E144_G147del
VIM-19	<i>F2L, L4V, L5I, K7S, L12M, I16V, I19V, F25H, V27G, D28E, S29P, S37N, VI45A, S192K, I200V, Y201H, I223V, Q228K, Q234E, F235V, K250Q, T253A, T260K, V265A</i>
VIM-20	H229R
VIM-23	R205S
VIM-24	R205L
VIM-25	<i>F2L, L4V, L5I, K7S, L12M, I16V, I19V, F25H, V27G, D28E, S29P, S37N</i> , A128K, <i>VI45A, S192N, I200V</i> , Y201L, E202A, <i>I223V, Q228K</i>

VIM-26	<i>F2L, L4V, L5I, K7S, L12M, I16V, I19V, F25H, V27G, D28E, S29P, S37N, V145A, S192N, I200V, Y201L, R205S, I223V, Q228K, Q234E, F235V, K250Q, T253A, T260K, V265A</i>
VIM-27	<i>F2L, L4V, L5I, K7S, L12M, I16V, I19V, F25H, V27G, D28E, S29P, S37N, A58S, V145A, S192N, I200V, Y201H, R205S, I223V, Q228K, Q234E, F235V, K250Q, T253A, T260K, V265A</i>
VIM-28	<i>F2L, L4V, L5I, K7S, L12M, I16V, I19V, F25H, V27G, D28E, S29P, S37N, V145A, S192N, I200V, Y201L, I223V, Q228K, Q234E, F235V, K250Q, T253A, T260K, V265A</i>
VIM-29	<i>F2L, L4V, L5I, K7S, L12M, I16V, I19V, F25H, V27G, D28E, S29P, S37N, V145A, S192K, I200V, Y201H, R205S, I223V, Q228K, H229R, Q234E, F235V, K250Q, T253A, T260K, V265A</i>
VIM-30	S37N
VIM-31	<i>Y201H, H229R</i>
VIM-32	<i>F2L, L4V, L5I, K7S, L12M, I16V, I19V, F25H, V27G, D28E, S29P, S37N, V145A, E146A, S192N, I200V, Y201H, R205S, I223V, Q228K, Q234E, F235V, K250Q, T253A, T260K, V265A</i>
VIM-33	<i>F2L, L4V, L5I, K7S, L12M, I16V, I19V, F25H, V27G, D28E, S29P, S37N, V145A, S192N, Y195F, I200V, Y201H, R205S, I223V, Q288K, Q234E, F235V, K250Q, T253A, T260K, V265A</i>
VIM-34	<i>F2L, L4V, L5I, K7S, L12M, I16V, I19V, F25H, V27G, D28E, S29P, S37N, V111I, V145A, S192N, Y195F, I200V, Y201H, R205S, I223V, Q288K, Q234E, F235V, K250Q, T253A, T260K, V265A</i>
VIM-35	<i>F2L, L4V, L5I, K7S, L12M, I16V, I19V, F25H, V27G, D28E, S29P, S37N, V145A, S192N, Y195F, I200V, Y201H, R205S, A212T, I223V, Q228K, Q234E, F235V, K250Q, T253A, T260K, V265A</i>
VIM-36	Q60R
VIM-37	<i>F2L, L4V, L5I, K7S, L12M, I16V, I19V, F25H, V27G, D28E, S29P, S37N, A58S, V145A, S192N, I200V, Y201H, I223V, Q228K, Q234E, F235V, K250Q, T253A, T260K, V265A</i>
VIM-38	<i>F2L, L4V, L5I, K7S, I16V, I19V, F25H, V27G, D28E, S29P, S37N, A128K, V145A, S192N, I200V, Y201L, E202A, I223V, Q228K, Q234E, F235V, K250Q, T253A, K257T, T260K</i>
VIM-39	<i>F2L, L4V, L5I, K7S, L12M, I16V, I19V, F25H, V27G, D28E, S29P, T35A, S37N, V145A, S192N, I200V, Y201L, R205S, I223V, Q228K, Q234E, F235V, K250Q, T253A, T260K, V265A</i>
VIM-40	<i>F2L, L4V, L5I, K7S, I16V, I19V, F25H, V27G, D28E, S29P, S37N, A143V, V145A, S192N, I200V, Y201H, I223V, Q228K, Q234E, F235V, K250W, T253A, T260K, V265A</i>
VIM-41	D213N
VIM-42	<i>F2L, L4V, L5I, K7S, I16V, I19V, F25H, V27G, D28E, S29P, S37N, V145A, S192N,</i>

	<i>I200V, Y201H, R205S, Q228K, Q234E, F235V, K250Q, T253A, T260K, V265A</i>
VIM-43	<i>F2L, L4V, L5I, K7S, I16V, I19V, A24V, F25H, V27G, D28E, S29P, S37N, V145A, S192N, I200V, Y201H, I223V, Q228K, Q234E, F235V, K250Q, T253A, T260K, V265A</i>
VIM-44	K257N
VIM-45	T35I
VIM-46	L4F, V36A
VIM-47	<i>L4V, L5V, K7S, V10F, L12M, I16L, I19V, F25H, V27G, D28E, S30R, A50D, Q60H, S61T, A65V, A89T, A93V, A110S, V125A, V145A, I150V, S192N, I200V, Y201L, T221G, I223V, Q234E, F235V, K250Q, T253A, V265A</i>
VIM-48	H259_N261del, R262G, V265A, E266K, E266_insIGGSQR
VIM-49	<i>F2L, L4V, L5I, K7S, L12M, I16V, I19V, F25H, V27G, D28E, S29P, S37N, A128K, V145A, S192N, I200V, Y201L, E202A, I223V, Q228K, Q234E, F235V, K250Q, T253A, K257T, T260K, V265A</i>
VIM-50	N148S, R205L
VIM-51	A208V
VIM-52	<i>F2L, L4V, L5I, K7S, L12M, I16V, I19V, F25H, V27G, D28E, S29P, S37N, V145A, S192N, I200V, Y201R, R205S, I223V, Q228K, Q234E, F235V, K250Q, T253A, T260K, V265A</i>
VIM-54	<i>F2L, L4V, L5I, K7S, L12M, I16V, I19V, F25H, V27G, D28E, S29P, S37N, V145A, N148S, S192N, I200V, Y201H, I223V, Q228K, Q234E, F235V, K250Q, T253A, T260K, V265A</i>
VIM-55	<i>F2L, L4V, L5I, K7S, L12M, I16V, I19V, F25H, V27G, D28E, S29P, S37N, V145A, S192K, I200V, Y201H, I223V, Q228K, H229R, Q234E, F235V, K250Q, T253A, T260K, V265A</i>

IMP Variant Sequence Alignment

```

          10          20          30          40          50          60
IMP-01  MSKLSVFFIFLFCSIATAAESLPDLKIEKLDEGVYVHTSFEEVNGWGVVPKHGLVVLVNA
IMP-02  .K. .F.LCVCFL...TA.GAR.....E.....S.....T
IMP-03  .....
IMP-04  .....P.....D.
IMP-05  ...F...M...TA.....T
IMP-06  .....
IMP-07  .K.....M.....ASG.A.....T
IMP-08  .K. .F.LCVCFL...TA.GAA.....E.....S.....T

```


IMP-11 D.....N.....Q.....V..
 IMP-12 D.....N.....A..G..FT..V.....Q.....
 IMP-13 D.....T.....N.....E..T.....Q.....
 IMP-14 D.....I.....N.....T..G..A.....Q.....
 IMP-15Q.....
 IMP-16 D.....A.....N.....S.....Q.....
 IMP-17 D.....T.....N.....E..T.....Q.....
 IMP-18 D.....I.....N..I.H..R.....T..G..A.....Q..S.....
 IMP-19 D.....T.....N.....T.....Q.....
 IMP-20 D.....T.....N.....T.....Q.....
 IMP-21 D.....N.....Q.....V..
 IMP-22 D.....Q.....
 IMP-23 D.....T.....N.....T.....Q.....
 IMP-24 D.....T.....N.....T.....Q.....
 IMP-25Q.....
 IMP-26Q.....
 IMP-27 D.....N.....TV.....Q.....
 IMP-28G.....Q.....
 IMP-29Q.....
 IMP-30Q.....
 IMP-31 D..I.....R..G.....A.....Q.....K..
 IMP-32 D.....I.....N.....T..G..A.....Q.....
 IMP-33 D.....T.....N.....T.....Q.....
 IMP-34G.....
 IMP-35 D..I.....R..G.....A.....Q.....K..
 IMP-37 D.....T.....N.....E..T.....Q.....
 IMP-38Q.....
 IMP-40S.....Q.....
 IMP-41 D.....N.....Q.....V..
 IMP-42Q.....
 IMP-43 D.....Q.....
 IMP-44 D.....S.....N.....Q.....V..
 IMP-45 D.....N..N.....R.....Q.....
 IMP-48 D.....T.....N.....T..G..A.....Q.....

IMP-13 S KY E . S Q . L S
 IMP-14 N KH . N . S . S . I Q K V
 IMP-15 K GS N NRV V
 IMP-16 N K S L I Q K V
 IMP-17 S KY S Q . L SE
 IMP-18 N S . S . I Q K V
 IMP-19 K S Q K V
 IMP-20 K S Q K V
 IMP-21 K S Q KN V
 IMP-22 . D QN K S Q K V
 IMP-23 K S Q K V
 IMP-24 K S Q K V
 IMP-25
 IMP-26 K G L
 IMP-27 K D . S A . D Q KE V
 IMP-28 K G . S NRV V
 IMP-29 G K S K NRV V
 IMP-30
 IMP-31 N . NA . E S H Q K
 IMP-32 N KH . Y . S . S . I Q K V
 IMP-33 S KY E . S Q . L S V
 IMP-34
 IMP-35 N . NA . E S H Q K
 IMP-37 S KY E . S Q . L S
 IMP-38 K G L
 IMP-40
 IMP-41 K S Q KN V
 IMP-42
 IMP-43 K AS K I HRV V
 IMP-44 K S Q KN V
 IMP-45 KY S K A NRV V
 IMP-48 N KH . N . S . S . I Q K V
 IMP-49 N S . S . I Q K V
 IMP-51 K AS K I HRV V

IMP-15L.....I.M.....S...T.N.....W.....K....
 IMP-16D...V...H.EI.M.R.N.....D.....W.....K....
 IMP-17 H.....L.....I.M.....S...K.....M.R.W...L...K....
 IMP-18 D.....L.....I.M.....S...I.N...Q.R.W.....
 IMP-19 D.....L.....I.M.V.....S...I.....R.W.....
 IMP-20 D.....L.....I.M.V.....S...I.....R.W.....
 IMP-21D...V...H.EK.I...N.....DI.....W.....
 IMP-22D...VV...H.EI.M.R.N.....DI.....W.....K....
 IMP-23 D.....L.....I.M.....S...I.....R.W.....
 IMP-24 D.....L.....I.M.....S...I.....R.W.....R....
 IMP-25S.....G.....
 IMP-26L.....I.....A.....
 IMP-27 H.....L...E...I.M.E.....S.G...T...T.H.R.W.....K....
 IMP-28L.....M.....R...H.....
 IMP-29D...V...H.EI.M.R.N.....DI.N.....W.....K....
 IMP-30
 IMP-31 D...Y...L.....E.T.M...N...S...I.G...R.W.....K...N
 IMP-32 D...Y...L.....I.M.....S...DI.V...R.W.....
 IMP-33 H.....L.....I.M.....S...K.....R.W...L...K....
 IMP-34
 IMP-35 D...Y...L.....E.T.M...N...S...I.G...R.W.....K....
 IMP-37 H.....L.....I.M.....S...K.....M.R.W...L...K....
 IMP-38L.....I.....G...A.....
 IMP-40
 IMP-41D...V...H.EK.I...N.....DI.....W.....
 IMP-42
 IMP-43L.....V.....R.....
 IMP-44D...V...H.EK.I...N.....DI.....W.....
 IMP-45L.....M.S.....G.DI.S.....W.T...F....
 IMP-48 D...Y...L.....I.M.....S...DI.V...R.W.....
 IMP-49 D.....L.....I.M.....S...I.N...Q.R.W.....
 IMP-51L.....V.....G.....R.....
 IMP-52
 IMP-53L.....M.S.....G.DI.S.....W.T...F....

IMP-54 D...Y...L...I.M...S...DI...V...R.W...
 IMP-55 ...K...
 IMP-56 D...L...I.M...SG...I.N...QR.W...
 IMP-58 ...D...VV...H...EI.M.R.N...DI...W...K...
 IMP-59 ...Y...L...I...A...
 IMP-60 ...
 IMP-61 ...
 IMP-62 ...L...I.M...SG...T.N...W...K...
 IMP-63 D...D...LK...I.M...S...I.N...W...K...
 IMP-64 H...L...E...I.M.E...SG...T...TH...R.W...K...
 IMP-66 ...
 IMP-67 H...L...E...I.M.E...SG...T...STH...R.W...K...
 IMP-68 ...D...V...H...EK.I...N...G...DI...W...
 IMP-69 D...L...I.M...S...I...R.W...
 IMP-70 ...I...

...|...

IMP-01 PSKPS--N
 IMP-02 ..Q.--.
 IMP-03--.
 IMP-04 ...L.--.
 IMP-05--.
 IMP-06--.
 IMP-07 L.....--.
 IMP-08 ..Q.--.
 IMP-09 -.TTA--H
 IMP-10--.
 IMP-11 -.NTV--H
 IMP-12 .LL.--.
 IMP-13 T.S.--.
 IMP-14 S.Q.--D
 IMP-15 ..L.--.
 IMP-16 ..Q.--.

IMP-17 T.S.--.
IMP-18 .LQ.--S
IMP-19 ..Q.--.
IMP-20 ..Q.--.
IMP-21 -.NTV--H
IMP-22 ..E.--.
IMP-23 ..Q.--.
IMP-24 ..Q.--.
IMP-25
IMP-26 ...L.--.
IMP-27 TLQ.--.
IMP-28
IMP-29 ..Q.--.
IMP-30
IMP-31 HHS.K---
IMP-32 S.Q.--D
IMP-33 T.S.--.
IMP-34
IMP-35 ..Q.N--.
IMP-37 T.SQ.TAS
IMP-38 ...L.--.
IMP-40
IMP-41 -.NTV--H
IMP-42
IMP-43 L.....
IMP-44 -.NTV--H
IMP-45 -.TTA--H
IMP-48 S.Q.--D
IMP-49 .LQ.--S
IMP-51 L.....
IMP-52
IMP-53 -.TTA--H
IMP-54 S.Q.--D
IMP-55

IMP-56 .LQ.--S
 IMP-58 ..E.--.
 IMP-59 ...L.--.
 IMP-60--.
 IMP-61--.
 IMP-62 ..L.--.
 IMP-63 .LL.--.
 IMP-64 TLQ.--.
 IMP-66--.
 IMP-67 TLQ.--.
 IMP-68 -.NTV--H
 IMP-69 ..Q.--.
 IMP-70--.

Table of IMP variant amino acid differences relative to IMP-1

IMP-2	S2K, S5F, F7L, F8C, I9V, F10C, L11F, F12L, A16T, T17A, A19G, E20A, S21R, D31E, P50S, A60T, E61D, K72T, T79N, S91T, R110Q, T133K, N140S, P159Q, R169K, I178V, Y181D, I191L, L200I, K202M, G206V, P213S, V218I, L226R, L228W, K243Q
IMP-3	E105G, S214G
IMP-4	S21P, N59D, R110Q, T133K, S137G, V162L, I191L, K202I, V218A, P244L
IMP-5	S5F, I9M, A16T, T17A, A60T, R110Q, T133K, V139A, N140S, N146K, R169N, K170R, I171V, I178V, I191V, K202M, L226R
IMP-6	S214G
IMP-7	S2K, I9M, T17A, A18S, A19G, S21A, A60T, E61D, R110Q, T133K, V139A, N140S, N146K, V150I, R169H, K170R, I171V, I178V, I191L, K202V, L226R, P241L
IMP-8	S2K, S5F, F7L, F8C, I9V, F10C, L11F, F12L, A16T, T17A, A19G, E20A, S21A, D31E, P50S, A60T, E61D, K72T, T79N, S91T, R110Q, T133K, N140S, P159Q, R169K, I178V, Y181D, I191L, L200I, K202M, P213S, V218I, L226R, L228W, K243Q
IMP-9	S5F, I9M, A16T, T17A, A19G, V49I, A60T, E61D, K76N, T79N, K87R, R110Q, T133K, N134Y, N140S, N146K, T158A, R169N, K170R, I171V, I178V, I191L, K202M, G206S, E217D, V218I, A221S, L228W, A231T, L235F, P241del, K243T, P244T, S245A, N246H
IMP-10	V49F
IMP-11	S2K, S5F, F7L, F8C, A16T, T17A, A19G, E20A, D31E, P50S, A60T, E61D, T79N, R110Q, E118V, T133K, N140S, P159Q, E168K, R169N, I178V, G187D, I191V, K196H, K199E, L200K, K202I, K207N, E217D, V218I, L228W, P241del, K243N, P244T,

	S245V, N246H
IMP-12	S2K, S5F, F7L, F8C, C13L, A16T, T17A, A18S, A19G, S21V, D31E, V36L, N44S, P50T, A60N, E61D, A71N, T79A, E83G, Y86F, K87T, I92V, R110Q, D127N, N140S, V150I, P159Q, R169N, I178V, Y181D, G187D, I191L, E192K, L200I, L202M, P213S, S214G, V218I, D220N, L228W, N236K, S242L, K243L
IMP-13	S2K, S5F, F7L, F8C, I9V, F10C, L11F, A16T, T17A, A19G, E20A, S21A, D31E, Y35F, P50T, A60T, E61D, K72T, T79N, K87E, S91T, R110Q, D127S, T133K, N134Y, G138E, N140S, P159Q, V162L, R169S, Y181H, I191L, L200I, K202M, P213S, V218K, L224M, L226R, L228W, V232L, N236K, P241T, K243S
IMP-14	S2K, S5F, F7L, F8C, I9V, L11F, S14N, T17V, A19E, D31E, N44K, G47S, P50T, N59K, A60N, E61D, F69I, T79N, S94T, S98G, G102A, R110Q, G128N, T133K, N134H, S137N, N140S, W142S, V144I, P159Q, R169K, I178V, Y181D, N185Y, I191L, L200I, K202M, P213S, E217D, V218I, A221V, L226R, L228W, P241S, K243Q, N246D
IMP-15	S2N, I9M, L11M, A16T, T17A, A19G, A60T, R110Q, T133K, V139G, N140S, K145N, R169N, K170R, I171V, I178V, I191L, L200I, K202M, P213S, V218T, D220N, L228W, N236K, K243L
IMP-16	S2K, S5F, F7L, F8C, A16T, T17A, A19G, D31E, E32D, P50T, V56F, A60T, E61D, T70A, T79N, T101S, R110Q, D127N, T133K, N140S, V144L, V150I, P159Q, R169K, I178V, G187D, I191V, K196H, K199E, L200I, K202M, K204R, K207N, E217D, L228W, N236K, K243Q
IMP-17	S2K, S5F, F7L, F8C, T9V, F10C, L11F, A16T, T17A, A19G, E20A, S21A, D31E, Y35F, P50T, A60T, E61D, K72T, T79N, K87E, S91T, R110Q, D127S, T133K, N134Y, N140S, P159Q, V162L, R169S, K170E, Y181H, I191L, L200I, K202M, P213S, V218K, L224M, L226R, L228W, V232L, N236K, P241T, K243S
IMP-18	S2K, S5F, F7L, F8C, I9V, L11F, F12L, S14N, T17A, A19D, E20D, D31E, E32K, N44K, P50T, N59K, A60N, E61D, F69I, T79N, V82I, R84H, K87R, S94T, S98G, G102A, R110Q, P113S, G128N, N140S, W142S, V144I, P159Q, R169K, I178V, Y181D, I191L, L200I, K202M, P213S, V218I, D220N, K225Q, L226R, L228W, S242L, K243Q, N246S
IMP-19	S2K, S5F, F7L, F8C, I9V, F10C, L11F, F12L, A16T, T17A, A19G, E20A, S21A, D31E, P50S, A60T, E61D, K72T, T79N, S91T, R110Q, T133K, N140S, P159Q, R169K, I178V, Y181D, I191L, L200I, K202M, G206V, P213S, V218I, L226R, L228W, K243Q
IMP-20	S2K, S5F, F7L, F8C, I9V, F10C, L11F, F12L, A16T, T17A, A19G, E20A, S21A, D31E, V49F, P50S, A60T, E61D, K72T, T79N, S91T, R110Q, T133K, N140S, P159Q, R169K, I178V, Y181D, I191L, L200I, K202M, G206V, P213S, V218I, L226R, L228W, K243Q
IMP-21	S2K, S5F, F7L, F8C, A16T, T17A, A19G, E20A, D31E, V49A, P50S, A60T, E61D, T79N, R110Q, E118V, T133K, N140S, P159Q, E168K, R169N, I178V, G187D, I191V, K196H, K199E, L200K, K202I, K207N, E217D, V218I, L228W, P241del, K243N, P244T, S245V, N246H
IMP-22	S2K, S5F, F7L, F8C, I9V, A16T, T17A, A19G, D31E, P50S, V56I, A60T, E61D, R110Q, E122D, K126Q, D127N, T133K, N140S, P159Q, R169K, I178V, G187D, I191V, E192V, K196H, K199E, L200I, K202M, K204R, K207N, E217D, V218I, L228W,

	N236K, K243E
IMP-23	S2K, S5F, F7L, F8C, I9V, F10C, L11F, F12L, A16T, T17A, A19G, E20A, S21A, D31E, V49F, P50S, A60T, E61D, K72T, T79N, S91T, R110Q, T133K, N140S, P159Q, R169K, I178V, Y181D, I191L, L200I, K202M, P213S, V218I, L226R, L228W, K243Q
IMP-24	S2K, S5F, F7L, F8C, I9V, F10C, L11F, F12L, A16T, T17A, A19G, E20A, S21A, D31E, P50S, A60T, E61D, K72T, T79N, S91T, R110Q, T133K, N140S, P159Q, R169K, I178V, Y181D, I191L, L200I, K202M, P213S, V218I, L226R, L228W, K239R, K243Q
IMP-25	G187S, S214G
IMP-26	S21P, V49F, N59D, R110Q, T133K, S137G, V162L, I191L, K202I, V218A, P244L
IMP-27	S2K, S5F, F7L, F8C, I9V, L11V, A16T, T17V, A19G, S21T, D24N, K26R, I27V, D31E, F40Y, N44K, P50T, V58I, N59G, E61D, T79N, S91T, I92V, R110Q, T133K, S137D, N140S, V144A, N146D, D159Q, R169K, K170E, I178V, Y181H, I191L, K196E, L200I, K202M, S203E, P213S, S214G, V218T, S222T, L223H, L226R, L228W, N236K, P241T, S242L, K243Q
IMP-28	S5F, I9M, A16T, T17A, K29R, A60T, E83G, R110Q, T133K, S137G, N140S, R169N, K170R, I171V, I178V, I191L, K202M, L226R, Q230H
IMP-29	S5F, F8L, A16T, T17A, A60T, R110Q, D127G, T133K, N140S, N146K, R169N, K170R, I171V, I178V, G187D, I191V, K196H, K199E, L200I, K202M, K204R, K207N, E217D, V218I, D220N, L228W, N236K, K243Q
IMP-30	E41K
IMP-31	S2K, L4I, S5F, F7L, I9V, A16T, T17A, A19G, L25I, G33D, E42K, V43I, N44T, V49I, P50T, A60T, E61D, L64I, T79R, E83G, T101A, R110Q, E118K, D127N, K129N, V130A, T133S, N140S, N146H, P159Q, R169K, Y181D, N185Y, I191L, K199E, L200T, K202M, K207N, P213S, V218I, D220G, L226R, L228W, N236K, K240N, P241H, S242H, K243S, S245K
IMP-32	S2K, S5F, F7L, F8C, I9V, L11F, S14N, T17V, A19E, D31E, N44K, G47S, P50T, N59K, A60N, E61D, F69I, T79N, S94T, S98G, G102A, R110Q, G128N, T133K, N134H, S137Y, N140S, W142S, V144I, P159Q, R169K, I178V, Y181D, N185Y, I191L, L200I, K202M, P213S, E217D, V218I, A221V, L226R, L228W, P241S, K243Q, N246D
IMP-33	S2K, S5F, F7L, F8C, I9V, F10C, L11F, A16T, T17A, A19G, E20S, D31E, Y35F, P50T, A60T, E61D, K72T, T79N, S91T, R110Q, D127S, T133K, N134Y, G138E, N140S, P159Q, V162L, R169S, I178V, Y181H, I191L, L200I, K202M, P213S, V218K, L226R, L228W, V232L, N236K, P241T, K243S
IMP-34	E105G
IMP-35	S2K, L4I, S5F, F7L, I9V, A16T, T17A, A19G, L25I, G33D, V43D, V49I, P50T, A60T, E61D, L64I, T79R, E83G, T101A, R110Q, E118K, D127N, K129N, V130A, T133E, N140S, N146H, P159Q, R169K, Y181D, N185Y, I191L, K199E, L200T, K202M, K207N, P213S, V218I, D220G, L226R, L228W, N236K, K243Q, S245N
IMP-37	S2K, S5F, F7L, F8C, I9V, F10C, L11F, A16T, T17A, A19G, E20A, S21A, D31E, Y35F, P50T, A60T, E61D, K72T, T79N, K87E, S91T, R110Q, D127S, T133K, N134Y, G138E,

	N140S, P159Q, V162L, R169S, Y181H, I191L, L200I, K202M, P213S, V218K, L224M, L226R, L228W, V232L, N236K, P241T, K243S, P244Q, S245_N246insTA, N246S
IMP-38	S21P, N59D, R110Q, T133K, S137G, V162L, I191L, K202I, S214G, V218A, P244L
IMP-40	V49F, F69S
IMP-41	S2K, S5F, F7L, F8C, A16T, T17A, A19G, E20A, D31E, V49F, P50S, A60T, E61D, T79N, R110Q, E118V, T133K, N140S, P159Q, E168K, R169N, I178V, G187D, I191V, K196H, K199E, L200K, K202I, K207N, E217D, V218I, L228W, P241del, K243N, P244T, S245V, N246H
IMP-42	G45R
IMP-43	S2K, I9M, T17A, A18S, A19G, S21A, V49F, A60T, E61D, R110Q, T133K, V139A, N140S, N146K, V150I, R169H, K170R, I171V, I178V, I191L, K202V, L226R, P241L
IMP-44	S2K, S5F, F7L, F8C, A16T, T17A, A19G, E20A, D31E, V49F, P50S, A60T, E61D, F69S, T79N, R110Q, E118V, T133K, N140S, P159Q, E168K, R169N, I178V, G187D, I191V, K196H, K199E, L200K, K202I, K207N, E217D, V218I, L228W, P241del, K243N, P244T, S245V, N246H
IMP-45	S5F, I9M, A16T, T17A, A19G, V49I, A60T, E61D, K76N, T79N, K87R, R110Q, T133K, N134Y, N140S, N146K, T158A, R169N, K170R, I171V, I178V, I191L, K202M, G206S, S214G, E217D, V218I, A221S, L228W, A231T, L235F, P241del, K243T, P244T, S245A, N246H
IMP-48	S2K, S5F, F7L, F8C, I9V, L11F, S14N, T17V, A19E, D31E, N44K, G47S, P50T, N59K, A60N, E61D, F69T, T79N, S94T, S98G, G102A, R110Q, G118N, T133K, N134H, S137N, N140S, W142S, V144I, P159Q, R169K, I178V, Y181D, N185Y, I191L, L200I, K202M, P213S, E217D, V218I, A221V, L226R, L228W, P241S, K243Q, N246D
IMP-49	S2K, S5F, F7L, F8C, I9V, L11F, F12L, S14N, T17A, A19D, E20D, D31E, E32K, N44K, V49F, P50T, N59K, A60N, E61D, F69I, T79N, V82I, R84H, K87R, S94T, S98G, G102A, R110Q, P113S, G128N, N140S, W142S, V144I, P159Q, R169K, I178V, Y181D, I191L, L200I, K202M, P213S, V218I, D220N, K225Q, L226R, L228W, S242L, K243Q, N246S
IMP-51	S2K, I9M, T17A, A18S, A19G, S21A, A60T, E61D, R110Q, T133K, V139A, N140S, N146K, V150I, R169H, K170R, I171V, I178V, I191L, K202V, S214G, L226R, P241L
IMP-52	L64I, V78G
IMP-53	S5F, I9M, A16T, T17A, A19G, V49I, A60T, E61D, K76N, T79N, K87R, R110Q, T133K, N134Y, N140S, N146K, P155S, T158A, R169N, K170R, I171V, I178V, I191L, K202M, G206S, S214G, E217D, V218I, A211S, L228W, A231T, L235F, P241del, K243T, P244T, S245A, N246H
IMP-54	S2K, S5F, F7L, F8C, I9V, L11F, S14N, T17V, A19E, D31E, N44K, G47S, P50T, N59K, A60N, E61D, F69V, T79N, S94T, S98G, G102A, R110Q, G128N, T133K, N134H, S137N, N140S, W142S, V144I, P159Q, R169K, I178V, Y181D, N185Y, I191L, L200I, K202M, P213S, E217D, V218I, A221V, L226R, L228W, P241S, K243Q, N246D

IMP-55	F12I, D31E, E41K, L172F, N185K
IMP-56	S2K, S5F, F7L, F8C, I9V, L11F, F12L, S14N, T17A, A19D, E20D, D31E, E32K, N44K, P50T, N59K, A60N, E61D, F69I, T79N, V82I, R84H, K87R, S94T, S98G, G102A, R110Q, P113S, G128N, N140S, W142S, V144I, P159Q, R169K, I178V, Y181D, I191L, L200I, K202M, P213S, S214G, V218I, D220N, K225Q, L226R, L228W, S242L, K243Q, N246S
IMP-58	S2K, S5F, F7L, F8C, I9V, A16T, T17A, A19G, D31E, V49F, P50S, V56I, A60T, E61D, R110Q, E122D, K126Q, D127N, T133K, N140S, P159Q, R169K, I178V, G187D, I191V, E192V, K196H, K199E, L200I, K202M, K204R, K207N, E217D, V218I, L228W, N236K, K243E
IMP-59	S21P, N59D, R110Q, T133K, S137G, V162L, N185Y, I191L, K202I, V218A, P244L
IMP-60	E168K
IMP-61	N108I
IMP-62	S2N, I9M, L11M, A16T, T17A, A19G, A60T, R110Q, T133K, V139G, N140S, K145N, R169N, K170R, I171V, I178V, I191L, L200I, K202M, P213S, S214G, V218T, D220N, L228W, N236K, K243L
IMP-63	S2K, S5F, F7L, F8C, C13L, A16T, T17A, A18S, A19G, S21V, D31E, V36L, N44S, P50T, A60N, E61D, A71N, T79A, E83G, Y86F, K87T, I92V, R110Q, D127N, N140S, V150I, P159Q, R169N, I178V, Y181D, G187D, I191L, E192K, L200I, K202M, P213S, V218I, D220N, L228W, N236K, S242L, K243L
IMP-64	S2K, S5F, F7L, F8C, T9V, L11V, A16T, T17V, S21T, D24N, K26R, I27V, D31E, F40Y, N44K, P50T, V58I, N59G, E61D, T79N, S91T, I92V, R110Q, T133K, S137D, N140S, V144A, N146D, P159Q, R169K, K170E, I178V, Y181H, I191L, K196E, L200I, K202M, S203E, P213S, S214G, V218T, S222T, L223H, L226R, L228W, N236K, P241T, S242L, K243Q
IMP-66	V48F
IMP-67	S2K, S5F, F7L, F8C, I9V, L11V, A16T, T17V, A19G, S21T, D24N, K26R, I27V, D31E, F40Y, N44K, P50T, V58I, N59G, E61D, T79N, S91T, I92V, R110Q, T133K, S137D, N140S, V144A, N146D, P159Q, R169K, K170E, I178V, Y181H, I191L, K196E, L200I, K202M, S203E, P213S, S214G, V218T, A221S, S222T, L223H, L226R, L228W, N236K, P241T, S242L, K243Q
IMP-68	S2K, S5F, F7L, F8C, A16T, T17A, A19G, E20A, D31E, P50S, A60T, E61D, T79N, R110Q, E118V, T133K, N140S, P159Q, E168K, R169N, I178V, G187D, I191V, K196H, K199E, L200K, K202I, K207N, S214G, E217D, V218I, L228W, P241del, K243N, P244T, S245V, N246H
IMP-69	S2K, S5F, F7L, F8C, I9V, F10C, L11F, F12L, A16T, T17A, A19G, E20A, S21T, D31E, P50S, A60T, E61D, K72T, T79N, S91T, R110Q, T133K, N140S, P159Q, R169K, I178V, Y181D, I191L, L200I, K202M, P213S, V218I, L226R, L228W, K243Q
IMP-70	L228I

Bibliography

- (1) Centers for Disease Control and Prevention. Achievements in Public Health, 1900-1999: Control of Infectious Diseases. *Morb. Mortal. Wkly. Rep.* **1999**, 48 (29), 621–629.
- (2) Fleming, A. On the Antibacterial Action of Cultures of a Penicillium, with Special Reference to Their Use in the Isolation of B. Influenzae. *Br. J. Exp. Pathol.* **1929**, 10 (8), 226–236.
- (3) Fletcher, C. First Clinical Use of Penicillin. *Br. Med. J.* **1984**, 289 (December), 1721–1723.
- (4) Chain, E.; Florey, H. W.; Gardner, A. D.; Heatley, N. G.; Jennings, M. A.; Orr-Ewing, J.; Sanders, A. G. Penicillin as a Chemotherapeutic Agent. *Lancet* **1940**, 236 (6104), 226–228.
- (5) Aminov, R. I. A Brief History of the Antibiotic Era: Lessons Learned and Challenges for the Future. *Front. Microbiol.* **2010**, 1 (134), 1–7.
- (6) Chopra, I.; Hesse, L.; O'Neill, A. J. Exploiting Current Understanding of Antibiotic Action for Discovery of New Drugs. *J. Appl. Microbiol. Symp. Suppl.* **2002**, 92, 4S–15S.
- (7) Rice, L. B. Federal Funding for the Study of Antimicrobial Resistance in Nosocomial Pathogens: No ESKAPE. *J. Infect. Dis.* **2008**, 197 (8), 1079–1081.
- (8) Lawe-Davies, O.; Bennett, S. WHO publishes list of bacteria for which new antibiotics are urgently needed <http://www.who.int/mediacentre/news/releases/2017/bacteria-antibiotics-needed/en/> (accessed May 9, 2018).
- (9) World Health Organization. *Critically Important Antimicrobials for Human Medicine - 5th Rev*; Geneva, 2017.
- (10) Kohanski, M. A.; Dwyer, D. J.; Collins, J. J. How Antibiotics Kill Bacteria: From Targets to Networks. *Nat. Rev. Microbiol.* **2010**, 8, 423–435.
- (11) McCoy, L. S.; Xie, Y.; Tor, Y. Antibiotics That Target Protein Synthesis. *Wiley Interdiscip. Rev. RNA* **2011**, 2, 209–232.
- (12) Schneider, T.; Sahl, H.-G. An Oldie but a Goodie - Cell Wall Biosynthesis as Antibiotic Target Pathway. *Int. J. Med. Microbiol.* **2010**, 300, 161–169.
- (13) Epanand, R. M.; Walker, C.; Epanand, R. F.; Magarvey, N. A. Molecular Mechanisms of Membrane Targeting Antibiotics. *Biochim. Biophys. Acta* **2016**, 1858, 980–987.
- (14) Falagas, M. E.; Kasiakou, S. K. Colistin: The Revival of Polymyxins for the Management of

- Multidrug-Resistant Gram-Negative Bacterial Infections. *Clin. Infect. Dis.* **2005**, *40*, 1333–1341.
- (15) Wishart, D. S.; Feunang, Y. D.; Guo, A. C.; Lo, E. J.; Marcu, A.; Grant, J. R.; Sajed, T.; Johnson, D.; Li, C.; Sayeeda, Z.; Assempour, N.; Iynkkaran, I.; Liu, Y.; Maciejewski, A.; Gale, N.; Wilson, A.; Chin, L.; Cummings, R.; Le, D.; Pon, A.; Knox, C.; Wilson, M. DrugBank 5.0: A Major Update to the DrugBank Database for 2018. *Nucleic Acids Res.* **2018**, *46*, D1074–D1082.
- (16) Data Provided by Infectious Disease Prevention and Control Branch of the Public Health Agency of Canada. Personal Communication. 2018.
- (17) *Canadian Antimicrobial Resistance Surveillance System 2017 Report*; Ottawa, ON, 2018.
- (18) Sauvage, E.; Kerff, F.; Terrak, M.; Ayala, J. A.; Charlier, P. The Penicillin-Binding Proteins: Structure and Role in Peptidoglycan Biosynthesis. *FEMS Microbiol. Rev.* **2008**, *32*, 234–258.
- (19) Munita, J. M.; Arias, C. A. Mechanisms of Antibiotic Resistance. *Microbiol. Spectr.* **2016**, *4* (2), 1–24.
- (20) Giedraitienė, A.; Vitkauskienė, A.; Naginienė, R.; Pavilionis, A. Antibiotic Resistance Mechanisms of Clinically Important Bacteria. *Medicina (Kaunas)*. **2011**, *47* (3), 137–146.
- (21) Santajit, S.; Indrawattana, N. Mechanisms of Antimicrobial Resistance in ESKAPE Pathogens. *Biomed Res. Int.* **2016**, *2016*.
- (22) Poole, K. Resistance to β -Lactam Antibiotics. *Cell. Mol. Life Sci.* **2004**, *61* (17), 2200–2223.
- (23) Drawz, S. M.; Bonomo, R. A. Three Decades of β -Lactamase Inhibitors. *Clin. Microbiol. Rev.* **2010**, *23* (1), 160–201.
- (24) Galleni, M.; Lamotte-Brasseur, J.; Raquet, X.; Dubus, A.; Monnaie, D.; Knox, J. R.; Frère, J.-M. The Enigmatic Catalytic Mechanism of Active-Site Serine β -Lactamases. *Biochem. Pharmacol.* **1995**, *49* (9), 1171–1178.
- (25) Page, M. I.; Badarau, A. The Mechanisms of Catalysis by Metallo β -Lactamases. *Bioinorg. Chem. Appl.* **2008**, 576297–576310.
- (26) Palzkill, T. Metallo- β -Lactamase Structure and Function. *Ann. N. Y. Acad. Sci.* **2013**, *1277*, 91–104.

- (27) Docquier, J.-D.; Mangani, S. An Update on β -Lactamase Inhibitor Discovery and Development. *Drug Resist. Updat.* **2018**, *36*, 13–29.
- (28) Bush, K.; Bradford, P. A. β -Lactams and β -Lactamase Inhibitors: An Overview. *Cold Spring Harb. Perspect. Med.* **2016**, *6*, 1–22.
- (29) Sanderson, J. B. Appendix 5 – Further Report of Researches Concerning the Intimate Pathology of Contagion. The Origin and Distribution of Microzymes (Bacteria) in Water, and the Circumstances Which Determine Their Existence in the Tissue and Liquids. In *Thirteenth Report of the Medical Officer of the Privy Council, with Appendix, 1870*; Her Majesty's Stationery Office: London, 1871; pp 48–69.
- (30) Selwyn, S. Pioneer Work on the “Penicillin Phenomenon”, 1870-1876. *J. Antimicrob. Chemother.* **1979**, *5*, 249–255.
- (31) Lister, J. A Contribution to the Germ Theory of Putrefaction and Other Fermentative Changes, and to the Natural History of Torulæ and Bacteria. *Trans. R. Soc. Edinburgh* **1875**, *27*, 313–348.
- (32) Tyndall, J. Observations on the Optical Department of the Atmosphere in Reference to the Phenomena of Putrefaction and Infection. *Philos. Trans. R. Soc. London* **1876**, *166*, 27–74.
- (33) Friday, J. A Microscopic Incident in a Monumental Struggle: Huxley and Antibiosis in 1875. *Br. J. Hist. Sci.* **1974**, *7* (1), 61–71.
- (34) Page, M. G. P. Beta-Lactam Antibiotics. In *Antibiotic Discovery and Development*; Dougherty, T. J., Pucci, M. J., Eds.; Springer: Boston, Ma, 2012; pp 79–117.
- (35) Fair, R. J.; Tor, Y. Antibiotics and Bacterial Resistance in the 21st Century. *Perspect. Medicin. Chem.* **2014**, *6*, 25–64.
- (36) Brotzu, G. Ricerche Su Di Un Nuovo Antibiotico (Research on a New Antibiotic). *Lav. dell'istituto d'Igiene di Cagliari* **1948**, 1–11.
- (37) Abraham, E. P.; Newton, G. G. F. The Structure of Cephalosporin C. *Biochem. J.* **1961**, *79*, 377–393.
- (38) Brown, A. G.; Butterworth, D.; Cole, M.; Hanscomb, G.; Hood, J. D.; Reading, C. Naturally-Occurring β -Lactamase Inhibitors with Antibacterial Activity. *J. Antibiot. (Tokyo)*. **1976**, *29*

- (6), 668–669.
- (39) Kahan, J. S.; Kahan, F. M.; Goegelman, R.; Currie, S. A.; Jackson, M.; Stapley, E. O.; Miller, T. W.; Miller, A. K.; Hendlin, D.; Mochales, S.; Hernandez, S.; Woodruff, H. B.; Birnbaum, J. Thienamycin, a New β -Lactam Antibiotic I. Discovery, Taxonomy, Isolation and Physical Properties. *J. Antibiot. (Tokyo)*. **1979**, *32* (1), 1–12.
- (40) Kahan, F. M.; Kropp, H.; Sundelof, J. G.; Birnbaum, J. Thienamycin: Development of Imipenem-Cilastatin. *J. Antimicrob. Chemother.* **1983**, *12* (Suppl. D), 1–35.
- (41) Leanza, W. J.; Wildonger, K. J.; Miller, T. W.; Christensen, B. G. N-Acetimidoyl- and N-Formimidoylthienamycin Derivatives: Antipseudomonal β -Lactam Antibiotics. *J. Med. Chem.* **1979**, *22* (12), 22–23.
- (42) Moellering, R. C.; Eliopoulos, G. M.; Sentochnik, D. E. The Carbapenems: New Broad Spectrum β -Lactam Antibiotics. *J. Antimicrob. Chemother.* **1989**, *24* (Suppl. A), 1–7.
- (43) Johnson, J. W. Cyclobutanone Analogues of β -Lactam Antibiotics as Inhibitors of Serine- and Metallo- β -Lactamases By, University of Waterloo, 2011.
- (44) Centers for Disease Control and Prevention. Antibiotic resistance threats in the United States, 2013 <https://www.cdc.gov/drugresistance/threat-report-2013/index.html> (accessed May 2, 2018).
- (45) Abraham, E. P.; Chain, E. An Enzyme from Bacteria Able to Destroy Penicillin. *Nature* **1940**, *146*, 837.
- (46) Aminov, R. I. The Role of Antibiotics and Antibiotic Resistance. *Environ. Microbiol.* **2009**, *11* (12), 2970–2988.
- (47) Holmes, A. H.; Moore, L. S. P.; Sundsfjord, A.; Steinbakk, M.; Regmi, S.; Karkey, A.; Guerin, P. J.; Piddock, L. J. V. Understanding the Mechanisms and Drivers of Antimicrobial Resistance. *Lancet* **2016**, *387*, 176–187.
- (48) Owens Jr., R. C.; Rice, L. Hospital-Based Strategies for Combating Resistance. *Clin. Infect. Dis.* **2006**, *42* (Suppl 4), S173–S181.
- (49) Lim, D.; Strynadka, N. C. J. Structural Basis for the β -Lactam Resistance of PBP2a from Methicillin-Resistant Staphylococcus Aureus. *Nat. Struct. Biol.* **2002**, *9* (11), 870–876.

- (50) Quinn, J. P.; Dudek, E. J.; DiVincenzo, C. A.; Lucks, D. A.; Lerner, S. A. Emergence of Resistance to Imipenem during Therapy for *Pseudomonas Aeruginosa* Infections. *J. Infect. Dis.* **1986**, *154* (2), 289–294.
- (51) Lynch, M. J.; Drusano, G. L.; Mobley, H. L. T. Emergence of Resistance to Imipenem in *Pseudomonas Aeruginosa*. *Antimicrob. Agents Chemother.* **1987**, *31* (12), 1892–1896.
- (52) El Amin, N.; Giske, C. G.; Jalal, S.; Keijsers, B.; Kronvall, G.; Wretling, B. Carbapenem Resistance Mechanisms in *Pseudomonas Aeruginosa*: Alterations of Porin OprD and Efflux Proteins Do Not Fully Explain Resistance Patterns. *Acta Pathol. Microbiol. Immunol. Scand.* **2005**, *113* (3), 187–196.
- (53) Bush, K.; Palzkill, T.; Jacoby, G. β -Lactamase Classification and Amino Acid Sequences for TEM, SHV, and OXA Extended-Spectrum and Inhibitor Resistant Enzymes <https://www.lahey.org/Studies/> (accessed Oct 18, 2018).
- (54) Pleiss, J. The Metallo- β -Lactamase Engineering Database <http://www.mbled.uni-stuttgart.de/> (accessed Oct 18, 2018).
- (55) National Center for Biotechnology Information. Bacterial Antimicrobial Resistance Reference Gene Database <https://www.ncbi.nlm.nih.gov/bioproject/PRJNA313047> (accessed Dec 18, 2018).
- (56) Johnson, A. P.; Woodford, N. Global Spread of Antibiotic Resistance : The Example of New Delhi Metallo- β -Lactamase (NDM)-Mediated Carbapenem Resistance. *J. Med. Microbiol.* **2013**, *62*, 499–513.
- (57) Miller, S. I.; Salama, N. R. The Gram-Negative Bacterial Periplasm: Size Matters. *PLoS Biol.* **2018**, *16* (1), e2004935.
- (58) Salton, M. R. J.; Kim, K. Structure. In *Medical Microbiology*; Baron, S., Ed.; Galveston, TX, 1996.
- (59) Razin, S. The Cell Membrane of Mycoplasma. *Ann. N. Y. Acad. Sci.* **1967**, *143* (1), 115–129.
- (60) Razin, S. Mycoplasma Membranes as Models in Membrane Research. In *Subcellular Biochemistry v. 20 Mycoplasma Cell Membranes*; Rotten, S., Kahane, I., Eds.; Springer Science + Business Media: New York, New York, 1993; pp 1–28.

- (61) Razin, S.; Yogev, D.; Naot, Y. Molecular Biology and Pathogenicity of Mycoplasmas. *Microbiol. Mol. Biol. Rev.* **1998**, *62* (4), 1094–1156.
- (62) Llarull, L. I.; Testero, S. A.; Fisher, J. F.; Mobashery, S. The Future of the β -Lactams. *Curr. Opin. Microbiol.* **2010**, *13*, 551–557.
- (63) Cabeen, M. T.; Jacobs-Wagner, C. Bacterial Cell Shape. *Nat. Rev. Microbiol.* **2005**, *3*, 601–610.
- (64) den Blaauwen, T.; de Pedro, M. A.; Nguyen-Distèche, M.; Ayala, J. A. Morphogenesis of Rod-Shaped Sacculi. *FEMS Microbiol. Rev.* **2008**, *32*, 321–344.
- (65) Korat, B.; Mottl, H.; Keck, W. Penicillin-binding Protein 4 of Escherichia Coli: Molecular Cloning of the DacB Gene, Controlled Overexpression, and Alterations in Murein Composition. *Mol. Microbiol.* **1991**, *5* (3), 675–684.
- (66) Spratt, B. G.; Pardee, A. B. Penicillin-Binding Proteins and Cell Shape in E. Coli. *Nature* **1975**, *254* (5500), 516–517.
- (67) Vollmer, W.; Blanot, D.; de Pedro, M. A. Peptidoglycan Structure and Architecture. *FEMS Microbiol. Rev.* **2008**, *32* (2), 149–167.
- (68) Goffin, C.; Ghuysen, J.-M. Multimodular Penicillin-Binding Proteins: An Enigmatic Family of Orthologs and Paralogs. *Microbiol. Mol. Biol. Rev.* **1998**, *62* (4), 1079–1093.
- (69) Nelson, D. E.; Young, K. D. Penicillin Binding Protein 5 Affects Cell Diameter, Contour, and Morphology of Escherichia Coli. *J. Bacteriol.* **2000**, *182* (6), 1714–1721.
- (70) Fisher, J. F.; Mobashery, S. The Sentinel Role of Peptidoglycan Recycling in the β -Lactam Resistance of the Gram-Negative Enterobacteriaceae and Pseudomonas Aeruginosa. *Bioorg. Chem.* **2014**, *56*, 41–48.
- (71) Priyadarshini, R.; Popham, D. L.; Young, K. D. Daughter Cell Separation by Penicillin-Binding Proteins and Peptidoglycan Amidases in Escherichia Coli. *J. Bacteriol.* **2006**, *188* (15), 5345–5355.
- (72) Vollmer, W.; Bertsche, U. Murein (Peptidoglycan) Structure, Architecture and Biosynthesis in Escherichia Coli. *Biochim. Biophys. Acta - Biomembr.* **2008**, *1778* (9), 1714–1734.
- (73) Macheboeuf, P.; Contreras-Martel, C.; Job, V.; Dideberg, O.; Dessen, A. Penicillin Binding

- Proteins: Key Players in Bacterial Cell Cycle and Drug Resistance Processes. *FEMS Microbiol. Rev.* **2006**, *30*, 673–691.
- (74) Litzinger, S.; Mayer, C. The Murein Sacculus. In *Prokaryotic Cell Wall Compounds - Structure and Biochemistry*; König, H., Claus, H., Varma, A., Eds.; Springer-Verlag Berlin Heidelberg: Mainz, Germany, 2010; pp 3–52.
- (75) Lee, M.; Heseck, D.; Blázquez, B.; Lastochkin, E.; Boggess, B.; Fisher, J. F.; Mobashery, S. Catalytic Spectrum of the Penicillin-Binding Protein 4 of *Pseudomonas Aeruginosa*, a Nexus for the Induction of B-Lactam Antibiotic Resistance. *J. Am. Chem. Soc.* **2015**, *137*, 190–200.
- (76) Dhar, S.; Kumari, H.; Balasubramanian, D.; Mathee, K. Cell-Wall Recycling and Synthesis in *Escherichia Coli* and *Pseudomonas Aeruginosa* – Their Role in the Development of Resistance. *J. Med. Microbiol.* **2018**, *67*, 1–21.
- (77) Suzuki, H.; Van Heijenoort, Y.; Tamura, T.; Mizoguchi, J.; Hirota, Y.; Van Heijenoort, J. In Vitro Peptidoglycan Polymerization Catalyzed by Penicillin Binding Protein 1b of *Escherichia Coli* K-12. *FEBS Lett.* **1980**, *110* (2), 245–249.
- (78) Ishino, F.; Mitsui, K.; Tamaki, S.; Matsushashi, M. Dual Enzyme Activities of Cell Wall Peptidoglycan Synthesis, Peptidoglycan Transglycosylase and Penicillin-Sensitive Transpeptidase, in Purified Preparations of *Escherichia Coli* Penicillin-Binding Protein 1A. *Biochem. Biophys. Res. Commun.* **1980**, *97* (1), 287–293.
- (79) Tamura, T.; Suzuki, H.; Nishimura, Y.; Mizoguchi, J.; Hirota, Y. On the Process of Cellular Division in *Escherichia Coli*: Isolation and Characterization of Penicillin-Binding Proteins 1a, 1b, and 3. *Proc. Natl. Acad. Sci. USA* **1980**, *77* (8), 4499–4503.
- (80) Terrak, M.; Ghosh, T. K.; Van Heijenoort, J.; Van Beeumen, J.; Lampilas, M.; Aszodi, J.; Ayala, J. A.; Ghuysen, J.-M.; Nguyen-Distèche, M. The Catalytic, Glycosyl Transferase and Acyl Transferase Modules of the Cell Wall Peptidoglycan-Polymerizing Penicillin-Binding Protein 1b of *Escherichia Coli*. *Mol. Microbiol.* **1999**, *34* (2), 350–364.
- (81) Schiffer, G.; Höltje, J.-V. Cloning and Characterization of PBP 1C, a Third Member of the Multimodular Class A Penicillin-Binding Proteins of *Escherichia Coli*. *J. Biol. Chem.* **1999**, *274* (45), 32031–32039.
- (82) Schwartz, U.; Seeger, K.; Wengenmayer, F.; Strecker, H. Penicillin-Binding Proteins of

- Escherichia Coli Identified with a 125I-Derivative of Ampicillin. *FEMS Microbiol. Lett.* **1981**, *10*, 107–109.
- (83) Hara, H.; Suzuki, H. A Novel Glycan Polymerase That Synthesizes Uncross-Linked Peptidoglycan in Escherichia Coli. *FEBS Lett.* **1984**, *168* (2), 155–160.
- (84) Di Berardino, M.; Dijkstra, A.; Stüber, D.; Keck, W.; Gubler, M. The Monofunctional Glycosyltransferase of Escherichia Coli Is a Member of a New Class of Peptidoglycan-Synthesising Enzymes. *FEBS Lett.* **1996**, *392*, 184–188.
- (85) Zapun, A.; Contreras-Martel, C.; Vernet, T. Penicillin-Binding Proteins and β -Lactam Resistance. *FEMS Microbiol. Rev.* **2008**, *32* (2), 361–385.
- (86) Spratt, B. G. Distinct Penicillin Binding Proteins Involved in the Division, Elongation, and Shape of Escherichia Coli K12. *Proc. Natl. Acad. Sci.* **1975**, *72* (8), 2999–3003.
- (87) Daniel, R. A.; Harry, E. J.; Errington, J. Role of Penicillin-Binding Protein PBP 2B in Assembly and Functioning of the Division Machinery of Bacillus Subtilis. *Mol. Microbiol.* **2000**, *35* (2), 299–311.
- (88) Zapun, A.; Vernet, T.; Pinho, M. G. The Different Shapes of Cocci. *FEMS Microbiol. Rev.* **2008**, *32* (2), 345–360.
- (89) Pagliero, E.; Chesnel, L.; Hopkins, J.; Croizé, J.; Dideberg, O.; Vernet, T.; Di Guilmi, A. M. Biochemical Characterization of Streptococcus Pneumoniae Penicillin-Binding Protein 2b and Its Implication in β -Lactam Resistance Biochemical Characterization of Streptococcus Pneumoniae Penicillin-Binding Protein 2b and Its Implication in β -Lactam Resi. *Antimicrob. Agents Chemother.* **2004**, *48* (5), 1848–1855.
- (90) Sassine, J.; Xu, M.; Sidiq, K. R.; Emmins, R.; Errington, J.; Daniel, R. A. Functional Redundancy of Division Specific Penicillin-Binding Proteins in Bacillus Subtilis. *Mol. Microbiol.* **2017**, *106* (2), 304–318.
- (91) Wei, Y.; Havasy, T.; McPherson, D. C.; Popham, D. L. Rod Shape Determination by the Bacillus Subtilis Class B Penicillin-Binding Proteins Encoded by PbpA and PbpH. *J. Bacteriol.* **2003**, *185* (16), 4717–4726.
- (92) Meberg, B. M.; Paulson, A. L.; Priyadarshini, R.; Young, K. D. Endopeptidase Penicillin-

- Binding Proteins 4 and 7 Play Auxiliary Roles in Determining Uniform Morphology of Escherichia Coli. *J. Bacteriol.* **2004**, *186* (24), 8326–8336.
- (93) Clarke, T. B.; Kawai, F.; Park, S.-Y.; Tame, J. R. H.; Dowson, C. G.; Roper, D. I. Mutational Analysis of the Substrate Specificity of Escherichia Coli Penicillin Binding Protein 4. *Biochemistry* **2009**, *48*, 2675–2683.
- (94) Gittins, J. R.; Phoenix, D. A.; Pratt, J. M. Multiple Mechanisms of Membrane Anchoring of Escherichia Coli Penicillin-Binding Proteins. *FEMS Microbiol. Rev.* **1994**, *13*, 1–12.
- (95) Harris, F.; Brandenburg, K.; Seydel, U.; Phoenix, D. Investigations into the Mechanisms Used by the C-Terminal Anchors of Escherichia Coli Penicillin-Binding Proteins 4, 5, 6 and 6b for Membrane Interaction. *Eur. J. Biochem.* **2002**, *269*, 5821–5829.
- (96) Stefanova, M. E.; Tomberg, J.; Olesky, M.; Hölftje, J.-V.; Gutheil, W. G.; Nicholas, R. A. Neisseria Gonorrhoeae Penicillin-Binding Protein 3 Exhibits Exceptionally High Carboxypeptidase and β -Lactam Binding Activities. *Biochemistry* **2003**, *42*, 14614–14625.
- (97) Judd, R. C.; Strange, J. C.; Pettit, R. K.; Shafer, W. M. Identification and Characterization of a Conserved Outer-membrane Protein of Neisseria Gonorrhoeae. *Mol. Microbiol.* **1991**, *5* (5), 1091–1096.
- (98) Shafer, W. M.; Judd, R. C. Gonococcal Penicillin-binding Protein 3 and the Surface-exposed 44kDa Peptidoglycan-binding Protein Appear to Be the Same Molecule. *Mol. Microbiol.* **1991**, *5* (5), 1097–1103.
- (99) Smith, J. D.; Kumarasiri, M.; Zhang, W.; Heseck, D.; Lee, M.; Toth, M.; Vakulenko, S.; Fisher, J. F.; Mobashery, S.; Chen, Y. Structural Analysis of the Role of Pseudomonas Aeruginosa Penicillin-Binding Protein 5 in β -Lactam Resistance. *Antimicrob. Agents Chemother.* **2013**, *57* (7), 3137–3146.
- (100) Nicholas, R. A.; Krings, S.; Tomberg, J.; Nicola, G.; Davies, C. Crystal Structure of Wild-Type Penicillin-Binding Protein 5 from Escherichia Coli: Implications for Deacylation of the Acyl-Enzyme Complex. *J. Biol. Chem.* **2003**, *278* (52), 52826–52833.
- (101) Vollmer, W.; Joris, B.; Charlier, P.; Foster, S. Bacterial Peptidoglycan (Murein) Hydrolases. *FEMS Microbiol. Rev.* **2008**, *32*, 259–286.

- (102) Guinane, C. M.; Cotter, P. D.; Ross, R. P.; Hill, C. Contribution of Penicillin-Binding Protein Homologs to Antibiotic Resistance, Cell Morphology, and Virulence of *Listeria Monocytogenes* EGDe. *Antimicrob. Agents Chemother.* **2006**, *50* (8), 2824–2828.
- (103) Morlot, C.; Noirclerc-Savoye, M.; Zapun, A.; Dideberg, O.; Vernet, T. The D,D-Carboxypeptidase PBP3 Organizes the Division Process of *Streptococcus Pneumoniae*. *Mol. Microbiol.* **2004**, *51* (6), 1641–1648.
- (104) Begg, K. J.; Dewar, S. J.; Donachie, W. D. A New *Escherichia Coli* Cell Division Gene, FtsK. *J. Bacteriol.* **1995**, *177* (21), 6211–6222.
- (105) van der Linden, M. P. G.; de Haan, L.; Hoyer, M. A.; Keck, W. Possible Role of *Escherichia Coli* Penicillin-Binding Protein 6 in Stabilization of Stationary-Phase Peptidoglycan. *J. Bacteriol.* **1992**, *174* (23), 7572–7578.
- (106) Romeis, T.; Höltje, J.-V. Penicillin-Binding Protein 7/8 of *Escherichia Coli* Is a DD-Endopeptidase. *Eur. J. Biochem.* **1994**, *224*, 597–604.
- (107) Henderson, T. A.; Templin, M.; Young, K. D. Identification and Cloning of the Gene Encoding Penicillin-Binding Protein 7 of *Escherichia Coli*. *J. Bacteriol.* **1995**, *177* (8), 2074–2079.
- (108) Noguchi, H.; Matsushashi, M.; Mitsushashi, S. Comparative Studies of Penicillin-Binding Proteins in *Pseudomonas Aeruginosa* and *Escherichia Coli*. *Eur. J. Biochem.* **1979**, *100*, 41–49.
- (109) Handfield, J.; Gagnon, L.; Dargis, M.; Huletsky, A. Sequence of the PonA Gene and Characterization of the Penicillin-Binding Protein 1A of *Pseudomonas Aeruginosa* PAO1. *Gene* **1997**, *199*, 49–56.
- (110) Legaree, B. A.; Daniels, K.; Weadge, J. T.; Cockburn, D.; Clarke, A. J. Function of Penicillin-Binding Protein 2 in Viability and Morphology of *Pseudomonas Aeruginosa*. *J. Antimicrob. Chemother.* **2007**, *59*, 411–424.
- (111) Chen, W.; Zhang, Y.-M.; Davies, C. Penicillin-Binding Protein 3 Is Essential for Growth of *Pseudomonas Aeruginosa*. *Antimicrob. Agents Chemother.* **2017**, *61* (1), e01651-16.
- (112) Rossi, C. G. A.; Gómez-Puertas, P.; Serrano, J. A. A. In Vivo Functional and Molecular

- Characterization of the Penicillin-Binding Protein 4 (DacB) of *Pseudomonas Aeruginosa*. *BMC Microbiol.* **2016**, *16* (234), 1–14.
- (113) Ropy, A.; Cabot, G.; Sánchez-Diener, I.; Aguilera, C.; Moya, B.; Ayala, J. A.; Oliver, A. Role of *Pseudomonas Aeruginosa* Low-Molecular-Mass Penicillin-Binding Proteins in AmpC Expression, β -Lactam Resistance, and Peptidoglycan Structure. *Antimicrob. Agents Chemother.* **2015**, *59*, 3925–3934.
- (114) Liao, X.; Hancock, R. E. W. Identification of a Penicillin-Binding Protein 3 Homolog , PBP3x , in *Pseudomonas Aeruginosa*: Gene Cloning and Growth Phase-Dependent Expression. *J. Bacteriol.* **1997**, *179* (5), 1490–1496.
- (115) Sainsbury, S.; Bird, L.; Rao, V.; Shepherd, S. M.; Stuart, D. I.; Hunter, W. N.; Owens, R. J.; Ren, J. Crystal Structures of Penicillin-Binding Protein 3 from *Pseudomonas Aeruginosa*: Comparison of Native and Antibiotic-Bound Forms. *J. Mol. Biol.* **2011**, *405* (1), 173–184.
- (116) Moyá, B.; Zamorano, L.; Juan, C.; Ge, Y.; Oliver, A. Affinity of the New Cephalosporin CXA-101 to Penicillin-Binding Proteins of *Pseudomonas Aeruginosa*. *Antimicrob. Agents Chemother.* **2010**, *54* (9), 3933–3937.
- (117) Curtis, N. A. C.; Orr, D.; Ross, G. W.; Boulton, M. G. Competition of β -Lactam Antibiotics for the Penicillin-Binding Proteins of *Pseudomonas Aeruginosa*, *Enterobacter Cloacae*, *Klebsiella Aerogenes*, *Proteus Rettgeri*, and *Escherichia Coli*: Comparison with Antibacterial Activity and Effects upon Bacterial Morpho. *Antimicrob. Agents Chemother.* **1979**, *16* (3), 325–328.
- (118) Spratt, B. G.; Cromie, K. D. Penicillin-Binding Proteins of Gram-Negative Bacteria. *Rev. Infect. Dis.* **1988**, *10* (4), 699–711.
- (119) Craig, W. A.; Andes, D. R. In Vivo Activities of Ceftolozane, a New Cephalosporin, with and without Tazobactam against *Pseudomonas Aeruginosa* and *Enterobacteriaceae*, Including Strains with Extended-Spectrum β -Lactamases, in the Thighs of Neutropenic Mice. *Antimicrob. Agents Chemother.* **2013**, *57* (4), 1577–1582.
- (120) Giancola, S. E.; Mahoney, M. V.; Bias, T. E.; Hirsch, E. B. Critical Evaluation of Ceftolozane–tazobactam for Complicated Urinary Tract and Intra-Abdominal Infections. *Ther. Clin. Risk Manag.* **2016**, *12*, 787–797.

- (121) Bassetti, M.; Vena, A.; Croxatto, A.; Righi, E.; Guery, B. How to Manage Pseudomonas Aeruginosa Infections. *Drugs Context* **2018**, *7*, 1–18.
- (122) Ceftolozane <https://www.drugbank.ca/drugs/DB09050> (accessed Jul 3, 2018).
- (123) Moyá, B.; Beceiro, A.; Cabot, G.; Juan, C.; Zamorano, L.; Alberti, S.; Oliver, A.; Oliver, A. Pan- β -Lactam Resistance Development in Pseudomonas Aeruginosa Clinical Strains: Molecular Mechanisms, Penicillin-Binding Protein Profiles, and Binding Affinities. *Antimicrob. Agents Chemother.* **2012**, *56* (9), 4771–4778.
- (124) Winkler, M. L.; Papp-Wallace, K. M.; Hujer, A. M.; Domitrovic, T. N.; Hujer, K. M.; Hurlless, K. N.; Tuohy, M.; Hall, G.; Bonomo, R. A. Unexpected Challenges in Treating Multidrug-Resistant Gram-Negative Bacteria: Resistance to Ceftazidime-Avibactam in Archived Isolates of Pseudomonas Aeruginosa. *Antimicrob. Agents Chemother.* **2015**, *59* (2), 1020–1029.
- (125) Hartman, B. J.; Tomasz, A. Low-Affinity Penicillin-Binding Protein Associated with r-Lactam Resistance in Staphylococcus Aureus. *J. Bacteriol.* **1984**, *158* (2), 513–516.
- (126) Utsui, Y.; Yokota, T. Role of an Altered Penicillin-Binding Protein in Methicillin- and Cephem-Resistant Staphylococcus Aureus. *Antimicrob. Agents Chemother.* **1985**, *28* (3), 397–403.
- (127) Ito, T.; Katayama, Y.; Asada, K.; Mori, N.; Tsutsumimoto, K.; Tiensasitorn, C.; Hiramatsu, K. Structural Comparison of Three Types of Staphylococcal Cassette Chromosome Mec Integrated in the Chromosome in Methicillin-Resistant Staphylococcus Aureus. *Antimicrob. Agents Chemother.* **2001**, *45* (5), 1323–1336.
- (128) Tsubakishita, S.; Kuwahara-Arai, K.; Sasaki, T.; Hiramatsu, K. Origin and Molecular Evolution of the Determinant of Methicillin Resistance in Staphylococci. *Antimicrob. Agents Chemother.* **2010**, *54* (10), 4352–4359.
- (129) Chambers, H. F.; Sachdeva, M. J.; Hackbarth, C. J. Kinetics of Penicillin Binding to Penicillin-Binding Proteins of Staphylococcus Aureus. *Biochem. J.* **1994**, *301*, 139–144.
- (130) Graves-Woodward, K.; Pratt, R. F. Reaction of Soluble Penicillin-Binding Protein 2a of Methicillin-Resistant Staphylococcus Aureus with β -Lactams and Acyclic Substrates: Kinetics in Homogeneous Solution. *Biochem. J.* **1998**, *332*, 755–761.

- (131) Lu, W.-P.; Sun, Y.; Bauer, M. D.; Paule, S.; Koenigs, P. M.; Kraft, W. G. Penicillin-Binding Protein 2a from Methicillin-Resistant *Staphylococcus Aureus*: Kinetic Characterization of Its Interactions with Beta-Lactams Using Electrospray Mass Spectrometry. *Biochemistry* **1999**, *38* (20), 6537–6546.
- (132) Pinho, M. G.; de Lencastre, H.; Tomasz, A. An Acquired and a Native Penicillin-Binding Protein Cooperate in Building the Cell Wall of Drug-Resistant *Staphylococci*. *Proc. Natl. Acad. Sci.* **2001**, *98* (19), 10886–10891.
- (133) Pinho, M. G.; Filipe, S. R.; De Lencastre, H.; Tomasz, A. Complementation of the Essential Peptidoglycan Transpeptidase Function of Penicillin-Binding Protein 2 (PBP2) by the Drug Resistance Protein PBP2A in *Staphylococcus Aureus*. *J. Bacteriol.* **2001**, *183* (22), 6525–6531.
- (134) Pucci, M. J.; Dougherty, T. J. Direct Quantitation of the Numbers of Individual Penicillin-Binding Proteins per Cell in *Staphylococcus Aureus*. *J. Bacteriol.* **2002**, *184* (2), 588–591.
- (135) Georgopapadakou, N. H. Penicillin-Binding Proteins and Bacterial Resistance to β -Lactams. *Antimicrob. Agents Chemother.* **1993**, *37* (10), 2045–2053.
- (136) Grundström, T.; Jaurin, B. Overlap between AmpC and Frd Operons on the *Escherichia Coli* Chromosome. *Proc. Natl. Acad. Sci.* **1982**, *79*, 1111–1115.
- (137) Olsson, O.; Bergström, S.; Normark, S. Identification of a Novel AmpC β -Lactamase Promoter in a Clinical Isolate of *Escherichia Coli*. *EMBO J.* **1982**, *1* (11), 1411–1416.
- (138) Bergström, S.; Olsson, O.; Normark, S. Common Evolutionary Origin of Chromosomal Beta-Lactamase Genes in Enterobacteria. *J. Bacteriol.* **1982**, *150* (2), 528–534.
- (139) Honoré, N.; Nicolas, M. H.; Cole, S. T. Inducible Cephalosporinase Production in Clinical Isolates of *Enterobacter Cloacae* Is Controlled by a Regulatory Gene That Has Been Deleted from *Escherichia Coli*. *EMBO J.* **1986**, *5* (13), 3709–3714.
- (140) Zeng, X.; Lin, J. β -Lactamase Induction and Cell Wall Metabolism in Gram-Negative Bacteria. *Front. Microbiol.* **2013**, *4*, 1–9.
- (141) Templin, M. F.; Edwards, D. H.; Höltje, J.-V. A Murein Hydrolase Is the Specific Target of Bulgecin in *Escherichia Coli*. *J. Biol. Chem.* **1992**, *267* (28), 20039–20043.

- (142) Park, J. T.; Uehara, T. How Bacteria Consume Their Own Exoskeletons (Turnover and Recycling of Cell Wall Peptidoglycan). *Microbiol. Mol. Biol. Rev.* **2008**, *72* (2), 211–227.
- (143) Jacobs, C.; Frère, J.-M.; Normark, S. Cytosolic Intermediates for Cell Wall Biosynthesis and Degradation Control Inducible β -Lactam Resistance in Gram-Negative Bacteria. *Cell* **1997**, *88*, 823–832.
- (144) Moya, B.; Dötsch, A.; Juan, C.; Blázquez, J.; Zamorano, L.; Haussler, S.; Oliver, A. β -Lactam Resistance Response Triggered by Inactivation of a Nonessential Penicillin-Binding Protein. *PLoS Pathog.* **2009**, *5* (3), e1000353.
- (145) Cheng, Q.; Li, H.; Merdek, K.; Park, J. T. Molecular Characterization of the β -N-Acetylglucosaminidase of Escherichia Coli and Its Role in Cell Wall Recycling. *J. Bacteriol.* **2000**, *182* (17), 4836–4840.
- (146) Höltje, J.-V.; Kopp, U.; Ursinus, A.; Wiedemann, B. The Negative Regulator of β -Lactamase Induction AmpD Is a N-Acetyl-Anhydromuramyl-L-Alanine Amidase. *FEMS Microbiol. Lett.* **1994**, *122*, 159–164.
- (147) Alksne, L. E.; Rasmussen, B. A. Expression of the AsbA1, OXA-12, and AsbM1 β -Lactamases in Aeromonas Jandaei AER 14 Is Coordinated by a Two-Component Regulon. *J. Bacteriol.* **1997**, *179* (6), 2006–2013.
- (148) Zamorano, L.; Moyà, B.; Juan, C.; Mulet, X.; Blázquez, J.; Oliver, A. The Pseudomonas Aeruginosa CreBC Two-Component System Plays a Major Role in the Response to β -Lactams, Fitness, Biofilm Growth, and Global Regulation. *Antimicrob. Agents Chemother.* **2014**, *58* (9), 5084–5095.
- (149) Yamamoto, K.; Hirao, K.; Oshima, T.; Aiba, H.; Utsumi, R.; Ishihama, A. Functional Characterization in Vitro of All Two-Component Signal Transduction Systems from Escherichia Coli. *J. Biol. Chem.* **2005**, *280* (2), 1448–1456.
- (150) Huang, H.-H.; Lin, Y.-T.; Chen, W.-C.; Huang, Y.-W.; Chen, S.-J.; Yang, T.-C. Expression and Functions of CreD, an Inner Membrane Protein in Stenotrophomonas Maltophilia. *PLoS One* **2015**, *10* (12), 1–16.
- (151) Hall, B. G.; Barlow, M. Evolution of the Serine β -Lactamases: Past , Present and Future. *Drug Resist. Updat.* **2004**, *7*, 111–123.

- (152) Medeiros, A. A. Evolution and Dissemination of β -Lactamases Accelerated by Generations of β -Lactam Antibiotics. *Clin. Infect. Dis.* **1997**, *24* (Suppl 1), S19-45.
- (153) Bodey, G. P.; Whitecar Jr., J. P.; Middleman, E.; Rodriguez, V. Carbenicillin Therapy for Pseudomonas Infections. *J. Am. Med. Assoc.* **1971**, *218* (1), 62–66.
- (154) Neu, H. C.; Labthavikul, P. Antibacterial Activity and , β -Lactamase Stability of Ceftazidime, an Aminothiazolyl Cephalosporin Potentially Active Against Pseudomonas Aeruginosa. *Antimicrob. Agents Chemother.* **1982**, *21* (1), 11–18.
- (155) Foord, R. D. Aspects of Clinical Trials with Ceftazidime Worldwide. *Am. J. Med.* **1985**, *79* (Suppl 2A), 110–113.
- (156) Philippon, A.; Labia, R.; Jacoby, G. Extended Spectrum β -Lactamases. *Antimicrob. Agents Chemother.* **1989**, *33* (8), 1131–1136.
- (157) Richmond, M. H.; Sykes, R. B. β -Lactamases of Gram-Negative Bacteria and Their Possible Physiological Role. *Adv. Microb. Physiol.* **1973**, *9*, 31–88.
- (158) Paterson, D. L.; Bonomo, R. A. Extended-Spectrum β -Lactamases: A Clinical Update. *Clin. Microbiol. Rev.* **2005**, *18* (4), 657–686.
- (159) Rodríguez-Baño, J.; Gutiérrez-Gutiérrez, B.; Machuca, I.; Pascual, A. Treatment of Infections Caused by Extended-Spectrum-Beta-Lactamase-, AmpC-, and Carbapenemase-Producing Enterobacteriaceae. *Clin. Microbiol. Rev.* **2018**, *31* (2), e00079-17.
- (160) Yong, D.; Toleman, M. A.; Giske, C. G.; Cho, H. S.; Sundman, K.; Lee, K.; Walsh, T. R. Characterization of a New Metallo- β -Lactamase Gene, Bla(NDM-1), and a Novel Erythromycin Esterase Gene Carried on a Unique Genetic Structure in Klebsiella Pneumoniae Sequence Type 14 from India. *Antimicrob. Agents Chemother.* **2009**, *53* (12), 5046–5054.
- (161) Pagano, M.; Martins, A. F.; Barth, A. L. Mobile Genetic Elements Related to Carbapenem Resistance in Acinetobacter Baumannii. *Brazilian J. Microbiol.* **2016**, *47* (4), 785–792.
- (162) Hudson, C. M.; Bent, Z. W.; Meagher, R. J.; Williams, K. P. Resistance Determinants and Mobile Genetic Elements of an NDM-1-Encoding Klebsiella Pneumoniae Strain. *PLoS One* **2014**, *9* (6), e99209.
- (163) van Duin, D.; Paterson, D. Multidrug Resistant Bacteria in the Community: Trends and

- Lessons Learned. *Infect. Dis. Clin. North Am.* **2016**, *30* (2), 377–390.
- (164) IDSA. Combating Antimicrobial Resistance: Policy Recommendations to Save Lives. *Clin. Infect. Dis.* **2011**, *52* (S5), S397–S428.
- (165) Newton, G. G. F.; Abraham, E. P. Cephalosporin C, a New Antibiotic Containing Sulphur and D- α -Aminoadipic Acid. *Nature* **1955**, *175*, 548.
- (166) Newton, G. G. F.; Abraham, E. P. Isolation of Cephalosporin C, a Penicillin-like Antibiotic Containing D- α -Aminoadipic Acid. *Biochem. J.* **1956**, *62*, 651–658.
- (167) Ayliffe, G. A. J. Ampicillin Inactivation and Sensitivity of Coliform Bacilli. *J. Gen. Microbiol.* **1963**, *30*, 339–348.
- (168) Jack, G. W.; Richmond, M. H. A Comparative Study of Eight Distinct β -Lactamases Synthesized by Gram-Negative Bacteria. *J. Gen. Microbiol.* **1970**, *61*, 43–61.
- (169) Richmond, M. H.; Jack, G. W.; Sykes, R. B. The β -Lactamases of Gram-Negative Bacteria Including Pseudomonads. *Ann. N. Y. Acad. Sci.* **1971**, *182*, 243–257.
- (170) Ambler, R. P. The Structure of β -Lactamases. *Philos. Trans. R. Soc. London. Ser. B Biol. Sci.* **1980**, *289* (1036), 321–331.
- (171) Jaurin, B.; Grundström, T. AmpC Cephalosporinase of Escherichia Coli K-12 Has a Different Evolutionary Origin from That of β -Lactamases of the Penicillinase Type. *Proc. Natl. Acad. Sci. USA* **1981**, *78* (8), 4897–4901.
- (172) Ouellette, M.; Bissonnette, L.; Roy, P. H. Precise Insertion of Antibiotic Resistance Determinants into Tn21-like Transposons: Nucleotide Sequence of the OXA-1. *Proc. Natl. Acad. Sci. USA* **1987**, *84*, 7378–7382.
- (173) Bush, K.; Jacoby, G. A. Updated Functional Classification of β -Lactamases. *Antimicrob. Agents Chemother.* **2010**, *54* (3), 969–976.
- (174) Bush, K.; Jacoby, G. A.; Medeiros, A. A. A Functional Classification Scheme for β -Lactamases and Its Correlation with Molecular Structure. *Antimicrob. Agents Chemother.* **1995**, *39* (6), 1211–1233.
- (175) Bush, K. Proliferation and Significance of Clinically Relevant β -Lactamases. *Ann. N. Y. Acad. Sci.* **2013**, *1277*, 84–90.

- (176) Liakopoulos, A.; Mevius, D.; Ceccarelli, D. A Review of SHV Extended-Spectrum β -Lactamases: Neglected Yet Ubiquitous. *FEMS Microbiol. Rev.* **2016**, *7*.
- (177) Hennequin, C.; Ravet, V.; Robin, F. Plasmids Carrying DHA-1 β -Lactamases. *Eur. J. Clin. Microbiol. Infect. Dis.* **2018**, *37*, 1197–1209.
- (178) Galleni, M.; Lamotte-Brasseur, J.; Rossolini, G. M.; Spencer, J.; Dideberg, O.; Frère, J.-M. Standard Numbering Scheme for Class B β -Lactamases. *Antimicrob. Agents Chemother.* **2001**, *45* (3), 660–663.
- (179) Hall, B. G.; Barlow, M. Revised Ambler Classification of β -Lactamases. *J. Antimicrob. Chemother.* **2005**, *55* (6), 1050–1051.
- (180) Bush, K. Recent Developments in β -Lactamase Research and Their Implications for the Future. *Rev. Infect. Dis.* **1988**, *10* (4), 681–690.
- (181) Bush, K. Classification of β -Lactamases: Groups 1, 2a, 2b, and 2b'. *Antimicrob. Agents Chemother.* **1989**, *33* (3), 264–270.
- (182) Bush, K. Classification of β -Lactamases: Group 2c, 2d, 2e, 3, and 4. *Antimicrob. Agents Chemother.* **1989**, *33* (3), 271–276.
- (183) Jacoby, G. A. β -Lactamase Nomenclature. *Antimicrob. Agents Chemother.* **2006**, *50* (4), 1123–1129.
- (184) Bradford, P. A. Extended-Spectrum β -Lactamases in the 21st Century: Characterization, Epidemiology, and Detection of This Important Resistance Threat. *Clin. Microbiol. Rev.* **2001**, *14* (4), 933–951.
- (185) ur Rahman, S.; Ali, T.; Ali, I.; Khan, N. A.; Han, B.; Gao, J. The Growing Genetic and Functional Diversity of Extended Spectrum Beta-Lactamases. *Biomed Res. Int.* **2018**, *2018*, 9519718.
- (186) Fonzé, E.; Vanhove, M.; Dive, G.; Sauvage, E.; Frère, J.-M.; Charlier, P. Crystal Structures of the *Bacillus Licheniformis* BS3 Class A β -Lactamase and of the Acyl-Enzyme Adduct Formed with Cefoxitin. *Biochemistry* **2002**, *41*, 1877–1885.
- (187) Díaz, N.; Sordo, T. L.; Merz, K. M.; Suárez, D. Insights into the Acylation Mechanism of Class A β -Lactamases from Molecular Dynamics Simulations of the TEM-1 Enzyme

- Complexed with Benzylpenicillin. *J. Am. Chem. Soc.* **2003**, *125* (3), 672–684.
- (188) Ke, W.; Bethel, C. R.; Papp-Wallace, K. M.; Pagadala, S. R. R.; Nottingham, M.; Fernandez, D.; Buynak, J. D.; Bonomo, R. A.; van den Akker, F. Crystal Structures of KPC-2 β -Lactamase in Complex with 3-Nitrophenyl Boronic Acid and the Penam Sulfone PSR-3-226. *Antimicrob. Agents Chemother.* **2012**, *56* (5), 2713–2718.
- (189) Pratt, R. F.; Loosemore, M. J. 6- β -Bromopenicillanic Acid, a Potent β -Lactamase Inhibitor. *Proc. Natl. Acad. Sci. USA* **1978**, *75* (9), 4145–4149.
- (190) Fisher, J.; Charnas, R. L.; Knowles, J. R. Kinetic Studies on the Inactivation of Escherichia Coli RTEM β -Lactamase by Clavulanic Acid. *Biochemistry* **1978**, *17* (11), 2180–2184.
- (191) Charnas, R. L.; Fisher, J.; Knowles, J. R. Chemical Studies on the Inactivation of Escherichia Coli RTEM β -Lactamase by Clavulanic Acid. *Biochemistry* **1978**, *17* (11), 2185–2189.
- (192) Knott-Hunziker, V.; Waley, S. G.; Orlek, B. S.; Sammes, P. G. Penicillinase Active Sites: Labelling of Serine-44 in β -Lactamase I by 6 β -Bromopenicillanic Acid. *FEBS Lett.* **1979**, *99* (1), 59–61.
- (193) Fisher, J.; Belasco, J. G.; Khosla, S.; Knowles, J. R. β -Lactamase Proceeds via an Acyl-Enzyme Intermediate. Interaction of the Escherichia Coli RTEM Enzyme with Cefoxitin. *Biochemistry* **1980**, *19* (13), 2895–2901.
- (194) Adachi, H.; Ohta, T.; Matsuzawa, H. Site-Directed Mutants, at Position 166, of RTEM-1 β -Lactamase That Form a Stable Acyl-Enzyme Intermediate with Penicillin. *J. Biol. Chem.* **1991**, *266* (5), 3186–3191.
- (195) Strynadka, N. C. J.; Adachi, H.; Jensen, S. E.; Johns, K.; Sielecki, A.; Betzel, C.; Sutoh, K.; James, M. N. G. Molecular Structure of the Acyl-Enzyme Intermediate in β -Lactam Hydrolysis at 1.7 Å Resolution. *Nature* **1992**, *359*, 700–705.
- (196) Chen, Y.; Bonnet, R.; Shoichet, B. K. The Acylation Mechanism of CTX-M β -Lactamase at 0.88 Å Resolution. *J. Am. Chem. Soc.* **2007**, *129* (17), 5378–5380.
- (197) Grigorenko, V. G.; Rubtsova, M. Y.; Uporov, I. V.; Ishtubaev, I. V.; Andreeva, I. P.; Shcherbinin, D. S.; Veselovsky, A. V.; Egorov, A. M. Bacterial TEM-Type Serine Beta-Lactamases: Structure and Analysis of Mutations. *Biochem. (Moscow), Suppl. Ser. B Biomed.*

- Chem.* **2018**, *12* (2), 87–95.
- (198) Page, M. G. P. Extended-Spectrum β -Lactamases: Structure and Kinetic Mechanism. *Clin. Microbiol. Infect.* **2008**, *14* (Suppl. 1), 63–74.
- (199) Poirel, L.; Héritier, C.; Podglajen, I.; Sougakoff, W.; Gutmann, L.; Nordmann, P. Emergence in *Klebsiella Pneumoniae* of a Chromosome-Encoded SHV β -Lactamase That Comprises the Efficacy of Imipenem. *Antimicrob. Agents Chemother.* **2003**, *47* (2), 755–758.
- (200) Bauernfeind, A.; Grimm, H.; Schweighart, S. A New Plasmidic Cefotaximase in a Clinical Isolate of *Escherichia Coli*. *Infection* **1990**, *18*, 294–298.
- (201) Cantón, R.; González-Alba, J. M.; Galán, J. C. CTX-M Enzymes: Origin and Diffusion. *Front. Microbiol.* **2012**, *3* (110), 1–19.
- (202) Shen, Z.; Ding, B.; Bi, Y.; Wu, S.; Xu, S.; Xu, X.; Guo, Q.; Wang, M. CTX-M-190, a Novel β -Lactamase Resistant to Tazobactam and Sulbactam, Identified in an *Escherichia Coli* Clinical Isolate. *Antimicrob. Agents Chemother.* **2017**, *61* (1), e01848-16.
- (203) Bevan, E. R.; Jones, A. M.; Hawkey, P. M. Global Epidemiology of CTX-M β -Lactamases: Temporal and Geographical Shifts in Genotype. *J. Antimicrob. Chemother.* **2017**, *72* (8), 2145–2155.
- (204) Yigit, H.; Queenan, A. M.; Anderson, G. J.; Domenech-Sanchez, A.; Biddle, J. W.; Steward, C. D.; Alberti, S.; Bush, K.; Tenover, F. C. Novel Carbapenem-Hydrolyzing β -Lactamase, KPC-1, from a Carbapenem-Resistant Strain of *Klebsiella Pneumoniae*. *Antimicrob. Agents Chemother.* **2001**, *45* (4), 1151–1161.
- (205) Pillai, D. R.; Melano, R.; Rawte, P.; Lo, S.; Tijet, N.; Fuksa, M.; Roda, N.; Farrell, D. J.; Krajden, S. *Klebsiella Pneumoniae* Carbapenemase, Canada. *Emerg. Infect. Dis.* **2009**, *15* (5), 827–829.
- (206) Munoz-Price, L. S.; Poirel, L.; Bonomo, R. A.; Schwaber, M. J.; Daikos, G. L.; Cormican, M.; Cornaglia, G.; Garau, J.; Giadkowski, M.; Hayden, M. K.; Kumarasamy, K.; Livermore, D. M.; Maya, J. J.; Nordmann, P.; Patel, J. B.; Paterson, D. L.; Pitout, J.; Villegas, M. V.; Wang, H.; Woodford, N.; Quinn, J. P. Clinical Epidemiology of the Global Expansion of *Klebsiella Pneumoniae* Carbapenemases. *Lancet Infect. Dis.* **2013**, *13* (9), 785–796.

- (207) van Duin, D.; Doi, Y. The Global Epidemiology of Carbapenemase-Producing Enterobacteriaceae. *Virulence* **2017**, 8 (4), 460–469.
- (208) Walther-Rasmussen, J.; Høiby, N. Class A Carbapenemases. *J. Antimicrob. Chemother.* **2007**, 60 (3), 470–482.
- (209) Dortet, L.; Poirel, L.; Abbas, S.; Oueslati, S.; Nordmann, P. Genetic and Biochemical Characterization of FRI-1, a Carbapenem-Hydrolyzing Class A β -Lactamase from *Enterobacter Cloacae*. *Antimicrob. Agents Chemother.* **2015**, 59 (12), 7420–7425.
- (210) Nicoletti, A. G.; Marcondes, M. F. M.; Martins, W. M. B. S.; Almeida, L. G. P.; Nicolás, M. F.; Vasconcelos, A. T. R.; Oliveira, V.; Gales, A. C. Characterization of BKC-1 Class A Carbapenemase from *Klebsiella Pneumoniae* Clinical Isolates in Brazil. *Antimicrob. Agents Chemother.* **2015**, 59 (9), 5159–5164.
- (211) Toth, M.; Vakulenko, V.; Antunes, N. T.; Frase, H.; Vakulenko, S. B. Class A Carbapenemase FPH-1 from *Francisella Philomiragia*. *Antimicrob. Agents Chemother.* **2012**, 56 (6), 2852–2857.
- (212) Mangat, C. S.; Boyd, D.; Janecko, N.; Martz, S.-L.; Desruisseau, A.; Carpenter, M.; Reid-Smith, R. J.; Mulvey, M. R. Characterization of VCC-1, a Novel Ambler Class A Carbapenemase from *Vibrio Cholerae* Isolated from Imported Retail Shrimp Sold in Canada. *Antimicrob. Agents Chemother.* **2016**, 60 (3), 1819–1825.
- (213) Girlich, D.; Poirel, L.; Nordmann, P. Novel Ambler Class A Carbapenem-Hydrolyzing β -Lactamase from a *Pseudomonas Fluorescens* Isolate from the Seine River, Paris, France. *Antimicrob. Agents Chemother.* **2010**, 54 (1), 328–332.
- (214) Ke, W.; Bethel, C. R.; Thomson, J. M.; Bonomo, R. A.; van den Akker, F. Crystal Structure of KPC-2: Insights into Carbapenemase Activity in Class A β -Lactamases. *Biochemistry* **2008**, 46 (19), 5732–5740.
- (215) Jacoby, G. A. AmpC β -Lactamases. *Clin. Microbiol. Rev.* **2009**, 22 (1), 161–182.
- (216) Galleni, M.; Amicosante, G.; Frère, J.-M. A Survey of the Kinetic Parameters of Class C β -Lactamases. *Biochem. J.* **1988**, 255, 123–129.
- (217) Philippon, A.; Arlet, G.; Jacoby, G. A. Plasmid-Determined AmpC-Type. *Antimicrob. Agents*

- Chemother.* **2002**, *46* (1), 1–11.
- (218) Conen, A.; Frei, R.; Adler, H.; Dangel, M.; Fux, C. A.; Widmer, A. F. Microbiological Screening Is Necessary to Distinguish Carriers of Plasmid-Mediated AmpC Beta-Lactamase-Producing Enterobacteriaceae and Extended-Spectrum Beta-Lactamase (ESBL)-Producing Enterobacteriaceae Because of Clinical Similarity. *PLoS One* **2015**, *10* (3), e0120688.
- (219) Nukaga, M.; Haruta, S.; Tanimoto, K.; Kogure, K.; Taniguchi, K.; Tamaki, M.; Sawai, T. Molecular Evolution of a Class C β -Lactamase Extending Its Substrate Specificity. *J. Biol. Chem.* **1995**, *270* (11), 5729–5735.
- (220) Oefner, C.; D’Arcy, A.; Daly, J. J.; Gubernator, K.; Charnas, R. L.; Heinze, I.; Hubschwerlen, C.; Winkler, F. K. Refined Crystal Structure of β -Lactamase from *Citrobacter freundii* Indicates a Mechanism for β -Lactam Hydrolysis. *Lett. To Nat.* **1990**, *343*, 284–288.
- (221) Fisher, J. F.; Meroueh, S. O.; Mobashery, S. Bacterial Resistance to β -Lactam Antibiotics: Compelling Opportunism, Compelling Opportunity. *Chem. Rev.* **2005**, *105* (2), 395–424.
- (222) Bauvois, C.; Ibuka, A. S.; Celso, A.; Alba, J.; Ishii, Y.; Frère, J.-M.; Galleni, M. Kinetic Properties of Four Plasmid-Mediated AmpC β -Lactamases. *Antimicrob. Agents Chemother.* **2005**, *49* (10), 4240–4246.
- (223) Lobkovsky, E.; Moews, P. C.; Liu, H.; Zhao, H.; Frère, J.-M.; Knox, J. R. Evolution of an Enzyme Activity: Crystallographic Structure at 2-Å Resolution of Cephalosporinase from the AmpC Gene of *Enterobacter Cloacae* P99 and Comparison with a Class A Penicillinase. *Proc. Natl. Acad. Sci. USA* **1993**, *90*, 11257–11261.
- (224) Kato-Toma, Y.; Iwashita, T.; Masuda, K.; Oyama, Y.; Ishiguro, M. PKa Measurements from Nuclear Magnetic Resonance of Tyrosine-150 in Class C β -Lactamase. *Biochem. J.* **2003**, *371*, 175–181.
- (225) Dubus, A.; Wilkin, J.-M.; Raquet, X.; Normark, S.; Frère, J.-M. Catalytic Mechanism of Active-Site Serine β -Lactamases: Role of the Conserved Hydroxy Group of the Lys-Thr(Ser)-Gly Triad. *Biochem. J.* **1994**, *301*, 485–494.
- (226) Tripathi, R.; Nair, N. N. Mechanism of Acyl–Enzyme Complex Formation from the Henry–Michaelis Complex of Class C B-Lactamases with B-Lactam Antibiotics. *J. Am. Chem. Soc.* **2013**, *135* (39), 14679–14690.

- (227) Tripathi, R.; Nair, N. N. Deacylation Mechanism and Kinetics of Acyl–Enzyme Complex of Class C β -Lactamase and Cephalothin. *J. Phys. Chem. B* **2016**, *120* (10), 2681–2690.
- (228) Bulychev, A.; Massova, I.; Miyashita, K.; Mobashery, S. Nuances of Mechanisms and Their Implications for Evolution of the Versatile β -Lactamase Activity: From Biosynthetic Enzymes to Drug Resistance Factors. *J. Am. Chem. Soc.* **1997**, *119* (33), 7619–7625.
- (229) Patera, A.; Blaszczyk, L. C.; Shoichet, B. K. Crystal Structures of Substrate and Inhibitor Complexes with AmpC β -Lactamase: Possible Implications for Substrate-Assisted Catalysis. *J. Am. Chem. Soc.* **2000**, *122* (43), 10504–10512.
- (230) Gherman, B. F.; Goldberg, S. D.; Cornish, V. W.; Friesner, R. A. Mixed Quantum Mechanical/Molecular Mechanical (QM/MM) Study of the Deacylation Reaction in a Penicillin Binding Protein (PBP) versus in a Class C β -Lactamase. *J. Am. Chem. Soc.* **2004**, *126* (24), 7652–7664.
- (231) Golemi, D.; Maveyraud, L.; Vakulenko, S.; Tranier, S.; Ishiwata, A.; Kotra, L. P.; Samama, J.-P.; Mobashery, S. The First Structural and Mechanistic Insights for Class D β -Lactamases : Evidence for a Novel Catalytic Process for Turnover of β -Lactam Antibiotics. *J. Am. Chem. Soc.* **2000**, *122* (7), 6132–6133.
- (232) Leonard, D. A.; Bonomo, R. A.; Powers, R. A. Class D β -Lactamases: A Reappraisal after Five Decades. *Acc. Chem. Res.* **2013**, *46* (11), 2407–2415.
- (233) Walther-Rasmussen, J.; Høiby, N. OXA-Type Carbapenemases. *J. Antimicrob. Chemother.* **2006**, *57* (3), 373–383.
- (234) Evans, B. A.; Amyes, S. G. B. OXA β -Lactamases. *Clin. Microbiol. Rev.* **2014**, *27* (2), 241–263.
- (235) Poirel, L.; Naas, T.; Nordmann, P. Diversity, Epidemiology, and Genetics of Class D β -Lactamases. *Antimicrob. Agents Chemother.* **2010**, *54* (1), 24–38.
- (236) Paetzel, M.; Danel, F.; de Castro, L.; Mosimann, S. C.; Page, M. G. P.; Strynadka, N. C. J. Crystal Structure of the Class D β -Lactamase OXA-10. *Nat. Struct. Biol.* **2000**, *7* (10), 918–925.
- (237) Maveyraud, L.; Golemi, D.; Kotra, L. P.; Tranier, S.; Vakulenko, S.; Mobashery, S.; Samama,

- J.-P. Insights into Class D β -Lactamases Are Revealed by the Crystal Structure of the OXA10 Enzyme from *Pseudomonas Aeruginosa*. *Structure* **2000**, 8 (12), 1289–1298.
- (238) Che, T.; Bonomo, R. A.; Shanmugam, S.; Bethel, C. R.; Pusztai-Carey, M.; Buynak, J. D.; Carey, P. R. Carboxylation and Decarboxylation of Active Site Lys 84 Controls the Activity of OXA-24 β -Lactamase of *Acinetobacter Baumannii*: Raman Crystallographic and Solution Evidence. *J. Am. Chem. Soc.* **2012**, 134, 11206–11215.
- (239) Golemi, D.; Maveyraud, L.; Vakulenko, S.; Samama, J.-P.; Mobashery, S. Critical Involvement of a Carbamylated Lysine in Catalytic Function of Class D β -Lactamases. *PNAS* **2001**, 98 (25), 14280–14285.
- (240) Leonard, D. A.; Hujer, A. M.; Smith, B. A.; Schneider, K. D.; Bethel, C. R.; Hujer, K. M.; Bonomo, R. A. The Role of OXA-1 β -Lactamase Asp66 in the Stabilization of the Active-Site Carbamate Group and in Substrate Turnover. *Biochem. J.* **2008**, 410 (3), 455–462.
- (241) Docquier, J.-D.; Calderone, V.; De Luca, F.; Benvenuti, M.; Giuliani, F.; Bellucci, L.; Tafi, A.; Nordmann, P.; Botta, M.; Rossolini, G. M.; Mangani, S. Crystal Structure of the OXA-48 β -Lactamase Reveals Mechanistic Diversity among Class D Carbapenemases. *Chem. Biol.* **2009**, 16 (5), 540–547.
- (242) Dale, J. W.; Smith, J. T. The Dimeric Nature of an R-Factor Mediated β -Lactamase. *Biochem. Biophys. Res. Commun.* **1976**, 68 (3), 1000–1005.
- (243) Pernot, L.; Frénois, F.; Rybkine, T.; L’Hermite, G.; Petrella, S.; Delettré, J.; Jarlier, V.; Collatz, E.; Sougakoff, W. Crystal Structures of the Class D β -Lactamase OXA-13 in the Native Form and in Complex with Meropenem. *J. Mol. Biol.* **2001**, 310, 859–874.
- (244) Franceschini, N.; Boschi, L.; Pollini, S.; Herman, R.; Perilli, M.; Galleni, M.; Frère, J.-M.; Amicosante, G.; Rossolini, G. M. Characterization of OXA-29 from *Legionella (Fluoribacter) Gormanii*: Molecular Class D β -Lactamase with Unusual Properties. *Antimicrob. Agents Chemother.* **2001**, 45 (12), 3509–3516.
- (245) Giuliani, F.; Docquier, J.-D.; Riccio, M. L.; Pagani, L.; Rossolini, G. M. OXA-46, a New Class D β -Lactamase of Narrow Substrate Specificity Encoded by a *BlaVIM-1*-Containing Integron from a *Pseudomonas Aeruginosa* Clinical Isolate. *Antimicrob. Agents Chemother.* **2005**, 49 (5), 1973–1980.

- (246) Sun, T.; Nukaga, M.; Mayama, K.; Braswell, E. H.; Knox, J. R. Comparison of β -Lactamases of Classes A and D: 1.5-Å Crystallographic Structure of the Class D OXA-1 Oxacillinase. *Protein Sci.* **2003**, *12*, 82–91.
- (247) Santillana, E.; Beceiro, A.; Bou, G.; Romero, A. Crystal Structure of the Carbapenemase OXA-24 Reveals Insights into the Mechanism of Carbapenem Hydrolysis. *Proc. Natl. Acad. Sci.* **2007**, *104* (13), 5354–5359.
- (248) Voha, C.; Docquier, J.-D.; Rossolini, G. M.; Fosse, T. Genetic and Biochemical Characterization of FUS-1 (OXA-85), a Narrow-Spectrum Class D β -Lactamase from *Fusobacterium Nucleatum* Subsp. Polymorphum. *Antimicrob. Agents Chemother.* **2006**, *50* (8), 2673–2679.
- (249) Krasauskas, R.; Labeikytė, D.; Markuckas, A.; Povilonis, J.; Armalytė, J.; Plančiūnienė, R.; Kavaliauskas, P.; Sužiedėlienė, E. Purification and Characterization of a New B-lactamase OXA-205 from *Pseudomonas Aeruginosa*. *Ann. Clin. Microbiol. Antimicrob.* **2015**, *14* (52), 1–8.
- (250) Fabiane, S. M.; Sohi, M. K.; Wan, T.; Payne, D. J.; Bateson, J. H.; Mitchell, T.; Sutton, B. J. Crystal Structure of the Zinc-Dependent β -Lactamase from *Bacillus Cereus* at 1.9 Å Resolution: Binuclear Active Site with Features of a Mononuclear Enzyme. *Biochemistry* **1998**, *37*, 12404–12411.
- (251) Concha, N. O.; Janson, C. A.; Rowling, P.; Pearson, S.; Cheever, C. A.; Clarke, B. P.; Lewis, C.; Galleni, M.; Frère, J.-M.; Payne, D. J.; Bateson, J. H.; Abdel-Meguid, S. S. Crystal Structure of the IMP-1 Metallo- β -Lactamase from *Pseudomonas Aeruginosa* and Its Complex with a Mecarptocarboxylate Inhibitor: Binding Determinants of a Potent, Broad-Spectrum Inhibitor. *Biochemistry* **2000**, *39*, 4288–4298.
- (252) Garcia-Saez, I.; Docquier, J.-D.; Rossolini, G. M.; Dideberg, O. The Three-Dimensional Structure of VIM-2, a Zn- β -Lactamase from *Pseudomonas Aeruginosa* in Its Reduced and Oxidised Form. *J. Mol. Biol.* **2008**, *375* (3), 604–611.
- (253) Zhang, H.; Hao, Q. Crystal Structure of NDM-1 Reveals a Common β -Lactam Hydrolysis Mechanism. *FASEB J.* **2011**, *25* (8), 2574–2582.
- (254) Palacios, A. R.; Mojica, M. F.; Giannini, E.; Taracila, M. A.; Bethel, C. R.; Alzari, P. M.;

- Otero, L. H.; Klinke, S.; Llarrull, L. I.; Bonomo, R. A.; Vila, A. J. The Reaction Mechanism of Metallo- β -Lactamases Is Tuned by the Conformation of an Active-Site Mobile Loop. *Antimicrob. Agents Chemother.* **2019**, *63*, e01754-18.
- (255) Nauton, L.; Kahn, R.; Garau, G.; Hernandez, J. F.; Dideberg, O. Structural Insights into the Design of Inhibitors for the L1 Metallo- β -Lactamase from *Stenotrophomonas Maltophilia*. *J. Mol. Biol.* **2008**, *375* (1), 257–269.
- (256) García-Sáez, I.; Mercuri, P. S.; Papamicael, C.; Kahn, R.; Frère, J. M.; Galleni, M.; Rossolini, G. M.; Dideberg, O. Three-Dimensional Structure of FEZ-1, a Monomeric Subclass B3 Metallo- β -Lactamase from *Fluoribacter Gormanii*, in Native Form and in Complex with D-Captopril. *J. Mol. Biol.* **2003**, *325* (4), 651–660.
- (257) Morán-Barrio, J.; Lisa, M.-N.; Larrieux, N.; Drusin, S. I.; Viale, A. M.; Moreno, D. M.; Buschiazzo, A.; Vila, A. J. Crystal Structure of the Metallo- β -Lactamase GOB in the Periplasmic Dizinc Form Reveals an Unusual Metal Site. *Antimicrob. Agents Chemother.* **2016**, *60* (10), 6013–6022.
- (258) Garau, G.; Bebrone, C.; Anne, C.; Galleni, M.; Frère, J.-M.; Dideberg, O. A Metallo- β -Lactamase Enzyme in Action: Crystal Structures of the Monozinc Carbapenemase CphA and Its Complex with Biapenem. *J. Mol. Biol.* **2005**, *345* (4), 785–795.
- (259) Fonseca, F.; Bromley, E. H. C.; Saavedra, M. J.; Correia, A.; Spencer, J. Crystal Structure of *Serratia Fonticola* Sfh-I: Activation of the Nucleophile in Mono-Zinc Metallo- β -Lactamases. *J. Mol. Biol.* **2011**, *411* (5), 951–959.
- (260) Garau, G.; García-Sáez, I.; Bebrone, C.; Anne, C.; Mercuri, P.; Galleni, M.; Frère, J.-M.; Dideberg, O. Update of the Standard Numbering Scheme for Class B β -Lactamases. *Antimicrob. Agents Chemother.* **2004**, *48* (7), 2347–2349.
- (261) Daiyasu, H.; Osaka, K.; Ishino, Y.; Toh, H. Expansion of the Zinc Metallo-Hydrolase Family of the β -Lactamase Fold. *FEBS Lett.* **2001**, *503*, 1–6.
- (262) Alderson, R. G.; Barker, D.; Mitchell, J. B. O. One Origin for Metallo- β -Lactamase Activity, or Two? An Investigation Assessing a Diverse Set of Reconstructed Ancestral Sequences Based on a Sample of Phylogenetic Trees. *J. Mol. Evol.* **2014**, *79*, 117–129.
- (263) Abraham, E. P.; Newton, G. G. A Comparison of the Action of Penicillinase on

- Benzylpenicillin and Cephalosporin N and the Competitive Inhibition of Penicillinase by Cephalosporin C. *Biochem. J.* **1956**, *63* (4), 628–634.
- (264) Kuwabara, S.; Abraham, E. P. Some Properties of Two Extracellular β -Lactamases from *Bacillus Cereus* 569/H. *Biochem. J.* **1967**, *103*, 859–861.
- (265) Sabath, L. D.; Abraham, E. P. Zinc as a Cofactor for Cephalosporinase from *Bacillus Cereus* 569. *Biochem. J.* **1966**, *98*, 11c–13c.
- (266) Saino, Y.; Kobayashi, F.; Inoue, M.; Mitsushashi, S. Purification and Properties of Inducible Penicillin β -Lactamase Isolated from *Pseudomonas Maltophilia*. *Antimicrob. Agents Chemother.* **1982**, *22* (4), 564–570.
- (267) Cuchural, G. J.; Malamy, M. H.; Tally, F. P. β -Lactamase-Mediated Imipenem Resistance in *Bacteroides Fragilis*. *Antimicrob. Agents Chemother.* **1986**, *30* (5), 645–648.
- (268) Shannon, K.; Phillips, I. The Effects on β -Lactam Susceptibility of Phenotypic Induction and Genotypic Derepression of β -Lactamase Synthesis. *J. Antimicrob. Chemother.* **1986**, *18* (Suppl E), 15–22.
- (269) Chang, Y.-T.; Lin, C.-Y.; Chen, Y.-H.; Hsueh, P.-R. Update on Infections Caused by *Stenotrophomonas Maltophilia* with Particular Attention to Resistance Mechanisms and Therapeutic Options. *Front. Microbiol.* **2015**, *6* (893), 1–20.
- (270) Watanabe, M.; Iyobe, S.; Inoue, M.; Mitsushashi, S. Transferable Imipenem Resistance in *Pseudomonas Aeruginosa*. *Antimicrob. Agents Chemother.* **1991**, *35* (1), 147–151.
- (271) Osano, E.; Arakawa, Y.; Wacharotayankun, R.; Ohta, M.; Horii, T.; Ito, H.; Yoshimura, F.; Kato, N. Molecular Characterization of an Enterobacterial Metallo β -Lactamase Found in a Clinical Isolate of *Serratia Marcescens* That Shows Imipenem Resistance. *Antimicrob. Agents Chemother.* **1994**, *38* (1), 71–78.
- (272) Walsh, T. R.; Toleman, M. A.; Poirel, L.; Nordmann, P. Metallo- β -Lactamases: The Quiet before the Storm? *Clin. Microbiol. Rev.* **2005**, *18* (2), 306–325.
- (273) Walsh, T. R. The Emergence and Implications of Metallo- β -Lactamases in Gram-Negative Bacteria. *Clin. Microbiol. Infect.* **2005**, *11* (Suppl 6), 2–9.
- (274) Queenan, A. M.; Bush, K. Carbapenemases: The Versatile Beta-Lactamases. *Clin. Microbiol.*

Rev. **2007**, *20* (3), 440--58, table of contents.

- (275) Oelschlaeger, P.; Ai, N.; DuPrez, K. T.; Welsh, W. J.; Toney, J. H. Evolving Carbapenemases: Can Medicinal Chemists Advance One Step Ahead of the Coming Storm? *J. Med. Chem.* **2010**, *53* (8), 3013–3027.
- (276) Matsumura, Y.; Peirano, G.; Motyl, M. R.; Adams, M. D.; Chen, L.; Kreiswirth, B.; DeVinney, R.; Pitout, J. D. D. Global Molecular Epidemiology of IMP-Producing Enterobacteriaceae. *Antimicrob. Agents Chemother.* **2017**, *61* (4), e02729-16.
- (277) Lauretti, L.; Riccio, M. L.; Mazzariol, A.; Cornaglia, G.; Amicosante, G.; Fontana, R.; Rossolini, G. M. Cloning and Characterization of Bla(VIM), a New Integron-Borne Metallo- β -Lactamase Gene from a Pseudomonas Aeruginosa Clinical Isolate. *Antimicrob. Agents Chemother.* **1999**, *43* (7), 1584–1590.
- (278) Matsumura, Y.; Peirano, G.; Devinney, R.; Bradford, P. A.; Motyl, M. R.; Adams, M. D.; Chen, L.; Kreiswirth, B.; Pitout, J. D. D. Genomic Epidemiology of Global VIM-Producing Enterobacteriaceae. *J. Antimicrob. Chemother.* **2017**, *72* (8), 2249–2258.
- (279) Chung, H.-S.; Hong, S. G.; Lee, Y.; Kim, M.; Yong, D.; Jeong, S. H.; Lee, K.; Chong, Y. Antimicrobial Susceptibility of Stenotrophomonas Maltophilia Isolates from a Korean Tertiary Care Hospital. *Yonsei Med. J.* **2012**, *53* (2), 439–441.
- (280) Shakil, S.; Azhar, E. I.; Tabrez, S.; Kamal, M. A.; Jabir, N. R.; Abuzenadah, A. M.; Damanhour, G. A.; Alam, Q. New Delhi Metallo- β -Lactamase (NDM-1): An Update. *J. Chemother.* **2011**, *23* (5), 35–38.
- (281) Walsh, T. R.; Weeks, J.; Livermore, D. M.; Toleman, M. A. Dissemination of NDM-1 Positive Bacteria in the New Delhi Environment and Its Implications for Human Health: An Environmental Point Prevalence Study. *Lancet Infect. Dis.* **2011**, *11* (5), 355–362.
- (282) Chowdhury, G.; Pazhani, G. P.; Sarkar, A.; Rajendran, K.; Mukhopadhyay, A. K.; Bhattacharya, M. K.; Ghosh, A.; Ramamurthy, T. Carbapenem Resistance in Clonally Distinct Clinical Strains of Vibrio Fluvialis Isolated from Diarrheal Samples. *Emerg. Infect. Dis.* **2016**, *22* (10), 1754–1761.
- (283) Huang, T.-W.; Wang, J.-T.; Lauderdale, T.-L.; Liao, T.-L.; Lai, J.-F.; Tan, M.-C.; Lin, A.-C.; Chen, Y.-T.; Tsai, S.-F.; Chang, S.-C. Complete Sequences of Two Plasmids in a BlaNDM-1-

- Positive *Klebsiella Oxytoca* Isolate from Taiwan. *Antimicrob. Agents Chemother.* **2013**, *57* (8), 4072–4076.
- (284) Boschi, L.; Mercuri, P. S.; Riccio, M. L.; Amicosante, G.; Galleni, M.; Frère, J.-M.; Rossolini, G. M. The *Legionella* (*Fluoribacter*) *Gormanii* Metallo- β -Lactamase: A New Member of the Highly Divergent Lineage of Molecular-Subclass B3 β -Lactamases. *Antimicrob. Agents Chemother.* **2000**, *44* (6), 1538–1543.
- (285) Saavedra, M. J.; Peixe, L.; Sousa, J. C.; Henriques, I.; Alves, A.; Correia, A. Sfh-I, a Subclass B2 Metallo- β -Lactamase from a *Serratia Fonticola* Environmental Isolate. *Antimicrob. Agents Chemother.* **2003**, *47* (7), 2330–2333.
- (286) Toleman, M. A.; Simm, A. M.; Murphy, T. A.; Gales, A. C.; Biedenbach, D. J.; Jones, R. N.; Walsh, T. R. Molecular Characterization of SPM-1, a Novel Metallo- β -Lactamase Isolated in Latin America: Report from the SENTRY Antimicrobial Surveillance Programme. *J. Antimicrob. Chemother.* **2002**, *50* (5), 673–679.
- (287) Murphy, T. A.; Catto, L. E.; Halford, S. E.; Hadfield, A. T.; Minor, W.; Walsh, T. R.; Spencer, J. Crystal Structure of *Pseudomonas Aeruginosa* SPM-1 Provides Insights into Variable Zinc Affinity of Metallo- β -Lactamases. *J. Mol. Biol.* **2006**, *357* (3), 890–903.
- (288) Castanheira, M.; Toleman, M. A.; Jones, R. N.; Schmidt, F. J.; Walsh, T. R. Molecular Characterization of a β -Lactamase Gene, BlaGIM-1, Encoding a New Subclass of Metallo- β -Lactamase. *Antimicrob. Agents Chemother.* **2004**, *48* (12), 4654–4661.
- (289) Lee, K.; Yum, J. H.; Yong, D.; Lee, H. M.; Kim, H. D.; Docquier, J.-D.; Rossolini, G. M.; Chong, Y. Novel Acquired Metallo- β -Lactamase Gene, BlaSIM-1, in a Class 1 Integron from *Acinetobacter Baumannii* Clinical Isolates from Korea. *Antimicrob. Agents Chemother.* **2005**, *49* (11), 4485–4491.
- (290) Sekiguchi, J.; Morita, K.; Kitao, T.; Watanabe, N.; Okazaki, M.; Miyoshi-Akiyama, T.; Kanamori, M.; Kirikae, T. KHM-1, a Novel Plasmid-Mediated Metallo- β -Lactamase from a *Citrobacter Freundii* Clinical Isolate. *Antimicrob. Agents Chemother.* **2008**, *52* (11), 4194–4197.
- (291) Poirel, L.; Rodríguez-Martínez, J.-M.; Al Naiemi, N.; Debets-Ossenkopp, Y. J.; Nordmann, P. Characterization of DIM-1, an Integron-Encoded Metallo- β -Lactamase from a *Pseudomonas*

- Stutzeri Clinical Isolate in the Netherlands. *Antimicrob. Agents Chemother.* **2010**, *54* (6), 2420–2424.
- (292) Yong, D.; Toleman, M. A.; Bell, J.; Ritchie, B.; Pratt, R.; Ryley, H.; Walsh, T. R. Genetic and Biochemical Characterization of an Acquired Subgroup B3 Metallo- β -Lactamase Gene, BlaAIM-1, and Its Unique Genetic Context in *Pseudomonas Aeruginosa* from Australia. *Antimicrob. Agents Chemother.* **2012**, *56* (12), 6154–6159.
- (293) Pollini, S.; Maradei, S.; Pecile, P.; Olivo, G.; Luzzaro, F.; Docquier, J.-D.; Rossolini, G. M. FIM-1, a New Acquired Metallo- β -Lactamase from a *Pseudomonas Aeruginosa* Clinical Isolate from Italy. *Antimicrob. Agents Chemother.* **2013**, *57* (1), 410–416.
- (294) Hong, D. J.; Bae, I. K.; Jang, I.-H.; Jeong, S. H.; Kang, H.-K.; Lee, K. Epidemiology and Characteristics of Metallo- β -Lactamase-Producing *Pseudomonas Aeruginosa*. *Infect. Chemother.* **2015**, *47* (2), 81–97.
- (295) Kazmierczak, K. M.; Rabine, S.; Hackel, M.; McLaughlin, R. E.; Biedenbach, D. J.; Bouchillon, S. K.; Sahn, D. F.; Bradford, P. A. Multiyear, Multinational Survey of the Incidence and Global Distribution of Metallo- β -Lactamase-Producing Enterobacteriaceae and *Pseudomonas Aeruginosa*. *Antimicrob. Agents Chemother.* **2016**, *60* (2), 1067–1078.
- (296) Logan, L. K.; Weinstein, R. A. The Epidemiology of Carbapenem-Resistant Enterobacteriaceae: The Impact and Evolution of a Global Menace. *J. Infect. Dis.* **2017**, *215* (Suppl 1), S28–S36.
- (297) Ghasemian, A.; Rizi, K. S.; Vardanjani, H. R.; Nojoomi, F. Prevalence of Clinically Isolated Metallo-Beta-Lactamase-Producing *Pseudomonas Aeruginosa*, Coding Genes, and Possible Risk Factors in Iran. *Iran. J. Pathol.* **2018**, *13* (1), 1–9.
- (298) Meini, M.-R.; Llarrull, L. I.; Vila, A. J. Overcoming Differences: The Catalytic Mechanism of Metallo- β -Lactamases. *FEBS Lett.* **2015**, *589*, 3419–3432.
- (299) Bounaga, S.; Laws, A. P.; Galleni, M.; Page, M. I. The Mechanism of Catalysis and the Inhibition of the *Bacillus Cereus* Zinc-Dependent β -Lactamase. *Biochem. J.* **1998**, *331*, 703–711.
- (300) Wang, Z.; Fast, W.; Benkovic, S. J. On the Mechanism of the Metallo- β -Lactamase from *Bacteroides Fragilis*. *Biochemistry* **1999**, *38*, 10013–10023.

- (301) Garrity, J. D.; Carenbauer, A. L.; Herron, L. R.; Crowder, M. W. Metal Binding Asp-120 in Metallo- β -Lactamase L1 from *Stenotrophomonas Maltophilia* Plays a Crucial Role in Catalysis. *J. Biol. Chem.* **2004**, *279* (2), 920–927.
- (302) Yamaguchi, Y.; Kuroki, T.; Yasuzawa, H.; Higashi, T.; Jin, W.; Kawanami, A.; Yamagata, Y.; Arakawa, Y.; Goto, M.; Kurosaki, H. Probing the Role of Asp-120(81) of Metallo-Beta-Lactamase (IMP-1) by Site-Directed Mutagenesis, Kinetic Studies, and X-Ray Crystallography. *J. Biol. Chem.* **2005**, *280* (21), 20824–20832.
- (303) Llarrull, L. I.; Fabiane, S. M.; Kowalski, J. M.; Bennett, B.; Sutton, B. J.; Vila, A. J. Asp-120 Locates Zn²⁺ for Optimal Metallo- β -Lactamase Activity. *J. Biol. Chem.* **2007**, *282* (25), 18276–18285.
- (304) Saz, A. K.; Lowery, D. L.; Jackson, L. J. Staphylococcal Penicillinase. *J. Bacteriol.* **1961**, *82*, 298–304.
- (305) Hou, J. P.; Poole, J. W. Measurement of β -Lactamase Activity and Rate of Inactivation of Penicillins by a PH-Stat Alkalimetric Titration Method. *J. Pharm. Sci.* **1972**, *61* (10), 1594–1598.
- (306) Perret, C. J. Iodometric Assay of Penicillinase. *Nature* **1954**, *174*, 1012–1013.
- (307) Novick, R. P. Micro-Iodometric Assay for Penicillinase. *Biochem. J.* **1962**, *83*, 236–240.
- (308) Sargent, M. G. Rapid Fixed-Time Assay for Penicillinase. *J. Bacteriol.* **1968**, *95* (4), 1493–1494.
- (309) Henry, R. J.; Housewright, R. D. Studies on Penicillinase. II. Manometric Method of Assaying Penicillinase and Penicillin, Kinetic of the Penicillin-Penicillinase Reaction, and the Effects of Inhibitors of Penicillinase. *J. Biol. Chem.* **1947**, *167*, 559–571.
- (310) O'Callaghan, C. H.; Morris, a; Kirby, S. M.; Shingler, a H. Novel Method for Detection of Beta-Lactamases by Using a Chromogenic Cephalosporin Substrate. *Antimicrob. Agents Chemother.* **1972**, *1* (4), 283–288.
- (311) Samuni, A. A Direct Spectrophotometric Assay and Determination of Michaelis Constants for the β -Lactamase Reaction. *Anal. Biochem.* **1975**, *63*, 17–26.
- (312) Schindler, P.; Huber, G. Use of PADAC, A Novel Chromogenic β -Lactamase Substrate, for

- the Detection of β -Lactamase Producing Organisms and Assay of β -Lactamase Inhibitors/Inactivators. In *Enzyme Inhibitors*, Verlag Chemie; Brodbeck, U., Ed.; Weinheim, West Germany, 1980; pp 169–176.
- (313) Jones, R. N.; Wilson, H. W.; Novick, W. J.; Barry, A. L.; Thornsberry, C. In Vitro Evaluation of CENTA, a New Beta-Lactamase-Susceptible Chromogenic Cephalosporin Reagent. *J. Clin. Microbiol.* **1982**, *15* (5), 954–958.
- (314) Jones, R. N.; Wilson, H. W.; Novick, W. J. In Vitro Evaluation of Pyridine-2-Azo-p-Dimethylaniline Cephalosporin, a New Diagnostic Chromogenic Reagent, an Comparison with Nitrocefin, Cephacetrile, and Other Beta-Lactam Compounds. *J. Clin. Microbiol.* **1982**, *15* (4), 677–683.
- (315) Yu, S.; Vosbeek, A.; Corbella, K.; Severson, J.; Schesser, J.; Sutton, L. D. A Chromogenic Cephalosporin for β -Lactamase Inhibitor Screening Assays. *Anal. Biochem.* **2012**, *428* (2), 96–98.
- (316) Gao, W.; Xing, B.; Tsien, R. Y.; Rao, J. Novel Fluorogenic Substrates for Imaging β -Lactamase Gene Expression. *J. Am. Chem. Soc.* **2003**, *125* (37), 11146–11147.
- (317) van Berkel, S. S.; Brem, J.; Rydzik, A. M.; Salimraj, R.; Cain, R.; Verma, A.; Owens, R. J.; Fishwick, C. W. G.; Spencer, J.; Schofield, C. J. Assay Platform for Clinically Relevant Metallo- β -Lactamases. *J. Med. Chem.* **2013**, *56* (17), 6945–6953.
- (318) Xie, H.; Mire, J.; Kong, Y.; Chang, M.; Hassounah, H. A.; Thornton, C. N.; Sacchettini, J. C.; Cirillo, J. D.; Rao, J. Rapid Point-of-Care Detection of the Tuberculosis Pathogen Using a BlaC-Specific Fluorogenic Probe. *Nat. Chem.* **2012**, *4* (10), 802–809.
- (319) Rolinson, G. N.; Stevens, S.; Batchelor, F. R.; Wood, J. C.; Chain, E. B. Bacteriological Studies on a New Penicillin-BRL.1241. *Lancet* **1960**, *276* (7150), 564–567.
- (320) Kiener, P. A.; Waley, S. G. Substrate-Induced Deactivation of Penicillinases Studies of β -Lactamase I by Hydrogen Exchange. *Biochem. J.* **1977**, *165*, 279–285.
- (321) Persaud, K. C.; Pain, R. H.; Virden, R. Reversible Deactivation of β -Lactamase by Quinacillin. Extent of the Conformational Change in the Isolated Transitory Complex. *Biochem. J.* **1986**, *237*, 723–730.

- (322) Fink, A. L.; Behner, K. M.; Tan, A. K. Kinetic and Structural Characterization of Reversibly Inactivated β -Lactamase. *Biochemistry* **1987**, *26* (14), 4248–4258.
- (323) Faraci, W. S.; Pratt, R. F. Mechanism of Inhibition of the PC1 β -Lactamase of *Staphylococcus Aureus* by Cephalosporins: Importance of the 3'-Leaving Group. *Biochemistry* **1985**, *24*, 903–910.
- (324) Faraci, W. S.; Pratt, R. F. Mechanism of Inhibition of RTEM-2 β -Lactamase by Cephamycins: Relative Importance of the 7 α -Methoxy Group and the 3' Leaving Group. *Biochemistry* **1986**, *25*, 2934–2941.
- (325) Charnas, R. L.; Then, R. L. Mechanism of Inhibition of Chromosomal β -Lactamases by Third-Generation Cephalosporins. *Rev. Infect. Dis.* **1988**, *10* (4), 752–760.
- (326) Mazzella, L. J.; Pratt, R. F. Effect of the 3'-Leaving Group on Turnover of Cephem Antibiotics by a Class C β -Lactamase. *Biochem. J.* **1989**, *259*, 255–260.
- (327) Powers, R. A.; Caselli, E.; Focia, P. J.; Prati, F.; Shoichet, B. K. Structures of Ceftazidime and Its Transition-State Analogue in Complex with AmpC β -Lactamase: Implications for Resistance Mutations and Inhibitor Design. *Biochemistry* **2001**, *40* (31), 9207–9214.
- (328) Mitchell, J. M.; Clasman, J. R.; June, C. M.; Kaitany, K.-C. J.; LaFleur, J. R.; Taracila, M. A.; Klinger, N. V.; Bonomo, R. A.; Wymore, T.; Szarecka, A.; Powers, R. A.; Leonard, D. A. Structural Basis of Activity against Aztreonam and Extended Spectrum Cephalosporins for Two Carbapenem-Hydrolyzing Class D β -Lactamases from *Acinetobacter Baumannii*. *Biochemistry* **2015**, *54* (10), 1976–1987.
- (329) Patel, M. P.; Hu, L.; Stojanoski, V.; Sankaran, B.; Prasad, B. V. V.; Palzkill, T. The Drug-Resistant Variant P167S Expands the Substrate Profile of CTX-M β -Lactamases for Oxyimino-Cephalosporin Antibiotics by Enlarging the Active Site upon Acylation. *Biochemistry* **2017**, *56* (27), 3443–3453.
- (330) Charnas, R. L.; Knowles, J. R. Inhibition of the RTEM β -Lactamase from *Escherichia Coli*. Interaction of the Enzyme with Derivatives of Olivanic Acid. *Biochemistry* **1981**, *20*, 2732–2737.
- (331) Easton, C. J.; Knowles, J. R. Inhibition of the RTEM β -Lactamase from *Escherichia Coli*. Interaction of the Enzyme with Derivatives of Olivanic Acid. *Biochemistry* **1982**, *21* (12),

2857–2862.

- (332) Zafaralla, G.; Mobashery, S. Facilitation of the $\Delta^2 \rightarrow \Delta^1$ Pyrroline Tautomerization of Carbapenem Antibiotics by the Highly Conserved Arginine-244 of Class A β -Lactamases during the Course of Turnover. *J. Am. Chem. Soc.* **1992**, *114* (4), 1505–1506.
- (333) Maveyraud, L.; Mourey, L.; Kotra, L. P.; Pedelacq, J.-D.; Guillet, V.; Mobashery, S.; Samama, J.-P. Structural Basis for Clinical Longevity of Carbapenem Antibiotics in the Face of Challenge by the Common Class A β -Lactamases from the Antibiotic-Resistant Bacteria. *J. Am. Chem. Soc.* **1998**, *120* (38), 9748–9752.
- (334) Nukaga, M.; Bethel, C. R.; Thomson, J. M.; Hujer, A. M.; Distler, A.; Anderson, V. E.; Knox, J. R.; Bonomo, R. A. Inhibition of Class A β -Lactamases by Carbapenems: Crystallographic Observation of Two Conformations of Meropenem in SHV-1. *J. Am. Chem. Soc.* **2008**, *130* (38), 12656–12662.
- (335) Beadle, B. M.; Shoichet, B. K. Structural Basis for Imipenem Inhibition of Class C β -Lactamases. *Antimicrob. Agents Chemother.* **2002**, *46* (12), 3978–3980.
- (336) Nagano, R.; Adachi, Y.; Imamura, H.; Yamada, K.; Hashizume, T.; Morishima, H. Carbapenem Derivatives as Potential Inhibitors of Various β -Lactamases, Including Class B Metallo- β -Lactamases. *Antimicrob. Agents Chemother.* **1999**, *43* (10), 2497–2503.
- (337) Bonnefoy, A.; Dupuis-Hamelin, C.; Steier, V.; Delachaume, C.; Seys, C.; Stachyra, T.; Fairley, M.; Guitton, M.; Lampilas, M. In Vitro Activity of AVE1330A, an Innovative Broad-Spectrum Non- β -Lactam β -Lactamase Inhibitor. *J. Antimicrob. Chemother.* **2004**, *54* (2), 410–417.
- (338) U.S. Food and Drug Administration. Drug Trials Snapshot: AVYCAZ (cIAI) <https://www.fda.gov/Drugs/InformationOnDrugs/ucm441042.htm> (accessed Dec 6, 2018).
- (339) Howarth, T. T.; Brown, A. G.; King, T. J. Clavulanic Acid, a Novel β -Lactam Isolated from *Streptomyces Clavuligerus*; X-Ray Crystal Structure Analysis. *J. Chem. Soc. Chem. Commun.* **1976**, 266–267.
- (340) Reading, C.; Cole, M. Clavulanic Acid: A Beta-Lactamase-Inhibiting Beta-Lactam from *Streptomyces Clavuligerus*. *Antimicrob. Agents Chemother.* **1977**, *11* (5), 852–857.

- (341) English, A. R.; Retsema, J. A.; Girard, A. E.; Lynch, J. E.; Barth, W. E. CP-45,899, a Beta-Lactamase Inhibitor That Extends the Antibacterial Spectrum of Beta-Lactams: Initial Bacteriological Characterization. *Antimicrob Agents Chemother* **1978**, *14* (3), 414–419.
- (342) Bush, K.; Macalintal, C.; Rasmussen, B. A.; Lee, V. J.; Yang, Y. Kinetic Interactions of Tazobactam with β -Lactamases from All Major Structural Classes. *Antimicrob. Agents Chemother.* **1993**, *37* (4), 851–858.
- (343) Micetich, R. G.; Maiti, S. N.; Spevak, P.; Hall, T. W.; Yamabe, S.; Ishida, N.; Tanaka, M.; Yamazaki, T.; Nakai, A.; Ogawa, K. Synthesis and β -Lactamase Inhibitory Properties of 2 β -[(1,2,3-Triazol-1-Yl)methyl]-2 α -Methylpenam-3 α -Carboxylic Acid 1,1-Dioxide and Related Triazolyl Derivatives. *J. Med. Chem.* **1987**, *30* (8), 1469–1474.
- (344) Brown, R. P. A.; Aplin, R. T.; Schofield, C. J. Inhibition of TEM-2 β -Lactamase from *Escherichia Coli* by Clavulanic Acid: Observation of Intermediates by Electrospray Ionization Mass Spectrometry. *Biochemistry* **1996**, *35* (38), 12421–12432.
- (345) Brown, R. P. A.; Aplin, R. T.; Schofield, C. J.; Frydrych, C. H. Mass Spectrometric Studies on the Inhibition of TEM-2 β -Lactamase by Clavulanic Acid Derivatives. *J. Antibiot. (Tokyo)*. **1997**, *50* (2), 184–185.
- (346) Kalp, M.; Buynak, J. D.; Carey, P. R. Role of E166 in the Imine to Enamine Tautomerization of the Clinical β -Lactamase Inhibitor Sulbactam. *Biochemistry* **2009**, *48*, 10196–10198.
- (347) Knowles, J. R. Penicillin Resistance: The Chemistry of β -Lactamase Inhibition. *Acc. Chem. Res.* **1985**, *18*, 97–104.
- (348) Therrien, C.; Levesque, R. C. Molecular Basis of Antibiotic Resistance and β -Lactamase Inhibition by Mechanism-Based Inactivators: Perspectives and Future Directions. *FEMS Microbiol. Rev.* **2000**, *24* (3), 251–262.
- (349) Buynak, J. D. Understanding the Longevity of the β -Lactam Antibiotics and of Antibiotic/ β -Lactamase Inhibitor Combinations. *Biochem. Pharmacol.* **2006**, *71* (7), 930–940.
- (350) Cartwright, S. J.; Coulson, A. F. W. A Semi-Synthetic Penicillinase Inactivator. *Nature* **1979**, *278*, 360–361.
- (351) Richter, H. G. F.; Angehrn, P.; Hubschwerlen, C.; Kania, M.; Page, M. G. P.; Specklin, J.-L.;

- Winkler, F. K. Design, Synthesis, and Evaluation of 2 β -Alkenyl Penam Sulfone Acids as Inhibitors of β -Lactamases. *J. Med. Chem.* **1996**, *39*, 3712–3722.
- (352) Phillips, O. A.; Reddy, A. V. N.; Setti, E. L.; Spevak, P.; Czajkowski, D. P.; Atwal, H.; Salama, S.; Micetich, R. G.; Maiti, S. N. Synthesis and Biological Evaluation of Penam Sulfones as Inhibitors of β -Lactamases. *Bioorganic Med. Chem.* **2005**, *13*, 2847–2858.
- (353) Loosemore, M. J.; Cohen, S. A.; Pratt, R. F. Inactivation of Bacillus Cereus β -Lactamase I by 6 β -Bromopenicillanic Acid: Kinetics. *Biochemistry* **1980**, *19*, 3990–3995.
- (354) Wise, R.; Andrews, J. M.; Patel, N. 6- β -Bromo- and 6- β -Iodo Penicillanic Acid, Two Novel β -Lactamase Inhibitors. *J. Antimicrob. Chemother.* **1981**, *7*, 531–536.
- (355) Sauvage, E.; Zervosen, A.; Dive, G.; Herman, R.; Amoroso, A.; Joris, B.; Fonzé, E.; Pratt, R. F.; Luxen, A.; Charlier, P.; Kreff, F. Structural Basis of the Inhibition of Class A β -Lactamases and Penicillin-Binding Proteins by 6- β -Iodopenicillanate. *J. Am. Chem. Soc.* **2009**, *131* (16), 15262–15269.
- (356) Arisawa, M.; Then, R. L. 6-Acetylmethylenepenicillanic Acid (Ro 15-1903), A Potent β -Lactamase Inhibitor. I. Inhibition of Chromosomally and R-Factor-Mediated β -Lactamases. *J. Antibiot. (Tokyo)*. **1982**, *35* (11), 1578–1583.
- (357) Arisawa, M.; Then, R. Inactivation of TEM-1 β -Lactamase by 6-Acetylmethylenepenicillanic Acid. *Biochem. J.* **1983**, *209*, 609–615.
- (358) Brenner, D. G.; Knowles, J. R. 6-(Methoxymethylene)Penicillanic Acid: Inactivator of RTEM β -Lactamase from Escherichia Coli. *Biochemistry* **1984**, *23*, 5839–5846.
- (359) Adam, S.; Then, R.; Angehrn, P. Potential Prodrugs of 6-Acetylmethylenepenicillanic Acid (Ro 15-1903). *J. Antibiot. (Tokyo)*. **1986**, *39* (6), 833–838.
- (360) Adam, S.; Then, R.; Angehrn, P. (6R)-6-(Substituted Methyl)Penicillanic Acid Sulfones: New Potent β -Lactamase Inhibitors. *J. Antibiot. (Tokyo)*. **1992**, *46* (4), 641–646.
- (361) Ehmman, D. E.; Jahić, H.; Ross, P. L.; Gu, R.-F.; Hu, J.; Durand-Réville, T. F.; Lahiri, S.; Thresher, J.; Livchak, S.; Gao, N.; Palmer, T.; Walkup, G. K.; Fisher, S. L. Kinetics of Avibactam Inhibition against Class A, C, and D β -Lactamases. *J. Biol. Chem.* **2013**, *288* (39), 27960–27971.

- (362) Shlaes, D. M. New β -Lactam- β -Lactamase Inhibitor Combinations in Clinical Development. *Ann. N. Y. Acad. Sci.* **2013**, *1277*, 105–114.
- (363) Merck & Co. Inc. *Merck Pipeline as of November 1, 2018*; 2018.
- (364) Papp-Wallace, K. M.; Nguyen, N. Q.; Jacobs, M. R.; Bethel, C. R.; Barnes, M. D.; Kumar, V.; Bajaksouzian, S.; Rudin, S. D.; Rather, P. N.; Bhavsar, S.; Ravikumar, T.; Deshpande, P. K.; Patil, V.; Yeole, R.; Bhagwat, S. S.; Patel, M. V.; van den Akker, F.; Bonomo, R. A. Strategic Approaches to Overcome Resistance against Gram-Negative Pathogens Using β -Lactamase Inhibitors and β -Lactam Enhancers: Activity of Three Novel Diazabicyclooctanes WCK 5153, Zidebactam (WCK 5107), and WCK 4234. *J. Med. Chem.* **2018**, *61* (9), 4067–4086.
- (365) Papp-Wallace, K. M.; Bonomo, R. A. New β -Lactamase Inhibitors in the Clinic. *Infect. Dis. Clin. North Am.* **2016**, *30* (2), 441–464.
- (366) King, D. T.; King, A. M.; Lal, S. M.; Wright, G. D.; Strynadka, N. C. J. Molecular Mechanism of Avibactam-Mediated B-Lactamase Inhibition. *ACS Infect. Dis.* **2015**, *1* (175–184).
- (367) Abboud, M. I.; Damblon, C.; Brem, J.; Smargiasso, N.; Mercuri, P.; Gilbert, B.; Rydzik, A. M.; Claridge, T. D. W.; Schofield, C. J.; Frère, J.-M. Interaction of Avibactam with Class B Metallo- β -Lactamases. *Antimicrob. Agents Chemother.* **2016**, *60*, 5655–5662.
- (368) Kiener, P. A.; Waley, S. G. Reversible Inhibitors of Penicillinases. *Biochem. J.* **1978**, *169*, 197–204.
- (369) Beesley, T.; Gascoyne, N.; Knott-Hunziker, V.; Petursson, S.; Waley, S. G.; Jaurin, B.; Grundström, T. The Inhibition of Class C β -Lactamases by Boronic Acids. *Biochem. J.* **1983**, *209*, 229–233.
- (370) Crompton, I. E.; Cuthbert, B. K.; Lowe, G.; Waley, S. G. β -Lactamase Inhibitors. The Inhibition of Serine β -Lactamases by Specific Boronic Acids. *Biochem. J.* **1988**, *251* (2), 453–459.
- (371) Weston, G. S.; Blázquez, J.; Baquero, F.; Shoichet, B. K. Structure-Based Enhancement of Boronic Acid-Based Inhibitors of AmpC β -Lactamase. *J. Med. Chem.* **1998**, *41* (23), 4577–4586.
- (372) Rojas, L. J.; Taracila, M. A.; Papp-Wallace, K. M.; Bethel, C. R.; Caselli, E.; Romagnoli, C.;

- Winkler, M. L.; Spellberg, B.; Prati, F.; Bonomo, R. A. Boronic Acid Transition State Inhibitors Active against KPC and Other Class a β -Lactamases: Structure-Activity Relationships as a Guide to Inhibitor Design. *Antimicrob. Agents Chemother.* **2016**, *60* (3), 1751–1759.
- (373) Hecker, S. J.; Reddy, K. R.; Totrov, M.; Hirst, G. C.; Lomovskaya, O.; Griffith, D. C.; King, P.; Tsivkovski, R.; Sun, D.; Sabet, M.; Tarazi, Z.; Clifton, M. C.; Atkins, K.; Raymond, A.; Potts, K. T.; Abendroth, J.; Boyer, S. H.; Loutit, J. S.; Morgan, E. E.; Durso, S.; Dudley, M. N. Discovery of a Cyclic Boronic Acid β -Lactamase Inhibitor (RPX7009) with Utility vs Class A Serine Carbapenemases. *J. Med. Chem.* **2015**, *58* (9), 3682–3692.
- (374) Hirst, G.; Reddy, R.; Hecker, S.; Totrov, M.; Griffith, D. C.; Rodny, O.; Dudley, M. N.; Boyer, S. Cyclic Boronic Acid Ester Derivatives and Therapeutic Uses Thereof. US9694025B2, 2017.
- (375) Lomovskaya, O.; Sun, D.; Rubio-Aparicio, D.; Nelson, K.; Tsivkovski, R.; Griffith, D. C.; Dudley, M. N. Vaborbactam: Spectrum of Beta-Lactamase Inhibition and Impact of Resistance Mechanisms on Activity in Enterobacteriaceae. *Antimicrob. Agents Chemother.* **2017**, *61* (11), e01443-17.
- (376) Werner, J. P.; Mitchell, J. M.; Taracila, M. A.; Bonomo, R. A.; Powers, R. A. Exploring the Potential of Boronic Acids as Inhibitors of OXA-24/40 β -Lactamase. *Protein Sci.* **2017**, *26* (3), 515–526.
- (377) Rahil, J.; Pratt, R. F. Phosphonate Monoester Inhibitors of Class A β -Lactamases. *Biochem. J.* **1991**, *275*, 793–795.
- (378) Rahil, J.; Pratt, R. F. Mechanism of Inhibition of the Class C β -Lactamase of Enterobacter Cloacae P99 by Phosphonate Monoesters. *Biochemistry* **1992**, *31* (25), 5869–5878.
- (379) Chen, C. C. H.; Rahil, J.; Pratt, R. F.; Herzberg, O. Structure of a Phosphonate-Inhibited β -Lactamase: An Analog of the Tetrahedral Transition State/Intermediate of β -Lactam Hydrolysis. *J. Mol. Biol.* **1993**, *234*, 165–178.
- (380) Li, N.; Rahil, J.; Wright, M. E.; Pratt, R. F. Structure-Activity Studies of the Inhibition of Serine β -Lactamases by Phosphonate Monoesters. *Bioorg. Med. Chem.* **1997**, *5* (9), 1783–1788.

- (381) Pratt, R. F.; Hammar, N. J. Salicyloyl Cyclic Phosphate, a “penicillin-like” Inhibitor of β -Lactamases. *J. Am. Chem. Soc.* **1998**, *120* (13), 3004–3006.
- (382) Kaur, K.; Lan, M. J. K.; Pratt, R. F. Mechanism of Inhibition of the Class C β -Lactamase of *Enterobacter Cloacae* P99 by Cyclic Acyl Phosph(on)Ates: Rescue by Return. *J. Am. Chem. Soc.* **2001**, *123* (43), 10436–10443.
- (383) Kaur, K.; Adediran, S. A.; Lan, M. J. K.; Pratt, R. F. Inhibition of β -Lactamases by Monocyclic Acyl Phosph(on)Ates. *Biochemistry* **2003**, *42* (6), 1529–1536.
- (384) Adediran, S. A.; Nukaga, M.; Baurin, S.; Frère, J.-M.; Pratt, R. F. Inhibition of Class D β -Lactamases by Acyl Phosphates and Phosphonates. *Antimicrob. Agents Chemother.* **2005**, *49* (10), 4410–4412.
- (385) Majumdar, S.; Adediran, S. A.; Nukaga, M.; Pratt, R. F. Inhibition of Class D β -Lactamases by Diaroyl Phosphates. *Biochemistry* **2005**, *44* (49), 16121–16129.
- (386) Majumdar, S.; Pratt, R. F. Inhibition of Class A and C β -Lactamases by Diaroyl Phosphates. *Biochemistry* **2009**, *48* (35), 8285–8292.
- (387) Jungheim, L. N.; Ternansky, R. J. Non- β -Lactam Mimics of β -Lactam Antibiotics. In *The Chemistry of β -Lactams*; Page, M. I., Ed.; Springer Science + Business Media: Bath, UK, 1992; pp 306–324.
- (388) Devi, P.; Rutledge, P. J. Cyclobutanone Analogues of β -Lactam Antibiotics: β -Lactamase Inhibitors with Untapped Potential? *ChemBioChem* **2017**, *18* (4), 338–351.
- (389) Gordon, E. M.; Plušćec, J.; Ondetti, M. A. Carbacyclic Isosteres of Penicillanic and Carbapenemic Acids. Synthesis of Bicyclo[3.2.0]Heptan-6-Ones as Potential Enzyme Inhibitors. *Tetrahedron Lett.* **1981**, *22* (20), 1871–1874.
- (390) Lowe, G.; Swain, S. Synthesis of a Cyclobutanone Analogue of a β -Lactam Antibiotic. *J. Chem. Soc. Perkin Trans. 1* **1985**, 391–398.
- (391) Johnson, J. W.; Gretes, M.; Goodfellow, V. J.; Marrone, L.; Heynen, M. L.; Strynadka, N. C. J.; Dmitrienko, G. I.; Goodfellow, Valerie, J.; Marrone, L.; Heynen, M. L.; Strynadka, N. C. J.; Dmitrienko, G. I. Cyclobutanone Analogues of β -Lactams Revisited: Insights into Conformational Requirements for Inhibition of Serine- and Metallo- β -Lactamases. *J. Am.*

- Chem. Soc.* **2010**, *132* (8), 2558–2560.
- (392) Abboud, M. I.; Kosmopoulou, M.; Krismanich, A. P.; Johnson, J. W.; Hinchliffe, P.; Claridge, T. D. W.; Spencer, J.; Schofield, C. J.; Dmitrienko, G. I. Cyclobutanone Mimics of Intermediates in Metallo- β -Lactamase Catalysis. *Chem. A Eur. J.* **2018**, *24*, 5734–5737.
- (393) Pfizer. A Study to Determine the Efficacy, Safety and Tolerability of Aztreonam-Avibactam (ATM-AVI) \pm Metronidazole (MTZ) Versus Meropenem (MER) \pm Colistin (COL) for the Treatment of Serious Infections Due to Gram Negative Bacteria. (REVISIT) NCT03329092 <https://clinicaltrials.gov/ct2/show/NCT03329092> (accessed Nov 21, 2018).
- (394) Karlowsky, J. A.; Kazmieczech, K. M.; de Jonge, B. L. M.; Hackel, M. A.; Sahm, D. F.; Bradford, P. A. In Vitro Activity of Aztreonam-Avibactam against Enterobacteriaceae and Clinical Laboratories in 40 Countries from 2012 to 2015. *Antimicrob. Agents Chemother.* **2017**, *61* (9), e00472-17.
- (395) Fast, W.; Sutton, L. D. Metallo- β -Lactamase: Inhibitors and Reporter Substrates. *Biochim. Biophys. Acta - Proteins Proteomics* **2013**, *1834* (8), 1648–1659.
- (396) Faridooon; Ul Islam, N. An Update on the Status of Potent Inhibitors of Metallo- β -Lactamases. *Sci. Pharm.* **2013**, *81* (2), 309–327.
- (397) McGeary, R. P.; Tan, D. T.; Schenk, G. Progress toward Inhibitors of Metallo- β -Lactamases. *Future Med. Chem.* **2017**, *9* (7), 673–691.
- (398) Rotondo, C. M.; Wright, G. D. Inhibitors of Metallo- β -Lactamases. *Curr. Opin. Microbiol.* **2017**, *39* (November), 96–105.
- (399) Bush, K. Characterization of β -Lactamases. *Antimicrob. Agents Chemother.* **1989**, *33* (3), 259–263.
- (400) Siemann, S.; Brewer, D.; Clarke, A. J.; Dmitrienko, G. I.; Lajoie, G.; Viswanatha, T. IMP-1 Metallo- β -Lactamase: Effect of Chelators and Assessment of Metal Requirement by Electrospray Mass Spectrometry. *Biochim. Biophys. Acta* **2002**, *1571* (3), 190–200.
- (401) King, A. M.; Reid-Yu, S. a; Wang, W.; King, D. T.; De Pascale, G.; Strynadka, N. C.; Walsh, T. R.; Coombes, B. K.; Wright, G. D. Aspergillomarasmine A Overcomes Metallo- β -Lactamase Antibiotic Resistance. *Nature* **2014**, *510*, 503–506.

- (402) Falconer, S. B.; Reid-Yu, S. A.; King, A. M.; Gehrke, S. S.; Wang, W.; Britten, J. F.; Coombes, B. K.; Wright, G. D.; Brown, E. D. Zinc Chelation by a Small-Molecule Adjuvant Potentiates Meropenem Activity in Vivo against NDM-1-Producing *Klebsiella Pneumoniae*. *ACS Infect. Dis.* **2016**, *1* (11), 533–543.
- (403) Laraki, N.; Franceschini, N.; Rossolini, G. M.; Santucci, P.; Meunier, C.; de Pauw, E.; Amicosante, G.; Frère, J.-M.; Galleni, M. Biochemical Characterization of the *Pseudomonas Aeruginosa* 101/1477 Metallo- β -Lactamase IMP-1 Produced by *Escherichia Coli*. *Antimicrob. Agents Chemother.* **1999**, *43* (4), 902–906.
- (404) Docquier, J.-D.; Lamotte-Brasseur, J.; Galleni, M.; Amicosante, G.; Frère, J.-M.; Rossolini, G. M. On Functional and Structural Heterogeneity of VIM-Type Metallo- β -Lactamases. *J. Antimicrob. Chemother.* **2003**, *51* (2), 257–266.
- (405) Thomas, P. W.; Zheng, M.; Wu, S.; Guo, H.; Liu, D.; Xu, D.; Fast, W. Characterization of Purified New Delhi Metallo- β -Lactamase-1. *Biochemistry* **2011**, *50* (46), 10102–10113.
- (406) Toney, J. H.; Hammond, G. G.; Fitzgerald, P. M. D.; Sharma, N.; Balkovec, J. M.; Rouen, G. P.; Olson, S. H.; Hammond, M. L.; Greenlee, M. L.; Gao, Y.-D. Succinic Acids as Potent Inhibitors of Plasmid-Borne IMP-1 Metallo- β -Lactamase. *J. Biol. Chem.* **2001**, *276* (34), 31913–31918.
- (407) Balkovec, J. M.; Hammond, G.; Greenlee, M. L.; Olson, S. H.; Rouen, G. P.; Toney, J. H. Novel Succinic Acid Metallo- β -Lactamase Inhibitors and Their Use in Treating Bacterial Infections. WO2001030149, 2001.
- (408) Moloughney, J. G.; Thomas, J. D.; Toney, J. H. Novel IMP-1 Metallo- β -Lactamase Inhibitors Can Reverse Meropenem Resistance in *Escherichia Coli* Expressing IMP-1. *FEMS Microbiol. Lett.* **2005**, *243* (1), 65–71.
- (409) Olsen, L.; Jost, S.; Adolph, H.-W.; Pettersson, I.; Hemmingsen, L.; Jørgensen, F. S. New Leads of Metallo- β -Lactamase Inhibitors from Structure-Based Pharmacophore Design. *Bioorganic Med. Chem.* **2006**, *14* (8), 2627–2635.
- (410) Horsfall, L. E.; Garau, G.; Liénard, B. M. R.; Dideberg, O.; Schofield, C. J.; Frère, J. M.; Galleni, M. Competitive Inhibitors of the CphA Metallo- β -Lactamase from *Aeromonas Hydrophila*. *Antimicrob. Agents Chemother.* **2007**, *51* (6), 2136–2142.

- (411) Hiraiwa, Y.; Morinaka, A.; Fukushima, T.; Kudo, T. Metallo- β -Lactamase Inhibitory Activity of Phthalic Acid Derivatives. *Bioorganic Med. Chem. Lett.* **2009**, *19*, 5162–5165.
- (412) Ishii, Y.; Eto, M.; Mano, Y.; Tateda, K.; Yamaguchi, K. In Vitro Potentiation of Carbapenems with ME1071, a Novel Metallo- β -Lactamase Inhibitor, against Metallo- β -Lactamase-Producing *Pseudomonas Aeruginosa* Clinical Isolates. *Antimicrob. Agents Chemother.* **2010**, *54* (9), 3625–3629.
- (413) Feng, L.; Yang, K.-W.; Zhou, L.-S.; Xiao, J.-M.; Yang, X.; Zhai, L.; Zhang, Y.-L.; Crowder, M. W. N-Heterocyclic Dicarboxylic Acids: Broad-Spectrum Inhibitors of Metallo- β -Lactamases with Co-Antibacterial Effect against Antibiotic-Resistant Bacteria. *Bioorganic Med. Chem. Lett.* **2012**, *22* (16), 5185–5189.
- (414) Hiraiwa, Y.; Saito, J.; Watanabe, T.; Yamada, M.; Morinaka, A.; Fukushima, T.; Kudo, T. X-Ray Crystallographic Analysis of IMP-1 Metallo- β -Lactamase Complexed with a 3-Aminophthalic Acid Derivative, Structure-Based Drug Design, and Synthesis of 3,6-Disubstituted Phthalic Acid Derivative Inhibitors. *Bioorg. Med. Chem. Lett.* **2014**, *24* (20), 4891–4894.
- (415) Hinchliffe, P.; Tanner, C. A.; Krismanich, A. P.; Labbé, G.; Goodfellow, V. J.; Marrone, L.; Desoky, A. Y.; Calvopiña, K.; Whittle, E. E.; Zeng, F.; Avison, M. B.; Bols, N. C.; Siemann, S.; Spencer, J.; Dmitrienko, G. I. Structural and Kinetic Studies of the Potent Inhibition of Metallo- β -Lactamases by 6-Phosphonomethylpyridine-2-Carboxylates. *Biochemistry* **2018**, *57* (12), 1880–1892.
- (416) Hiraiwa, Y.; Morinaka, A.; Fukushima, T.; Kudo, T. Metallo- β -Lactamase Inhibitory Activity of 3-Alkyloxy and 3-Amino Phthalic Acid Derivatives and Their Combination Effect with Carbapenem. *Bioorganic Med. Chem.* **2013**, *21* (18), 5841–5850.
- (417) Livermore, D. M.; Mushtaq, S.; Morinaka, A.; Ida, T.; Maebashi, K.; Hope, R. Activity of Carbapenems with ME1071 (Disodium 2,3-Diethylmaleate) against Enterobacteriaceae and *Acinetobacter* Spp. With Carbapenemases, Including NDM Enzymes. *J. Antimicrob. Chemother.* **2013**, *68* (1), 153–158.
- (418) Maret, W. Zinc and Sulfur: A Critical Biological Partnership. *Biochemistry* **2004**, *43* (12), 3301–3309.

- (419) Mollard, C.; Moali, C.; Papamicael, C.; Damblon, C.; Vessilier, S.; Amicosante, G.; Schofield, C. J.; Galleni, M.; Frère, J.-M.; Roberts, G. C. K. Thiomandelic Acid, a Broad Spectrum Inhibitor of Zinc β -Lactamases: Kinetic and Spectroscopic Studies. *J. Biol. Chem.* **2001**, *276* (48), 45015–45023.
- (420) Siemann, S.; Clarke, A. J.; Viswanatha, T.; Dmitrienko, G. I. Thiols as Classical and Slow-Binding Inhibitors of IMP-1 and Other Binuclear Metallo- β -Lactamases. *Biochemistry* **2003**, *42* (6), 1673–1683.
- (421) Jin, W.; Arakawa, Y.; Yasuzawa, H.; Taki, T.; Hashiguchi, R.; Mitsutani, K.; Shoga, A.; Yamaguchi, Y.; Kurosaki, H.; Shibata, N.; Ohta, M.; Goto, M. Comparative Study of the Inhibition of Metallo- β -Lactamases (IMP-1 and VIM-2) by Thiol Compounds That Contain a Hydrophobic Group. *Biol. Pharm. Bull.* **2004**, *27* (6), 851–856.
- (422) Antony, J.; Gresh, N.; Olsen, L.; Hemmingsen, L.; Schofield, C. J.; Bauer, R. Binding of D- and L-Captopril Inhibitors to Metallo- β -Lactamase Studied by Polarizable Molecular Mechanics and Quantum Mechanics. *J. Comput. Chem.* **2002**, *23* (13), 1281–1296.
- (423) Brem, J.; van Berkel, S. S.; Zollman, D.; Lee, S. Y.; Gileadi, O.; McHugh, P. J.; Walsh, T. R.; McDonough, M. A.; Schofield, C. J. Structural Basis of Metallo- β -Lactamase Inhibition by Captopril Stereoisomers. *Antimicrob. Agents Chemother.* **2016**, *60*, 142–150.
- (424) Lassaux, P.; Hamel, M.; Gulea, M.; Delbrück, H.; Mercuri, P. S.; Horsfall, L.; Dehareng, D.; Kupper, M.; Frère, J.-M.; Hoffmann, K.; Galleni, M.; Bebrone, C. Mercaptophosphonate Compounds as Broad-Spectrum Inhibitors of the Metallo- β -Lactamases. *J. Med. Chem.* **2010**, *53* (13), 4862–4876.
- (425) Hinchliffe, P.; González, M. M.; Mojica, M. F.; González, J. M.; Castillo, V.; Saiz, C.; Kosmopoulou, M.; Tooke, C. L.; Llarrull, L. I.; Mahler, G.; Bonomo, R. A.; Vila, A. J.; Spencer, J. Cross-Class Metallo- β -Lactamase Inhibition by Bisthiazolidines Reveals Multiple Binding Modes. *PNAS* **2016**, No. August, 1–10.
- (426) Atkinson, A. B.; Robertson, J. I. S. Captopril in the Treatment of Clinical Hypertension and Cardiac Failure. *Lancet* **1979**, *314* (8147), 836–839.
- (427) Rydzik, A. M.; Brem, J.; Berkel, S. S. Van; Pfeffer, I.; Makena, A.; Claridge, T. D. W.; Schofield, C. J. Monitoring Conformational Changes in the NDM-1 Metallo- β -Lactamase by

- 19 F NMR Spectroscopy**. *Angew. Chem. Int. Ed. Engl.* **2014**, *126*, 3193–3197.
- (428) García-Sáez, I.; Hopkins, J.; Papamichael, C.; Franceschini, N.; Amicosante, G.; Rossolinill, G. M.; Galleni, M.; Frère, J.-M.; Dideberg, O. The 1.5-Å Structure of *Chryseobacterium Meningosepticum* Zinc β -Lactamase in Complex with the Inhibitor, D-Captopril. *J. Biol. Chem.* **2003**, *278* (26), 23868–23873.
- (429) Liénard, B. M. R.; Garau, G.; Horsfall, L.; Karsisiotis, A. I.; Damblon, C.; Lassaux, P.; Papamichael, C.; Roberts, G. C. K.; Galleni, M.; Dideberg, O.; Frère, J.-M.; Schofield, C. J. Structural Basis for the Broad-Spectrum Inhibition of Metallo- β -Lactamases by Thiols. *Org. Biomol. Chem.* **2008**, *6* (13), 2282–2294.
- (430) Brem, J.; van Berkel, S. S.; Aik, W.; Rydzik, A. M.; Avison, M. B.; Pettinati, I.; Umland, K.-D.; Kawamura, A.; Spencer, J.; Claridge, T. D. W.; McDonough, M. A.; Schofield, C. J. Rhodanine Hydrolysis Leads to Potent Thioenolate Mediated Metallo- β -Lactamase Inhibition. *Nat. Chem.* **2014**, *6* (12), 1084–1090.
- (431) Brem, J.; Van Berkel, S. S.; McDonough, M. A.; Schofield, C. J. Beta Lactamase Inhibitors. US2017/0369433 A1, 2017.
- (432) Captopril <https://www.drugbank.ca/drugs/DB01197> (accessed Nov 28, 2018).
- (433) Munday, R. Toxicity of Thiols and Disulphides: Involvement of Free-Radical Species. *Free Radic. Biol. Med.* **1989**, *7* (6), 659–673.
- (434) Mendgen, T.; Steuer, C.; Klein, C. D. Privileged Scaffolds or Promiscuous Binders: A Comparative Study on Rhodanines and Related Heterocycles in Medicinal Chemistry. *J. Med. Chem.* **2012**, *55*, 743–753.
- (435) Payne, D. J.; Bateson, J. H.; Gasson, B. C.; Proctor, D.; Khushi, T.; Farmer, T. H.; Tolson, D. A.; Bell, D.; Skett, P. W.; Marshall, A. C.; Reid, R.; Ghosez, L.; Combret, Y.; Marchand-Brynaert, J. Inhibition of Metallo- β -Lactamases by a Series of Mercaptoacetic Acid Thiol Ester Derivatives. *Antimicrob. Agents Chemother.* **1997**, *41* (1), 135–140.
- (436) Payne, D. J.; Bateson, J. H.; Gasson, B. C.; Khushi, T.; Proctor, D.; Pearson, S. C.; Reid, R. Inhibition of Metallo- β -Lactamases by a Series of Thiol Ester Derivatives of Mercaptophenylacetic Acid. *FEMS Microbiol. Lett.* **1997**, *157*, 171–175.

- (437) Greenlee, M. L.; Laub, J. B.; Balkovec, J. M.; Hammond, M. L.; Hammond, G. G.; Pompliano, D. L.; Epstein-Toney, J. H. Synthesis and SAR of Thioester and Thiol Inhibitors of IMP-1 Metallo- β -Lactamase. *Bioorganic Med. Chem. Lett.* **1999**, *9*, 2549–2554.
- (438) Hammond, G. G.; Huber, J. L.; Greenlee, M. L.; Laub, J. B.; Young, K.; Silver, L. L.; Balkovec, J. M.; Pryor, K. D.; Wu, J. K.; Leitinger, B.; Pompliano, D. L.; Toney, J. H. Inhibition of IMP-1 Metallo- β -Lactamase and Sensitization of IMP-1-Producing Bacteria by Thioester Derivatives. *FEMS Microbiol. Lett.* **1999**, *459*, 289–296.
- (439) Roll, D. M.; Yang, Y.; Wildey, M. J.; Bush, K.; Lee, M. D. Inhibition of Metallo- β -Lactamases by Pyridine Monothiocarboxylic Acid Analogs. *J. Antibiot. (Tokyo)*. **2010**, *63* (5), 255–257.
- (440) Faridoo; Hussein, W. M.; Vella, P.; Ul Islam, N.; Ollis, D. L.; Schenk, G.; McGeary, R. P. 3-Mercapto-1,2,4-Triazoles and N-Acylated Thiosemicarbazides as Metallo- β -Lactamase Inhibitors. *Bioorganic Med. Chem. Lett.* **2012**, *22* (1), 380–386.
- (441) Siemann, S.; Evanoff, D. P.; Marrone, L.; Clarke, A. J.; Viswanatha, T.; Dmitrienko, G. I. N-Arylsulfonyl Hydrazones as Inhibitors of IMP-1 Metallo- β -Lactamase. *Antimicrob. Agents Chemother.* **2002**, *46* (8), 2450–2457.
- (442) Minond, D.; Saldanha, S. A.; Subramaniam, P.; Spaargaren, M.; Fotsing, J. R.; Weide, T.; Fokin, V.; Sharpless, B.; Frère, J.; Hodder, P. Inhibitors of VIM-2 by Screening Pharmacologically Active and Click-Chemistry Compound Libraries. *Bioorg. Med. Chem. Lett.* **2009**, *17* (14), 5027–5037.
- (443) Weide, T.; Saldanha, S. A.; Minond, D.; Spicer, T. P.; Fotsing, J. R.; Spaargaren, M.; Frère, J.-M.; Bebrone, C.; Sharpless, K. B.; Hodder, P. S.; Fokin, V. V. NH-1,2,3-Triazole Inhibitors of the VIM-2 Metallo- β -Lactamase. *ACS Med. Chem. Lett.* **2010**, *1*, 150–154.
- (444) Payne, D. J.; Hueso-Rodríguez, J. A.; Boyd, H.; Concha, N. O.; Janson, C. A.; Gilpin, M.; Bateson, J. H.; Cheever, C.; Niconovich, N. L.; Pearson, S.; Rittenhouse, S.; Tew, D.; Díez, E.; Pérez, P.; de la Fuente, J.; Rees, M.; Rivera-Sagredo, A. Identification of a Series of Tricyclic Natural Products as Potent Broad-Spectrum Inhibitors of Metallo- β -Lactamases. *Antimicrob. Agents Chemother.* **2002**, *46* (6), 1880–1886.
- (445) Toney, J. H.; Fitzgerald, P. M. D.; Grover-Sharma, N.; Olson, S. H.; May, W. J.; Sundelof, J.

- G.; Vanderwall, D. E.; Cleary, K. A.; Grant, S. K.; Wu, J. K.; Kozarich, J. W.; Pompliano, D. L.; Hammond, G. G. Antibiotic Sensitization Using Biphenyl Tetrazoles as Potent Inhibitors of *Bacteroides Fragilis* Metallo- β -Lactamase. *Chem. Biol.* **1998**, *5* (4), 185–196.
- (446) Bellosillo, B.; Colomer, D.; Pons, G.; Gil, J. Mitoxantrone, a Topoisomerase II Inhibitor, Induces Apoptosis of B-Chronic Lymphocytic Leukaemia Cells. *Br. J. Haematol.* **1998**, *100*, 142–146.
- (447) Fox, E. J. Mechanism of Action of Mitoxantrone. *Neurology* **2004**, *63* (12 Suppl 6), S15–S18.
- (448) Mitoxantrone <https://www.drugbank.ca/drugs/DB01204> (accessed Apr 13, 2018).
- (449) Hortobágyi, G. N. Anthracyclines in the Treatment of Cancer An Overview. *Drugs* **1997**, *54* (Suppl. 4), 1–7.
- (450) Cahill, S. T.; Cain, R.; Wang, D. Y.; Lohans, C. T.; Wareham, D. W.; Oswin, H. P.; Mohammed, J.; Spencer, J.; Fishwick, C. W. G.; McDonough, M. A.; Schofield, C. J.; Brema, J. Cyclic Boronates Inhibit All Classes of β -Lactamases. *Antimicrob. Agents Chemother.* **2017**, *61* (4), 1–13.
- (451) Brem, J.; Cain, R.; Cahill, S.; McDonough, M. A.; Clifton, I. J.; Jiménez-Castellanos, J.-C.; Avison, M. B.; Spencer, J.; Fishwick, C. W. G.; Schofield, C. J. Structural Basis of Metallo- β -Lactamase, Serine- β -Lactamase and Penicillin-Binding Protein Inhibition by Cyclic Boronates. *Nat. Commun.* **2016**, *7*, 1–8.
- (452) Bebrone, C.; Moali, C.; Mahy, F.; Rival, S.; Docquier, J. D.; Rossolini, G. M.; Fastrez, J.; Pratt, R. F.; Frère, J.-M.; Galleni, M. CENTA as a Chromogenic Substrate for Studying β -Lactamases. *Antimicrob. Agents Chemother.* **2001**, *45* (6), 1868–1871.
- (453) Ghavami, A.; Labbé, G.; Brem, J.; Goodfellow, V. J.; Marrone, L.; Tanner, C. A.; King, D. T.; Lam, M.; Strynadka, N. C. J.; Pillai, D. R.; Siemann, S.; Spencer, J.; Schofield, C. J.; Dmitrienko, G. I. Assay for Drug Discovery: Synthesis and Testing of Nitrocefin Analogues for Use as β -Lactamase Substrates. *Anal. Biochem.* **2015**, *486*, 75–77.
- (454) de las Heras, R.; Fry, S. R.; Li, J.; Arel, E.; Kachab, E. H.; Hazell, S. L.; Huang, C.-Y. Development of Homogeneous Immunoassays Based on Protein Fragment Complementation. *Biochem. Biophys. Res. Commun.* **2008**, *370* (1), 164–168.

- (455) Dereeper, A.; Audic, S.; Claverie, J. M.; Blanc, G. BLAST-EXPLORER Helps You Build Datasets for Phylogenetic Analysis. *Evol. Biol.* **2010**, *10* (8), 8–13.
- (456) Dereeper, A.; Guignon, V.; Blanc, G.; Audic, S.; Buffet, S.; Chevenet, F.; Dufayard, J. F.; Guindon, S.; Lefort, V.; Lescot, M.; Claverie, J. M.; Gascuel, O. Phylogeny.Fr: Robust Phylogenetic Analysis for the Non-Specialist. *Nucleic Acids Res.* **2008**, *36* (Web Server issue), 465–469.
- (457) Edgar, R. C. MUSCLE: Multiple Sequence Alignment with High Accuracy and High Throughput. *Nucleic Acids Res.* **2004**, *32* (5), 1792–1797.
- (458) Castresana, J. Selection of Conserved Blocks from Multiple Alignments for Their Use in Phylogenetic Analysis. *Mol. Biol. Evol.* **2000**, *17* (4), 540–552.
- (459) Guindon, S.; Gascuel, O. A Simple, Fast, and Accurate Algorithm to Estimate Large Phylogenies by Maximum Likelihood. *Syst. Biol.* **2003**, *52* (5), 696–704.
- (460) Anisimova, M.; Gascuel, O. Approximate Likelihood-Ratio Test for Branches: A Fast, Accurate and Powerful Alternative. *Syst. Biol.* **2006**, *55* (4), 539–552.
- (461) Chevenet, F.; Brun, C.; Bañuls, A. L.; Jacq, B.; Christen, R. TreeDyn: Towards Dynamic Graphics and Annotations for Analyses of Trees. *BMC Bioinformatics* **2006**, *7*, 1–9.
- (462) Hall, T. A. BioEdit: A User-Friendly Biological Sequence Alignment Editor and Analysis Program for Windows 95/98/NT. *Nucleic Acids Symp. Ser.* **1999**, *41*, 95–98.
- (463) Sambrook, J.; Fritsch, E. F.; Maniatis, T. *Molecular Cloning*, 2nd ed.; Nolan, C., Ed.; Cold Spring Harbor Laboratory Press: Cold Spring Harbor, NY, 1989.
- (464) Franceschini, N.; Caravelli, B.; Docquier, J.-D.; Galleni, M.; Frère, J.-M.; Amicosante, G.; Rossolini, G. M. Purification and Biochemical Characterization of the VIM-1 Metallo- β -Lactamase. *Antimicrob. Agents Chemother.* **2000**, *44* (11), 3003–3007.
- (465) Poirel, L.; Naas, T.; Nicolas, D.; Collet, L.; Bellais, S.; Cavallo, J.-D.; Nordmann, P. Characterization of VIM-2, a Carbapenem-Hydrolyzing Metallo- β -Lactamase and Its Plasmid- and Integron-Borne Gene from a *Pseudomonas Aeruginosa* Clinical Isolate in France. *Antimicrob. Agents Chemother.* **2000**, *44* (4), 891–897.
- (466) Tsukamoto, K.; Tachibana, K.; Yamazaki, N.; Ishii, Y.; Ujiie, K.; Nishida, N.; Sawai, T. Role

- of Lysine-67 in the Active Site of Class C B-lactamase from *Citrobacter Freundii* GN346. *Eur. J. Biochem.* **1990**, *188* (1), 15–22.
- (467) Copeland, R. A. *Enzymes. A Practical Introduction to Structure, Mechanism, and Data Analysis*, 2nd Editio.; Wiley-VCH: New York, New York, 2000.
- (468) Brem, J.; Struwe, W. B.; Rydzik, A. M.; Tarhonskaya, H.; Pfeffer, I.; Flashman, E.; van Berkel, S. S.; Spencer, J.; Claridge, T. D. W.; McDonough, M. A.; Benesch, J. L. P.; Schofield, C. J. Studying the Active-Site Loop Movement of the São Paulo Metallo- β -Lactamase-1. *Chem. Sci.* **2015**, *6*, 956–963.
- (469) Wang, X.; Li, H.; Zhao, C.; Chen, H.; Liu, J.; Wang, Z.; Wang, Q.; Zhang, Y.; He, W.; Zhang, F.; Wang, H. Novel NDM-9 Metallo- β -Lactamase Identified from a ST107 *Klebsiella Pneumoniae* Strain Isolated in China. *Int. J. Antimicrob. Agents* **2014**, *44* (1), 90–91.
- (470) Tada, T.; Shrestha, B.; Miyoshi-Akiyama, T.; Shimada, K.; Ohara, H.; Kirikae, T.; Pokhrel, B. M. NDM-12, a Novel New Delhi Metallo- β -Lactamase Variant from a Carbapenem-Resistant *Escherichia Coli* Clinical Isolate in Nepal. *Antimicrob. Agents Chemother.* **2014**, *58* (10), 6302–6305.
- (471) Makena, A.; Brem, J.; Pfeffer, I.; Geffen, R. E. J.; Wilkins, S. E.; Tarhonskaya, H.; Flashman, E.; Phee, L. M.; Wareham, D. W.; Schofield, C. J. Biochemical Characterization of New Delhi Metallo- β -Lactamase Variants Reveals Differences in Protein Stability. *J. Antimicrob. Chemother.* **2015**, *70* (2), 463–469.
- (472) Makena, A.; Düzgün, A. Ö.; Brem, J.; McDonough, M. A.; Rydzik, A. M.; Abboud, M. I.; Saral, A.; Çiçek, A. Ç.; Sandalli, C.; Schofield, C. J. Comparison of Verona Integron-Borne Metallo- β -Lactamase (VIM) Variants Reveals Differences in Stability and Inhibition Profiles. *Antimicrob. Agents Chemother.* **2016**, *60* (3), 1377–1384.
- (473) Widmann, M.; Pleiss, J. Protein Variants Form a System of Networks: Microdiversity of IMP Metallo-Beta-Lactamases. *PLoS One* **2014**, *9* (7).
- (474) Sancenon, V.; Goh, W. H.; Sundaram, A.; Er, K. S.; Johal, N.; Mukhina, S.; Carr, G.; Dhakshinamoorthy, S. Development, Validation and Quantitative Assessment of an Enzymatic Assay Suitable for Small Molecule Screening and Profiling: A Case-Study. *Biomol. Detect. Quantif.* **2015**, *4*, 1–9.

- (475) Henderson, P. J. F. *Statistical Analysis of Enzyme Kinetic Data*; Eisenthal, R., Danson, M. J., Eds.; Oxford, UK, 1993.
- (476) Cleland, W. W. *Statistical Analysis of Enzyme Kinetic Data*; 1967; Vol. 29.
- (477) Torol, S.; Kasap, M. Purification and Characterization of OXA-23 from *Acinetobacter Baumannii*. *J. Enzyme Inhib. Med. Chem.* **2013**, *28* (4), 836–842.
- (478) Stojanoski, V.; Chow, D.-C.; Fryszczyn, B.; Hu, L.; Nordmann, P.; Poirel, L.; Sankaran, B.; Prasad, B. V. V.; Palzkill, T. Structural Basis for Different Substrate Profiles of Two Closely Related Class D β -Lactamases and Their Inhibition by Halogens. *Biochemistry* **2015**, 150504140859003.
- (479) Kumar, S.; Adediran, S. A.; Nukaga, M.; Pratt, R. F. Kinetics of Turnover of Cefotaxime by the Enterobacter Cloacae P99 and GCl β -Lactamases: Two Free Enzyme Forms of the P99 β -Lactamase Detected by a Combination of Pre- and Post-Steady State Kinetics. *Biochemistry* **2004**, *43* (9), 2664–2672.
- (480) Faheem, M.; Rehman, M. T.; Danishuddin, M.; Khan, A. U. Biochemical Characterization of CTX-M-15 from Enterobacter Cloacae and Designing a Novel Non- β -Lactam- β -Lactamase Inhibitor. *PLoS One* **2013**, *8* (2), 1–10.
- (481) Ourghanlian, C.; Soroka, D.; Arthur, M. Inhibition by Avibactam and Clavulanate of the β -Lactamases KPC-2 and CTX-M-15 Harboring the Substitution N132G in the Conserved SDN Motif. *Antimicrob. Agents Chemother.* **2017**, *61* (3), e02510-16.
- (482) Maryam, L.; Khan, A. U. A Mechanism of Synergistic Effect of Streptomycin and Cefotaxime on CTX-M-15 Type β -Lactamase Producing Strain of E. Cloacae: A First Report. *Front. Microbiol.* **2016**, *7* (2007), 1–11.
- (483) Papp-Wallace, K. M.; Bethel, C. R.; Distler, A. M.; Kasuboski, C.; Taracila, M.; Bonomo, R. A. Inhibitor Resistance in the KPC-2 Beta-Lactamase, a Preeminent Property of This Class A Beta-Lactamase. *Antimicrob. Agents Chemother.* **2010**, *54* (2), 890–897.
- (484) Papp-Wallace, K. M.; Taracila, M.; Hornick, J. M.; Hujer, A. M.; Hujer, K. M.; Distler, A. M.; Endimiani, A.; Bonomo, R. A. Substrate Selectivity and a Novel Role in Inhibitor Discrimination by Residue 237 in the KPC-2 β -Lactamase. *Antimicrob. Agents Chemother.* **2010**, *54* (7), 2867–2877.

- (485) Moali, C.; Anne, C.; Lamotte-Brasseur, J.; Gros Lambert, S.; Devreese, B.; Van Beeumen, J.; Galleni, M.; Frère, J.-M. Analysis of the Importance of the Metallo- β -Lactamase Active Site Loop in Substrate Binding and Catalysis. *Chem. Biol.* **2003**, *10*, 319–329.
- (486) Kim, Y.; Tesar, C.; Mire, J.; Jedrzejczak, R.; Binkowski, A.; Babnigg, G.; Sacchettini, J.; Joachimiak, A. Structure of Apo- and Monometalated Forms of NDM-1-A Highly Potent Carbapenem-Hydrolyzing Metallo- β -Lactamase. *PLoS One* **2011**, *6* (9), 1–12.
- (487) Thomas, P. W.; Spicer, T.; Cammarata, M.; Brodbelt, J. S.; Hodder, P.; Fast, W. An Altered Zinc-Binding Site Confers Resistance to a Covalent Inactivator of New Delhi Metallo-Beta-Lactamase-1 (NDM-1) Discovered by High-Throughput Screening. *Bioorg. Med. Chem.* **2013**, *21* (11), 3138–3146.
- (488) Yang, H.; Aitha, M.; Hetrick, A. M.; Richmond, T. K.; Tierney, D. L.; Crowder, M. W. Mechanistic and Spectroscopic Studies of Metallo- β -Lactamase NDM-1. *Biochemistry* **2012**, *51*, 3839–3847.
- (489) Murphy, T. A.; Simm, A. M.; Toleman, M. A.; Jones, R. N.; Walsh, T. R. Biochemical Characterization of the Acquired Metallo- β -Lactamase SPM-1 from *Pseudomonas Aeruginosa*. *Antimicrob. Agents Chemother.* **2003**, *47* (2), 582–587.
- (490) Marchiaro, P.; Tomatis, P. E.; Mussi, M. A.; Pasteran, F.; Viale, A. M.; Limansky, A. S.; Vila, A. J. Biochemical Characterization of Metallo- β -Lactamase VIM-11 from a *Pseudomonas Aeruginosa* Clinical Strain. *Antimicrob. Agents Chemother.* **2008**, *52* (6), 2250–2252.
- (491) Fonseca, F.; Arthur, C. J.; Bromley, E. H. C.; Samyn, B.; Moerman, P.; Saavedra, M. J.; Correia, A.; Spencer, J. Biochemical Characterization of Sfh-I, a Subclass B2 Metallo- β -Lactamase from *Serratia Fonticola* UTAD54. *Antimicrob. Agents Chemother.* **2011**, *55* (11), 5392–5395.
- (492) Crowder, M. W.; Walsh, T. R.; Banovic, L.; Pettit, M.; Spencer, J. Overexpression, Purification, and Characterization of the Cloned Metallo-Beta-Lactamase L1 from *Stenotrophomonas Maltophilia*. *Antimicrob. Agents Chemother.* **1998**, *42* (4), 921–926.
- (493) Labbé, G.; de Groot, S.; Rasmusson, T.; Milojevic, G.; Dmitrienko, G. I.; Guillemette, J. G. Evaluation of Four Microbial Class II Fructose 1,6-Bisphosphate Aldolase Enzymes for Use as Biocatalysts. *Protein Expr. Purif.* **2011**, *80* (2), 224–233.

- (494) Kimura, S.; Ishii, Y.; Yamaguchi, K. Evaluation of Dipicolinic Acid for Detection of IMP- or VIM- Type Metallo- β -Lactamase-Producing *Pseudomonas Aeruginosa* Clinical Isolates. *Diagn. Microbiol. Infect. Dis.* **2005**, *53* (3), 241–244.
- (495) Chen, A. Y.; Thomas, P. W.; Stewart, A. C.; Bergstrom, A.; Cheng, Z.; Miller, C.; Bethel, C. R.; Marshall, S. H.; Credille, C. V.; Riley, C. L.; Page, R. C.; Bonomo, R. A.; Crowder, M. W.; Tierney, D. L.; Fast, W.; Cohen, S. M. Dipicolinic Acid Derivatives as Inhibitors of New Delhi Metallo- β -Lactamase-1. *J. Med. Chem.* **2017**, *60* (17), 7267–7283.
- (496) Morrison, J. F.; Walsh, C. T. *The Behavior and Significance of Slow-Binding Enzyme Inhibitors*; 1988; Vol. 61.
- (497) Goličnik, M.; Stojan, J. Slow-Binding Inhibition. A Theoretical and Practical Course for Students. *Biochem. Mol. Biol. Educ.* **2004**, *32* (4), 228–235.
- (498) Institute, C. and L. S. *Methods for Dilution Antimicrobial Susceptibility Tests for Bacteria That Grow Aerobically; Approved Standard-Tenth Edition M07-A10*; Clinical and Laboratory Standards Institute: Wayne, PA, USA, 2015.
- (499) Copeland, R. A. *Evaluation of Enzyme Inhibitors in Drug Discovery*; John Wiley & Sons, Inc.: Hoboken, New Jersey, 2005.
- (500) Institute, C. and L. S. *Performance Standards for Antimicrobial Susceptibility Testing; Twenty-Fifth Informational Supplement M100-S25*; Clinical and Laboratory Standards Institute: Wayne, PA, USA, 2015.
- (501) Labbé, G.; Krismanich, A. P.; de Groot, S.; Rasmusson, T.; Shang, M.; Brown, M. D. R.; Dmitrienko, G. I.; Guillemette, J. G. Development of Metal-Chelating Inhibitors for the Class II Fructose 1,6-Bisphosphate (FBP) Aldolase. *J. Inorg. Biochem.* **2012**, *112*, 49–58.
- (502) Wommer, S.; Rival, S.; Heinz, U.; Galleni, M.; Frère, J.-M.; Franceschini, N.; Amicosante, G.; Rasmussen, B.; Bauer, R.; Adolph, H.-W. Substrate-Activated Zinc Binding of Metallo- β -Lactamases. *J. Biol. Chem.* **2002**, *277* (27), 24142–24147.
- (503) Kliebe, C.; Nies, B. A.; Meyer, J. F.; Tolxdorff-Neutzling, R. M.; Wiedemann, B. Evolution of Plasmid-Coded Resistance to Broad-Spectrum Cephalosporins. *Antimicrob. Agents Chemother.* **1985**, *28* (2), 302–307.

- (504) Jacoby, G. A.; Medeiros, A. A. More Extended-Spectrum β -Lactamases. *Antimicrob. Agents Chemother.* **1991**, *35* (9), 1697–1704.
- (505) Mulvey, M. R.; Bryce, E.; Boyd, D.; Ofner-Agostini, M.; Christianson, S.; Simor, A. E.; Paton, S. Ambler Class A Extended-Spectrum Beta-Lactamase-Producing *Escherichia Coli* and *Klebsiella Spp.* in Canadian Hospitals. *Antimicrob. Agents Chemother.* **2004**, *48* (4), 1204–1214.
- (506) Pitout, J. D. D.; Hanson, N. D.; Church, D. L.; Laupland, K. B. Population-Based Laboratory Surveillance for *Escherichia Coli*-Producing Extended-Spectrum Beta-Lactamases: Importance of Community Isolates with BlaCTX-M Genes. *Clin. Infect. Dis.* **2004**, *38*, 1736–1741.
- (507) Castanheira, M.; Farrell, S. E.; Krause, K. M.; Jones, R. N.; Sader, H. S. Contemporary Diversity of β -Lactamases among Enterobacteriaceae in the Nine U.S. Census Regions and Ceftazidime-Avibactam Activity Tested against Isolates Producing the Most Prevalent β -Lactamase Groups. *Antimicrob. Agents Chemother.* **2014**, *58* (2), 833–838.
- (508) Bush, K. A Resurgence of β -Lactamase Inhibitor Combinations Effective against Multidrug-Resistant Gram-Negative Pathogens. *Int. J. Antimicrob. Agents* **2015**, *46* (5), 483–493.
- (509) Tsang, W. Y.; Dhanda, A.; Schofield, C. J.; Frère, J.-M.; Galleni, M.; Page, M. I. The Inhibition of Metallo- β -Lactamase by Thioxo-Cephalosporin Derivatives. *Bioorg. Med. Chem. Lett.* **2004**, *14* (7), 1737–1739.
- (510) Scorciapino, M. A.; Mallocci, G.; Serra, I.; Milenkovic, S.; Moynié, L.; Naismith, J. H.; Desarbre, E.; Page, M. G. P.; Ceccarelli, M. Complexes Formed by the Siderophore-Based Monosulfactam Antibiotic BAL30072 and Their Interaction with the Outer Membrane Receptor PiuA of *P. Aeruginosa*. *Biometals* **2019**, *32*, 155–170.
- (511) Wilson, B. R.; Bogdan, A. R.; Miyazawa, M.; Hashimoto, K.; Tsuji, Y. Siderophores in Iron Metabolism: From Mechanism to Therapy Potential. *Trends Mol. Med.* **2016**, *22* (12), 1077–1090.
- (512) Nukaga, M.; Abe, T.; Venkatesan, A. M.; Mansour, T. S.; Bonomo, R. A.; Knox, J. R. Inhibition of Class A and Class C β -Lactamases by Penems: Crystallographic Structures of a Novel 1,4-Thiazepine Intermediate. *Biochemistry* **2003**, *42*, 13152–13159.

- (513) Page, M. G. P.; Dantier, C.; Desarbre, E. In Vitro Properties of BAL30072, a Novel Siderophore Sulfactam with Activity against Multiresistant Gram-Negative Bacilli. *Antimicrob. Agents Chemother.* **2010**, *54* (6), 2291–2302.
- (514) Dmitrienko, G. I.; Ghavami, A.; Goodfellow, V. J.; Johnson, J. W.; Krismanich, A. P.; Marrone, L.; Viswanatha, T.; Viswanatha, S. Cephalosporin Derivatives Useful as Beta-Lactamase Inhibitors and Compositions and Methods of Use Thereof. US 2012/0329770 A1, 2012.
- (515) Nicodemo, A. C.; Garcia Paez, J. I. Antimicrobial Therapy for *Stenotrophomonas Maltophilia* Infections. *Eur. J. Clin. Microbiol. Infect. Dis.* **2007**, *26* (4), 229–237.
- (516) Falagas, M. E.; Valkimadi, P.-E.; Huang, Y.-T.; Matthaiou, D. K.; Hsueh, P.-R. Therapeutic Options for *Stenotrophomonas Maltophilia* Infections beyond Co-Trimoxazole: A Systematic Review. *J. Antimicrob. Chemother.* **2008**, *62*, 889–894.
- (517) Adegoke, A. A.; Stenström, T. A.; Okoh, A. I. *Stenotrophomonas Maltophilia* as an Emerging Ubiquitous Pathogen: Looking beyond Contemporary Antibiotic Therapy. *Front. Microbiol.* **2017**, *8* (NOV), 1–18.
- (518) The European Committee on Antimicrobial Susceptibility Testing. Breakpoint tables for interpretation of MICs and zone diameters. Version 7.0 <http://www.eucast.org>.
- (519) Papp-Wallace, K. M.; Winkler, M. L.; Gatta, J. A.; Taracila, M. A.; Chilakala, S.; Xu, Y.; Johnson, J. K.; Bonomo, R. A. Reclaiming the Efficacy of β -Lactam- β -Lactamase Inhibitor Combinations: Avibactam Restores the Susceptibility of CMY-2-Producing *Escherichia Coli* to Ceftazidime. *Antimicrob. Agents Chemother.* **2014**, *58* (8), 4290–4297.
- (520) Masuda, G.; Nakamura, K.; Yajima, T.; Saku, K. Bacteriostatic and Bactericidal Activities of β -Lactam Antibiotics Enhanced by the Addition of Low Concentrations of Gentamicin. *Antimicrob. Agents Chemother.* **1980**, *17* (3), 334–336.
- (521) Satta, G.; Cornaglia, G.; Mazzariol, A.; Golini, G.; Valisena, S.; Fontana, R. Target for Bacteriostatic and Bactericidal Activities of β -Lactam Antibiotics against *Escherichia Coli* Resides in Different Penicillin-Binding Proteins. *Antimicrob. Agents Chemother.* **1995**, *39* (4), 812–818.
- (522) Singh, M. P.; Petersen, P. J.; Weiss, W. J.; Janso, J. E.; Luckman, S. W.; Lenoy, E. B.;

- Bradford, P. A.; Testa, R. T.; Greenstein, M. Mannopectimycins, New Cyclic Glycopeptide Antibiotics Produced by *Streptomyces Hygroscopicus* LL-AC98: Antibacterial and Mechanistic Activities. *Antimicrob. Agents Chemother.* **2003**, *47* (1), 62–69.
- (523) Calabrese, E. J.; Baldwin, L. A. U-Shaped Dose-Responses in Biology, Toxicology, and Public Health. *Annu. Rev. Public Health* **2001**, *22*, 15–33.
- (524) Owen, S. C.; Doak, A. K.; Ganesh, A. N.; Nedyalkova, L.; McLaughlin, C. K.; Shoichet, B. K.; Shoichet, M. S. Colloidal Drug Formulations Can Explain “Bell-Shaped” Concentration-Response Curves. *ACS Chem. Biol.* **2014**, *9* (3), 777–784.
- (525) Denton, M.; Kerr, K. G. Microbiological and Clinical Aspects of Infection Associated with *Stenotrophomonas Maltophilia*. *Clin. Microbiol. Rev.* **1998**, *11* (1), 57–80.
- (526) Vila, J.; Marco, F. Lectura Interpretada Del Antibiograma de Bacilos Gramnegativos No Fermentadores. *Enferm. Infecc. Microbiol. Clin.* **2002**, *20* (6), 304–312.
- (527) Samonis, G.; Karageorgopoulos, D. E.; Maraki, S.; Levis, P.; Dimopoulou, D.; Spernovasilis, N. A.; Kofteridis, D. P.; Falagas, M. E. *Stenotrophomonas Maltophilia* Infections in a General Hospital: Patient Characteristics, Antimicrobial Susceptibility, and Treatment Outcome. *PLoS One* **2012**, *7* (5).
- (528) García-Rodríguez, J.; García Sánchez, J. E.; García García, M. I.; García Sánchez, E.; Muñoz Bellido, J. L. Antibiotic Susceptibility Profile of *Xanthomonas Maltophilia*. *Diagn. Microbiol. Infect. Dis.* **1991**, *14*, 239–243.
- (529) Pankuch, G. A.; Jacobs, M. R.; Rittenhouse, S. F.; Appelbaum, P. C. Susceptibilities of 123 Strains of *Xanthomonas Maltophilia* to Eight β -Lactams (Including β -Lactam- β -Lactamase Inhibitor Combinations) and Ciprofloxacin Tested by Five Methods. *Antimicrob. Agents Chemother.* **1994**, *38* (10), 2317–2322.
- (530) Muñoz Bellido, J. L.; Muñoz Criado, S.; García García, I.; Alonso Manzanares, M. A.; Gutiérrez Zufiaurre, M. N.; García-Rodríguez, J. A. In Vitro Activities of β -Lactam- β -Lactamase Inhibitor Combinations against *Stenotrophomonas Maltophilia*: Correlation between Methods for Testing Inhibitory Activity, Time-Kill Curves, and Bactericidal Activity. *Antimicrob. Agents Chemother.* **1997**, *41* (12), 2612–2615.
- (531) Sader, H. S.; Jones, R. N. Antimicrobial Susceptibility of Uncommonly Isolated Non-Enteric

Gram-Negative Bacilli. *Int. J. Antimicrob. Agents* **2005**, 25 (2), 95–109.

- (532) Farrell, D. J.; Sader, H. S.; Jones, R. N. Antimicrobial Susceptibilities of a Worldwide Collection of *Stenotrophomonas Maltophilia* Isolates Tested against Tigecycline and Agents Commonly Used for *S. Maltophilia* Infections. *Antimicrob. Agents Chemother.* **2010**, 54 (6), 2735–2737.
- (533) Milne, K. E. N.; Gould, I. M. Combination Antimicrobial Susceptibility Testing of Multidrug-Resistant *Stenotrophomonas Maltophilia* from Cystic Fibrosis Patients. *Antimicrob. Agents Chemother.* **2012**, 56 (8), 4071–4077.
- (534) San Gabriel, P.; Zhou, J.; Tabibi, S.; Chen, Y.; Trauzzi, M.; Saiman, L. Antimicrobial Susceptibility and Synergy Studies of *Stenotrophomonas Maltophilia* Isolates from Patients with Cystic Fibrosis. *Antimicrob. Agents Chemother.* **2004**, 48 (1), 168–171.
- (535) Jackson, J. J.; Kropp, H. Differences in Mode of Action of β -Lactam Antibiotics Influence Morphology, LPS Release and in Vivo Antibiotic Efficacy. *J. Endotoxin Res.* **1996**, 3 (3), 201–218.
- (536) Thompson, R. C. Use of Peptide Aldehydes to Generate Transition-State Analogs of Elastase. *Biochemistry* **1973**, 12 (1), 47–51.
- (537) Gelb, M. H.; Svaren, J. P.; Abeles, R. H. Fluoro Ketone Inhibitors of Hydrolytic Enzymes. *Biochemistry* **1985**, 24 (8), 1813–1817.
- (538) Imperiali, B.; Abeles, R. H. Inhibition of Serine Proteases by Peptidyl Fluoromethyl Ketones. *Biochemistry* **1986**, 25, 3760–3767.
- (539) Wolfenden, R. Analog Approaches the Structure of the Transition State in Enzyme Reactions. *Acc. Chem. Res.* **1972**, 5 (1), 10–18.
- (540) Schramm, V. L. Enzymatic Transition States and Transition State Analog Design. *Annu. Rev. Biochem.* **1998**, 67, 693–720.
- (541) Schramm, V. L. Enzymatic Transition States, Transition-State Analogs, Dynamics, Thermodynamics, and Lifetimes. *Annu. Rev. Biochem.* **2011**, 80, 703–732.
- (542) Lowe, G.; Swain, S. Synthesis of 7 β -Phenylacetamido-6-Oxo-2-Oxabicyclo[3.2.0]Heptane-4 α -Carboxylic Acid, a Cyclobutanone Analogue of a β -Lactam Antibiotic. *J. Chem. Soc.*

- Chem. Commun.* **1983**, 1279–1281.
- (543) Lange, G.; Savard, M. E.; Viswanatha, T.; Dmitrienko, G. I. Synthesis of 4-Carboxy-2-Thiabicyclo [3.2.0] Heptan-6-Ones via 3-Carboxy-2,3-Dihydrothiophenes: Potential β -Lactamase Inhibitors. *Tetrahedron Lett.* **1985**, 26 (15), 1791–1794.
- (544) Meth-Cohn, O.; Reason, A. J.; Roberts, S. M. Carbocyclic Analogues of Penicillin. *J. Chem. Soc. Chem. Commun.* **1982**, 90–92.
- (545) Cocuzza, A. J.; Boswell, G. A. Cyclobutanone Analogs of β -Lactam Antibiotics: Synthesis of N-Acetyldeazathienamycin. *Tetrahedron Lett.* **1985**, 26 (44), 5363–5366.
- (546) Johnson, J. W.; Evanoff, D. P.; Savard, M. E.; Lange, G.; Ramadhar, T. R.; Assoud, A.; Taylor, N. J.; Dmitrienko, G. I. Cyclobutanone Mimics of Penicillins: Effects of Substitution on Conformation and Hemiketal Stability. *J. Org. Chem.* **2008**, 73 (18), 6970–6982.
- (547) Feng, B. Y.; Shoichet, B. K. A Detergent-Based Assay for the Detection of Promiscuous Inhibitors. *Nat. Protoc.* **2006**, 1 (2), 550–553.
- (548) Irwin, J. J.; Duan, D.; Torosyan, H.; Doak, A. K.; Ziebart, K. T.; Sterling, T.; Tumanian, G.; Shoichet, B. K. An Aggregation Advisor for Ligand Discovery. *J. Med. Chem.* **2015**, 58, 7076–7087.
- (549) Ehlert, F. G. R.; Linde, K.; Diederich, W. E. What Are We Missing? The Detergent Triton X-100 Added to Avoid Compound Aggregation Can Affect Assay Results in an Unpredictable Manner. *ChemMedChem* **2017**, 12, 1419–1423.
- (550) Deming, W. E. *Statistical Adjustment of Data*; Dover Publications, Inc.: New York, New York, 1964.
- (551) Medeiros, A. A.; O'Brien, T. F.; Wacker, W. E. C.; Yulug, N. F. Effect of Salt Concentration on the Apparent In-Vitro Susceptibility of Pseudomonas and Other Gram-Negative Bacilli to Gentamicin. *J. Infect. Dis.* **1971**, 124, S59–S64.
- (552) Boyle, V. J.; Fancher, M. E.; Ross, R. W. Rapid, Modified Kirby-Bauer Susceptibility Test with Single, High-Concentration Antimicrobial Disks. *Antimicrob. Agents Chemother.* **1973**, 3 (3), 418–424.
- (553) Ducours, M.; Rispal, P.; Danjean, M. P.; Imbert, Y.; Dupont, E.; Traissac, E. M.; Grosleron, S.

- Bordetella Bronchiseptica Infection. *Med. Mal. Infect.* **2017**, *47* (7), 453–458.
- (554) Henderson, D. W.; Gorer, P. A. The Treatment of Certain Experimental Anaerobic Infections with Sulphapyridine and with Immune Sera and the Problem of Synergistic Action. *J. Hyg. (Lond)*. **1940**, *40* (3), 345–364.
- (555) Hoyt, A. Studies upon Growth Phases of Clostridium Septicum. *J. Bacteriol.* **1935**, *30* (3), 243–251.
- (556) Stephenson, D.; Ross, H. E. The Chemotherapy of Cl. Welchii Type A and Cl. Septique Infections in Mice. *Br. Med. J.* **1940**, *1* (4133), 471–475.
- (557) Hawking, F. Prevention of Gas-Gangrene Infections in Experimental Wounds by Local Application of Sulphonamide Compounds and by Sera. *Br. Med. J.* **1941**, *1* (4181), 263–268.
- (558) Dafaalla, E. N.; Soltys, M. A. Studies on Agglutination of Red Cells by Clostridia. *Br. J. Exp. Pathol.* **1951**, *32* (6), 510–515.
- (559) Denisuik, A. J.; Lagacé-Wiens, P. R. S.; Pitout, J. D.; Mulvey, M. R.; Simner, P. J.; Taylor, F.; Karlowsky, J. A.; Hoban, D. J.; Adam, H. J.; Zhanel, G. G. Molecular Epidemiology of Extended-Spectrum β -Lactamase-, AmpC β -Lactamase- and Carbapenemase-Producing Escherichia Coli and Klebsiella Pneumoniae Isolated from Canadian Hospitals over a 5 Year Period: CANWARD 2007-11. *J. Antimicrob. Chemother.* **2013**, *68* Suppl 1, 57–65.